United States
Environmental Protection
Agency

EPA-600/R-04-072
July 2004

Electrostatic Precipitator (ESP) Training Manual

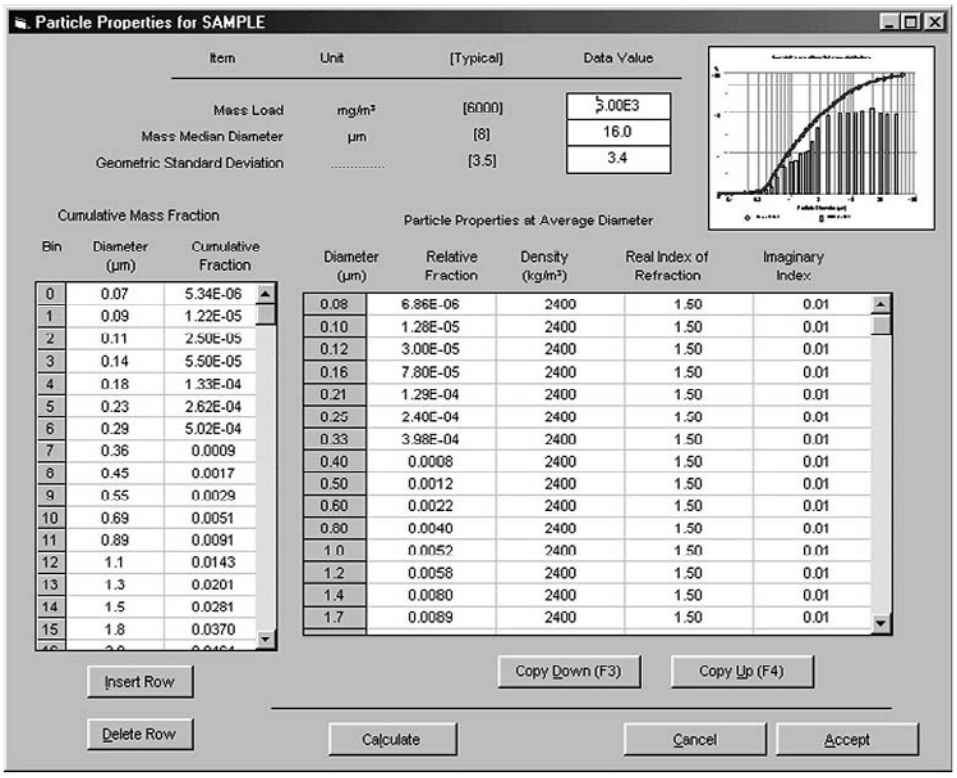

EPA-600/R-04/072
July 2004

Electrostatic Precipitator (ESP) Training Manual

Prepared by:

Kenneth Parker and Norman Plaks

Under subcontract to:

ARCADIS Geraghty & Miller
4915 Prospectus Drive, Suite F
Durham, NC 27713

EPA Contract No. 68-C-99-201, Work Assignment 4-30

EPA Project Officer: Ravi K. Srivastava
National Risk Management Research Laboratory
Research Triangle Park, NC 27711

Prepared for:

U.S. Environmental Protection Agency
Office of Research and Development
Washington, DC 20460

Abstract

This manual assists engineers in using a computer program, the ESPVI 4.0W, that models all elements of an electrostatic precipitator (ESP). Once an ESP is accurately modeled, the model can be used as an analytical tool to diagnose problems and to suggest ways to improve efficiency. In terms of emissions or electrical use, it can predict the results from various fuels and predict the benefit of equipment additions such as gas conditioning. The manual teaches the engineer how to operate the program and discusses the underlying mathematics. A great deal of attention is given to the practical workings of an ESP. Electrical issues are considered, including the detection and control of reverse ionization, electrode design, and various strategies for controlling and optimizing electric energy use. Mechanical matters such as flue gas cooling and conditioning are discussed as are the characteristics of flue gas that result from various fuels, the particles the flue gases contain, and the electrical qualities of the particles.

Foreword

The U.S. Environmental Protection Agency (EPA) is charged by Congress with protecting the Nation's land, air, and water resources. Under a mandate of national environmental laws, the Agency strives to formulate and implement actions leading to a compatible balance between human activities and the ability of natural systems to support and nurture life. To meet this mandate, EPA's research program is providing data and technical support for solving environmental problems today and building a science knowledge base necessary to manage our ecological resources wisely, understand how pollutants affect our health, and prevent or reduce environmental risks in the future.

The National Risk Management Research Laboratory (NRMRL) is the Agency's center for investigation of technological and management approaches for preventing and reducing risks from pollution that threaten human health and the environment. The focus of the Laboratory's research program is on methods and their cost-effectiveness for prevention and control of pollution to air, land, water, and subsurface resources; protection of water quality in public water systems; remediation of contaminated sites, sediments and ground water; prevention and control of indoor air pollution; and restoration of ecosystems. NRMRL collaborates with both public and private sector partners to foster technologies that reduce the cost of compliance and to anticipate emerging problems. NRMRL's research provides solutions to environmental problems by: developing and promoting technologies that protect and improve the environment; advancing scientific and engineering information to support regulatory and policy decisions; and providing the technical support and information transfer to ensure implementation of environmental regulations and strategies at the national, state, and community levels.

This publication has been produced as part of the Laboratory's strategic long-term research plan. It is published and made available by EPA's Office of Research and Development to assist the user community and to link researchers with their clients.

Lawrence W. Reiter, Acting Director.
National Risk Management Research Laboratory

EPA Review Notice

This report has been peer and administratively reviewed by the U.S. Environmental Protection Agency and approved for publication. Mention of trade names or commercial products does not constitute endorsement or recommendation for use.

This document is available to the public through the National Technical Information Service, Springfield, Virginia 22161.

Table of Contents

List of Tables viii
List of Figures ix
List of Acronyms xi
Nomenclature xii
Chapter 1 Overview 1-1
1.1 Introduction 1-1
1.2 Basics 1-3
1.3 ESP Model Development 1-6
1.4 ESPVI 4.0W Operation 1-9
1.5 Data Entry Menus 1-11
1.6 Calculation Menus 1-17
Chapter 2 Relationship of Electrostatic Precipitation to the ESPVI 4.0W 2-1
2.1 Production of an Electric Field to Create Corona and Ions 2-1
2.2 Charging of the Particles by the Ions 2-3
2.3 Effect of the Charged Particles on the Electric Field 2-5
2.4 Migration of Charged Particles through the Electric Field 2-6
2.5 Collection of the Charged Particles 2-9
2.6 Modeling an ESP with ESPVI 4.0W 2-10
2.7 Performance Calculation by the Standard Method 2-15
2.8 Review of Results 2-16
2.9 Graphs 2-18
2.10 Example 1: Varying the Height of an ESP 2-24
2.11 Example 2: Changing the Gas Velocity of an ESP 2-26
2.12 Example 3: Adding a Fourth Section 2-28
Chapter 3 Electrical Energization 3-1
3.1 Basic Operation of Main Frequency Equipment 3-1
3.2 High Voltage Equipment Supply Ratings 3-4
3.2.1 Mean ESP Current 3-4
3.2.2 Primary RMS Current 3-4
3.2.3 ESP Peak Voltage under No-Load Conditions 3-5
3.2.4 Apparent Input Power 3-5
3.2.5 Rectifier Equipment Nameplate Ratings 3-5
3.3 ESPVI 4.0W Operating Voltages 3-6
3.4 Generating V-I Data and Electrical Operating Points 3-12
3.5 Other Computational Methods 3-16
3.6 The Effects of Varying the High Voltage 3-17
3.7 The Effect of Low Voltage on One Section 3-18
3.8 The Effect of Changing the Peak-to-Average Voltage Ratio 3-19
3.9 The Effect of Increasing the Resistivity of Fly Ash 3-20
Chapter 4 Impact of Mechanical Features on Electrical Operation 4-1
4.1 Corona Discharge Electrodes 4-1
4.2 Discharge Electrode Formats 4-3

4.3 Spacing of Discharge Electrodes 4-4
4.4 Collector Electrodes 4-6
4.5 Specific Power Usage 4-6
4.6 ESP Sectionalization 4-8
4.7 High Tension Insulators 4-10
4.8 Electrical Clearances 4-11
4.9 Deposit Removal from the Collector and Discharge Systems 4-13
4.10 Hopper Dust Removal 4-14
4.11 Reentrainment from Hoppers 4-14
4.12 Electrode Design with ESPVI 4.0W 4-15
4.13 Sneakage/Rapping/Turbulence with ESPVI 4.0W 4-19
4.14 Modeling a Complex Electrode 4-24
4.14.1 Modeling the Complex Tape and Needle Electrode with Needles Parallel to the Gas Flow Using a Single Electrode Element 4-25
4.14.2 Modeling the Complex Tape and Needle Electrode with the Needles Parallel to the Gas Flow Using an Array of Electrode Elements 4-29
4.14.3 Modeling the Complex Tape and Needle Electrode with Needles Normal to the Flow 4-30
Chapter 5 Gas Characteristics that Impact ESP Design and Operation 5-1
5.1 Composition 5-1
5.2 Temperature 5-2
5.3 Pressure 5-3
5.4 Gas Flow Rate and Velocity 5-4
5.5 Viscosity and Density 5-7
5.6 Flue Gas Properties with ESPVI 4.0W 5-7
5.7 Changing Gas Temperature 5-9
5.8 Changing SO_2 Concentration 5-10
Chapter 6 Characteristics of the Particles and their Impact on ESP Performance 6-1
6.1 Space Charge 6-1
6.2 Concentration 6-2
6.3 Particle Sizing 6-3
6.4 Particle Shape and Composition 6-3
6.5 Particle Resistivity 6-4
6.5.1 Factors that Affect Particle Resistivity 6-5
6.5.2 The Effect of High Resistivity on the ESP 6-6
6.5.3 Correlation between ESP Performance and Particulate Resistivity 6-9
6.5.4 Electrical Conditions for ESPs Collecting Resistive and High Resistivity Dust 6-11
6.5.5 Low Resistivity Ash and Its Effect on Performance 6-12
6.6 Particle Properties in ESPVI 4.0W 6-13
6.7 Reverse Modeling Particle Size Distribution Using the Space Charge Effect on the Electrical Conditions 6-15
Chapter 7 Enhancing the Performance of Existing ESPs—Mechanical 7-1
7.1 Increasing the Size of the ESP 7-1
7.2 Flue Gas Conditioning 7-2
7.3 Humidity Conditioning 7-4

7.4 Reducing Inlet Gas Temperature 7-5
7.5 Mechanical Enhancement Evaluations with ESPVI 4.0W 7-5
Chapter 8 Enhancing the Performance of Existing ESPs—Electrical 8-1
8.1 Electrical Methods of Mitigating Reverse Ionization 8-1
8.1.1 Intermittent Energization (IE) 8-1
8.1.2 Comparison of IE with Traditional DC Energization 8-3
8.1.3 Pulse Energization 8-4
8.1.4 Summary of Resistivity Effects on ESP Performance 8-5
8.2 Reverse Ionization Detection and Corona Power Control 8-7
8.3 Automatic Voltage Control and Instrumentation 8-8
8.4 Specific Power Control 8-9
8.4.1 Control by the Use of IE 8-9
8.4.2 Supervisory Computer Control Using a Gateway Approach 8-9
8.5 Advanced Computer Control Functions 8-10
8.6 Switched Mode Power Supplies (SMPS) 8-11
8.6.1 The Development of SMPS 8-12
8.6.2 System Requirements 8-12
8.6.3 SMPS Design Considerations 8-13
8.6.4 SMPS Circuit Configurations 8-14
8.6.5 Practical Application of SMPS Systems 8-14
8.6.6 Summary of SMPS Equipment Operation 8-16
Chapter 9 Troubleshooting, Faultfinding, and Identification 9-1
9.1 Electrical Operating Conditions 9-2
9.2 Deposit Removal from the Internals 9-5
9.3 Discharge Electrode and Collector System Voltage—Current Relationships 9-5
9.3.1 Clean Air Load Characteristic 9-6
9.3.2 Operational Curves with Gas passing through the System 9-7
9.4 Dirty Air Load Test, without Gas Passing through System 9-9
9.5 Collector and Discharge Electrode Alignment 9-10
9.6 High Tension Insulators 9-11
9.7 Hopper Problems 9-11
9.8 Gas Distribution and Air In-leakage 9-12
9.9 Changing Inlet Gas Conditions 9-13
9.9.1 Particle Resistivity 9-13
9.9.2 Particle Sizing and Opacity Monitoring 9-13
9.10 Systematic Fault Finding Procedure 9-13
Chapter 10 References 10-1
Appendix A Installing and Setting Up ESPVI 4.0W A-1
Appendix B Internal Composition and Text of the Data Files B-1

List of Tables

Table 3-1. The Effects of Varying High Voltage on ESP Performance 3-18
Table 3-2. The Effect of Low Voltage on One Section on ESP Performance 3-18
Table 3-3. Effect of Changing Peak-to-Average Voltage Ratio on ESP Performance .. 3-19
Table 3-4. The Effect of Fly Ash Resistivity on ESP Performance 3-22
Table 4-1. Recommended Clearances for ESPs 4-13
Table 4-2. Comparison of Modeled Electrode Complex Tape and Needle Electrode with Needles Parallel to Gas Flow under Air Load Conditions .. 4-26
Table 4-3. Comparison of Modeled Electrode Complex Tape and Needle Electrode with Needles Normal to Gas Flow under Air Load Conditions 4-31
Table 5-1. The Effect of Gas Temperature on ESP Efficiency 5-9
Table 5-2. The Effect of SO_2 Concentration on ESP Efficiency 5-11
Table 6-1. Electrical Operating Conditions for a 3-Section ESP 6-2
Table 7-1. Performance Enhancement from Flue Gas Conditioning Approaches 7-2
Table 8-1. Current and Voltages with IE Compared to Values obtained with DC Energization 8-3
Table 9-1. Most Common Electrical Problems – Control Cubicle Information 9-3
Table 9-2. Examination of TR Panel Meter Readings 9-4
Table 9-3. Schematic of Rapping System Examination 9-5

List of Figures

Figure 1-1. Basic parallel plate ESP arrangement. 1-3
Figure 1-2. Main window of the ESPVI 4.0W. 1-10
Figure 1-3. “ESP Design” data window. 1-11
Figure 1-4. “Operating Voltages” data entry window. 1-12
Figure 1-5. “Electrode Design” data entry window. 1-13
Figure 1-6. “Sneakage/Rapping/Turbulence” data entry window. 1-14
Figure 1-7. “Gas Properties” data entry window. 1-15
Figure 1-8. “Particle Properties” data entry window. 1-16
Figure 2-1. Relative field strength between the electrodes for a tubular ESP arrangement. 2-2
Figure 2-2. Voltage current curves for a well operating ESP showing the effects of space charge corona suppression. 2-6
Figure 2-3. Particle penetration by size. 2-8
Figure 2-4. “ESP Design” window for SAMPLE ESP. 2-11
Figure 2-5. Results of computation by standard method for SAMPLE. 2-16
Figure 2-6. “Main Results” for the SAMPLE ESP. 2-17
Figure 2-7. “Plan Views of ESP” for SAMPLE ESP. 2-18
Figure 2-8. “V-I Operating Points” for SAMPLE ESP. 2-19
Figure 2-9. “Electrode Arrangements” for SAMPLE ESP. 2-20
Figure 2-10. “Inlet Particle Distribution” for SAMPLE ESP. 2-21
Figure 2-11. “Differential Particle Distribution” for SAMPLE ESP. 2-22
Figure 2-12. “Wave Forms by Section” showing full-wave energization for SAMPLE ESP. 2-23
Figure 2-13. “Design of ESP” window for SAMPLE1—changing the height. 2-25
Figure 2-14. “Main Results” for SAMPLE1—changing the height. 2-26
Figure 2-15. “Design of ESP” window for SAMPLE2—changing the gas velocity 2-27
Figure 2-16. “Main Results” for the SAMPLE2—changing the gas velocity. 2-28
Figure 2-17. “Main Results” for SAMPLE3—increasing the number of sections. 2-29
Figure 3-1. Typical main frequency rectifier equipment. 3-1
Figure 3-2. Typical DC wave forms as applied to the ESP. 3-3
Figure 3-3. Half-wave energization ESPVI 4.0W graph representation. 3-9
Figure 3-4. IE ESPVI 4.0W graph representation. 3-10
Figure 3-5. ”Calculation Options” window. 3-15
Figure 3-6. “Automatic V-I” calculations for SAMPLE operating with resistive dust. 3-21
Figure 3-7. “Fixed V-I” calculations for SAMPLE operating with resistive dust. 3-22
Figure 4-1. V-I characteristics indicating the corona threshold voltage for different electrode diameters. 4-2
Figure 4-2. Typical discharge electrode types. 4-2
Figure 4-3. Typical air load V-I characteristics for various electrode formats 4-3
Figure 4-4. Effect of electrode spacing on specific current. 4-5
Figure 4-5. Typical NIS collector sheet profiles. 4-6
Figure 4-6. Effect of specific power absorption on ESP efficiency. 4-7
Figure 4-7. Effect of ESP sectionalization on performance. 4-9

Figure 4-8. Effect of sectionalization on specific current production. 4-10
Figure 4-9. Effect of tracking across high tension insulator. 4-11
Figure 4-10. Cold-pipe electrode arrangement. 4-17
Figure 4-11. Tape and needle corona discharge electrode. 4-25
Figure 4-12. Complex tape and needle with needles parallel to gas flow using single element and array under air load conditions. 4-27
Figure 4-13. An array simulating the tape and needle electrode parallel to flow. 4-29
Figure 4-14. Complex tape and needle with needles normal to gas flow using single element under air load conditions. 4-32
Figure 5-1. Typical corona characteristics of gas mixtures. 5-2
Figure 5-2. Effect of gas temperature on ESP efficiency. 5-3
Figure 5-3. Effect of gas velocity on ESP efficiency 5-4
Figure 5-4. Variation of efficiency with gas velocity standard deviation 5-5
Figure 5-5. Skewed velocity distribution profile. 5-6
Figure 6-1. Effects of temperature and moisture on fly ash resistivity 6-4
Figure 6-2. The effect of sulfur in coal plus sodium in ash on fly ash resistivity 6-6
Figure 6-3. Representation of the conditions arising across a collector dust deposit. 6-7
Figure 6-4. Typical V-I curves for different dust resistivities. 6-9
Figure 6-5. The effect of sodium oxide in the ash on an ESP's efficiency 6-10
Figure 6-6. The effect of sulfur in coal and sodium in ash on ESP performance. 6-11
Figure 6-7. Effect of resistivity on allowable current density in an ESP. 6-12
Figure 6-8. V-I curves from unknown particle and two different known particle characteristics in SAMPLE7 6-17
Figure 7-1. Generic arrangement of a dual, sulfur trioxide plus ammonia, conditioning system. 7-4
Figure 7-2. Impact of temperature variations for a range of fuels. 7-5
Figure 8-1. Typical wave forms with IE. 8-2
Figure 8-2. Typical voltage wave form comparison obtained with pulse and DC energization 8-5
Figure 8-3. Voltage/current characteristics for different fly ash resistivities. 8-6
Figure 8-4. V-I curves indicating peak, mean, and trough voltage levels. 8-7
Figure 8-5. Supervisory computer control system. 8-10
Figure 8-6. Block diagram of a typical SMPS system. 8-13
Figure 8-7. Comparison of voltage wave forms from conventional and SMPS energization systems. 8-15
Figure 8-8. Reduction in electrical recovery times following a flashover with SMPS operation. 8-15
Figure 9-1. Identification of potential ESP fault areas. 9-2
Figure 9-2. Static V-I characteristic of an ESP field. 9-6
Figure 9-3. Typical V-I characteristics for good fly ash. 9-7
Figure 9-4. V-I characteristics indicating operational performance problems. 9-8
Figure 9-5. Abnormal operational V-I characteristics. 9-9
Figure 9-6. Comparison of V-I characteristics for clean and dirty collector plates. 9-10

List of Acronyms

AC	Alternating current
AVC	Automatic voltage control
DC	Direct current
DOS	Disk operating system (Now considered obsolete)
EPA	U.S. Environmental Protection Agency
EPRI	Electric Power Research Institute
ESP	Electrostatic precipitator
ESPM	An electrostatic precipitator model marketed by EPRI
FGC	Flue gas conditioning
HT	High tension
NIS	Newly independent states
NO_X	Term that includes all oxides of nitrogen species
O/C	Open circuit
O/S	Out of service (Fault condition)
PC	Personal computer
PLC	Programmable logic control
PM	Particulate matter
ppm	Parts per million
pps	Pulses per second
RMS	Root mean square
SCA	Specific collector area
SI	Metric system of measurements
SMPS	Switched mode power supply
TR	Transformer rectifier
V-I	Voltage current characteristic

Nomenclature

Symbol	Description	Unit
$\mathbf{A_o}$	Area of grounded collector electrode or plate	m^2
D	Particle diameter	µm
D	Degree of Intermittence	--
D	Charge ratio, reciprocal of D	--
e	Electronic charge	C
E	Electric field	v/m
$\boldsymbol{E_f}$	Efficiency	%
$\boldsymbol{\varepsilon_o}$	Permittivity of free space	F/m
FF	Form factor	--
I	Current – Subscripts denote type of current	A
K	Boltzmann's constant	J/s m^2 °C
m	Particle mass	kg
n	Transformer turns ratio	--
η	Viscosity	Pa×s
ω	Migration velocity in Deutsch equation applied to whole ESP	m/s
ω_k	Migration velocity in modified Deutsch equation	m/s
P	Power	W
Q	Particle charge	C
ρ	Space charge density	C/m^3
S	Apparent input power	W
t	Time – Subscripts denote type of time	s
T	Temperature – Subscripts denote type of temperature	°C
$\mathbf{V_c}$	Corona onset voltage	kV
Vf	Volumetric gas flow rate	m^3/s
$\mathbf{X_{lsc}}$	Short circuit reactance	---
W	Migration velocity applied to individual particle	m/s

Chapter 1
Overview

This chapter discusses the basics of electrostatic precipitation and provides the overview of electrostatic precipitator (ESP) model development. It presents the model and its capabilities by introducing the various pull-down menus that are used to enter data. It also discusses menu items from which completed results can be obtained.

1.1 Introduction

Particulate matter (PM) is emitted as a pollutant from many industrial processes, including coal-fired utility boilers. The control technology used to collect the majority of this PM is the ESP. A necessary tool for the ESP owner or operator is a means to understand how the unit works; when it is, or is not, functioning properly; how to identify and correct problems; and what options are available to improve its performance.

The science and understanding of electrostatic precipitation has in recent years reached a high level. The physics of the electric fields, the charging of particles within the field, their migration velocity and collection, and the effect of the charged particles have become well understood. The mathematics that describes the physics has evolved. Low-cost, powerful personal computers (PCs) that are capable of finding solutions for the ESP's mathematical physics have become readily available. Software programs to perform the complicated calculations and predict the ESP's performance have been written. The ESPVI 4.0W Performance Prediction Model (ESPVI 4.0W) is an advanced and accurate ESP model capable of predicting the performance of an ESP.

This manual utilizes a combined approach of ESP theory and modeling using ESPVI 4.0W and demonstrates how they relate to each other. The manual brings in those aspects of precipitation that have to be based on empirical approaches rather than theory, and introduces troubleshooting both by traditional and modeling means where applicable.

Individuals participating in this program will be operating the ESPVI 4.0W electrostatic precipitator performance prediction model on PCs using the Microsoft Windows operating system. It is assumed that the participants are familiar with computers and the Windows operating system. What will be included in the program are those aspects of operating the computer that are specific to ESPVI 4.0W. Aspects that are generally handled by the Windows operating system will generally be given less attention.

The organization of this manual generally follows the data entering process to ESPVI 4.0W. Once the set up of ESPVI 4.0W becomes familiar, users will probably establish their own approach to using the model, but the manual is expected to remain a valuable reference.

The basic principle of electrostatic precipitation is that gas-borne particles are passed through an electric field where they are initially charged by means of a corona discharge. Charged particles are then deflected across the electric field and deposited on collecting electrodes. Therefore, the process is considered to be comprised of the following components:

- Production of an electric field to create corona and ions
- Charging of the particles by the ions
- Effect of the charged particles on the electric field
- Migration of the charged particles through the field
- Collection and removal of the charged particles

An ESP must be designed and installed in a manner consistent with the type of PM the unit will collect and its required collection efficiency. Once the ESP is erected and operating, it must be maintained in a manner that retains its original operating characteristics. The training program that this manual supports discusses all of the above and is integrally linked to ESPVI 4.0W.

Chapter 1 presents the basic structure of the ESPVI 4.0W. It introduces the various interfaces into which data is entered and from which computational results are obtained.

Chapter 2 discusses much of the theory that relates to electrostatic precipitation operation and to the ESPVI 4.0W. Many factors considered in the theory relate to the physical dimensions of the ESP. This chapter shows how physical information is entered into ESPVI 4.0W to allow it to provide collection efficiency output computations. The effects on particle collection arising from changes to ESP configuration will also be discussed.

By definition, an ESP operates by the application of high-voltage electrostatic fields. In Chapter 3, the application of high-voltage electrical energization to the ESP and to ESPVI 4.0W is presented, and the application of different electrical conditions and their effects are investigated.

Chapter 4 discusses many of the ESP's mechanical aspects that affect electrical conditions and performance. Part of the work is concerned with the corona discharge electrodes and the entering of their properties into ESPVI 4.0W, which, along with the energization and particle characteristics, control the voltage current relationships. Also considered are the non-ideal effects such as sneakage, which is the fraction of gas that bypasses the collection zone of an ESP section, and rapping reentrainment.

The effects of gas flow, composition, and temperature on the ESP and their introduction into ESPVI 4.0W are covered in Chapter 5.

Chapter 6 examines the effects of particles in the gas stream on the ESP and how this information is entered into ESPVI 4.0W.

It is often necessary to upgrade the performance of an existing ESP. One mechanical approach is increasing the size of the unit. Other mechanical options are considered in

Chapter 7, including the use of flue gas conditioning techniques. The use of ESPVI 4.0W to evaluate these options is also presented.

Other upgrading options make use of improved electrical energization. These options are explained in Chapter 8 and then evaluated using ESPVI 4.0W.

The collection efficiency of an ESP may degrade due to a mechanical or electrical problem. Procedures for evaluating the causes are discussed in Chapter 9.

1.2 Basics

The fundamental principle of operation of an ESP is that the particles are passed through an electrical field where they receive an electrical charge. Charged particles are then deflected across the field and collected on a grounded plate. Most industrial ESPs are based on a single stage approach in which both charging and migration across the field (precipitation) take place within the same set of electrodes, as illustrated in Figure 1-1

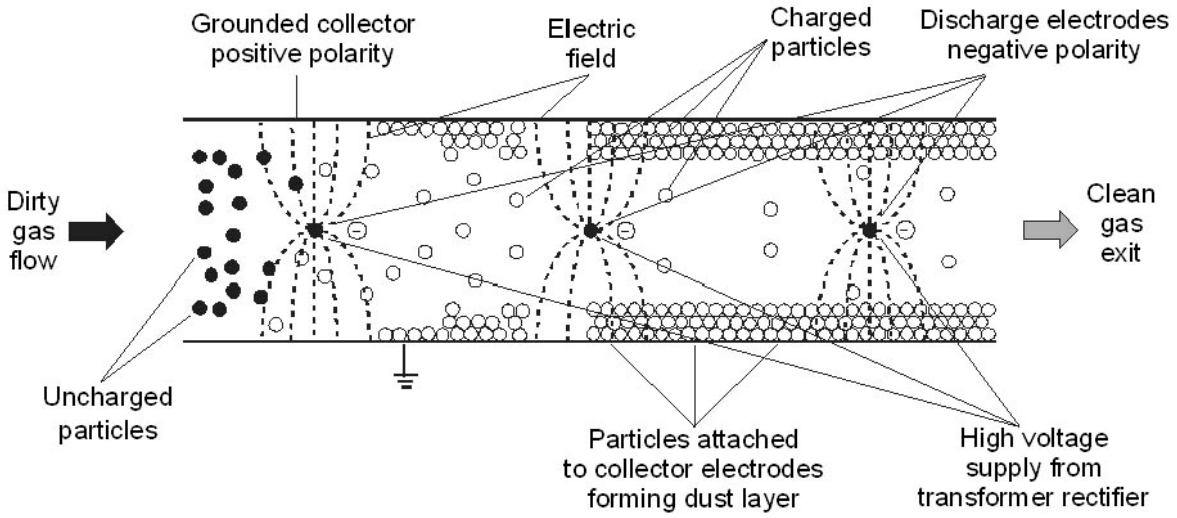

Figure 1-1. Basic parallel plate ESP arrangement.

In practice, for large gas flow rates, single stage ESP normally takes the form of a series of vertical parallel plates, usually termed receiving (or collecting) electrodes, which are normally at ground potential, having insulated discharging elements positioned midway between them. For a 400 mm collector electrode spacing, the discharging elements, ranging from simple 3 mm round wires to specially designed spiked forms, are typically energized at an average direct current (DC) voltage of around minus 70 kV. The voltage may be higher or lower for other collector spacing.

Adjacent to the small diameter electrode elements, the resultant high electrical field ionizes the gas molecules, forming both positive and negative ions. The positive ions are immediately captured by the negatively charged electrodes, while the negative ions and any

electrons, generally referred to as a corona discharge, migrate under the influence of the electric field into the inter electrode space. As the gas-borne particles pass through the inter-electrode space, the larger particles receive an electric charge either by collision with the ions/electrons or by induction charging for the smallest particles. The charged particles then move under the influence of the electric field and migrate to the collecting electrodes, where the charge subsequently leaks away to the ground.

To ensure that the collection process in a dry precipitator is continuous, the collector electrodes are usually mechanically rapped after a period of time to remove the deposited material. The frequency and intensity of the rapping is important, for it is necessary to minimize rapping reentrainment and to maximize collection efficiency. The rapping should be such as to shear the deposited dust from the collector surface in an agglomerated form that is large enough to fall through the gas flow into receiving hoppers, rather than exploding the layer from the collection surface, which would result in severe particle reentrainment.

Although the corona wind emanating from the discharge electrodes coupled with incipient flashover should assist in keeping the discharge electrodes free of dust, it is normal practice to either rap or vibrate the discharge system to ensure optimum corona production.

In practice, the advantage of the horizontal flow unit is that, to attain the high efficiencies demanded to meet the current emission standard, several separate sections or fields can be readily arranged in series. The number of series fields supplied depends not only on the overall efficiency required, but also on the supplier's preferences. In general terms, when working with easily collected dusts, three field arrangements are typical for efficiencies above 99 percent. For efficiency requirements above 99.5 percent, four or more fields may be found on many installations.

Until the recent development of switched mode power supplies (SMPS), most currently installed industrial ESPs were electrically energized from main supply frequency-rectified, high-voltage equipment. This comprises a suitably designed and insulated step-up transformer, the output from which can be controlled by adjusting the incoming main supply voltage level. The transformer output is then rectified to produce a high negative DC voltage. The magnitude of the peak voltage can exceed 100kV, depending on the ESP design, collector spacing, and such.

Different approaches to sizing of ESPs are in use today. One of the more popular is the use of "performance factors" derived from the measurement of efficiency at a plant having similar mechanical, electrical, and process characteristics. This approach is most useful for equipment suppliers who have developed large data bases of the performance of the equipment that they have supplied in the past. This approach is based on the work of Deutsch and others.

Deutsch, an early theoretical investigator, working in the mid 1920s, proposed that the performance, or collection, efficiency of an ESP took the form of an exponential equation. His work ultimately led to his now famous equation in which the efficiency, $\boldsymbol{E_f}$, is given by Equation 1.1:

$$E_f = 1 - e^{-A\omega/Vf} \qquad 1.1$$

where ω is the effective migration velocity, **A** is the area of grounded collecting electrode or plate, and ***Vf*** is the actual gas volumetric flow rate.

The above relationship was used for many years to relate the size of the ESP, collection efficiency, and gas flow rate for plants operating on similar requirements and inlet conditions. Used in that way, the relationship is applied to the whole ESP regardless of the number of sections or operating conditions. Although the formula is theoretically based, when used by itself it is no more than a useful method of comparing ESP performance levels.

It was in the 1960s, when difficulties arose in meeting more stringent emission requirements, that modifications to the traditional Deutsch relationship were considered. One of the better-known modifications was that derived by Matts and Ohnfeldt, who produced the relationship given in Equation 1.2 below, termed the Modified Deutsch Formula, for deriving an improved working value of the "effective migration velocity" ω_k:

$$\omega_k = ln\ [1/(1 - E_f)]^2\ Vf/A \qquad 1.2$$

The practical implication of these modified approaches is that, for a change in efficiency, based on an installed plant whose operational data is known, the required plate area increase is around twice that derived from the straight Deutsch Formula. It should be noted that the actual values of ω_k and the exponent, which is shown as 2 in Equation 1.2, are derived from a database of ESPs that are similar to the unit that is to be evaluated. They have little scientific or physical meaning and essentially do little more than provide a curve fitting means. The accuracy of the Matts and Ohnfeldt relationship decreases for ESPs whose configuration and operation differs from the ESPs in the database.

For evaluation and sizing of an ESP for which there is not sufficient information for accurate application of the Matts and Ohnfeldt relationship, or if precise determination is needed of what is happening inside the ESP, other methods must be used. These other methods must work from first principles, starting with Poisson's equation given in Equation 1.3:

$$\nabla^2 V = - \rho/\varepsilon_o \qquad 1.3$$

where **V** is the voltage; ρ is the space charge density, and ε_o is the permittivity of free space.

Because the space charge is attributable to the corona current, solving Poisson's equation allows the development of voltage/current relationships. By application of suitable physical relationships involving the electrode geometry and spacing, the corona onset and voltage/current curves are determined. As part of the overall process, the electric fields for particle charging and collection are established.

Following the "first principle" process, it is necessary to charge the particles, compute their true migration velocity, and then collect them. Collecting the particles continues to make use

of the Deutsch equation, but this time it is applied in its scientifically derived, rigorous form. To go even further, some modes of ESP operation (specifically reverse ionization) subject particles to charging by positive ions (bipolar charging).

The set up and solving of all of the physical relationships that describe the internal activities within a modern ESP requires the solution of a very large number of complex mathematical equations. The availability of modern, powerful computers has made it possible to prepare programs for determining the performance of an ESP from first principles.

A modern, powerful ESP performance prediction model is ESPVI 4.0W, the program to be described by this manual. When loaded with various operating parameters from the ESP, ESPVI 4.0W will accurately predict ESP performance. It will do this, not only for the total ESP, but also section by section. Moreover, it will provide the total particle collection and the collection by particle size as an output. It can be used both as a standard, again section-by-section, against which the performance of a full-scale ESP can be judged and also as a powerful tool for troubleshooting purposes. Finally, before making expensive changes to either the configuration or the operation of a full-scale ESP, changes can be modeled on the computer to accurately determine the effects on particle collection. Additionally, when it senses that reverse ionization is occurring, ESPVI 4.0W includes a bipolar charging capability to determine the effects on the particles by positive ions. ESPVI 4.0W is also a very powerful design tool for sizing an ESP for use in a new installation.

It is the purpose of this manual to examine how the characteristics of the gas and dust presented to the ESP affect performance and how the mechanical and electrical arrangements can be optimized. Consequently, the manual will comprise basic theory and practical considerations and discuss how ESPVI 4.0W can be used to investigate the performance of existing ESPs as well as how their performance can be optimized. It will be seen that the basic electrical and physical activities that occur within an ESP are needed as input to the ESPVI 4.0W. Once entered with the correct parameters, ESPVI 4.0W will accurately describe the performance of the ESP from which the parameters were obtained.

1.3 ESP Model Development

The ESPVI 4.0W has been developed to allow the user to accurately predict ESP performance. This model is the result of many separate research efforts that have been drawn together in to a close-knit working relationship.

The program has been designed for ease of use. It runs on Windows compatible computers. It controls the data entry with a menu-structured interface, and makes the results of intermediate calculations available to appropriate parts as input data. The outputs are presented in a variety of forms, both tabular and graphical. The ESPVI 4.0W is the latest in a long series of model development activities under the sponsorship of the U.S. Environmental Protection Agency (EPA) that started in the early 1970s (Plaks, 1998).

The heart of the modern ESP model presented earlier is the well-known Deutsch equation, which in its rigorous form computes the probability that a particle traveling in the turbulent

interior of an ESP will enter the laminar layer at the collecting surface. If the particle entering the laminar layer is charged and an electric field exists at the collecting surface, then its migration velocity assures its collection. This differs from the Deutsch equation used in its non-rigorous form in which a single pseudo migration velocity, sometimes called a rate parameter, is used to represent all of the particles in the gas stream regardless of their size.

In the modern, computerized model, the Deutsch equation is used in its rigorous form. It requires all of the particles for which it is performing the calculation have the same migration velocity, which in this case is the true migration velocity and not a rate parameter. To handle this requirement, the particle size distribution is divided into a number of narrow size increments, for each of which the migration velocity is computed. The computed migration velocity is the maximum velocity attained by the charged particle in the electric field, subject to the viscous drag of the gas. Before computation of the migration velocity, the charge of the particles in each size increment is determined. Depending on the particle size, the model uses diffusion, field charging, or some combination of both. In addition, the computation is divided into a number of ESP length increments, usually one for each electrode element. For each of the length increments, the particle charge corrected for charging time and migration velocity are recomputed. The changing electrical conditions from one increment to the next are accommodated in the calculations. Finally, a double summation, for both the particle size and length increments, is performed to give the overall ESP collection efficiency.

The basic model just described characterizes the early model series, which appeared in various versions between July 1972 and January 1991. The initial versions in this series performed their computations on mainframe computers. As the newer versions were developed, they were adapted to desktop computers. Computational methods to handle the wire/duct geometry and empirical treatment of non-ideal factors including sneakage, velocity distribution, and reentrainment, were added to the basic model. As the series developed, data from actual ESPs were used to validate and improve the accuracy of the models, and computational time was decreased. This series achieved its ultimate capability with the release of the final version, the Self-Consistent Deutschian Model. This version rigorously handled the space charge and its effect on ESP performance in the computations, and consequently provided the greatest accuracy of the models in this series.

An important aspect of this early series of models is related to the electrode configuration as they handle electrical voltages and currents. The modeled electrode configurations are evenly spaced, round wires. ESPs with unevenly spaced electrodes or non-round wires introduce inaccuracies. The early series of models takes and accepts as input both the voltage and the current for the performance computations. It makes no difference to the models whether or not the currents are useful. The current can be inappropriate for a number of reasons such as back corona, leakage, or misalignment. These models assume that all of the current is useful corona current and use it in computations, thereby introducing additional inaccuracies.

The next stage in the evolution of ESP models was the present series known as ESPVI. The objective was to develop a program that could perform all the computations of the early series, and model the various electrode configurations both in commercial use and being developed. Version 1.0 (Interactive ESP Computer Model) was released in September 1986.

The ESPVI series went through Versions 2.0, 3.0, and 3.2, which were developed and tested, but not released. In June 1992 ESPVI 4.0 was released, followed in January 1996 by ESPVI 4.0a. All of the ESPVI models through ESPVI 4.0a used the Disk Operating System (DOS).

The ESPVI 4.0 and 4.0a series includes the finding of solutions for Poisson's equation, which relates electric field and space charge. This allows introduction of current and electrode geometry as well as space charge, both particle and ionic. The ESPVI 4.0x models for given high-voltages, electrode configuration, and particle characteristics calculate the corona current. ESPVI 4.0x always use the computed current for the performance prediction calculations rather than the actual ESP current. As far as the ESPVI 4.0x models are concerned, the calculated currents are the only useful currents within the ESP. If actual ESP currents differ from the calculated currents, either the model has not been set up properly, or some problem exists within the ESP. This last situation indicates how the ESPVI 4.0x models can be useful for troubleshooting an ESP.

Individual electrode elements can be set to any size or spacing. By use of different electrode element combinations or settings, virtually any electrode configuration in commercial use can be simulated. Also included is both flat-plate and cold-pipe geometry to further increase their usefulness. The ESP is divided into a length increment for each electrode element. This allows space charge to be computed very rigorously, increment-by-increment and electrode-by-electrode. The rigorous computation of the space charge effect by ESPVI 4.0 and 4.0a allows them to actually match the corona current suppression, which causes the lower currents seen in the inlet sections of ESPs. A major difference between ESPVI 4.0 and 4.0a is the use of improved particle charging algorithms including the bipolar charging as experienced with back corona. A number of additional features have been added to improve operation and accuracy. ESPVI 4.0a is superior to and is the successor to ESPVI 4.0.

An important ESP performance prediction model is ESPM, which is a proprietary model commercially marketed by the Electric Power Research Institute (EPRI). ESPM has many of the capabilities that are inherent in ESPVI 4.0a. A major difference is the requirement of ESPM that, very much like the early models described above, all corona discharge electrodes be inputted as the same round wire diameter and be set for equal spacing. This limits ESPM's ability to accurately simulate many of the electrode configurations currently in commercial use. ESPM does have some additional features, useful to the electric utility industry, such as an internal resistivity calculator for coal ash. However, with its additional features, ESPVI 4.0a was one of the most advanced and accurate of the ESP models available.

The EPA ESPVI 4.0a and EPRI's ESPM, which use the same internal algorithms for computing, will provide similar accuracy and results for modeling ESPs with equally spaced corona discharge electrodes. The data requirements for both models, when operating with round equally spaced electrodes are greater than the early models. These models, in-turn, have a wider range of applicability to differing ESPs and operating conditions. To take advantage of this increased flexibility requires more skill on the part of the person performing the modeling to assure that the model is truly representing the ESP. ESPVI 4.0a and ESPM use menus and entry forms for ease of data loading.

In addition to being able to model simple electrode configurations, ESPVI 4.0a is able to accurately model non-uniformly spaced electrodes, such as the spiral and wire mast, and special shaped electrodes such as the increasingly popular rigid type or the tape and needle electrodes. To accurately model these more complex ESP configurations requires both a greater amount of data input than all other models and a still higher level of skill on the part of the user. In turn, ESPVI 4.0a has the widest range of applicability and usefulness of all of the prior ESP models and provides the largest amount of useful output information. It is also the only known model that can work in either the SI (metric) or non-metric system of units. To accurately model these more complex ESP configurations, larger and more complex input is required.

Recently, the DOS model, ESPVI 4.0a, was upgraded to work with the Windows operating system as ESPVI 4.0W. Operating in the Windows system makes ESPVI 4.0W significantly simpler to use than its predecessor while retaining all of its inherent accuracy and capabilities. In addition to being able to operate with Windows, several minor improvements were made to the model to further increase its accuracy and usefulness. These will be discussed later in this manual. Installation and set up of ESPVI 4.0W are discussed in Appendix A.

1.4 ESPVI 4.0W Operation

Upon opening ESPVI 4.0W, a small window appears with two command buttons labeled English and Russian. Once the language button is clicked, a new window will open, as shown in Figure 1-2. This window is called the main window. Across the top of the window there is a number of pull-down menus: “File”, “Data Entry and Editing”, “Calculate V-I Curve”, “Performance Calc”, “Show Results”, “Graphs”, and “Help”. The large white space in the window below the pull-down menu bar is the area where graphs generated by the model are displayed. The graphs generated by ESPVI 4.0W will be discussed later in the manual.

The first pull down-menu on the left is labeled “File”. This menu contains typical Windows entry commands. Included are file management commands, printing, and exiting the program. This menu will be discussed in more detail later in this chapter. The remaining pull-down menus will be discussed briefly here and in more detail later in the manual.

These are:

- “Data Entry and Editing” provides various commands that allow entry of data for the ESPs to be modeled in either metric or non-metric system of units. The “Notes” command under this menu allows a few lines of notes to be entered in the master file concerning the ESP being modeled.
- “Calculate V-I Curve” provides several methods for calculating the electrical conditions within the ESP that is being modeled.
- “Performance Calc” provides several methods for computing the performance for the ESP that is being modeled.
- “Show Results” provides the modeling results in text form.
- “Graphs” provides graphical output for modeling results.
- “Help” provides help information about the model.

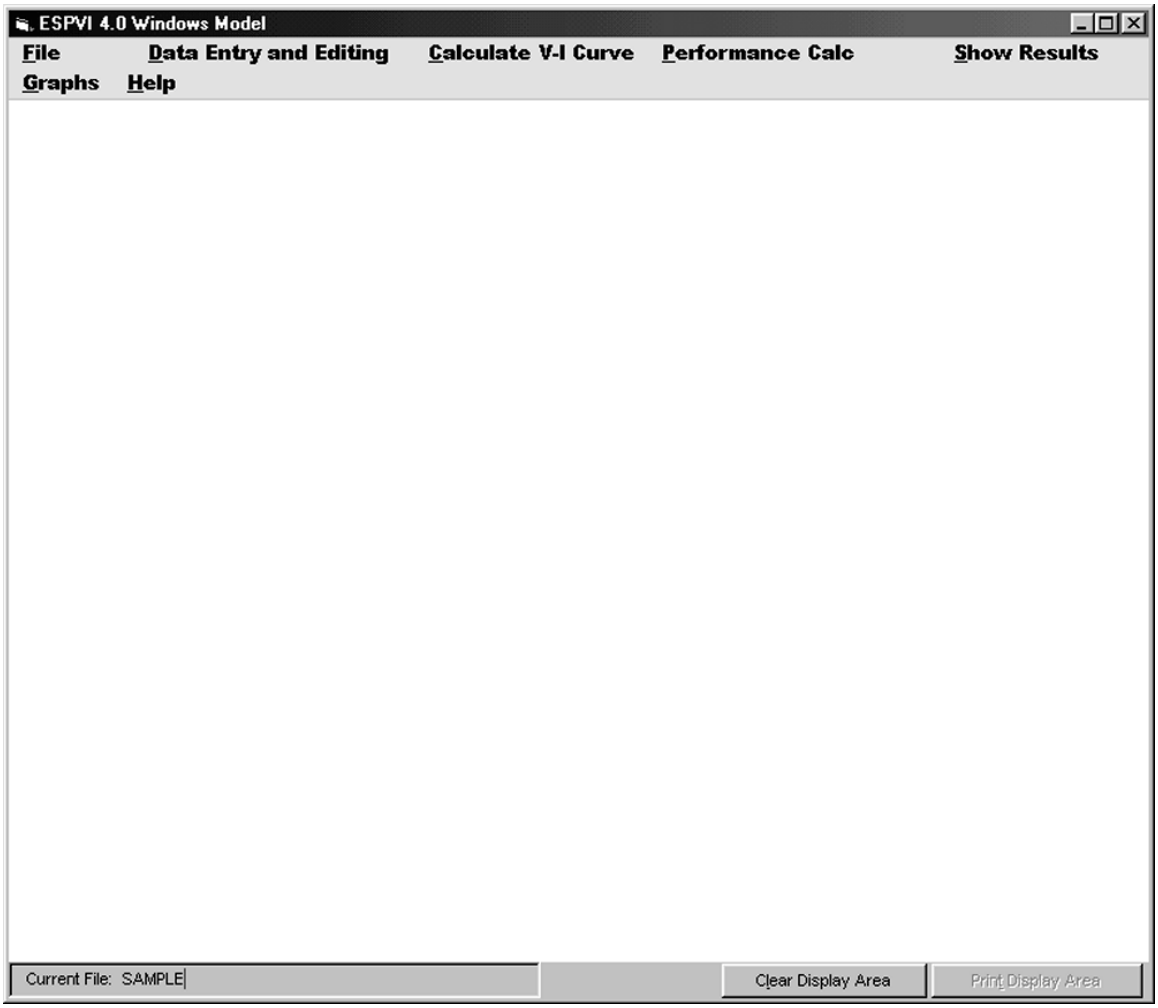

Figure 1-2. Main window of ESPVI 4.0W.

It should be noted that the pull-down menu names in Figure 1-2, and some of the subsequent figures are shown arranged on two lines. Depending on the computer and the size of the window, the names may appear on one line. Operation of ESPVI 4.0W is the same for both situations.

Part of the approach to making data entry as simple as possible is the data file structure. ESPVI 4.0W saves the data in a series of files. An example of a complete set of files with their internal text is shown in Appendix B. This set, which is the SAMPLE ESP, is for a simple three-section (field) ESP. It is one of the examples supplied with ESPVI 4.0W. The complete set for the SAMPLE ESP consists of SAMPLE.mst; SAMPLE.esp; SAMPLExx.elc; SAMPLE.srt; SAMPLE.gas; and SAMPLE.prt. Note that SAMPLExx.elc is a series of files in which “Electrode Design” stores the electrode data for each section in a separate file numbered sequentially from xx = 01 up to 0n, in which n is the number of sections.

The master file, SAMPLE.mst, contains the names of the other data files that are used for a particular modeling run. In this way, a system of data files can be built up that may operate as a library. The SAMPLE.esp file holds both the physical characteristics of the ESP and its electrical properties. SAMPLExx.elc files contain the "Electrode Design" input data; SAMPLE.srt file contains the "Sneakage/Rapping/Turbulence" input data; SAMPLE.gas file contains the "Gas Properties" input data, and finally SAMPLE.prt file contains the "Particle Properties" input data.

1.5 Data Entry Menus

Referring to the main window, Figure 1-2, click on "File" and then on "Open", which allows viewing of a list of master files of ESPs for which files exist. It may be shown as SAMPLE or SAMPLE.mst depending on the computer and operating system. SAMPLE.mst should be chosen. The word SAMPLE is used here to denote the name of a data set; typically, a data set would be named after the plant where the modeled ESP is located. Please note that the characters in the name can be either upper or lower case. When a master is chosen under "Open", the master file and the five other files are loaded into the program.

Moving on, next click "Data Entry and Editing" and then "Design of ESP", which brings up the "ESP Design for SAMPLE" data entry window shown in Figure 1-3. "ESP Design" is the

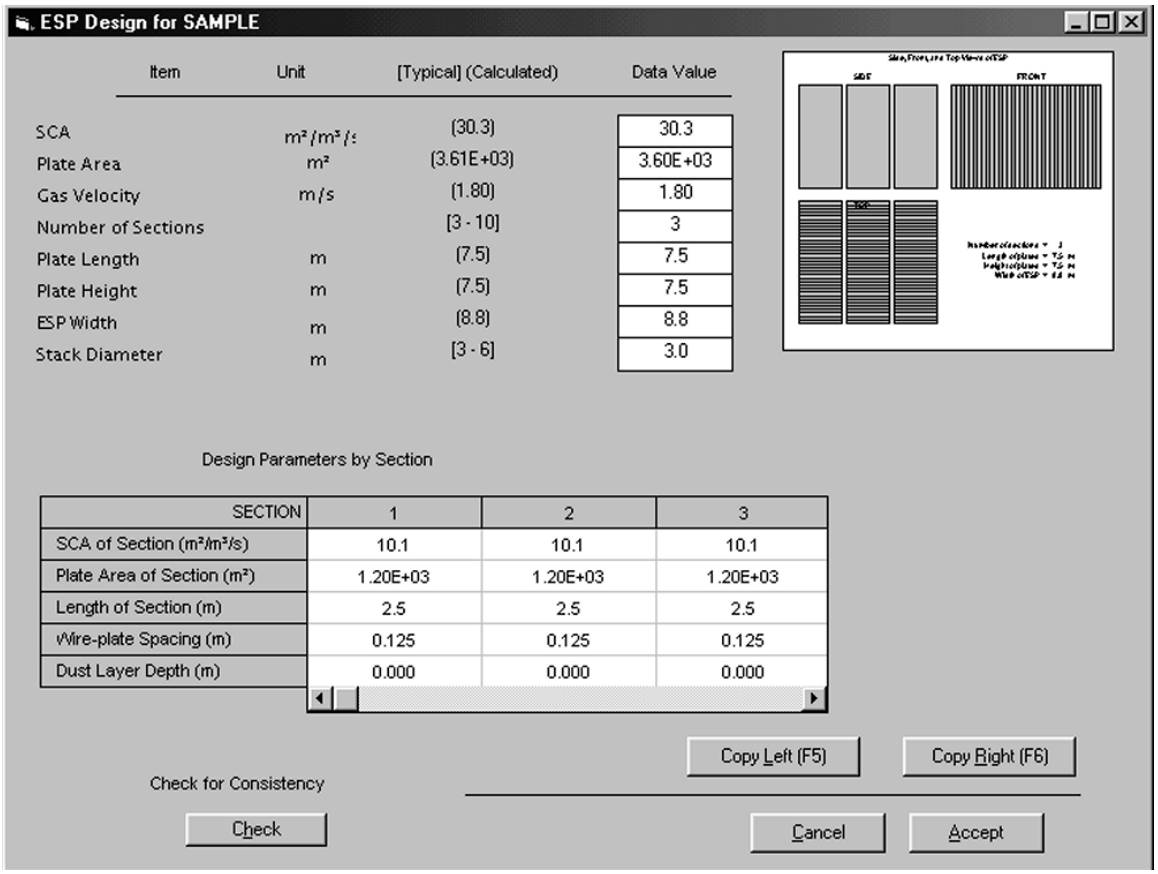

Figure 1-3. "ESP Design" data window.

form for which all of the physical data input for the ESP is entered, with the exception of the electrode data. It also contains the gas velocity. The use of the “ESP Design” data entry form will be discussed in detail in Chapter 2 of this manual.

Next click on “Data Entry and Editing” and then on “Operating Voltages”, which brings up the “Operating Voltages for SAMPLE” data entry window, shown in Figure 1-4. In this data entry form, all of the electrical data for the modeled ESP is entered. It is noted once again that all of the data entered into “ESP Design”, Figure 1-3, and “Operating Voltages”, Figure 1-4, go into the data file with the suffix esp, of which SAMPLE.esp is an example. The use of the “Operating Voltages”, Figure 1-4, data entry window will be discussed in detail in Chapter 3 of this manual.

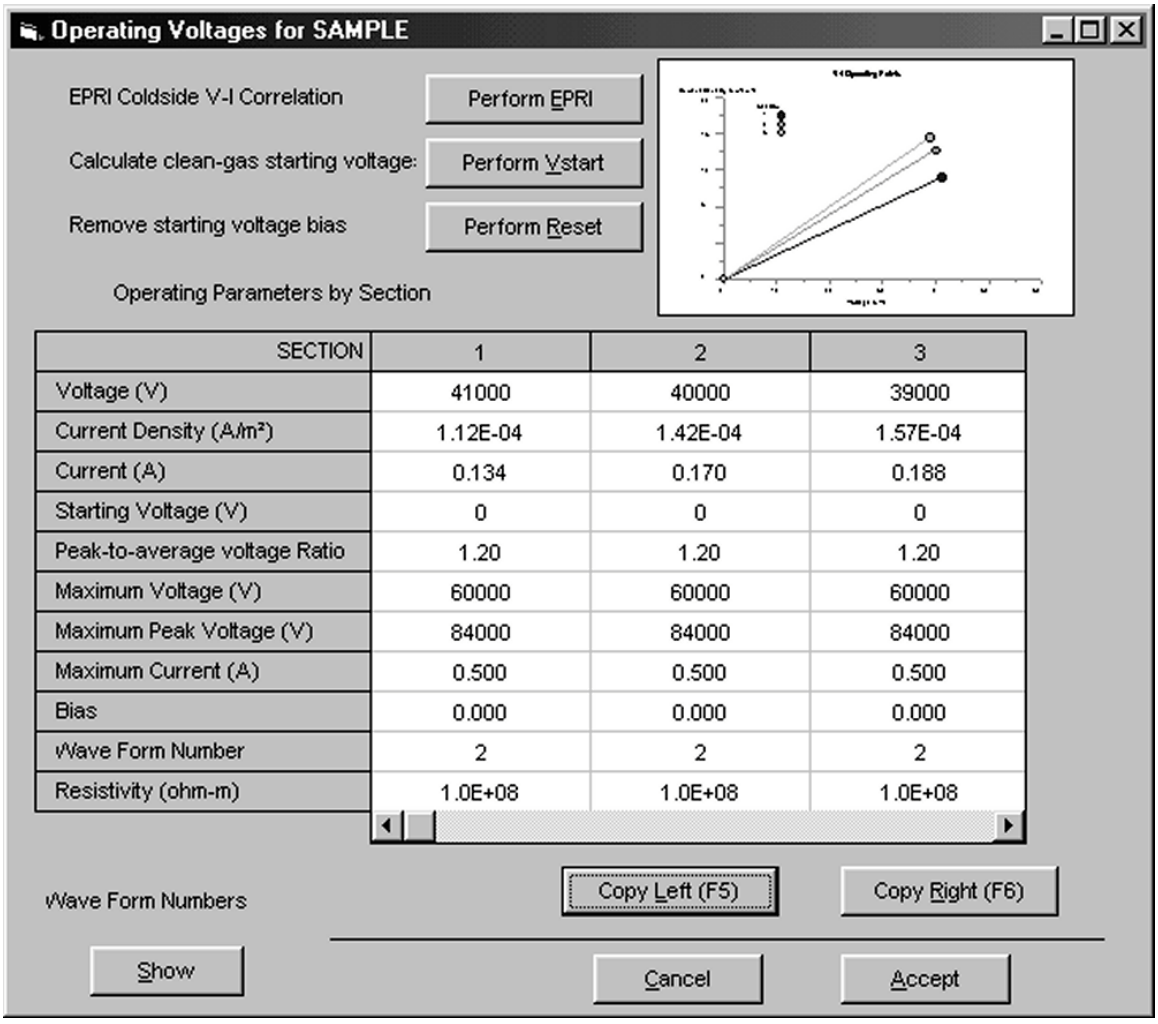

Figure 1-4. “Operating Voltages” data entry window.

The next data entry form to open under “Data Entry and Editing” is “Electrode Design”, which is shown as Figure 1-5. All of the data that pertains to the corona discharge electrode configuration is entered in this form. The use of this data input window is discussed in detail in Chapter 4 of this manual.

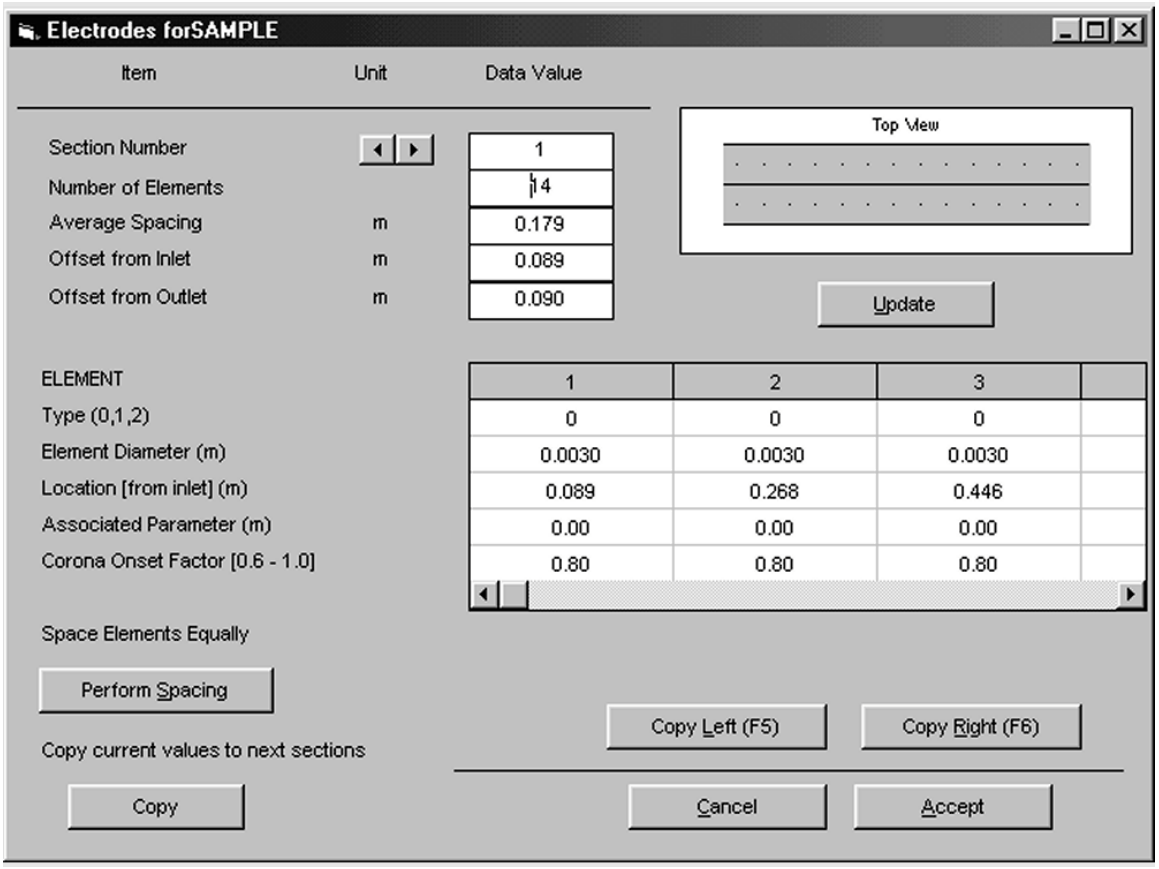

Figure 1-5. “Electrode Design” data entry window.

The “Sneakage/Rapping/Turbulence” window under “Data Entry and Editing” is shown as Figure 1-6. The non-ideal factors which are not definable from first principles and which must consequentially be dealt with empirically are entered into this form window. This data entry form is described in detail in Chapter 4 of this manual.

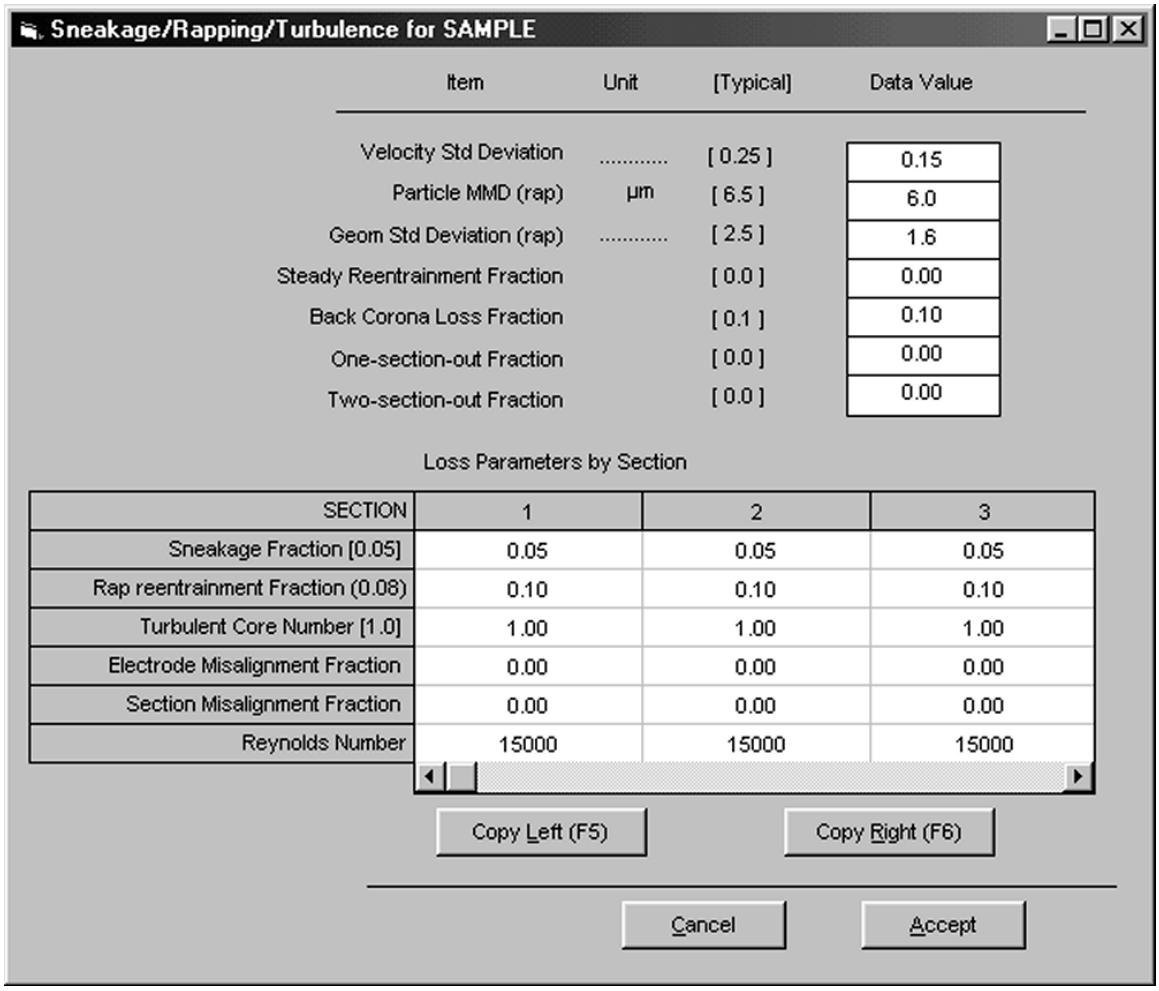

Figure 1-6. “Sneakage/Rapping/Turbulence” data entry window.

In addition, under “Data Entry and Editing”, there is “Gas Properties” window shown in Figure 1-7. All of the gas properties, including temperature, pressure, flow rate, and composition, are entered into this form window. Chapter 5 of this manual explains the use of this window.

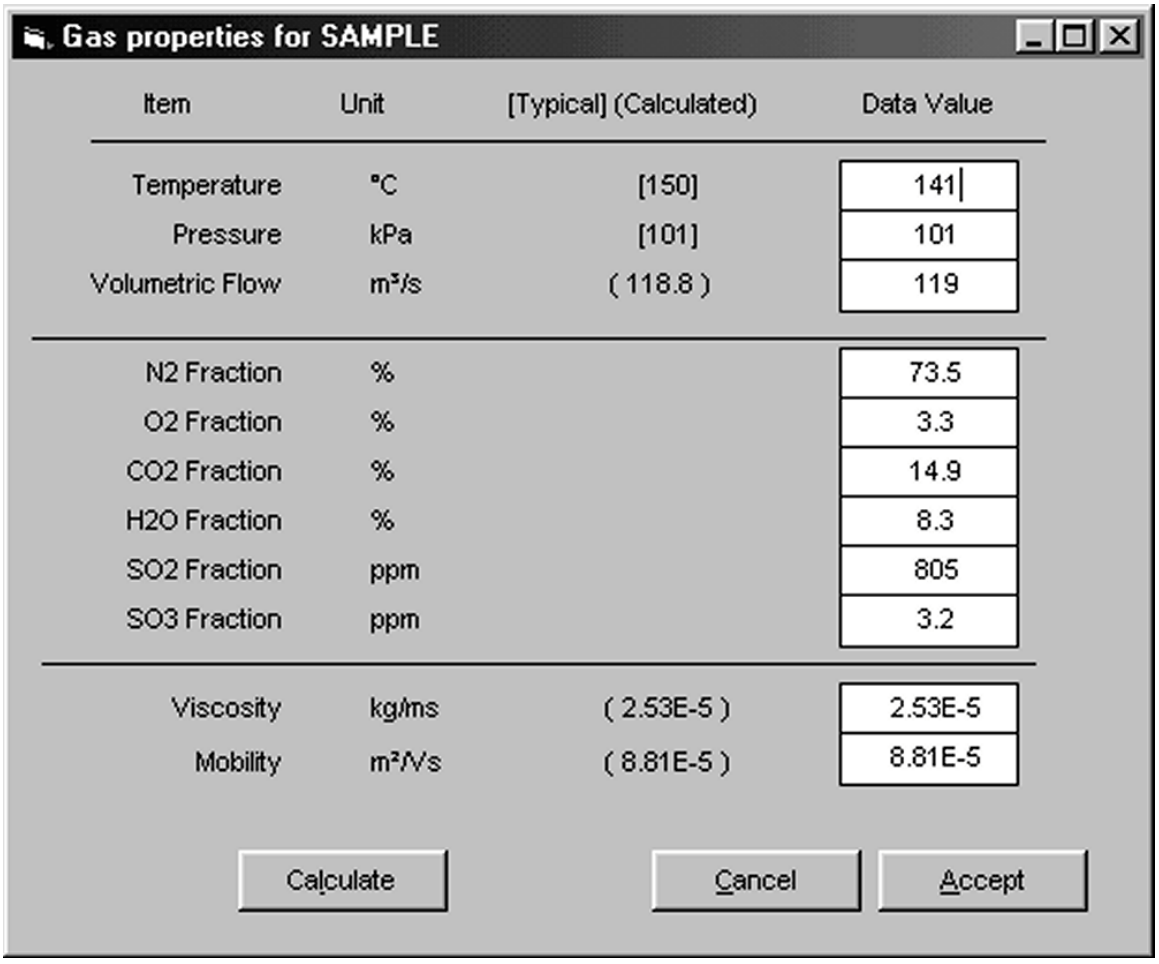

Figure 1-7. “Gas Properties” data entry window.

The last of the data entry window forms under “Data Entry and Editing” on the main window is the “Particle Properties” form shown as Figure 1-8. Particle properties are entered onto this form, which is discussed in Chapter 6.

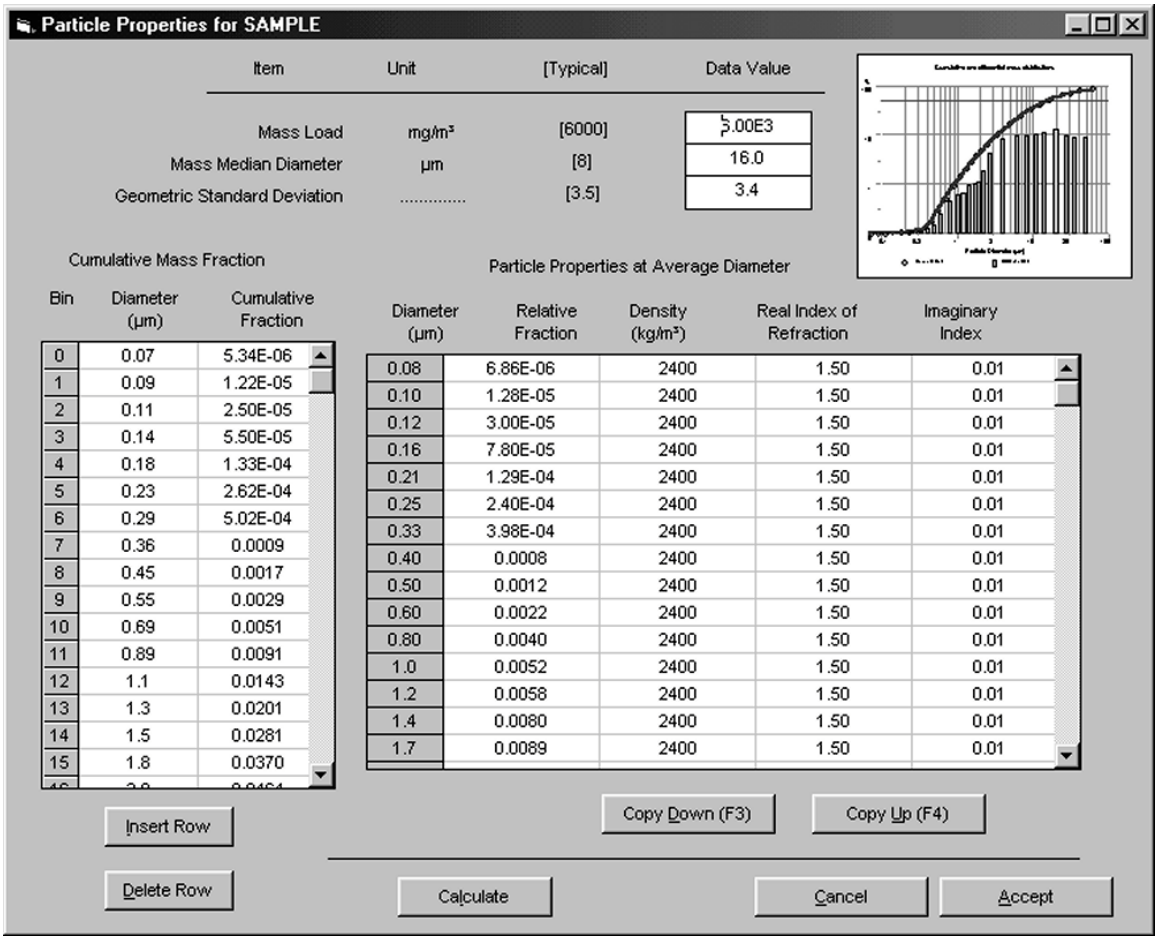

Figure 1-8. “Particle Properties” data entry window.

The operating philosophy of the program is that the various input window forms can be used to modify the ESP data, thereby allowing the effects of the changes to be evaluated by ESPVI 4.0W. Any number of changes can be made and the effects noted. However, changes made to the input forms do not become permanent until the files are saved. Saving of files can be done at any time by clicking “Save” under “File” on the main window. When exiting the program, ESPVI 4.0W will inquire if the files are to be saved. If the files are not saved, the original input data will remain in the files.

To model a new ESP, it is necessary to develop a set of files specific to that unit. With ESPVI 4.0W there are two ways to do this. The first is to click on “File” on the main window and then on “New”. ESPVI 4.0W asks for a name that it assigns to the copies of a file named @DEFAULT. Accordingly, a set of the @DEFAULT files must be in the directory in which ESPVI 4.0W is creating the new set of files. The newly created files will be @DEFAULT with its new name. At that point the data inputs of the new set of ESP files are configured as

desired, and then saved. The second approach is to open one of the existing ESP files and make the necessary changes that define the new ESP. Then, under "File", click **Save As** and provide a name. With either approach, the results are a set of files for the new ESP. The original set of ESP files that were the basis for the new ESP remains in place. One problem with the second approach is the possibility of overwriting the original set of files if "Save" is used instead of "Save As". "Save" simply overwrites the existing file with the current values, but "Save As" creates a new file with a new name. To prevent overwriting an existing file, the first approach is probably the safest.

All the files loaded or saved for a specific ESP by the program must be in one location on the disk. To avoid the mixing of files of different ESPs it may be desirable to set up a folder for each one. The "Save As" feature allows this to be done.

For a particular ESP configuration it is often desirable to try changing some of the input parameters, such as particle properties, that would result from use of different coals. To do this, it is necessary to change the appropriate input data and then use "Save As" under "File" with a new name. This creates a new file set while retaining the original file set.

1.6 Calculation Menus

On the main window, Figure 1-2, are two pull-down menus "Calculate V-I Curve" and "Performance Calc". These two pull-down menus contain the menu items that command ESPVI 4.0W to go through its various computations once the appropriate data has been entered into the menu items under "Data Entry and Editing". These two pull-down menus will be discussed briefly in this chapter and in greater detail in subsequent chapters of the manual.

The "Calculate V-I Curve" menu items make use of the various inputs under "Data Entry and Editing" that affect the voltage and current for an ESP. These include electrode configuration and particle and gas properties. For the inputs, it finds solutions to Poisson's equation. For the two menu items **Automatic V-I** and **Fixed V-I**, ESPVI 4.0W starts at the corona onset point where the current is zero. ESPVI 4.0W increases the voltage by a small amount and computes the current. This process continues until, at some point, ESPVI 4.0W stops the upward voltage step process. The difference between **Automatic V-I** and **Fixed V-I** is the criteria that they use for controlling the point at which ESPVI 4.0W stops the upward steps.

The **Elemental V-I (Graphical)** under the "Calculate V-I Curve" pull-down menu presents a graph for each ESP section and provides the voltage current characteristics for each of the electrode elements. It will be shown later as being useful for observing the effects of decreasing space charge while going through the ESP and also for helping evaluate the effects of different electrodes and the onset of reverse ionization.

The **Calculation Options** on the "Calculate V-I Curve" pull-down menu allows changing some of the criteria that affect the operation of the **Automatic V-I** and **Fixed V-I**, including where they stop their voltage steps and the characteristics of the steps. Other criteria for

Automatic V-I and **Fixed V-I** are the result of various entries that were made under “Data Entry and Editing”.

Display Operating Points reproduces the electrical conditions that were entered as **Operating Voltages** under “Data Entry and Editing”. It allows the entries to be viewed but not changed. To change the entries it is necessary to go back to **Operating Voltages**.

“Performance Calc” on the main window, Figure 1-2, contains the menu items that, with the electrical conditions computed by the “Calculate V-I Curve” or by entering unique electrical conditions, provides the ESP performance. In general, this command causes the calculation by the Deutsch equation of the electrical integration velocity and collection.

The first menu item on the “Performance Calc” pull down menu is the **Standard Method**. It uses the electrical conditions in **Operating Voltages** under “Data Entry and Editing”. **Adjust Peak Factor**, **Adjust Offset Factor**, **Adjust Particle Distribution**, **Compute Maldistribution**, and **Adjust Ion Mobility** cause an adjustment to some other parameter before ESPVI 4.0W makes its performance calculation. It is used as a means for helping ESPVI 4.0W match its results to the actual ESP.

Chapter 2
Relationship of Electrostatic Precipitation to the ESPVI 4.0W

This chapter describes the process of an electric field production in an ESP, effect of charged particles on this field, migration of charged particles in an electric field, and their collection in an ESP. Further, this chapter discusses electrostatic precipitation theory and presents a related operation of the ESPVI 4.0W. Physical dimensions of the ESP and their role on model performance as well as the effect of changes to ESP configuration are considered below.

2.1 Production of an Electric Field to Create Corona and Ions

Investigations into the physics of ionization date back to the middle of the 19th century and are still ongoing. For simplicity, because of the ease of creating analytical solutions, some of the following refers to historical work as applied to wire/tube forms of ESP, although the same arguments apply to wire/plate forms of ESP.

The earliest investigations were concerned with developing voltage current relationships of corona discharge and the effects of different means of electrical energization. In 1862, Gaugain, working with concentric cylinders, found that for a given outer diameter electrode, the electrical breakdown voltage was primarily dependent on the radius of the central emitter electrode.

Roentgen, in 1878, working with point/plane electrodes, found that a certain voltage had to be applied to initiate a corona current flow. This corona onset voltage was dependent on the sharpness of the point, gas pressure, and polarity of the point electrode.

The next significant finding can be attributed to work carried out by Townsend in 1915. He noted that the appearance of the corona discharge with negative ionization of the discharge element was very different from when the electrode was positively energized. In the case of negative energization, the corona appears as bright flares, which tend to move across the surface of the electrode. With positive energization, the corona appears as a diffuse glow surrounding the electrode. Other differences found were that, with negative energization, the corona had a distinctive hissing sound, and the corona initiation voltage was lower and the breakdown potential higher than those of the positively charged corona.

When ESPs are used for gaseous applications, ions are produced by high voltage electric input. Figure 2-1 indicates a typical electric field distribution across the inter-electrode area, between a small diameter emitter and a much larger passive electrode.

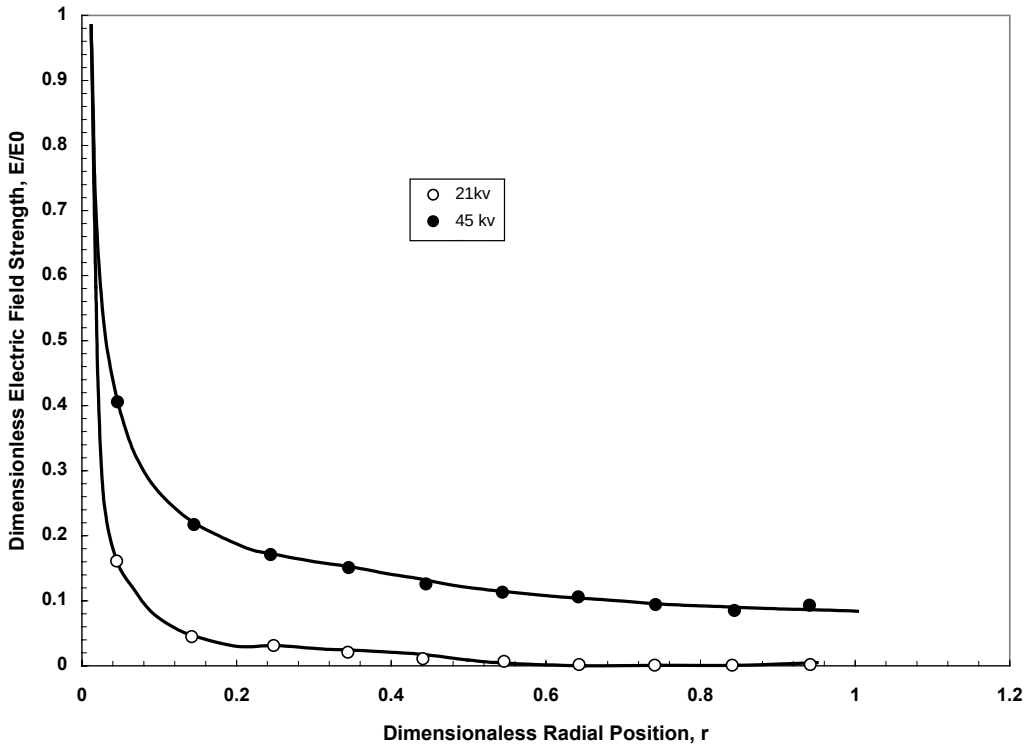

Figure 2-1. Relative field strength between the electrodes for a tubular ESP arrangement.

From the curve it is obvious that the electric field adjacent to the emitter is extremely high. It is this electrical stress that increases with higher applied voltage until it reaches a level that excites any free electrons in the immediate vicinity and causes corona to form. These fast moving electrons acquire sufficient energy to collide with gas molecules and produce further free electrons and positive ions. Townsend, working in this area, proposed the concept of a chain reaction or electron avalanche. In this mechanism, each new electron produced by ionization generates new electrons in ever increasing numbers.

In practice, with a negatively energized system, as the electrons rapidly move across the field area they collide with, and attach themselves to, gaseous molecules to produce negative ions. Any positive ions are attracted towards the discharge element and, upon reaching the element, take no further part in the process.

There is an abundance of free electrons adjacent to the discharge element. However, the number of free electrons decreases as the distance from the element increases, and there is a corresponding increase in the number of negative ions. Within a relatively short (compared to the distance to the collector electrode) distance from the corona discharge electrode, the free electrons disappear and are completely replaced by the ions.

Negative corona is a feature of gases that exhibit appreciable electron attachment and is, therefore, sensitive to gas composition and temperature. The corona can range from virtually zero to being a highly stable discharge, depending on operating characteristics. As indicated earlier, the visual appearance of negative corona takes the form of tufts, which look like

bright glow points. These glow points are characterized as intermittent, or Trichel pulses, which, on a plain smooth emitter, rapidly move about. The number of tufts and their luminescence increases as the energizing voltage is raised, producing a higher corona current discharge.

2.2 Charging of the Particles by the Ions

For industrial ESPs, in which negative ionization is used because of its lower corona initiation voltage and higher breakdown potential, particle charging occurs in the area between the active plasma region and the passive electrode surface. This area contains a high space charge having neutral molecules, negative ions, plus some free electrons, all moving towards the passive electrode because of the electric field.

As the gas borne particles enter the space charge region of the field, two charging mechanisms occur: (1) by ion attachment, that is to say field or impact charging, and (2) by ion diffusion charging. Field or impact charging predominates for particles greater than about 0.8 to 1 μm. Diffusion charging is essential for particles less than 0.2 μm diameter. Both processes occur in the intermediate size range but neither dominates.

Field charging requires the presence of an electric field to drive the free mobile charge carriers, whereas the diffusion process is based on randomly moving gas ions. The gas ions arise through temperature effects as described by the kinetic theory of gases (Brownian motion). The field charging level for a particle of a specific size that is subject to an electric field of specific intensity achieves a specific saturation charge in a finite length of time. On the other hand, the diffusion charging level that a particle achieves never does achieve a saturation charge. Instead, it reaches some level of charge, dependent on the electric field, above which further increases become less probable. For practical purposes, this level may be considered a sort of saturation charge.

Classical charging theory provides the saturation charge, **q**, for field charging as given in Equation 2.1 below:

$$\mathbf{q = 3\ \pi\ \varepsilon_o\ d^2\ E} \qquad 2.1$$

where **d** is the particle diameter, $\boldsymbol{\varepsilon_o}$ is the permittivity of free space, and **E** is the electric field.

Diffusion charging, **Q**, is given by Equation 2.2 below:

$$\mathbf{Q = \tfrac{1}{2}\ d\ K\ T/e^2} \qquad 2.2$$

where **d** is the diameter, **K** is the Boltzmann constant, **T** is the absolute temperature, and **e** is the electronic charge. Equation 2.2 is somewhat simplistic in that it does not consider a full set of electric field effects. These are considered in the more advanced particle charge relationships that have been developed.

The significance of Equation 2.1 is that the saturation charge of a particle is proportional to the electrical field and to the square of its size; that is to say, the larger the electric field, the greater the charge. In practice, it is the peak electric field that is dominant. The higher the peak electric field, the greater is the charge that the particle ultimately attains.

As mentioned before, a particle subject to diffusion charging never does achieve its saturation charge. Therefore, Equation 2.2 can be considered the charge that a diffusion charging process achieves. The level of charge that a particle subject to diffusion charge achieves is proportional to the electric field.

Over the years, a great deal of analytical work has been carried out to define the relationships that include both diffusion and field charging. This includes work by Cochet (1961), by Smith and McDonald (1976), and by others. The significance of Cochet's work was in bridging the region between diffusion and field charging in which neither dominates. Later, Smith and McDonald more rigorously and precisely improved the analytical understanding of the continuum between the two charging regimes. Their work provided a relationship that covered the complete range of particle sizes. It set the stage for including the full size spectrum for particle charging in ESP modeling.

The important step in particle charging, which set the stage for rapid ESP modeling and is especially important in respect to ESPVI 4.0W, is the work by Lawless (1996). In this work, an analytical model was formulated that gave good agreement with both unipolar and bipolar charging data. Furthermore, it achieved this along with continuum charging between diffusion and field charging. The Lawless charging model is used within ESPVI 4.0W to provide both unipolar and bipolar charging.

The presence of reverse ionization, or back corona, as discussed later in this manual, gives rise to positive ions in the gas stream. Positive ions, in turn, modify the charge on the particles. The ESPVI 4.0W computes both the amount of diffusion charge and field charge that each particle size acquires. Bipolar charging is also included to allow ESPVI 4.0W to consider the effects of back ionization when necessary.

ESPVI 4.0W divides the particle size spectrum for an ESP (0.07-70.0 μm), which is in the form of a log-normal distribution, into 27 discrete size fractions. For each size fraction, ESPVI 4.0W computes both the diffusion and the field charge levels. Because time is a factor for both charging mechanisms, ESPVI 4.0W considers it, as it relates to the velocity of the gases through the ESP, in computing the level of charge. This means that the further the particle travels into the ESP, the higher is the level of charge that it acquires, up to its maximum level.

In the particle size range from about 0.2 to about 0.8 μm in which neither field nor diffusion charging mechanisms dominate, both processes work on the particles and contribute to their total charge. The Brownian motion of the particles below about 0.2 μm assists in their collection, although they acquire relatively low levels of charge. Particles above the submicron size acquire relatively large levels of charge, which makes their capture and collection relatively effective. Particles in this intermediate submicron size range do not have

sufficient Brownian motion nor do they acquire sufficiently high levels of charge to provide effective capture. Consequently, they are the most difficult size of particles to capture and collect by the electrostatic precipitation process. In a well performing ESP, these submicron particles can form a significant portion of the total PM that passes through the device.

It can be shown that, with good electrical conditions, most field charged particles reach around 90 percent of their full saturation charge in less than 0.1 s; the diffusion charging of the particles can take longer depending on the abundance of negative ions that are present. Hence, it can be assumed that, on entering a precipitation field having a typical exposure/treatment time of 3 to 5 s, the particles achieve their maximum charge.

2.3 Effect of the Charged Particles on the Electric Field

Charged particles entering the electric field within an ESP have the effect of modifying the electric field. For this discussion, the term charged particles, includes electrons, ions and actual particles that have an electric charge on them. Each charged particle has its own electric field. A volume containing a cloud of charged particles, which is called the space charge, has an electric field that is contributed to by the individual particles. The electron component makes only a very small contribution to the space charge because they either travel very rapidly out of the cloud or, more likely, give up their charge to a gas molecule to form an ion. The majority of the ions travel quite rapidly out of the charged particle cloud to the collecting surface, thereby making a small but significant contribution to the space charge. A small percentage of the ions in an ESP transfer their charge to the particles, which tend to drift more slowly out of the electric field. The lower mobility of the charged dust particles causes them to make the largest contribution to the space charge within an ESP.

The effect of space charge is to weaken the electric field near the corona discharge electrodes, thereby suppressing some of the corona and its generation of ions. It essentially accomplishes this by raising the corona onset voltage, $\mathbf{V_c}$, as shown by Equation 2.3 below:

$$\mathbf{V_c = V + \psi\,(\rho)} \qquad 2.3$$

Where $\boldsymbol{\psi\,(\rho)}$ is a function of the space charge, $\boldsymbol{\rho}$, that elevates the corona onset voltage, **V,** to a new voltage level, $\mathbf{V_c}$. If it increases the corona onset up to the level of the applied voltage, it can essentially shut down the corona.

Going back to Figure 1-1, which depicted basic parallel plate ESP arrangement, as the particles enter the ion cloud formed by the first discharge electrode, they start to acquire charge. These charged particles add to the space charge. The effect of the increased space charge is to decrease the corona current. As the particles travel through the ESP and are removed by the collection process, the space charge and the corona suppression decrease.

In a well operating ESP, the voltage and currents change when going from inlet to outlet sections. The voltage starts at some high level in the first section and decreases, section by section. The current, which is lowest in the first section, increases in each of the following ESP sections. Typical V-I curves are shown as Figure 2-2 for a well operating typical ESP.

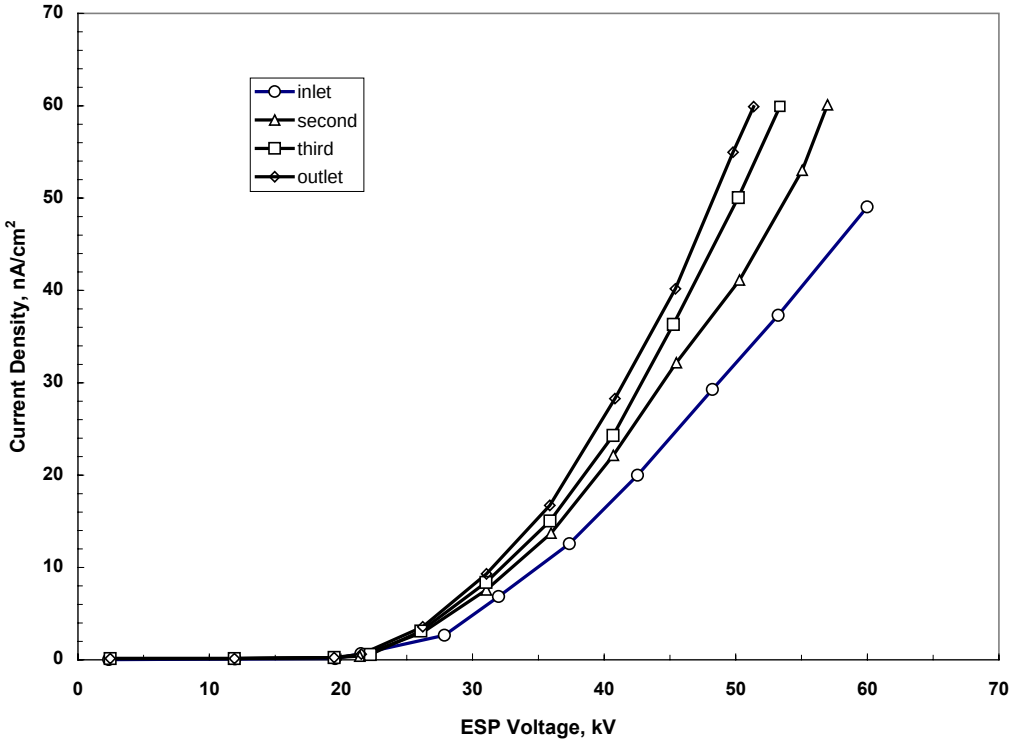

Figure 2-2. Voltage current curves for a well operating ESP showing the effects of space charge corona suppression.

The space charge effect and its consequences will be discussed in detail in Chapter 6.

The ESPVI 4.0W does, from first principles, find solutions for Poisson's equation for different ESP configurations and operating conditions. It accurately computes the space charge and the resultant corona suppression from inlet to outlet as the particles are charged and collected. The voltage current data generated by ESPVI 4.0W shows the effect of decreasing space charge corona suppression in going from inlet to outlet of the ESP being modeled. If the ESP that is being modeled does not show the same decreasing space charge corona suppression, it is an indication that some problem may exist in the unit. The effects of particles on the operation of the ESP will be considered in detail later.

2.4 Migration of Charged Particles through the Electric Field

Migration velocity, **W**, is the velocity that a charged particle achieves in a quiescent gas. It is a balance between the coulombic (or electrical), viscous, and inertial forces, which leads to Equation 2.4 below:

$$\mathbf{W = (QE)/(3\,\pi\,d\,\eta)\,[1 - \exp\{-3\,\pi\,d\,\eta\,t\}/m]} \qquad 2.4$$

where **Q** is particle charge, **E** is electric field, **d** is the particle diameter, **η** is the viscosity, **t** is the time, and **m** is the particle mass. The numerator **QE** is the electrical force acting on the

particle. Its denominator, $\mathbf{3 \pi d \eta}$, is the resisting viscous force. The exponential, time dependent inertial force, is generally of short duration, which does eventually go to zero, leaving the migration velocity in its steady state form, which is the terminal velocity. However, until it goes to zero, it must be considered since it does affect collection. Once it does go to zero, Equation 2.4 becomes the terminal velocity that the particle ultimately achieves.

For rigorous accuracy, the Cunningham slip correction to Stokes law for the smaller particles must be applied to the ratio of the coulombic to the viscous force. The Cunningham slip correction factor, whose value is significant for very small particles, essentially goes to zero for particles in the micron range and larger.

ESPVI 4.0W does explicitly determine the migration velocity, taking into consideration the decrease of the inertial force with time. It also applies the correct particle-size-dependent Cunningham slip factor.

From Equations 2.1 and 2.4, once it has achieved its steady state form, Equation 2.5 can be derived as:

$$\mathbf{W = (\varepsilon_o d E^2)/\eta} \qquad 2.5$$

The significance of this relationship is that, for particles dominated by field charging:

- Theoretically, the limiting field charge on the particle is proportional to the radius squared because the migration velocity of the particle will increase with particle size.
- Since the electric field is proportional to the applied voltage, the migration velocity is proportional to the voltage squared.

These observations suggest, in practical terms, that the larger particles are more easily collected than the smaller ones. The exception is those smaller particles whose charging is dominated by the diffusion process and are generally easily collected because of their inherent Brownian motion. It also suggests that it is desirable for the unit to operate with voltages as high as possible for maximum collection efficiency in an ESP. The particles of those sizes, about 0.2 to 0.8 μm, for which neither diffusion or field charging dominate, will have the lowest migration velocity and which are the most difficult to collect in an ESP.

Figure 2-3, which was generated directly by ESPVI 4.0W, shows the results of its computations of penetration by particle size for an actual ESP. It should be noted that penetration is:

Penetration = 1 - Efficiency

ESPVI 4.0W computes both the diffusion and field charging levels for each particle size increment. In the range from about 0.2 to 0.8 μm where neither diffusion nor field charging dominates the penetration. It should be further noted, as will be seen later, that larger amounts of the sub-micron particles will be collected as changes are made to the ESP to

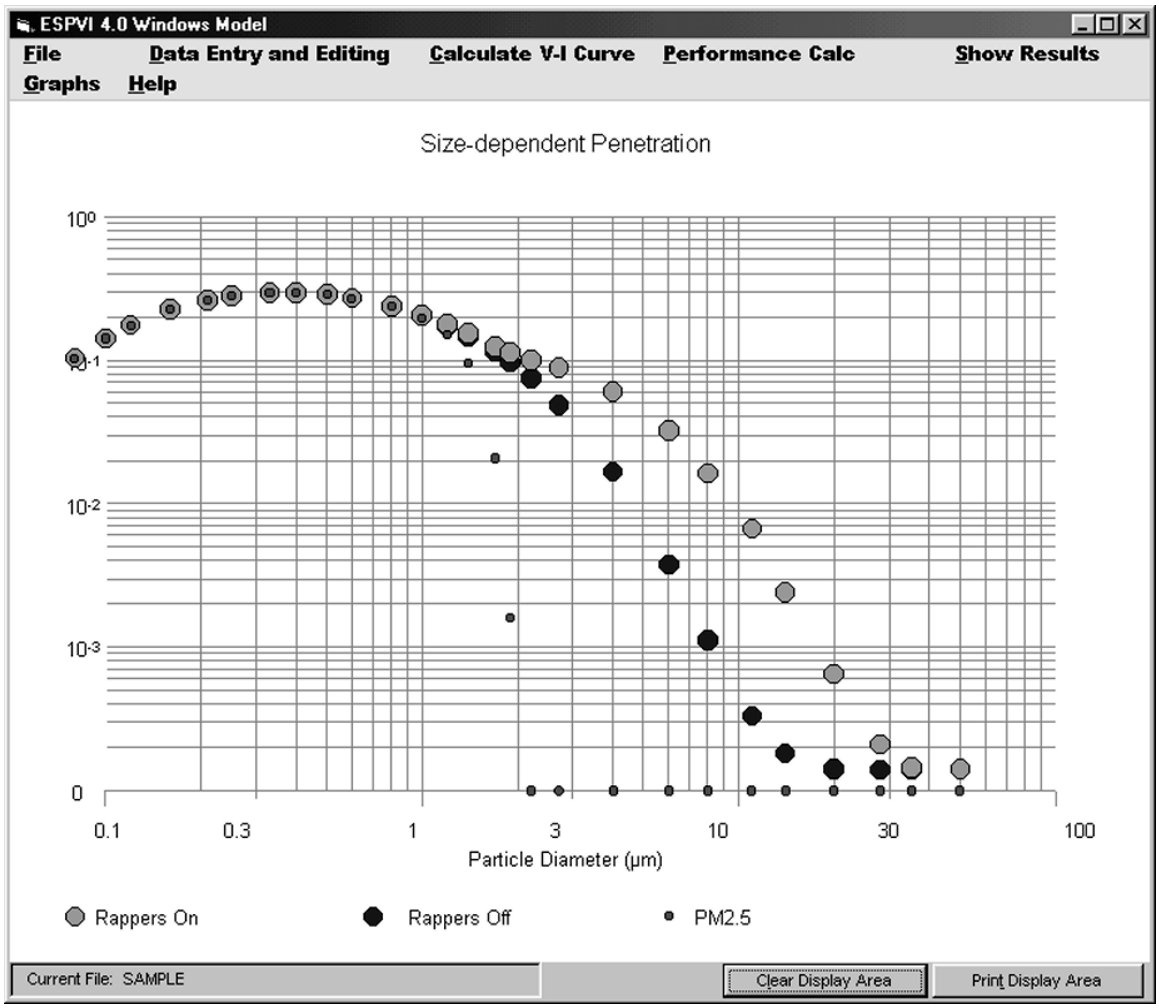

Figure 2-3. Particle penetration by size.

improve its performance. The “Rappers on” and “Rappers off” curves in Figure 2-3 show the contribution that the rapping reentrainment makes to the overall particle penetration. The reentrained particles, as will be seen in Chapter 4, have a mean size of about 6 µm. Once a modeling run is made with ESPVI 4.0W, it is interesting and informative to have it generate the curve equivalent to Figure 2-3 in order to see the effects on collection of the various particle sizes when changing the conditions in the ESP being modeled.

Figure 2-3 shows the rapping emissions compared to the non-rapping emissions. It further shows that the large particles are the most easily collected ones. As the efficiency of the ESP is increased, the effect is to further decrease the penetration of the remaining particles.

It should be noted that, as the collection efficiency of the sub-micron particles is improved, more and more of the remaining dust emissions are the result of rapping reentrainment, especially from of the outlet section. For a high efficiency ESP, it would be expected that up to half of the residual emissions would be due to rapping reentrainment.

From the above discussion, it will be appreciated that the performance of an ESP is dependent on having sufficient current capability to satisfy ion production for charging the particles. In addition, the voltage should be sufficiently high to generate an electric field in order to create the ions and to precipitate the particles.

Although the foregoing portrays the theoretical approach to the migration of charged particles through an electric field, the calculated figures of theoretical migration velocity should not be confused with the "effective migration velocity". The latter is derived from plant efficiency measurements and the specific surface area of the ESP. The "effective migration velocity" derived from measured efficiencies and the specific collection area for the ESP should more realistically be considered as a measure of a precipitation performance factor rather than a measure of the average theoretical particle migration velocity. It is used with the Deutsch equation, or its modified variants, as applied to a total ESP without regard to its configuration and operating conditions.

For a fundamental determination of ESP performance, such as that embodied in ESPVI 4.0W, the Deutsch equation is used in its more scientifically rigorous form. This is done in conjunction with the particle charging migration velocity means discussed earlier.

2.5 Collection of the Charged Particles

Deutsch's derivation (Deutsch, 1922) of his equation for the collection of particles in an ESP was done on a rigorous basis. The equation for the efficiency, E_f, is given by Equation 2.6:

$$E_f = 1 - \exp\left[- (A_0/V_f)\, W\right] \qquad 2.6$$

where A_0 is the area, V_f is the volumetric flow rate of the gas, and W is the migration velocity of the particles. This derivation incorporates several major assumptions:

- The particle concentration is uniform at any cross section of the ESP. This implies turbulent conditions that impart motion to the particles more intense than the migration velocity.
- There is uniform velocity through the ESP except at the boundary layer of the collecting surface, where the flow is laminar.
- The migration velocity in the laminar boundary layer near the collecting surface is a constant for all particles.

Later, White derived the equation by considering the probability that a particle entering the ESP would avoid the laminar layer thereby avoiding capture and penetrating to the outlet. Generally, the flow through all industrial ESPs is turbulent. This fulfills the requirement of the first two major assumptions.

The last of the major assumptions above would be simple if all of the particles were of the same size and the electrical and operating conditions were unchanged from inlet to outlet of the ESP. However, operating industrial ESPs generally collect a mix of particle sizes, which would certainly cause there to be a mixture of migration velocities by what had been seen earlier in this Chapter. In addition, as has been seen, there is a space charge in the ESP that

changes from inlet to outlet, and this space charge, in turn, affects the electrical conditions, thereby further affecting the migration velocity.

The last assumption is implemented in ESPVI 4.0W by the division of the particle distribution spectrum into a number of size increments and the ESP length into a number of short length increments. For each particle size segment and each length increment, the particle charge for both field and diffusion, and hence migration velocities, are calculated and then used in Equation 2.6. It is assumed that each of the particles size segments represents a unique size, and that the migration velocity for each of the length increments represents the local migration velocity.

The collection of the particles by the Deutsch relationship does involve the ESP geometry, especially the collector electrode area. Deutsch also considers the gas flow through the ESP. The first data entry window, "Design of ESP" in the "Data Entry and Editing" pull-down menu, is the first portion of the presentation that considers collector area and gas velocity. Therefore, working with the ESPVI 4.0W can be initiated at this time. It will initially show how the ESP collector areas and spacing are entered and will give gas velocity. At this time the operation of ESPVI 4.0W can be initiated.

2.6 Modeling an ESP with ESPVI 4.0W

For ESP modeling with ESPVI 4.0W, the particle size distribution is divided into 27 narrow size segments which are sufficiently narrow to be treated as one specific size for calculating the total charge and migration velocity. In ESPVI 4.0W, the ESP length is divided into a number of short segments, one for each corona discharge electrode. For each of the length segments, the electrical conditions are computed taking into consideration the electrode size and the space charge caused by all of the particles in its portion of the gas stream. In each length segment, the Deutsch equation is allowed to separately compute the amount of each particle segment that is collected. By this means, the assumption that all particles have the same migration velocity is fulfilled. Finally, at the outlet of the ESP, the quantity for each of the particle size segments that has penetrated is summed together to provide the total penetration.

To start the modeling of an ESP in ESPVI 4.0W, it is necessary to provide the dimensions of the unit as input. Included in such data is the number of sections, height, width, section length, number and width of lanes or passages, gas velocity, and specific collector areas. Data to be entered into the "ESP Design" window form is generally data that is relatively easy to obtain. All of the data asked for should be entered if it is known. ESPVI 4.0W provides the check for the interrelationship between the data. For example, the sum of the individual section areas must equal the total area. Another example is that the gas volume flow must be equal to the gas velocity multiplied by the ESP's height multiplied by its width. If interrelationships such as these are inconsistent, ESPVI 4.0W will not allow the modeling to proceed until the inconsistency is corrected. The modeler may determine all of the correct data values and then enter them into ESPVI 4.0W. A second option is to enter a few of the data values and then allow ESPVI 4.0W to calculate the rest. For the second option, if insufficient data has been provided to allow the remaining data values to be calculated,

additional data values will have to be entered. The best approach is to manually calculate as much of the ESP dimension-related and gas flow data as possible, and then enter them into ESPVI 4.0W. Doing it this way will minimize errors. For illustration purposes, a set of ESP data called SAMPLE has been loaded into the ESPVI 4.0W.

At this point, the set of ESP data that comes with the program, called SAMPLE, should be loaded. To load SAMPLE, go to the "File" pull-down menu on the main window, Figure 1-2, and choose **Open** to allow SAMPLE to be opened. To start entering data, go to the main window (Figure 1-2) and first click on "Data Entry and Editing" and then on "ESP Design", which comes up on the screen as shown in Figure 1-3.

The last entry under the "Data Entry and Editing" pull-down menu is labeled "SI". This allows switching the units in ESPVI 4.0W between metric and non-metric system. If ESPVI 4.0W is initially opened in Russian, only the metric system can be used. If the program is opened in English, "SI" will allow switching between metric and non-metric units.

Open the "ESP Design" window, which provides much of the dimensional information that describes SAMPLE ESP. This window is shown here as Figure 2-4. As the various text box

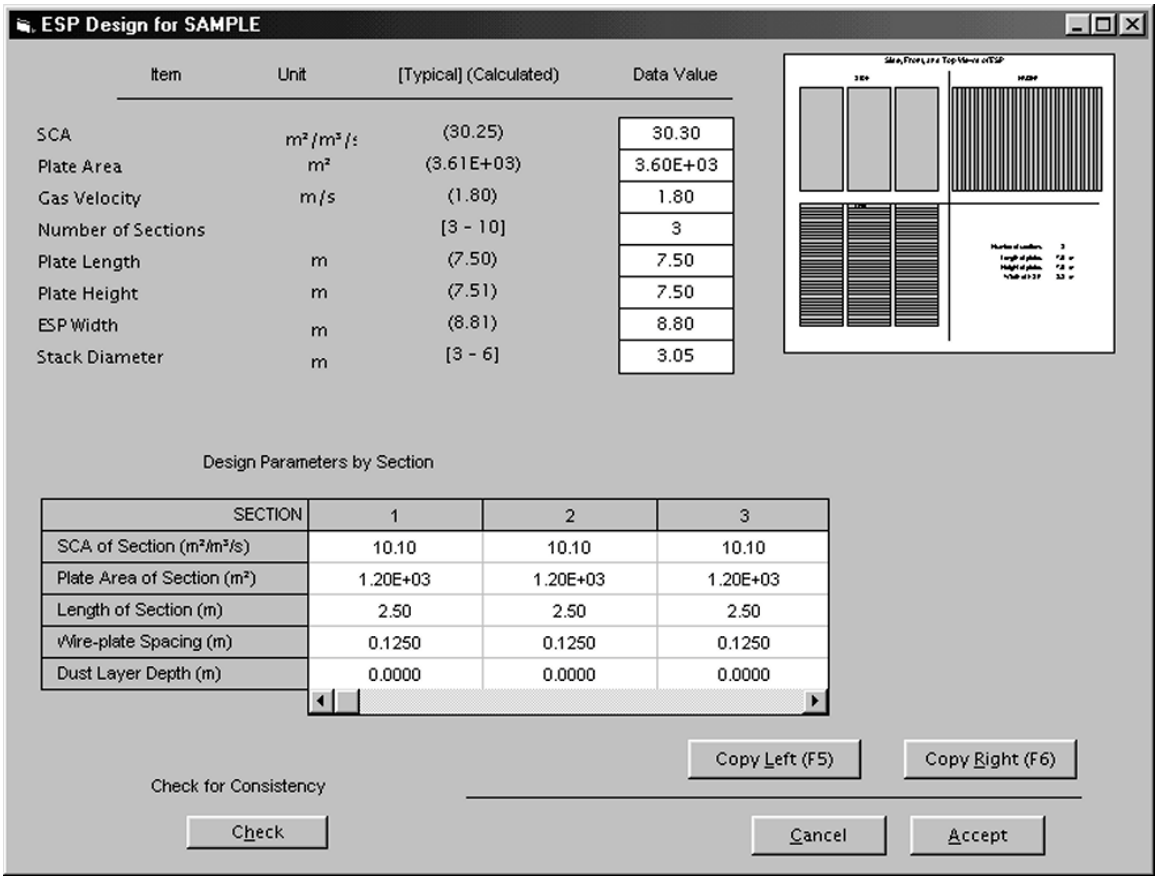

Figure 2-4. "ESP Design" window for SAMPLE ESP.

inputs and commands are discussed, reference can be made to Figure 2-4 and to SAMPLE in the computer.

The “ESP Design” window is divided into two areas. The text boxes in the upper portion are for data representative of the total ESP. The text boxes in the lower portion are for data that is entered by section. As an added feature, the upper right-hand of the window contains an image that shows a top, side, and frontal views of the ESP being modeled. This image and those on other data input windows under the “Data Entry and Editing” pull-down menus are shown in larger scale in the “Graphs” pull down menu.

When describing the design of an ESP, the practice of dividing a total ESP into separate, parallel chambers that are essentially independent of each other should be kept in mind. Using values of gas volume flow, plate areas, and other parameters specific to that chamber, ESPVI 4.0W can be used to describe a single chamber. Using the total gas volume flow, total plate area, total currents, along with the average voltages for each electrical section, ESPVI 4.0W can also model the entire ESP. When reading an ESP specification, it is important to discern whether it is being applied to one chamber or to the whole ESP. Data inputs for the total ESP will be considered first.

SCA (specific collector area) on the total ESP part of “ESP Design” is the total collector electrode area divided by the gas volume flow rate. The calculated value is computed in just that way, using the current value of total plate area and the gas volume flow. The SI units for this variable are square meters per cubic meters per second, or seconds per meter, and typical values will fall between 20 for a very small ESP to 200 or more for a very large ESP. Generally, the larger the SCA, the more efficient the collection will be, but many other factors enter the performance. Strictly speaking, SCA is a derived quantity that is completely determined by plate area and volume flow. In practice, it is so widely used to describe an ESP that it is included as a separate variable. If either the total collector area or the gas volume flow is changed, so will the calculated SCA value change.

Plate Area on the “ESP Design” window form is the total area of the grounded collector electrode surface area or plates. For ESPVI 4.0W, the surface area is the surface parallel to the direction of flow. If any portion is not parallel, it is taken as the projected area that is parallel to the direction of flow. The area of any stiffeners or baffles should not be counted as collecting surface, although some dust will be collected there. A simple way for calculating the total plate area is to first calculate the plate area of the sections and then sum them to provide the total. The sectional area is equal to two times the height times the section length times the number of lanes or passages. If the SCA is known, multiplying it by the gas volume flow will equal the total plate area. Plate area can vary over a very wide range, so there are no typical values for it.

Gas Velocity on the “ESP Design” window form is the rate at which the gas stream is traveling through the ESP. This parameter generally falls between 1 and 2 m/s. Some cases are encountered that are either higher or lower. Many high efficiency ESPs are designed for a velocity of 1.5 m/s or less. At higher velocities, reentrainment may increase. The calculated value of velocity is computed here by dividing the gas volume flow by the product of height

and width of the ESPs (cross-sectional area). The width is the distance between the centerlines of the two outside grounded collector electrodes or plates. Occasionally the term "active cross section area" is encountered in practice, which is the height times the number of the facial opening to the passages. The active cross sectional area should not be used unless it is actually equal to the ESP's height times width. The value of gas velocity plays a critical role in ESPVI 4.0W and should be as accurate as possible. In Chapter 5, which deals with the ESP's gas characteristics, the total flow volume is provided as input data. ESPVI 4.0W calculates the cross sectional area, then multiplies it by the gas velocity, and compares it to the total flow volume. If there is an inconsistency, ESPVI 4.0W will not allow the modeling to proceed until it is corrected.

The **Number of Sections** on the "ESP Design" window form in an ESP is typically between 3 and 10 in the direction of gas flow. Often a section is referred to as a field. "Section" refers to electrical sectionalization, which is a portion of the ESP that has all corona discharge electrodes operating at the same voltage. In this model, the assumption is that the gas flow is well mixed between sections. It is assumed that rapping is confined to one section at a time. If there are two or more electrical sections within one rapping section, the number of sections is set equal to the number of rapping sections. This also means that an average voltage for the section would be used along with the sum of the currents for the two electrical sections. An electrical section may span two rapping sections for some ESPs. This situation is difficult to set up in ESPVI 4.0W. In the absence of accurate rapping data for the two rapping sections, they should be treated as one electrical section and one rapping section. If there is accurate rapping data, it may be treated as two electrical sections and two rapping sections.

Plate Length on the "ESP Design" window form is the total length of the plates in the direction of flow. It is assumed for this input parameter that the individual sectional lengths are placed end-to-end without counting the space that is normally between them. This value will typically be between 6 and 20 m, usually at 2 to 5 m per section. The overall length can be entered manually, or ESPVI 4.0W will calculate it if enough other data is available to take advantage of the interrelationships present in the ESP. The calculated value is the sum of the sectional lengths. Note that the total external length of an ESP will usually be longer than this value because of the space that is located between sections for maintenance access. Only the sum of the actual plate lengths should be used.

Plate Height on the "ESP Design" window form is the vertical dimension of the grounded collector electrodes or plates. The plate height is usually 6 to 15 m. The plate height can be entered manually, or ESPVI 4.0W will calculate it if possible. The calculated value is computed from the gas volume flow, gas face velocity, and width of the ESP. ESP performance is not known to depend on plate height, but sneakage should, in practice, be less for taller plates because the non-electrified zones on top and bottom are less in comparison to the electrified zones. Rapping reentrainment might be greater with taller plates, because the longer distance for ash to fall provides more opportunity for reentrainment.

ESP Width on the "ESP Design" window form is the distance between the centerlines of the two outside grounded collector electrodes or plates. The ESP width can either be entered manually, or ESPVI 4.0W can try to calculate it if sufficient other data has been entered.

Stack Diameter on the "ESP Design" window form is the internal diameter of the smokestack where a transmissometer or opacity meter would be placed. ESPVI 4.0W does compute stack opacity using the stack diameter for the path length. ESPVI 4.0W's opacity computations make use of real and imaginary indices of refraction that are appropriate for many coal fly ashes. These values are entered on the "Particle Properties" window form, Figure 1-8. If different values are desired, they should be entered in that location. If there is no interest in having ESPVI 4.0W compute opacity, the stack diameter can be ignored.

The **SCA of Section** on the "ESP Design" window form is the specific collector area of the individual section. It is the grounded collector area of the section divided by the gas volume flow. SCA values typically range from about 8 to 40 s/m or more. The total SCA is the sum of the individual section SCAs.

The **Plate Area of Section** on the "ESP Design" window form is the area of the grounded collector electrode surface area or plates area of the section. To determine a section's plate area, go to **Plate Area** in the total ESP section above, in the window for specific instructions. The total plate area is the sum of the section areas.

The **Length of Section** on the "ESP Design" window form is the length of the particular section of the ESP from inlet to outlet. A typical value for this variable is 2 to 5 m. The usual practice is to maintain certain height to length ratios, which means the taller the height, the longer the section length. The total plate length is the combined length of the individual sections, assuming that there is no space between them.

The **Wire-plate Spacing** on the "ESP Design" window form assumes that the corona-generating site is located on the centerline between the grounded collector electrodes or plates. Therefore, the **Wire-plate Spacing** is one-half the distance between the collector electrodes and is entered in meters. Typical collector spacing ranges from about 225 mm in older ESPs to as much as 450 mm in some of the newer units. The collecting plates of some ESPs are pocketed for improved collection performance and rigidity. In this case, the **Wire-plate Spacing** is the distance from the centerline to the surface of the collector directly under the discharge electrode. If the corona discharge site is not on the centerline, the discharge electrode is treated differently, as will be seen in a subsequent chapter of the manual.

Dust Layer Depth on the "ESP Design" window form is the thickness of the collected dust layer. It is used to modify the corona onset voltage, which is a function of the wire-plate separation. In addition, the voltage drop in the dust layer is also computed. The dust layer voltage drop affects the electric field in the wire-plate gap. Generally, there is little effect until the layer is 2 or 3 mm thick and the resistivity is above 1×10^9 ohm-m. When back corona is detected, the voltage drop across the layer is held fixed at the value of the breakdown voltage.

There are several command buttons on the on the "ESP Design" window form. Two on the lower right hand side, which are labeled **Copy Left** and **Copy Right**, are used with the sectional input data portion of the window. These command buttons allow data that is entered

for one section to be copied to the other sections. For example if an SCA value is entered for the input section of the ESP and the same value is desired for the other sections, click on the **Copy Right** button. Alternatively, the SCA data for the other sections could be entered manually for each of them.

Three other command buttons along the very bottom of the "ESP Design" window form are labeled **Check**, **Cancel**, and **Accept**. The **Check** button **Checks for Consistency** of the data that has been entered to the window form. If there are inconsistencies, small windows will appear that provide options for correcting the inconsistencies. In accepting the option, ESPVI4.0W should not be allowed to change an input that is known to be correct. Only data that is known to be incorrect should be allowed to change. It is recommended that, before data is entered to ESPVI 4.0W, that the various inputs be determined with a calculator to make certain that correct choices are made when going through the **Check for Consistency**.

The **Accept** command button closes the "ESP Design" window with its current data contents so that the modeling can proceed. ESPVI 4.0W will not allow the modeling calculation to proceed if there are data inconsistencies. Clicking on **Accept** only allows the calculations to proceed with the window's current contents. It does not save the contents, which, if desired, must be done by means of "Save", which is under "File" in the main window. Clicking on the **Cancel** command button closes the window and restores the data entries last saved.

2.7 Performance Calculation by the Standard Method

Once the SAMPLE files have been loaded, go to the "Performance Calc" pull-down menu in the main window, Figure 1-2, and choose **Standard Method**. There are several calculation choices, but **Standard Method** will be used for the present. The other calculation choices will be studied later in this program. **Standard Method** allows the voltage that has been entered to find a solution to Poisson's equation for the ESP parameters that have been set. Figure 2-5 shows the first set of results for **Standard Method**.

Some interesting observations can be made from Figure 2-5, which shows some of the computed conditions for the three sections of SAMPLE. The middle column, which lists the voltages, has to its immediate right the calculated average current density in nanoamperes (1×10^{-9} A) per square centimeter. The next column lists the average current densities that were entered. It is noted that they differ. If SAMPLE was an actual ESP and if all of the data were entered precisely and represented that ESP, then it would be expected that the two sets of currents would generally agree with each other. Other columns list the sectional and

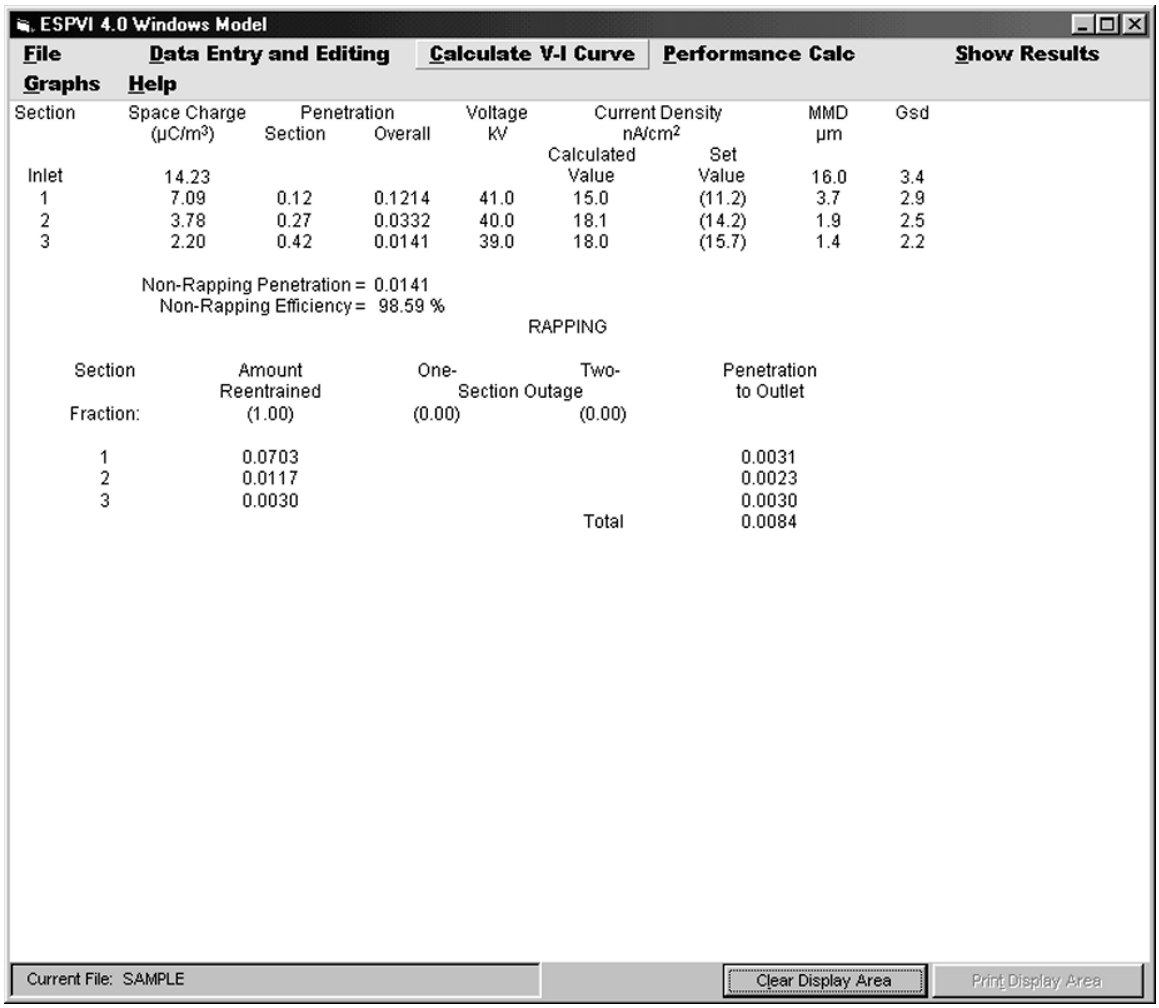

Figure 2-5. Results of computation by standard method for SAMPLE.

overall particle penetration, not including rapping reentrainment. At the right hand side is the inlet and outlet particle size distribution in terms of lognormal mass mean diameter and geometric standard deviation, again not including rapping reentrainment. The inlet and outlet particle size distribution clearly shows that the larger particles are easily captured and that the ones that penetrate are the sub-micron sizes.

2.8 Review of Results

Once the performance calculations are completed, the next step is to review the results. This is done with the “Show Results” pull-down menu, which is located in the main window, Figure 1-2.

The first item on the ”Show Results” menu is **All Results,** which provides all of the output results of any computational run. It opens with a screen that shows the performance of the

ESP for that computational run. The subsequent screens are brought up by means of a small window with two command buttons, **Continue** and **Cancel**.

The second item on the "Show Results" pull-down menu is **Main Results,** which provides the initial overall view of the ESP's performance of **All Results** and which is shown as Figure 2-6.

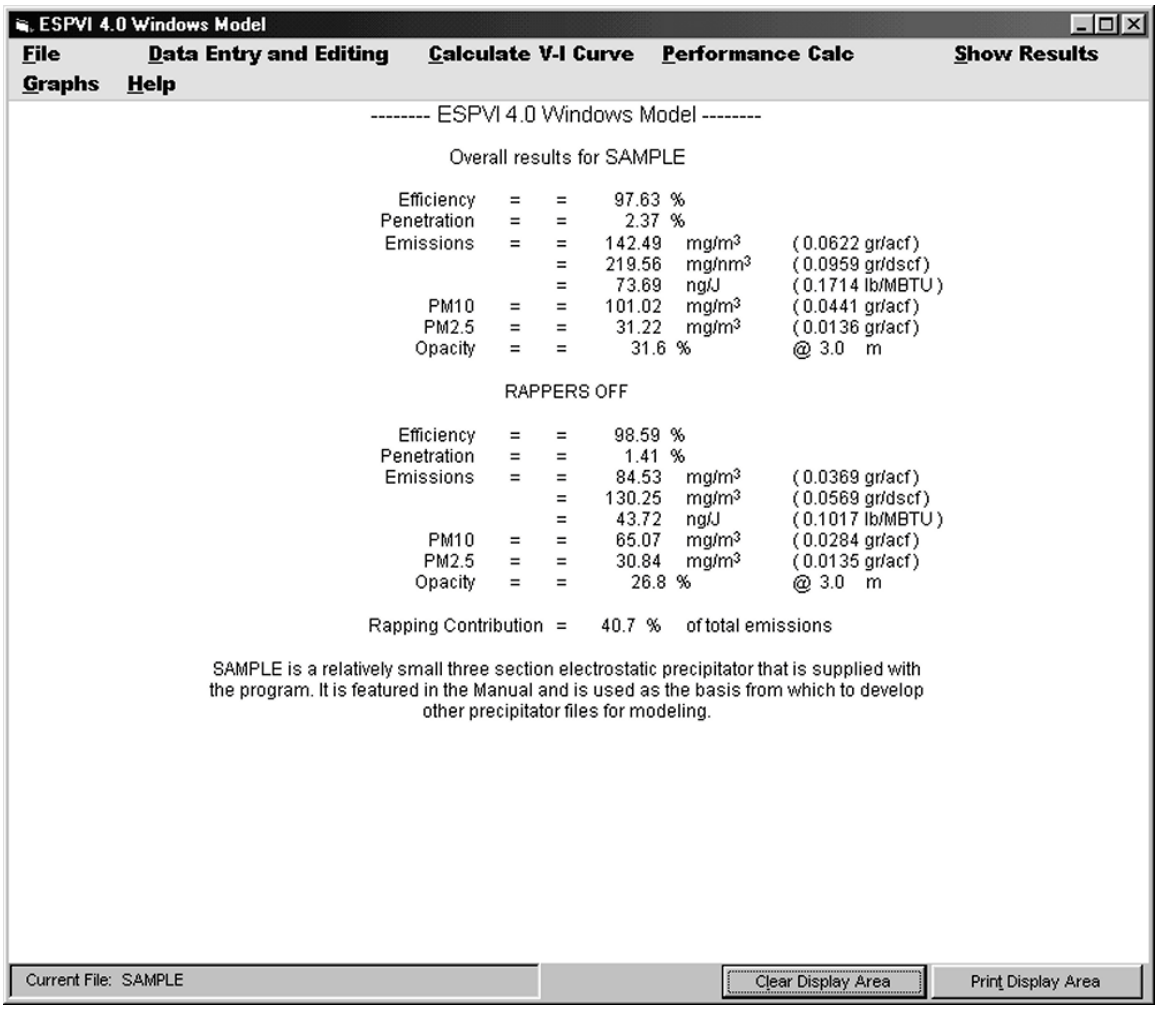

Figure 2-6. "Main Results" for the SAMPLE ESP.

The remaining items on the "Show Results" pull-down menu**—Section Parameters, Electrode Descriptions, Nonideal Factors, Particle Properties, and Size-dependent Penetration—**are the individual outputs that can be viewed in sequence in **All Results**

2.9 Graphs

The “Graphs” pull-down menu on the main window, Figure 1-2, provides a number of images including layout plans and graphs. The first on the pull-down menu is “Plan Views of ESP”. Assuming SAMPLE has been opened in ESPVI 4.0W, choosing “Graphs” provides the plan of SAMPLE shown in Figure 2-7, which provides side, top, and front views. The primary purpose for this ESP plan view is to provide an extra means for checking how accurately the ESP data were entered.

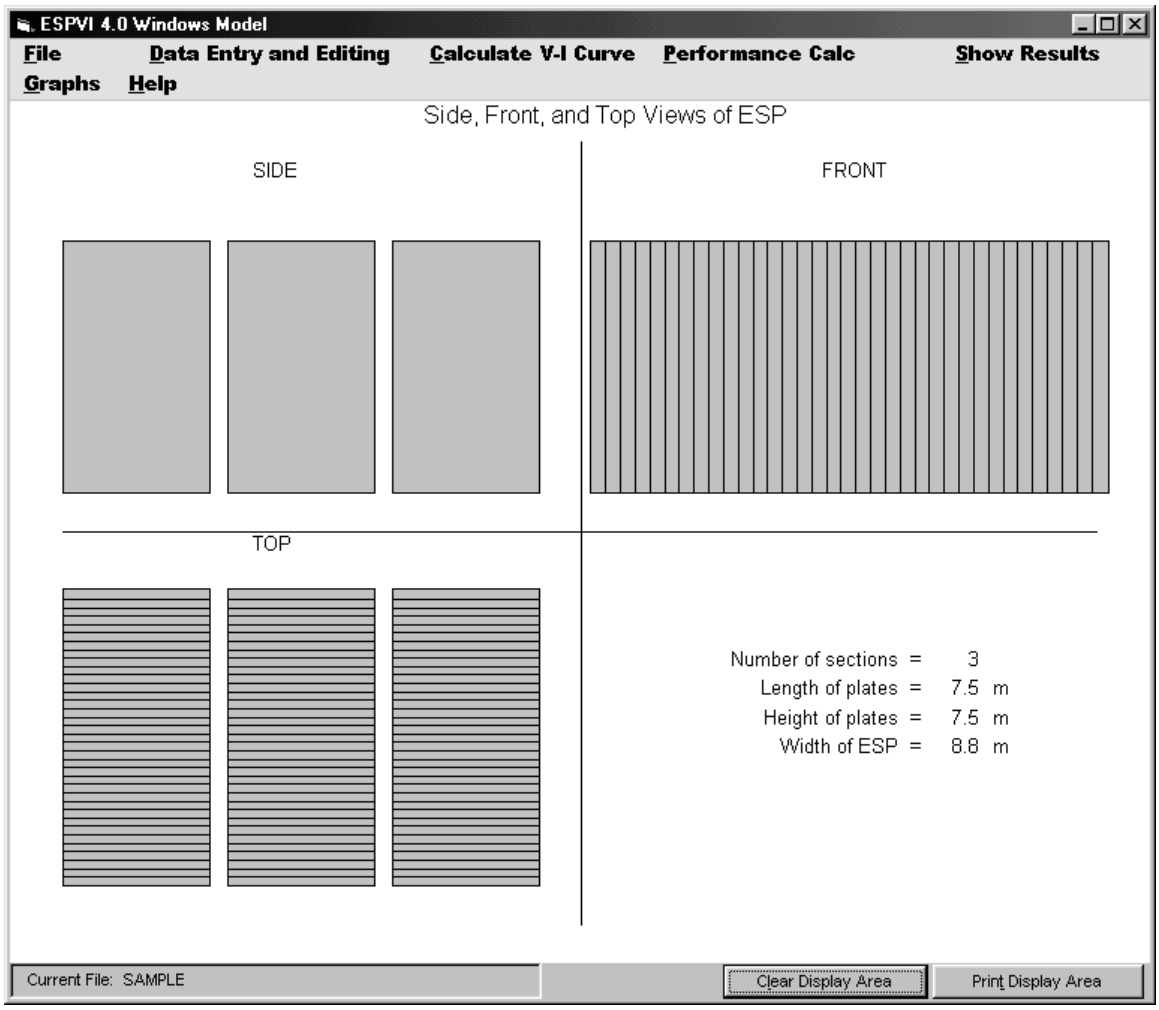

Figure 2-7. “Plan Views of ESP” for SAMPLE ESP.

The second item is “V-I Operating Points”, which can appear in three differing forms, one of which is shown as Figure 2-8. The graph in Figure 2-8 provides the corona onset and the electrical operating points for each of SAMPLE’s three sections. The line between the corona onset and operating point shows their connection and is not the actual voltage current curve. The one in Figure 2-8 is for normal operation with space charge causing an increase in the corona onset voltages. It will be seen in Chapter 3 of this manual that if the **Perform Vstart** command button is used in the “Operating Voltages” window, the three corona onset voltages would be set for clean gas operation with no space charge. With no space charge, the three corona onset points would all be the same. The third possibility would occur before “Standard Method” or other computational operation was performed. In that case, the three corona onset points would be at zero volts.

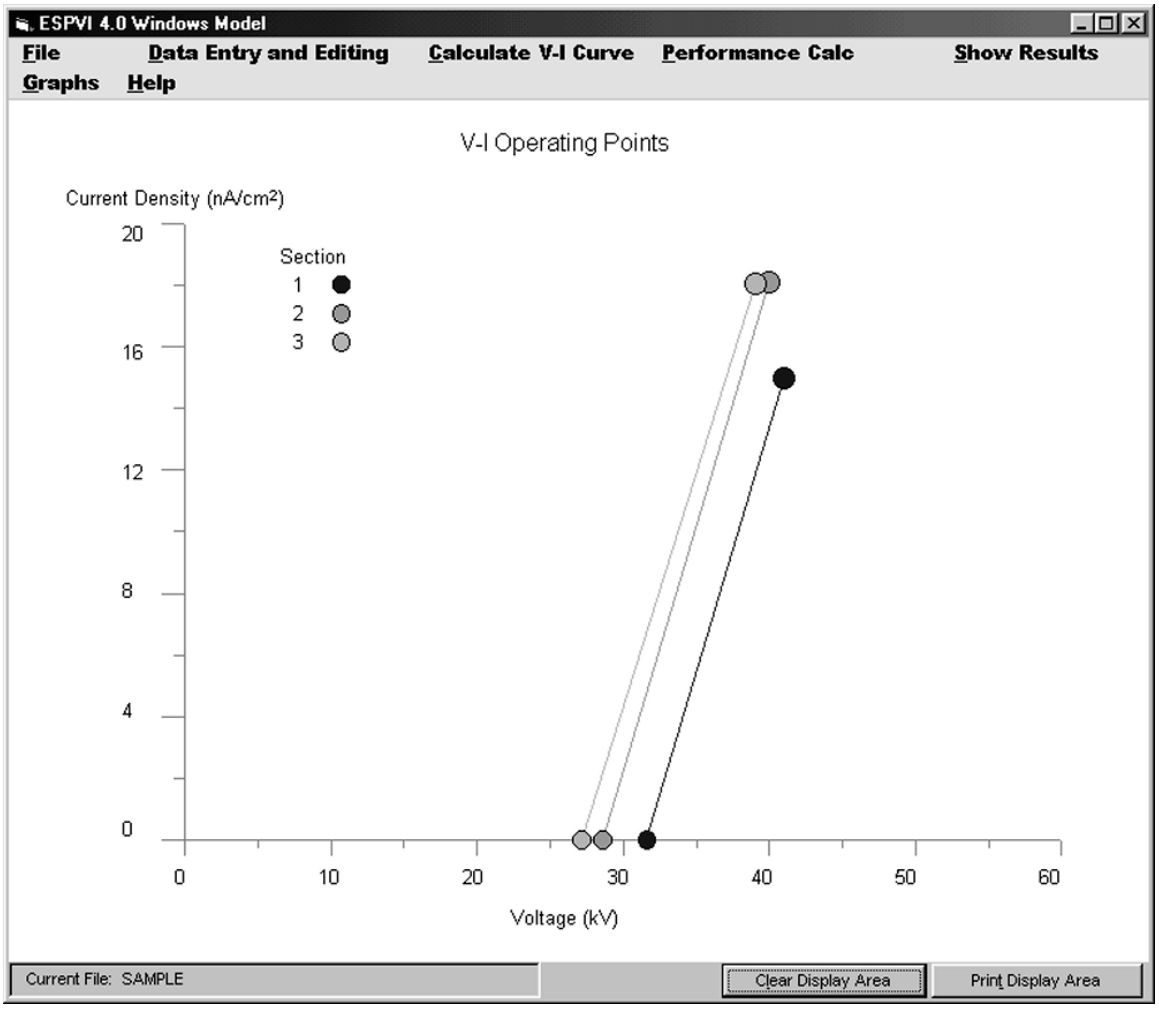

Figure 2-8. “V-I Operating Points” for SAMPLE ESP.

"Electrode Arrangements", as shown in Figure 2-9, is essentially an enlarged version of the top view of the ESP from "Plan Views of ESP" with the electrodes visible. The visibility of the electrodes in the graphical display is a function of their diameter, which makes them difficult at times to see clearly in the representation for some electrode properties.

Figure 2-9. "Electrode Arrangements" for SAMPLE ESP.

The “Inlet Particle Distribution” of Figure 2-10, shows the plot of the histogram cumulative and differential particle size distribution data from “Particle Properties”, which was shown in Figure 1-8.

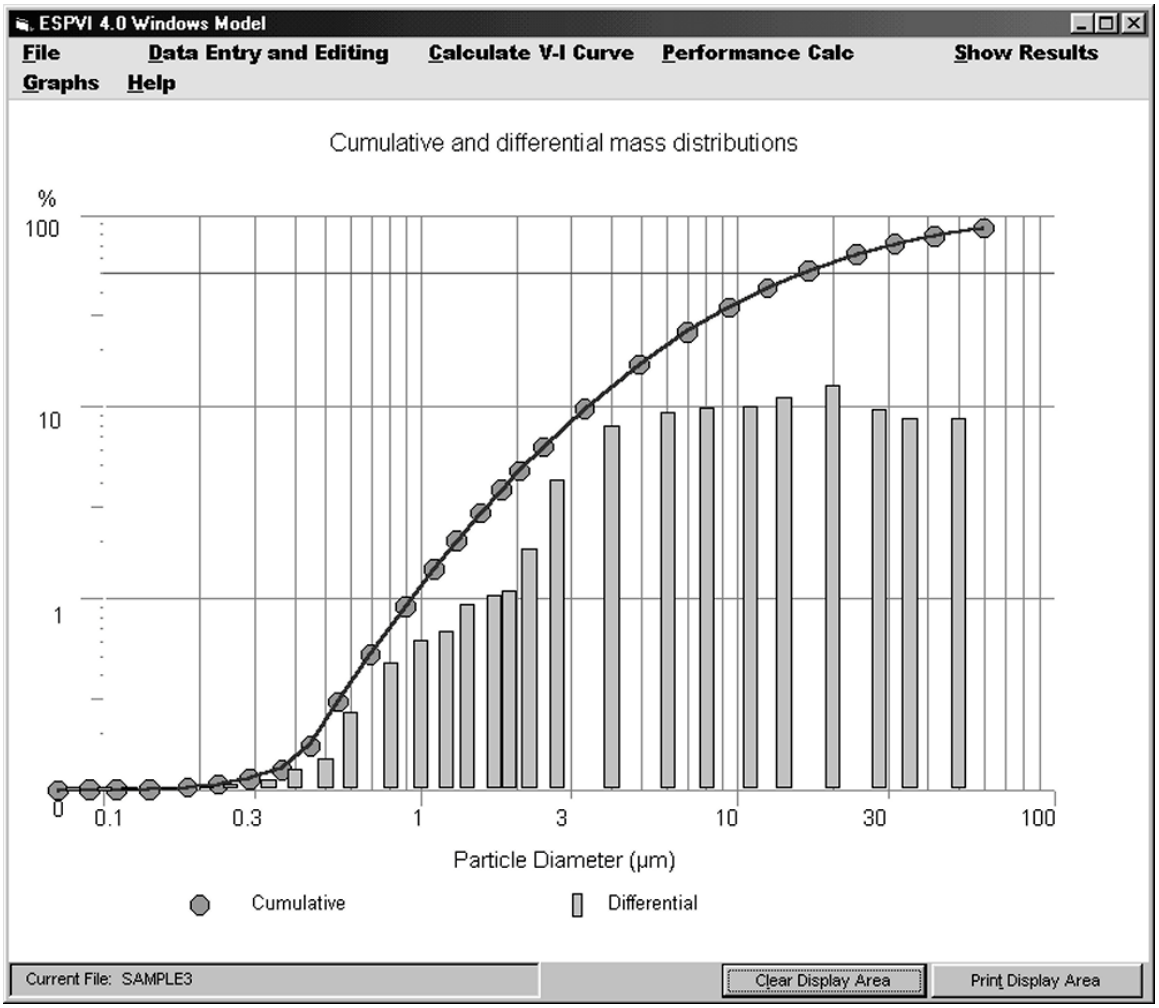

Figure 2-10. “Inlet Particle Distribution” for SAMPLE ESP.

The next item under “Graphs” is the “Differential Particle Distributions” shown as Figure 2-11. This graph qualitatively shows both inlet and outlet data by mass and by number of particles. For the inlet, the dominant mass of particles is with the larger ones, but the greatest number is among the smaller ones. This shows clearly that the great number of fine particles has a very large effect on the formation of the space charge in an ESP although they might individually have little mass.

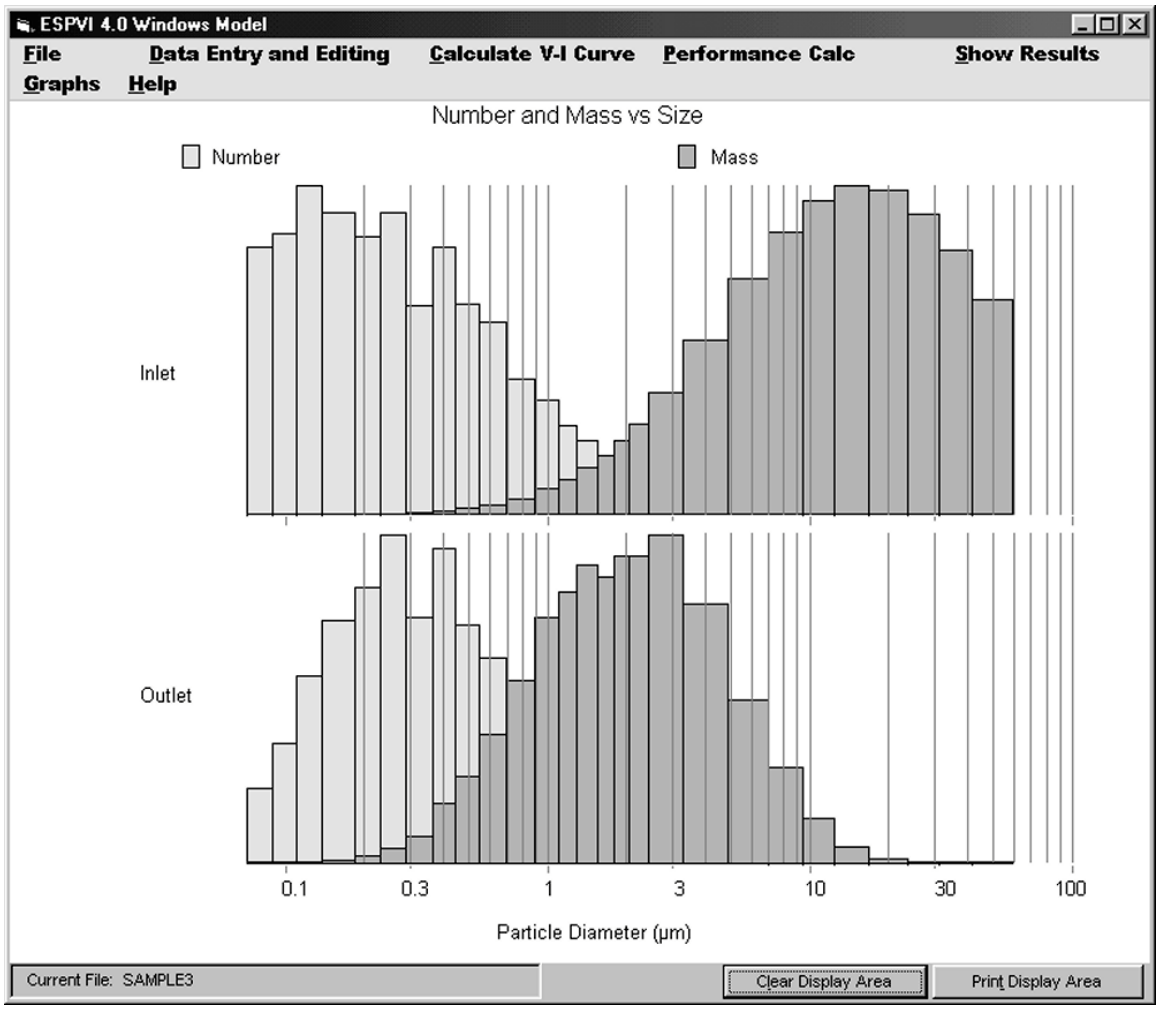

Figure 2-11. “Differential Particle Distribution” for SAMPLE ESP.

The final graph under “Graphs” is “Wave Forms by Section”. The wave form for the first section or field of SAMPLE, which is operating with full-wave energization, is shown in Figure 2-12. The two arrow buttons at the bottom of the window can access the remaining sections. The energization for SAMPLE is a full wave whose rectified half-waves are seen as faint dotted lines. The 25.2 kV interrupted line is the minimum or corona onset voltage. The interrupted horizontal line (41.0 kV) above it is the average or panel-meter reading. The energization from the transformer rectifier (TR) set provides charge to the electrical capacitance of the ESP section. Between these peaks, the voltage decreases as the charge is drained off by the corona current. Wave form is discussed in greater detail in Chapter 3 of this manual.

At this point, three examples will be worked on that make use of the inputs to “ESP Design”. These will include changes to SAMPLE’s height and gas velocity as well as the addition of a fourth section (field). Other changes should be also experimented with using procedures similar to those used in these examples.

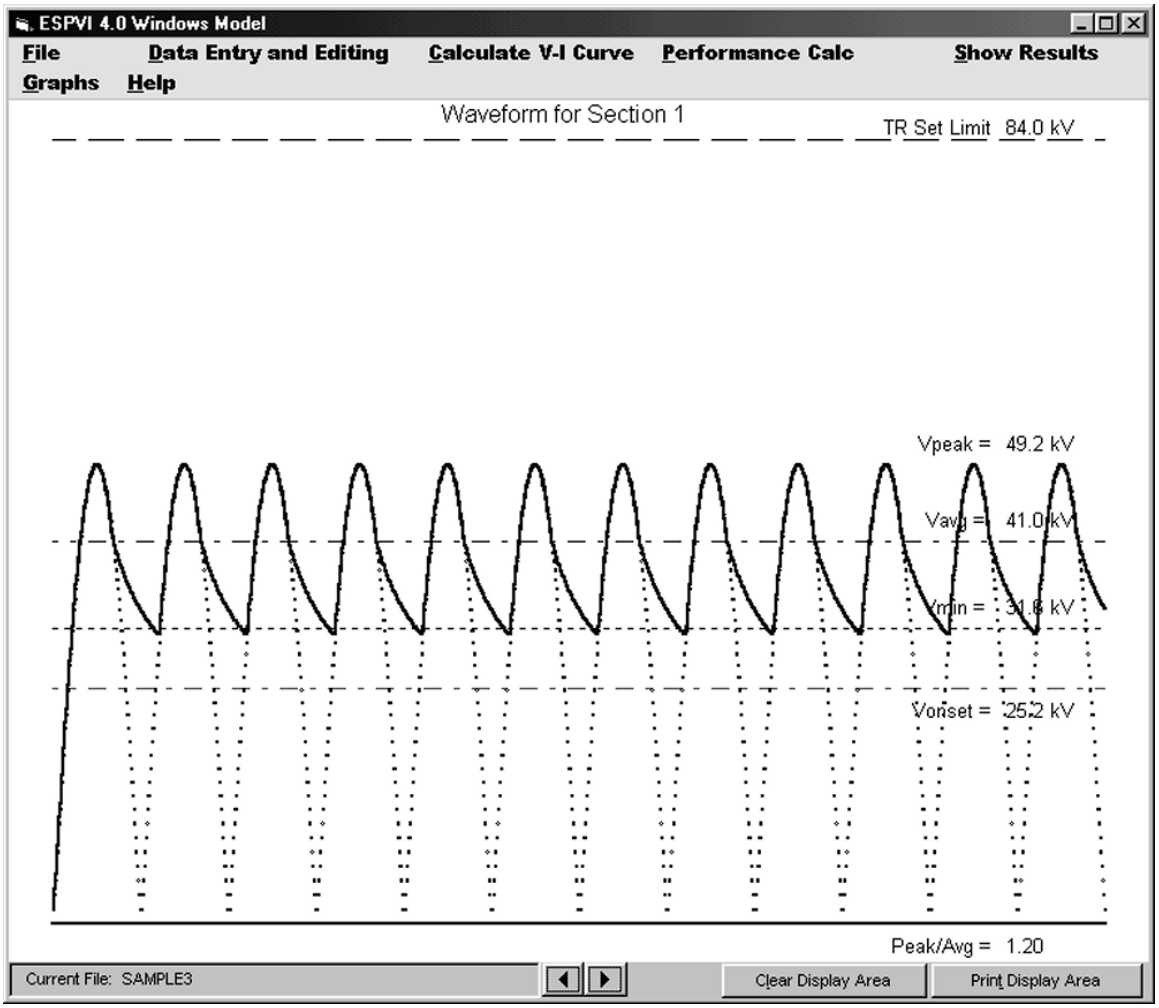

Figure 2-12. “Wave Forms by Section” showing full-wave energization for SAMPLE ESP.

2.10 Example 1: Varying the Height of an ESP

The objective of the three examples below is to demonstrate that the performance of an ESP is closely tied to its characteristics, or parameters. The majority of the input parameters for "ESP Design", which are the physical dimensions, are easily determined and consequently should be quite accurate. The gas velocity can also be determined, but with accuracy that is less certain than the physical dimensions are.

It should be noted that the results from ESPVI 4.0W are quite repeatable. However, depending on the files and how they were created, the computer, and the operating system, very slight deviations in some of the outputs are sometimes seen. These are generally less then a few percent and are certainly less than the error in the data that is usually available, which has a more profound effect.

In Example 1, a plate height of 7.5 m will be increased to 8.5 m, without changing the gas flow volume, particle characteristics, and electrical conditions. Increasing the plate height will increase the collector electrode area and will require a decrease in the gas velocity. The increase in the collector electrode area will cause an increase in the SCA. The increased SCA would be expected to result in increased collection efficiency.

As a first step, it is always recommended that calculations be made manually for input into ESPVI 4.0W. Using the data from "ESP Design" for SAMPLE, the following calculations are made:

Plate Area = 3600 m^2 × 8.5 m / 7.5 m = 4080 m^2

Plate Area of Section = Sectional area = 4080/3 = 1360 m^2

Gas Velocity = Volume flow / width × height = 119 m^3/s /(8.8 m × 8.5 m) = 1.59 m/s

SCA = Total area / volume flow rate = 4080 m^2 / 119 m^3/s = 34.3 $m^2/m^3/s$ (s/m)

SCA of Section = Total SCA / Number of sections = 34.3/3 = 11.4

In ESPVI 4.0W, SAMPLE needs to be opened. Next, under "File", choose "New" and name the new file ESP SAMPLE 1. Under "Data Entry and Editing", "ESP Design" should be chosen to input the new calculations.

It is good practice to enter as much information as possible into ESPVI 4.0W and then to allow **Check for Consistency** to check the results. Next, the values calculated above are entered. After entering the plate area for the first section, use the **Copy Right** command button to load the plate area data in sections 2 and 3. Then, the **Check for Consistency** command button is used to check results for completeness and accuracy. Once everything on the "ESP Design" menu appears correct, use the **Accept** command button to close the form. Figure 2-13 shows "ESP Design" window loaded with the input data for SAMPLE 1.

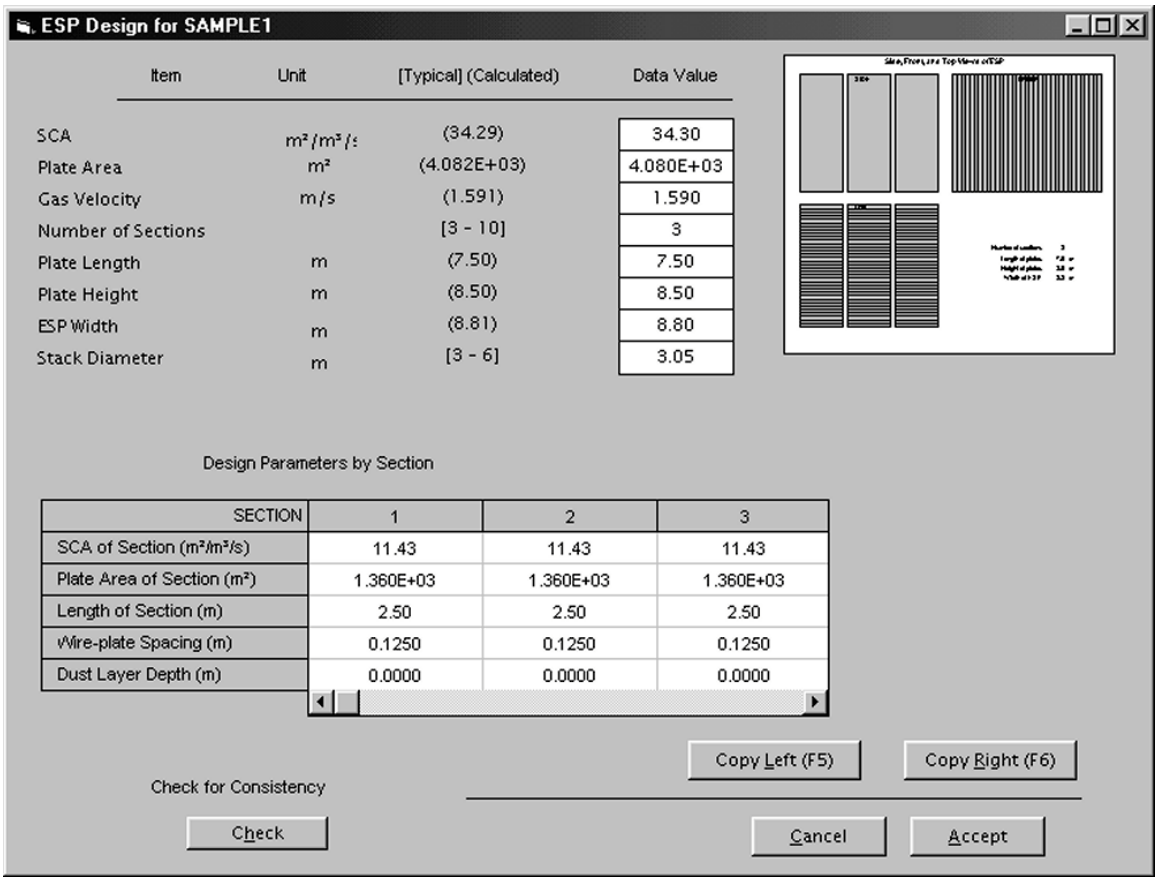

Figure 2-13. “Design of ESP” window for SAMPLE1—changing the height.

At this point, **Standard Method** in the “Performance Calc” pull-down menu is used to make the necessary computations that are seen as **Main Results** in the “Show Results” pull-down menu and presented here as Figure 2-14. Save the new data for SAMPLE 1.

In comparing the emissions, the change in penetration is more informative than efficiency is. Penetration is the uncollected portion that has evaded collection by the ESP. Looking at the reduction of the penetration provides the actual reduction in the emissions. By comparing the two penetrations, it is seen that increasing the height from 7.5 to 8.5 m, which increased the collection area by about 13 percent, reduced the emissions by about 22 percent. If the size of the ESP is further increased, so would the collection efficiency.

The reverse of increasing the collector area is to decrease it. The expected result would be to decrease the performance and thereby lower the collection efficiency.

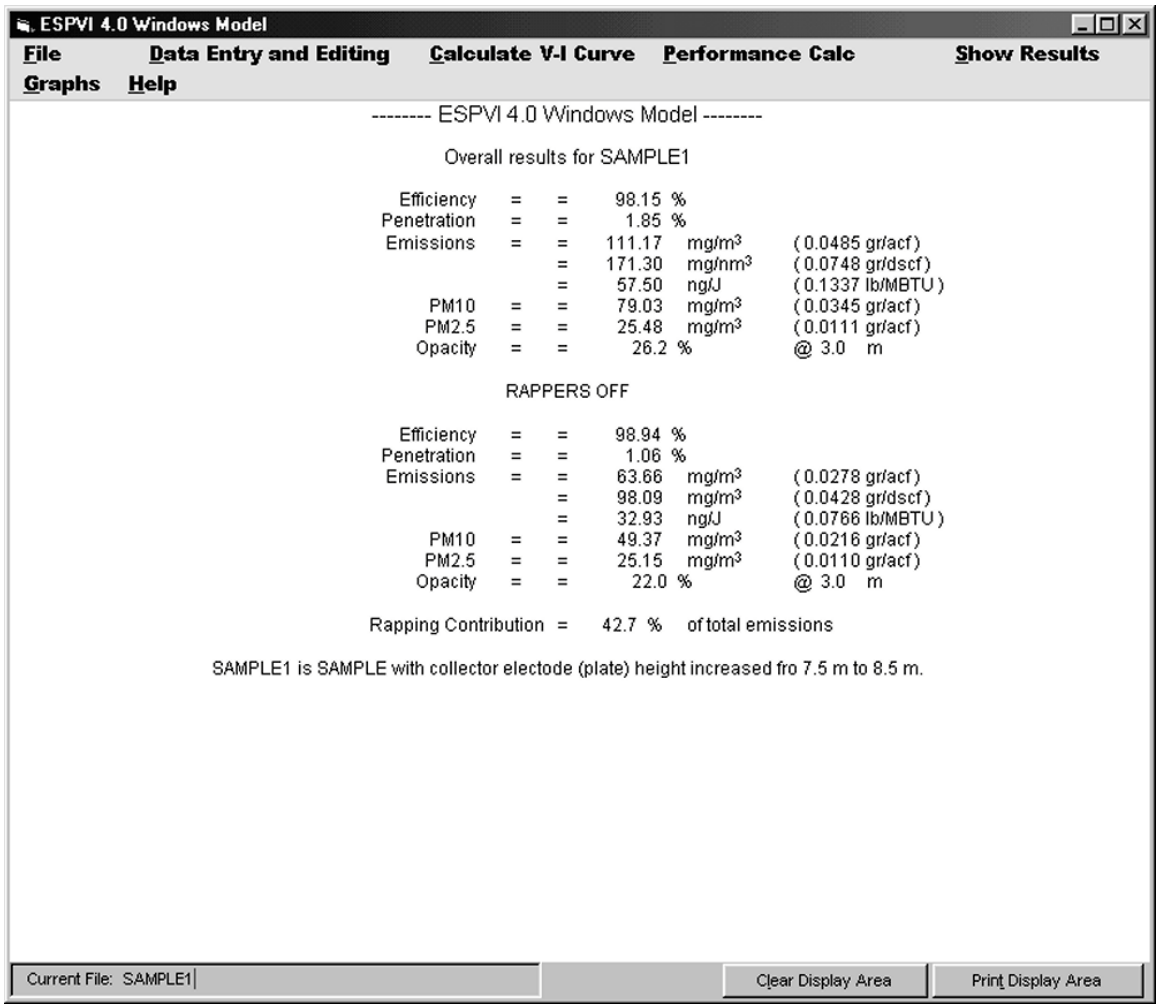

Figure 2-14. “Main Results” for SAMPLE1—changing the height.

2.11 Example 2: Changing the Gas Velocity of an ESP

Decreasing the inlet gas velocity to the ESP has the effect of decreasing the volume of gas flow, which increases the SCA. Looking at it another way, if the gas velocity decreases, the gas residence time in the ESP increases, and the collection efficiency would be expected to improve.

The gas velocity in SAMPLE is 1.80 m/s. For this example the gas velocity will be arbitrarily reduced by 25 percent to 1.35 m/s. Using a similar procedure as in Section 2.10, calculations are made as follows:

> **Volumetric Flow** =velocity flow × width × height = 1.35 m/s × 8.8 m × 7.5 m = 89.1 m^3/s.
>
> **SCA** = Total area / volume flow rate = 3600 m^2 / 89.1 m^3/s = 40.4 s/m.

This time instead of choosing **New** under "File", start with SAMPLE. On "Design of ESP" enter the new total **SCA** and **Gas Velocity**. This time use **Check for Consistency** to make the remaining changes realizing that the gas velocity has to change and the SCA needs to be changed in the three-ESP sections. Once the changes are made, **Accept** them.

Because the gas volume flow has to change, go to "Gas Properties" to determine whether it has been entered correctly as 89.1 m^3/s. If there are problems in setting up the data using **Check for Consistency**, complete the procedure manually.

Once everything is correctly entered, use "Standard Method" and then go to "Show Results". Finally, use "Save As" under "File" to save the file with the new name SAMPLE2. For this ESP operating with the reduced gas velocity, the "ESP Design" is shown as Figure 2-15 and the "Main Results" in Figure 2-16.

A comparison between SAMPLE and SAMPLE 2 shows a penetration reduction from 2.37 to 1.33 percent. This is a reduction of particulate emissions of about 44 percent, which is a significant decrease. It is understood that the opposite effect would occur if the gas velocity were increased.

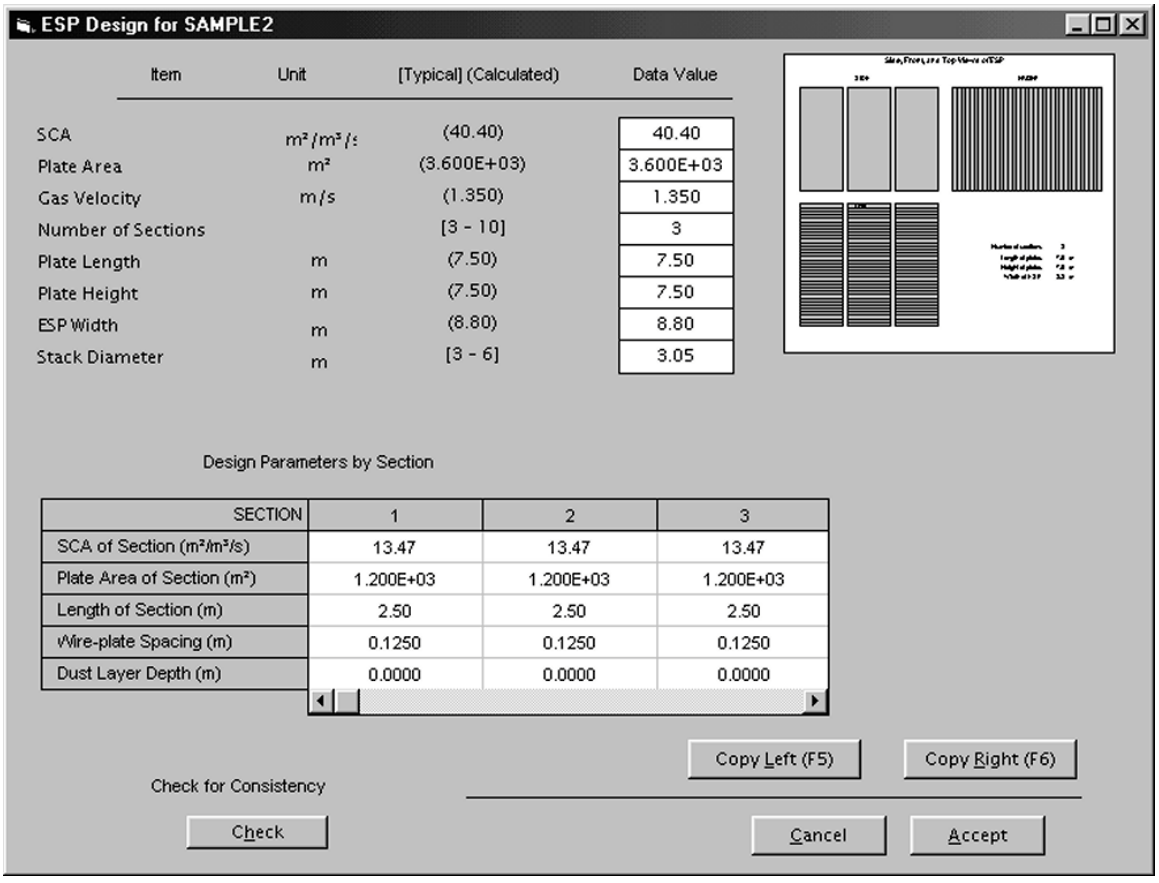

Figure 2-15. "Design of ESP" window for SAMPLE2—changing the gas velocity.

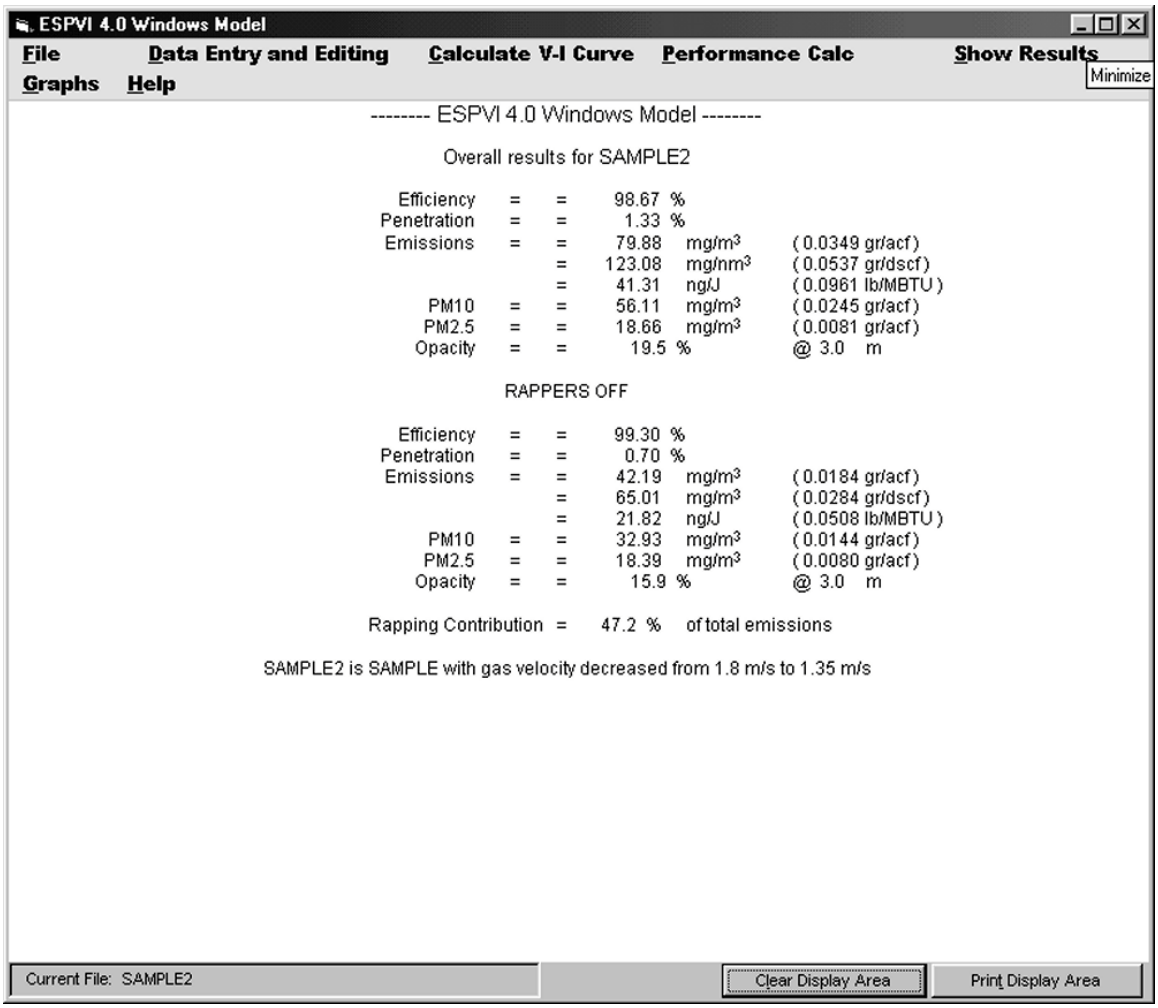

Figure 2-16. “Main Results” for the SAMPLE2—changing the gas velocity.

2.12 Example 3: Adding a Fourth Section

Adding additional sections (fields) to an ESP is a means for increasing the collector electrode area and, consequently, the SCA. As had been seen in the previous sections, increasing the SCA does increase the performance of the ESP. Increasing the SCA with an additional ESP section provides the increased advantage of optimizing the electrical conditions for the added collector electrode area. Adding an additional section or field is only practical if there is available space to perform the addition.

For this example, the additional section will be identical to the existing sections. This means that the collector electrode area will be 3,600 + 1,200 = 4,800 m. The SCA will be 30.3 + 10.1 = 40.4 s/m. The total length will be 7.5 + 2.5 = 10 m. All other parameters will remain the same.

In ESPVI 4.0W “Open” SAMPLE and then choose “New” and name it SAMPLE3. Go to “ESP Design” and enter the new parameters:

Plate Area = 4,800 m

SCA = 40.4 s/m

Plate Length = 10 m

Also, change "Number of Sections" from 3 to 4. Use **Check for Consistency** to determine the accuracy of the information entered. At this point examine "Plan Views of ESP" and compare the 4-section ESP on the screen to the 3-section unit in Figure 2-7 for SAMPLE.

Use the "Standard Method" to allow ESPVI 4.0W to make its necessary calculations. Compare the screen to Figure 2-5 for SAMPLE. Observe that ESPVI 4.0W has made calculations for four sections rather than the three for SAMPLE.

Going to "Main Results", Figure 2-17, it is apparent that there is a significant improvement of performance in comparison to that of SAMPLE, Figure 2-6. The particle penetration or emissions has gone from about 2.37 percent to 1.05 percent, which is a decrease of about 56 percent. Once completed, "Save" SAMPLE3.

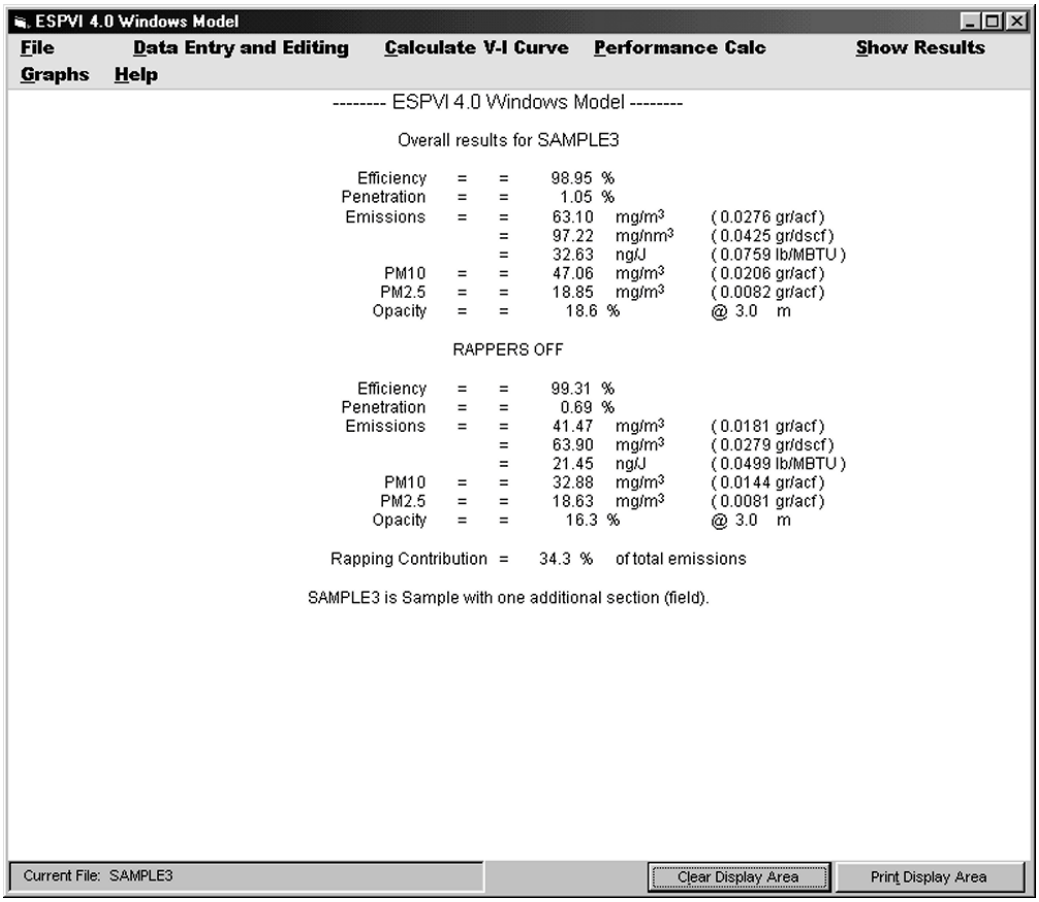

Figure 2-17. "Main Results" for SAMPLE3—increasing the number of sections.

Chapter 3
Electrical Energization

Most modern ESP installations are invariably energized from main frequency rectified equipment utilizing the latest electrical and electronic components. Generally the transformer input conditions are controlled by anti-parallel-connected, thyristor-controlled rectifiers, which in turn are controlled by microprocessor-based automatic voltage control (AVC) system. Although the supply is usually a fully rectified voltage, many modern designs have the facility of intermittent energization for helping to meet specific fly ash conditions or for power saving while meeting a target emission. Some of these modern concepts will be discussed in detail in Chapter 7, Enhancing the Performance of Existing ESPs—Electrical.

3.1 Basic Operation of Main Frequency Equipment

The basic circuitry of the electrical equipment is shown in Figure 3-1 for a conventional 50 Hz power supply. Full wave rectification setup is illustrated. However, half wave rectification has also been used from time-to-time with the full wave rectifier replaced with a half wave device. The capacitor (C_{EP}) in Figure 3-1 represents the electrical capacitance of the electrodes and high voltage distribution system, which becomes charged during each voltage. The resistor (R_{EP}) represents the current drain, mainly from the corona discharge, which draws charge from the capacitance thereby reducing the voltage between cycles.

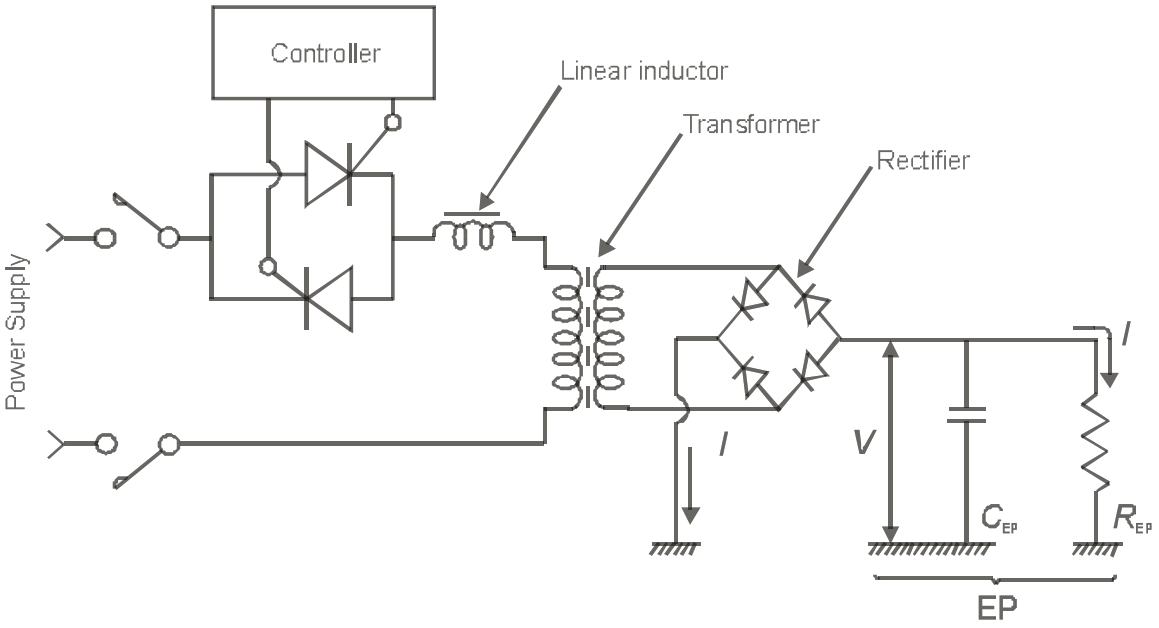

Figure 3-1. Typical main frequency rectifier equipment.

The output voltage of the power supply applied to an ESP bus section is controlled by varying the firing angle of the thyristors in the controller portion of the circuit; this can be done by delaying or advancing the firing instant in relation to the zero crossing (crossover) of the line voltage. When the thyristor fires, it changes from a state of high resistance to low resistance, and the primary current starts increasing. The current limiting inductor, the leakage inductance of the high voltage transformer, and the ESP load determine the magnitude and duration of the current. The amplitude of the secondary voltage is directly proportional to the transformer turns ratio. The amplitude difference between the primary and the secondary current is inversely related to the transformer turns ratio.

Typical full wave rectifier wave forms are shown in Figure 3-2. As seen previously in Chapter 1, ESPVI 4.0W provides wave forms as graphic outputs that are specific to the ESP that is being modeled.

The ESP voltage shown in Figure 3-2 has a considerable ripple, because of the inherent capacitance of the ESP section. In general, the ESP voltage is characterized by its peak, mean (or average), and minimum values. The peak voltage depends on the charge delivered the ESP's capacitance in one current pulse, specifically, the area beneath the current pulse. Since charge is drawn from the ESP capacitance in the time interval between the arrival of successive current pulses, the value of the mean voltage decreases. The mean (or average) voltage is normally the secondary panel voltage meter reading. In ESP operation, the peak voltage creates the electric field that is dominant in the particle charging process. The mean (or average) voltage causes the electric field that is dominant in the collection process. The minimum voltage is the lowest value that the voltage normally goes to during a cycle. In a well operating ESP, the lowest value for the minimum voltage is the corona onset voltage. It is possible for the minimum voltage to fall below corona onset between cycles in an ESP operating in the reverse ionization, or back corona, regime. The ESPVI 4.0W refers to mean value of the voltage as the average value of the voltage. For the purposes of this document, mean and average voltages are used interchangeably.

The earliest practical firing of the thyristor is influenced by the value of the ESP voltage at the firing instant, which is equal to minimum voltage. This value is greater than the corona onset voltage and is influenced by the ESP geometry and process conditions. With normal ESP loads and a 50 Hz power supply, the earliest practical firing is in the order of 2 to 3 ms, corresponding to a firing angle of 36° to 54°.

The primary current, **I**, an important parameter in ESP operation, is not continuous; instead, it flows for brief periods established by the energization frequency, the charging of the electrical capacitance, and the rate at which the charge is withdrawn. Various current considerations are the peak current, $\mathbf{I_p}$; the root mean square (RMS) current, $\mathbf{I_r}$**;** and the mean current, $\mathbf{I_m}$. The $\mathbf{I_r}$ current is the panel meter reading for the primary current. The form factor (FF) of the ESP current is an important quantity linking $\mathbf{I_r}$ and $\mathbf{I_m}$ that must be considered and is defined in Equation 3.1.

$$\mathbf{FF = I_r / I_m} \qquad 3.1$$

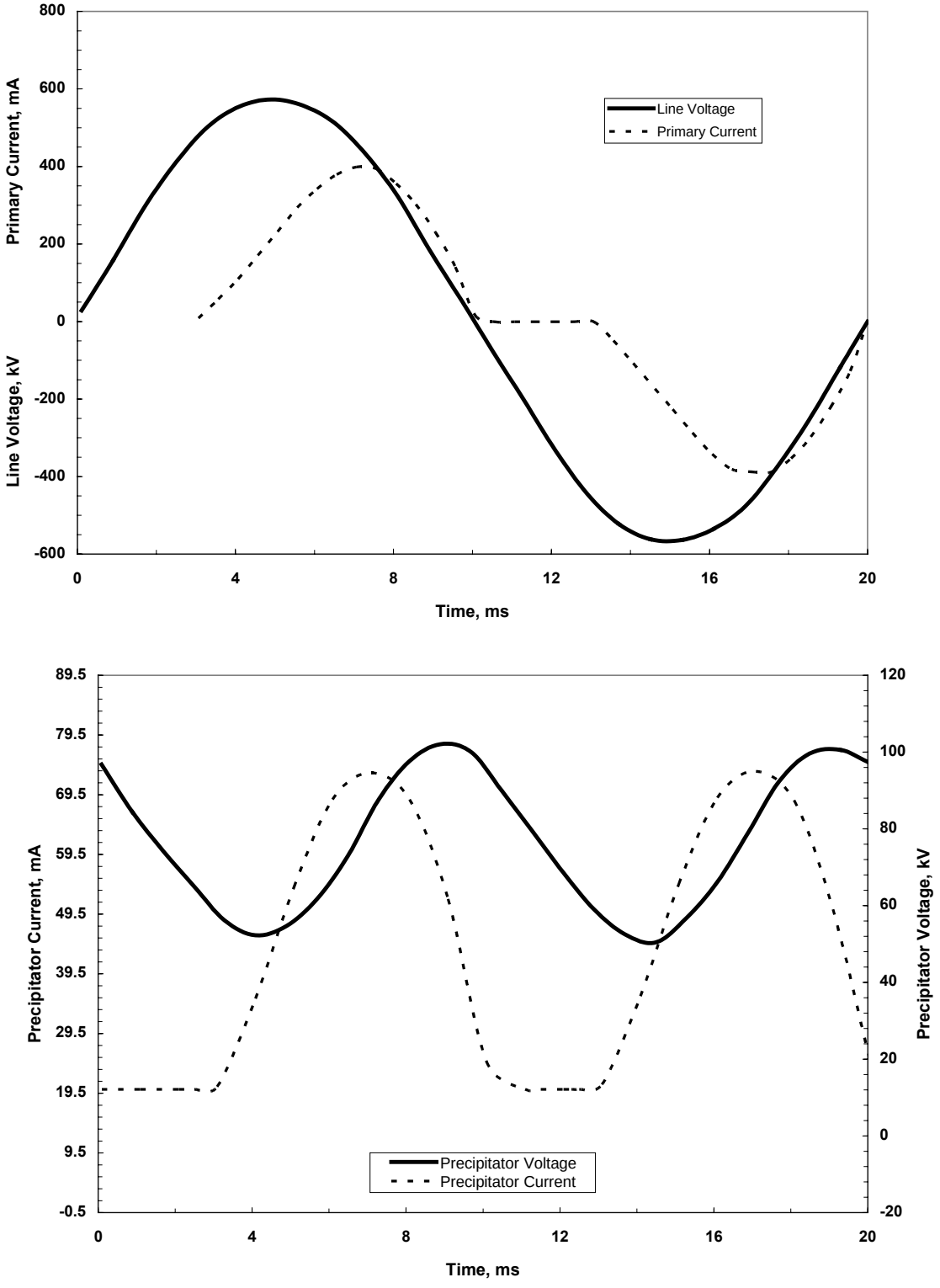

Figure 3-2. Typical DC wave forms as applied to the ESP.

Since the ESP current is not a pure sinusoidal wave, it is not easy to theoretically calculate its true mean and RMS values. Equations 3.2 and 3.3 approximate the mean and RMS values for the typical current wave form shown in Figure 3-2.

$$I_m = 2 (I_p / \pi) (t_f / t_{1/2}) \quad 3.2$$

$$I_r = I_p (t_f / (2 t_{1/2}))^{½} \quad 3.3$$

where $t_{½}$ is the ½ cycle time, which is 10 m seconds for a 50 Hz supply, and t_f is the firing period.

3.2 High Voltage Equipment Supply Ratings

The high voltage power supply for an ESP is characterized by the transformer turns ratio, **n**, and the short circuit impedance present in the main circuit. This impedance is predominantly inductive and is composed of the leakage reactance of the transformer (typically 5 to 10 percent) and the linear inductor, which is introduced purposely in order to significantly increase the short circuit impedance, as illustrated in Figure 3-1. The basic aim of the additional impedance is to limit the current surges that might occur during sparking in the ESP to (a) increase the life of the ESP internals, (b) protect the electrical equipment against overload, and (c) obtain a more stable electrical operation. The short circuit impedance value used by most of the equipment manufacturers is in the order of 30–40 percent, which limits the current surges on short circuit to some 3 or 2.5 times the rated load current value. By knowing the short circuit impedance/reactance and the transformer turns ratio, all the important quantities of the power supply can be determined for different ESP loads. The ratings can be expressed in different ways, but here, the European practice will be used.

3.2.1 Mean ESP Current

Referring to Figure 3-1, the mean secondary current value, I_S **mean**, is given by Equation 3.4 as

$$I_S \text{ mean} = 1/T \int_o^T I_0(t)dt \quad 3.4$$

where $I_0(t)$ is the ESP current and **T** is the period of the line frequency.

It should be noted that the rated ESP mean current is the maximum mean current the power supply is able to deliver to a load without exceeding the design primary current value.

3.2.2 Primary RMS Current

The primary RMS current value is defined as given by Equation 3.5.

$$I_p^2 = 1/T \int_o^T I_p^2(t)\, dt \quad \text{or} \quad I_p = n \cdot FF \cdot I_s nom \quad 3.5$$

where, **n** is the transformer turns ratio, **FF** is the form factor (typically 1.35 to 1.4), and $\mathbf{I_s nom}$ is the rated ESP mean current.

3.2.3 ESP Peak Voltage under No-Load Conditions

At no-load, the output current of the power supply, $\mathbf{I_s}$, is zero, and the primary current is therefore equal to the magnetizing current of the high voltage transformer. As this is negligible compared with the rated primary current, the peak voltage at no-load is as given by Equation 3.6.

$$\mathbf{V_s\, peak} = \sqrt{2}.\mathbf{n}\, \mathbf{V_L} \qquad 3.6$$

where $\mathbf{V_L}$ is the rated RMS value of the line voltage.

3.2.4 Apparent Input Power

This quantity is especially important in the physical sizing of the electrical installation, cabling, switch gear, and such. The apparent input power **S** is defined as given by Equation 3.7.

$$\mathbf{S} = \mathbf{I_p} \times \mathbf{V_L} \qquad 3.7$$

The active input power **P** is correspondingly given by Equation 3.8.

$$\mathbf{P} = \mathbf{S} \cos \varphi_1 \qquad 3.8$$

where φ_1 is the phase angle between the line voltage and the fundamental frequency component (50 Hz) of the primary current. ($\mathbf{Cos}\ \varphi_1$ is normally known as the power factor.)

The active power cannot be expressed as a rated value because it varies with the ESP load for the same rated ESP mean current. The active power is normally measured with a wattmeter or calculated by means of computer simulation. The power factor is normally better than 0.8 at full rated current, assuming the form factor is approximately 1.4.

3.2.5 Rectifier Equipment Nameplate Ratings

The following illustrates some typical rectifier equipment nameplate ratings.

Rated ESP mean current	$\mathbf{I_s}$	1200 mA
Rated ESP peak voltage	$\mathbf{V_p}$	110 kV
Line voltage	$\mathbf{V_L}$	415 V RMS
Short circuit reactance:	$\mathbf{X_{Lsc}}$	35 percent
Design form factor:	**FF**	1.4

The transformer turns ratio can be derived as

$$\mathbf{n} = \frac{\mathbf{1}}{\sqrt{2}} \frac{\mathbf{V_p}}{\mathbf{V_L\,nom}} = \frac{1}{\sqrt{2}} \frac{110000}{415} = 187$$

The ESP rated RMS current $\mathbf{I_o}$ is given by

$$\mathbf{I_o\,RMS} = \mathbf{I_o\,nom} \times \mathbf{FF} = 1200 \times 1.4 = 1680 \text{ mA}$$

The rated primary RMS current is

$$\mathbf{I_p\ RMS} = \mathbf{n} \times \mathbf{I_0}\,\text{RMS} = 187 \times 1.68 = 314\text{A}$$

The rated apparent power is

$$\mathbf{S = I_p\ RMS} \times \mathbf{V_L\ RMS} = 314 \times 415 = 130.4 \text{ kW}$$

Some of the rectifier equipment nameplate ratings are used as input parameters for the ESPVI 4.0W. These will be discussed later.

3.3 ESPVI 4.0W Operating Voltages

From the main window, Figure 1-2, go through the pull-down menu “Data Entry and Editing” to bring up the “Operating Voltages” window, Figure 1-4. On the lower two-thirds of the window, there is a large group of text boxes in which to enter the electrical data by section. These are the voltages and currents for each electrical section, which are parameters for determining ESP performance that are probably second in importance only to the physical parameters such as the collector electrode area.

ESPVI 4.0W is a unique model that can find a solution to Poisson’s equation using the ESP parameters that are provided as input. It starts from first principles taking into consideration the electrode configuration and the particle characteristics to find the solution to Poisson’s equation, which provides the corona current for a given voltage. This model allows input of current or current density values, but it is strictly for comparison purposes only. The parameter that controls the collection performance calculation is the operating voltage. ESPVI 4.0W considers reverse ionization or back corona. Particle charging uses an improved algorithm that is faster, more accurate, and allows for effects of bipolar charging.

Despite the improvements in back corona prediction with ESPVI 4.0W, there are still cases of back corona that remain difficult to explain. Such cases may have back corona in only a small fraction of the electrodes, but to such a degree that it determines the voltage and current density for the whole section. ESPVI 4.0W assumes that all the current delivered by the corona wires is useful for charging particles. However, if there are electrical problems, such as leakage across insulators, or if large amounts of back corona are present in the current value that is entered, then a large part of that current is not useful. The current is either being wasted in localized hot-spots, or else it is entering the gas stream as positive ions and actually discharging most of the negatively charged particles.

The first line in the data entry text box is the **Voltage** applied to the corona discharge electrodes. There are several options for entering this voltage. One of these is to enter the voltage directly, which is usually done if there are accurately measured values available. This is what was done in Chapter 2 of this manual when the "Standard Method" of calculation was used. Later in this chapter other calculation methods will be shown that automatically insert the voltage values.

Still another method is the "EPRI Coldside V-I Correlation" seen on the upper side of the window, which will be discussed later in this chapter. Voltages for cold-side ESPs typically range from less than 30 to more than 70 kV, depending on discharge electrode and collector electrode spacing and particle resistivity. Because of the space charge effect of the particulate in the gas stream, the current densities in inlet sections may be noticeably lower than in outlet sections, while at the same time, the voltages would be higher at the inlet sections than at the outlet sections. Current densities may typically range from about 5×10^{-5}–2×10^{-4} A/m² in the inlet section to 2×10^{-4}–5×10^{-4} A/m² in the outlet sections, if no back corona is present. Under high resistivity or high space charge conditions, current densities may be lower.

The **Current Density** and **Current** entry box values are for comparison purposes only. Measured values may be recorded here, but will be replaced by calculated values when the "Calculate V-I Curve" or "Performance Calc" menu options are exercised. The significance is that the computed currents are what ESPVI 4.0W says the ESP should be doing if its operating parameters are the same as the input settings of ESPVI 4.0W. If they differ, it could mean that the ESPVI 4.0W inputs are not correctly set to the true ESP parameters. Alternatively, it could mean that the ESP is not working correctly. The **Current** is the total current for the section. The **Current Density** is the **Current** divided by the section area.

The **Starting Voltage** box on the "Operating Voltages" window uses theoretical considerations to calculate the V-I corona onset point for each electrical section, assuming no particles in the gas stream. It is not necessary to enter a voltage here; ESPVI 4.0W will insert the appropriate value when it makes its calculation. When the ESP performance is calculated, the onset voltage in the box will be updated to account for space charge effects. It is included here as an option for use in comparing with measured or estimated operating voltages. In cases with high resistivity dusts, the operating voltage should be closer to the corona onset voltage than it would be for lower resistivity dusts. The current increases with increasing operating voltage. The higher the resistivity of the dust the lower is the allowable current to prevent back corona or reverse ionization.

The **Peak-to-Average Voltage Ratio** is a number greater than 1. An ESP section acts like a capacitor in parallel with a resistor. During one wave form cycle, the capacitor is charged to its maximum voltage, after which the charge drains off to a lower level, mainly because of the corona current, which causes the voltage to decrease. It is repeated again at the next cycle. The average voltage between the peak and the minimum is normally the panel meter reading. There is significance to these voltage values. Particle charging is dominated by the peak electric field and collection is dominated by the average electric field. Therefore, a higher **Peak-to-Average Voltage Ratio** would cause there to be a higher level of charge on

the particles, which results in a higher migration velocity and, therefore, collection. A full-scale ESP's performance is therefore sensitive to the **Peak-to-Average Voltage Ratio**.

The ESPVI 4.0W considers these two electric fields (peak and average) during its computations. For the most accurate modeling, it is desirable to use actual values of peak to average voltage, which are different for half wave, full wave, and IE. Please note that elsewhere in this document the word average voltage is also called mean voltage. Therefore, where one or the other is encountered, they both mean the same. If no **Peak-to-Average Voltage Ratio** data are available, a reasonable value would be 1.2 for full-wave energization. A higher value should be used for half-wave energization.

Three additional inputs that are requested in the "Operating Voltages" window text box are **Maximum Voltage**, **Maximum Peak Voltage**, and **Maximum Current**, which are related to the electrical energization power supplies. These values can usually be obtained from the manufacturer's specifications. They can also be referred to as the rectifier equipment nameplate ratings discussed elsewhere in this chapter (3.2.5). If the values are not known, then set them to zero as a sign that there are no valid numbers for the parameters. These power supply limits, as will be seen later, are used to control the "Automatic V-I" calculations in the "Calculate V-I Curve" pull-down menu. If these values are left at zero, they will not affect the calculations. They should also be left at zero for calculations by the "Standard Method" performed in the manner of Chapter 2.

The maximum current rating for a section should be the sum of the ratings for all TR sets that supply the section plate area. The total current may exceed the rating of one power supply, but should not exceed the rating of all supplies together. Some common TR sets maximum ratings are 45 or 55 kV average voltage, 63 or 70 kV peak voltage, and 500, 1000, or 1500 mA average current. ESPs that require more current will usually have multiple units operating in parallel.

The **Wave Form** box, in the "Operating Voltages" window, Figure 1-4, allows the choice of one of a number of possible wave forms ranging from pure (filtered) DC to a very intermittent form of energization. Except for pure DC, the voltage is assumed to vary as the absolute value of a main frequency sine wave, with whole half cycles either present or absent. The wave form is entered section by section into the **Wave Form** data entry box. Each wave form has its own unique number. As it is possible to have a different wave form in each section of a full-scale ESP, it is possible to have a different wave form in each section in ESPVI 4.0W. The wave form is chosen by entering the Wave Form Numbers into the appropriate place in the **Wave Form** text box. The lower left corner of the window has a command button, **Show**, which calls up a small window that lists the various wave forms and their numbers that are available for entering into the text boxes.

Full wave energization, which is chosen by entering Number 2, has every half cycle present and was presented as Figure 2-12 as developed by ESPVI 4.0W.

Half wave energization, which is chosen by entering Number 3, has alternate half cycles present; there is no energization supplied between the half cycles. A half wave representation

as developed by ESPVI 4.0W can be viewed directly in ESPVI 4.0W as part of its “Graphs” capability. It differs from the full wave representation by only having every half-cycle provided by the TR set.

An example of half-wave energization as generated by ESPVI 4.0W is shown as Figure 3-3, which illustrates the alternate half-cycles provided by the TR set.

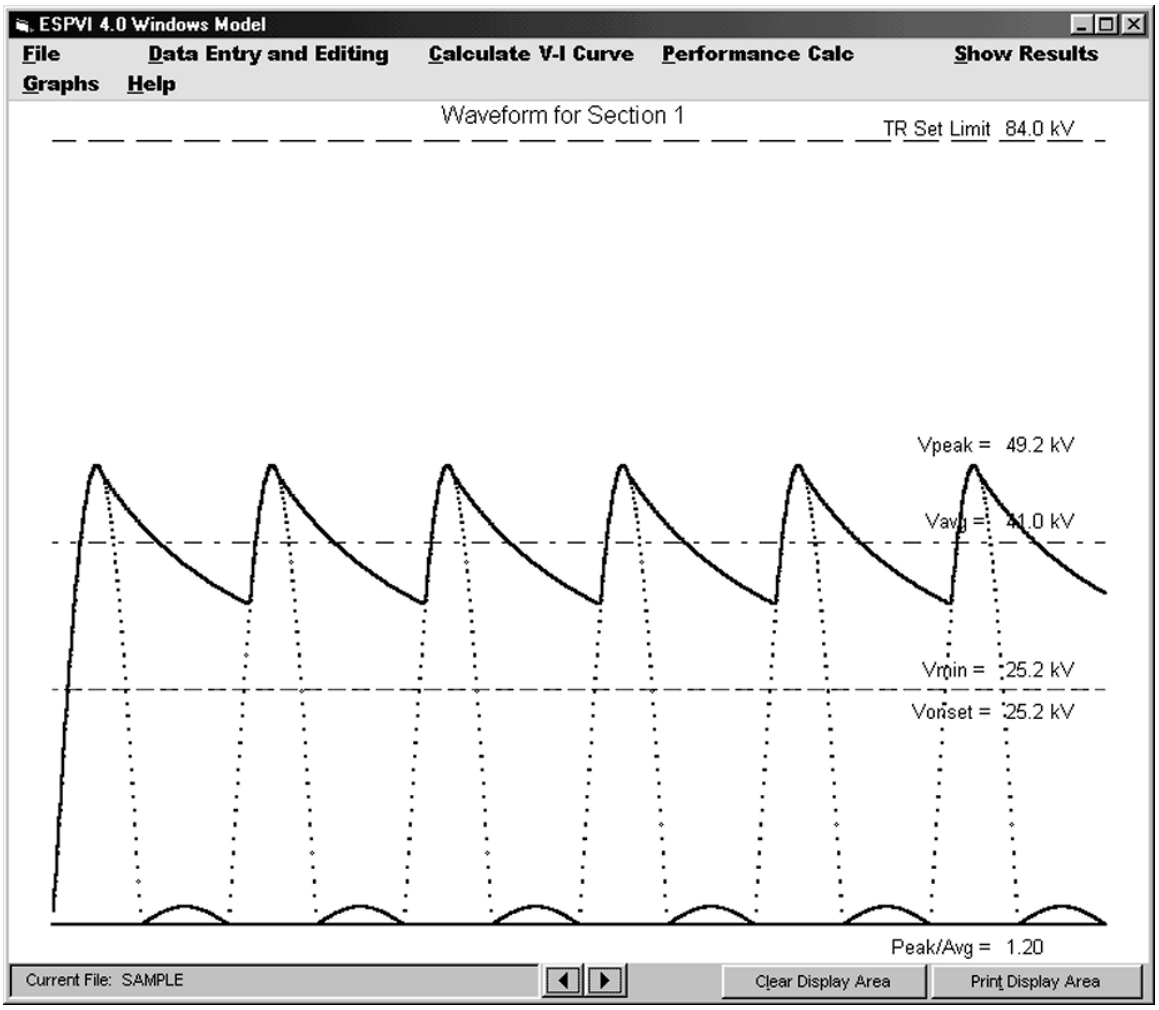

Figure 3-3. Half-wave energization ESPVI 4.0W graph representation.

The level of IE is chosen by entering the appropriate number of interrupts in the half-cycle energization for the set number of half cycles. A half cycle of energization is then provided followed by the interruption. The **Wave Form** entry window refers to IE by an alternate name—semi pulse or, as in ESPVI 4.0W, SemiPulse. As an example, SemiPulse 1:8 means that in each intermittent period of four cycles there is one half cycle energized followed by seven half cycles that are not, as shown in Figure 3-4. The term SemiPulse ratio used in ESPVI 4.0W is often called the degree of intermittence, or D. The D is the ratio of the

number of half cycles in the IE period to the number of energized half cycles. In this document and in the ESPVI 4.0W, the D and the SemiPulse ratio are used interchangeably. An IE representation as developed by ESPVI 4.0W is presented as Figure 3-4. It shows a D of 8, which is one half cycle of energization provided every 8 half cycles resulting from entries into the **Wave Form** window. SemiPulse IE is considered in significantly greater detail in Chapter 7.

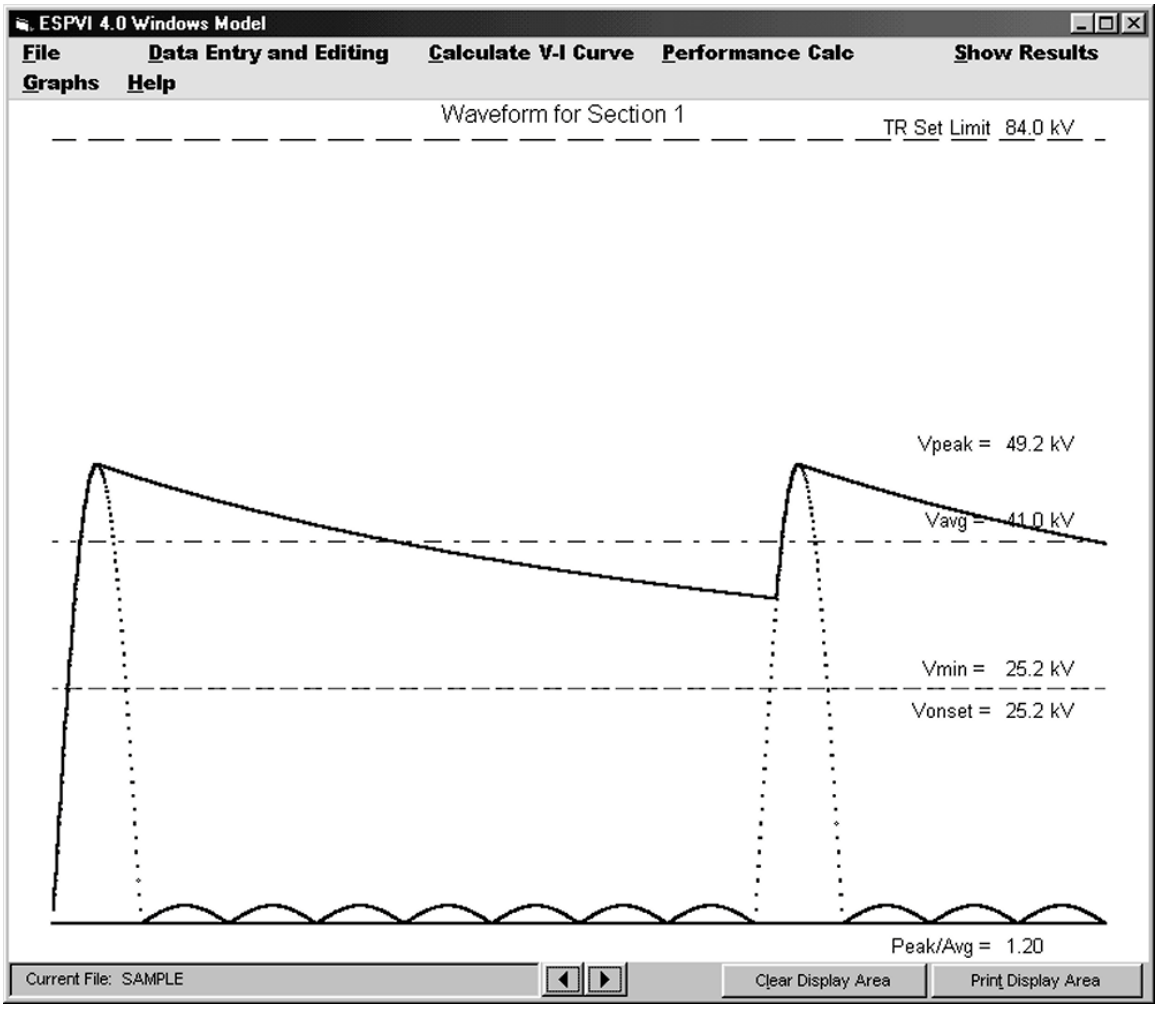

Figure 3-4. IE ESPVI 4.0W graph representation.

Filtered DC as such is not used in industrial precipitation practice. However, it does provide a useful service for an emerging method of energization, SMPS. The energization from SMPS is the rectified product of a type of alternating power significantly higher in frequency than the normal main supply provides. The small amount of ripple along with the capacitance of the energized ESP section makes it appear very much like pure DC. SMPS energization is described in more detail in Chapter 7.

Resistivity in the "Operating Voltages" window text box is the value of the particulate resistivity. It typically ranges between 10^7 and 10^{11} ohm-m or higher. ESPVI 4.0W uses the resistivity for several purposes, the first is to sense the onset of reverse ionization and to start using its bipolar charging feature. Referring back to Figure 1-2, "ESP Design", there is a data entry for "Dust Layer Depth". If "Dust Layer Depth" is entered, ESPVI 4.0W will use the resistivity to compute its effect on the electric field between the discharge and collector electrodes. ESPVI 4.0W will show no difference for resistivity lower than 1×10^5 ohm-m, although there may be some in practice, particularly with regard to steady reentrainment of the collected particles that is commonly found to occur when collecting low resistivity particle matter with an ESP. The resistivity value is used in picking the operating points from the EPRI correlation.

The three command buttons on the left upper side of the "Operating Voltages" window are for the **EPRI Coldside V-I Correlation**, **Calculate clean-gas starting voltage**, and **Remove starting voltage bias**. The **Calculate clean-gas starting voltage** calculates the corona onset voltage, which is then filled into the **Starting Voltage** text box discussed earlier in this chapter. **Remove starting voltage bias** is used to restore the corona factor to its initial value when the optional calculation method **Adjust Onset Factor** is chosen. The use of the **Adjust Onset Factor** calculation option will be explained later in this chapter.

The **EPRI Coldside V-I Correlation** is an option that uses a correlation of operating ESP voltages and current densities to provide values that depend on the dust resistivity. The correlation, which was originally developed by EPRI, had been based on a set of comprehensive tests for 17 operating ESPs in the United States having collector electrode spacing that ranged from 229 to 305 mm. The resistivity of the dust collected for the 17 ESPs ranged from a low of 1.6×10^8 to a maximum of 6.9×10^{10} ohm-m. The EPRI correlation was developed by finding limits of useful current density corresponding to the onset of back corona and may be used to see how much average current density can be attained for a given resistivity. It is a correlation derived from ESPs operating with the low fly ash inlet concentrations, which give rise to relatively low space charge, commonly found in the United States. Therefore, the EPRI correlation would not be expected to give good results with high ash coals such as are used to a considerable extent in the Newly Independent States (NIS). The correlation may be useful, under appropriate conditions, when actual operating voltages and currents are not available.

As has been seen, ESPVI 4.0W graphically shows the shape of the wave form, including the peak, average, and corona onset voltages. This allows a comparison to be made, using an oscilloscope, to the actual ESP wave form. The peak to average voltage ratio of the ESP can be determined and ESPVI 4.0W set accordingly.

It might be found that the ESP's operating voltage is either less or more than ESPVI 4.0W says it should be. In such cases, the electrode diameter or the corona onset factor may be adjusted to bring the onset voltage of ESPVI 4.0W to its correct level.

Although the corona onset voltage may be calculated and displayed, it is not essential. It will be calculated as a part of the automatic V-I Calculation.

As mentioned earlier, **Copy Left** and **Copy Right** are used with the sectional input data portion of the window. These command buttons allow data that is entered for one section to be copied to the other sections.

Two other command buttons along the bottom of the "Operating Voltages" window form are labeled **Cancel**, and **Accept**. The **Accept** command button closes the "Operating Voltages" window with its current data contents so that the modeling can proceed. Clicking on **Accept** only allows the calculations to proceed with the window's current contents. It does not save the contents, which, if desired, must be done by means of "Save", which is under "File" in the main window. Clicking on the **Cancel** command button closes the window and restores the data entries last saved.

3.4 Generating V-I Data and Electrical Operating Points

In Chapter 2 of this manual, after the ESP's data was loaded into ESPVI 4.0W, "Standard Method" was used to determine the performance. With "Standard Method", voltage and current values were assigned to each of the ESP's sections or fields. ESPVI 4.0W then performed computations in which it determined the level of current for each of the sections and given voltage. The performance of the ESP for those electrical conditions was also provided. The difference between the assigned and the calculated currents provided some indication as to whether the entered parameters to ESPVI 4.0W accurately described the ESP being modeled.

ESPVI 4.0W provides other means for assigning electrical conditions to the ESP being modeled. The "Calculate V-I Curve" pull-down menu on the "main window" brings up several choices, the first of which is "Automatic V-I". The "Automatic V-I" choice will calculate a voltage current (V-I) operating point by stepping the peak voltage upward in increments, starting at corona onset. With each increment, it also provides an average voltage and a current. It will stop the upward voltage steps when one or more of the following conditions are met:

- Sparking conditions are sensed, indicated by an asterisk (*) next to the voltage value.
- Back corona conditions are sensed for several corona elements, which is indicated by a * next to the current density value.
- The maximum ratings of the TR set entered into "Operating Voltages" are met.

Sensing sparking onset is according to a protocol built into ESPVI 4.0W that suggests whether or not the conditions for sparking exist. The criterion for back corona is based on the resistivity of the particle matter and the maximum current in the section. The TR set limits (voltage and current) are inputs requested by the "Operating Voltages" window as seen in Figure 1-4 and as discussed in Chapter 3.2.5. If zero values are used for the TR set limits (to indicate unknown values), stopping the voltage step increases in "Automatic V-I" will be only for sparking or back corona. Sensing sparking onset and reverse ionization or back corona by ESPVI 4.0W is based on theoretical considerations, is provided for guidance purposes only, and should not be relied on exclusively. It should always be supported by actual operating data and experience.

When “Automatic V-I” is chosen, the calculations for the first section are performed in small step increments. A small auxiliary window named “Pause to view” appears with two command buttons labeled **Continue** and **Cancel**. If **Continue** is chosen, ESPVI 4.0W will continue and will repeat the procedure for the next section. This can be continued until the curves are drawn for all sections of the ESP. If **Cancel** is chosen, the process will halt with the last section for which “Calculate V-I Curve” was performed.

After completion of “Automatic V-I”, it is possible to go directly to “Show Results” to determine the expected performance of the ESP with the new electrical conditions. Alternatively, it is also possible to go through the intermediate step of “Standard Method” where it will be observed that there is no difference between the calculated and the set values of current density.

The next choice on the “Calculate V-I Curve” pull-down menu is “Fixed V-I”, which steps through voltages from the corona onset voltage to a maximum peak value. At each voltage level, the current for each element is calculated, and the particle charging and collection are evaluated. Algorithms to predict sparking and back corona are built into ESPVI 4.0W. If ESPVI 4.0W senses that sparking will occur, an asterisk appears by the voltage in the **Peak V** column. If back corona is predicted, an asterisk appears by the current density in the **Avg j** column. The sparking prediction is based on theoretical conditions. Sparking at lower voltages can be present in an ESP because of mechanical or electrical problems.

The calculation involves both the peak and the valley (minimum) voltages for a pulsating wave form as shown in the graph representation of Figures 2.12, 3.3, and 3.4. The peak voltage dominates the particle charging because the electric field and the current density are strongest during the peaks. If the voltage decreases to corona onset between peaks, the valley voltage is the corona onset voltage plus the offset due to space charge. Time-averaged electric fields are used for the particle collection process, and time-averaged current densities are shown on the screen.

Since the peak and average voltage are both used in the calculation, the average voltage and peak-to-average ratio are also shown on the screen. A calculated space charge, corresponding to the space charge under the first element of the section is displayed to indicate the amount of charging taking place. The section calculation sums the current contributions of each element for the overall current density. The minimum voltage is the lowest value from among all the elements.

Both “Automatic V-I” and “Fixed V-I” present the data in both tabular and graphical forms for the whole section at once, as if the panel voltmeters and ammeters were reading it. When finished doing the calculations for the ESP, all V-I curves are shown together on the graph on the right side of the page.

The “Element V-I (Graphical)” on the “Calculate V-I Curve” pull-down menu performs the same calculations as “Fixed V-I” but presents the results differently; it can only present graphical results. Instead of presenting a summed curve, each element's current density is

plotted on a graph as a function of the voltage steps. It proceeds until the maximum peak voltage is reached. A maximum of fifteen elements is shown on the screen; elements beyond fifteen are calculated but not displayed. The current density represents the total current delivered by each element to the area served by that element. When similar elements serve different areas, the current densities may be different, although the currents from each element may be almost identical. This could result from interaction with neighboring elements whose spacing, or even absence, may be different.

If flat-plate elements are included, they will count among the fifteen presented, but no curve will be produced. Very often, element curves will lie atop one another or be grouped in families that are nearly identical, especially under low space charge conditions. In such cases, it is not important to distinguish the individual contributions. For the inlet section, the particle space charge effects will usually separate the element curves considerably, with the very first element having very little current. This is considered normal operation for an ESP. If several elements have very little current, it may be a sign of high particle loading with space charge suppression of corona.

All three “Calculate V-I Curve” menu items, “Automatic V-I”, “Fixed V-I”, and “Element V-I (Graphical)” leave the section voltages changed in “Operating Voltages”. It is important to remember: whatever that last voltage on a section was set to, either manually or by calculation, this is the voltage which will be used to determine the ESP's performance.

To restore the original saved voltages for an ESP go into “File” and then “Open” that file. This might be done if, after using one of the methods under “Calculate V-I Curve”, all of the original voltages will have been changed.

If the ESP that is being worked on in ESPVI 4.0W is ever saved by either using “Save” under the “File” pull down menu or saved when exiting the program, whatever values are entered at that time will become the saved values. Unless it is certain that, the present values need to be kept, avoid using the “Save” command.

The “Calculation Options” on the “Calculate V-I Curve” pull-down menu calls up a window with a set of text boxes that controls both the graphical displays and the number of steps and voltage limits in the V-I calculations, as shown in Figure 3-5. The default values in Figure 3-5 are always the same when the program is opened; changed values remain fixed until specifically changed or if ESPVI 4.0W is closed.

Starting at the top, **First section to calculate**, allows the V-I calculation to skip prior sections, using the voltage value previously set. This will be useful when sections require widely differing limits for the calculations or when changes are made to the outlet sections while keeping the inlet sections constant.

The second item, **Maximum peak voltage**, sets the limit for the highest or last step for the voltage current V-I curve calculations for either the “Fixed V-I” section curves or the “Element V-I” curves.

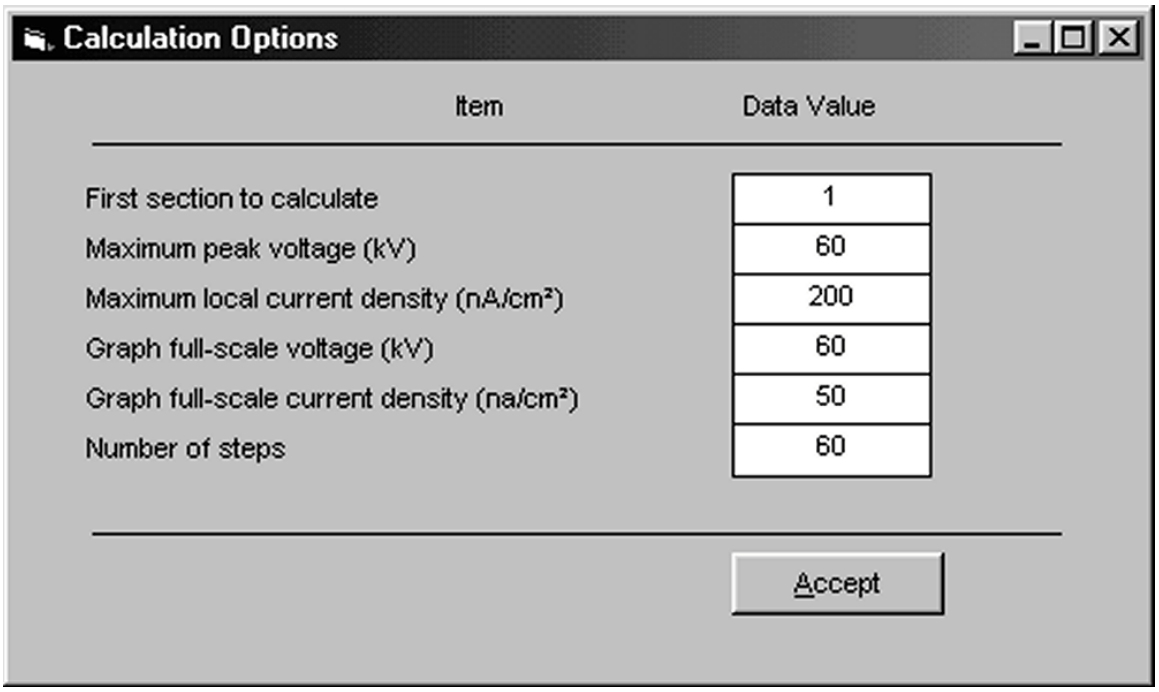

Figure 3-5. ”Calculation Options” window.

The third is **Maximum local current density**, which is a current density limit that will be invoked during the calculations. Once the average current density for the section or field equals or exceeds this value, the calculation will stop. This is applicable to the “Fixed V-I” section curves or the “Element V-I” curves.

The **Graph full-scale voltage** sets the upper limit on the graphed voltage current (V-I) curves. It refers to the average voltage, however, and is not a precise value. In order to keep the axis labels properly located, the actual maximum value will be a number chosen somewhat larger than the one used as input. For full wave and half wave energization, the peak voltage of 60 kV and the maximum graph voltage (average) of 40 kV are roughly equivalent. This, the next graph option, and **Number of Steps** are available to all of the “Calculate V-I Curves” calculations.

The **Graph full-scale current density** sets the upper limit for displaying the average value of current density. It, too, is not a precise number, but causes a more convenient value to be picked for displaying the labels on the vertical axis.

The **Number of steps** determines how many voltage steps are to be taken between the corona onset voltage and the maximum peak voltage. Ten to fifteen are convenient, but more steps are possible. The limit in having all of the steps on the screen at one time is about 39, after which no additional steps will be written. However, for some operations additional graph points will continue to be plotted.

After making a choice in “Calculation Options” click on **Accept** to close the window. Remember that any option chosen on this window disappears when ESPVI 4.0W is closed.

3.5 Other Computational Methods

Some experience has already been had with “Standard Method” for determining performance of the ESP based on input data in place among the various window forms of “Data Entry and Editing”. As had been demonstrated, “Standard Method” determines the performance of the ESP whose input parameters are included in the various window forms under “Data Entry and Editing”. It has also been demonstrated that, in doing so, there could be disagreement between the set and calculated currents. It has been further learned that the reason for the difference is a possible mismatch between the actual operating parameters of the ESP and the corresponding data entered into ESPVI 4.0W.

“Performance Calc” pull-down menu allows a choice of several other computational methods. All of these reset various input parameters to make ESPVI 4.0W match the calculated currents for each section to the entered “set” currents. These adjustment methods are useful if the currents are accurately measured and if the ESP is in good mechanical and electrical condition. By these computational methods, the effects of changes to these parameters can be explored to determine if they can realistically explain differences between the entered “set” current and the calculated current.

The first is “Adjust Peak Factor”. In “Operating Voltages”, is the text box data entry **Peak-to-average voltage ratio** which sets the ratio of the peak to the average voltage as can be seen in the wave form representation of Figure 2-12. The value of the peak-to-average ratio does have a significant effect on ESP performance. It is sensitive to the electrode geometry and the TR set configuration. The peak voltage dominates the level of charge placed on the particles, and the average voltage effects their collection.

The “Adjust Peak Factor” command on the “Calculate V-I Curve” pull-down menu instructs ESPVI 4.0W to reset the **Peak-to-average voltage ratio** for all sections of the ESP so that the calculated and set currents are the same. If TR set limits have been provided, it will not allow the **Peak-to-average voltage ratio** to be set to a value outside the limit.

The next is “Adjust Onset Factor”. The **Corona Onset Factor** has been set for each element in each section in “Electrode Design”. “Adjust Onset Factor” will attempt to apply an independent correction to each of the section’s **Corona Onset Factor**, without going outside the allowable range of 0.6 to 1.0. **Remove starting voltage bias** on “Operating Voltages” will reset the adjusted corona onset factor. Alternately, “Open” can be used to restore the original value.

In will be shown in Chapter 6, that the gas property called ion mobility plays an important role in determining the voltage and current curves for an ESP. On the “Gas Properties” window, the ion mobility is shown as **Mobility**. To reconcile the calculated currents to the “set” currents, ESPVI 4.0W will modify the ion mobility of the gas.

Each of these adjustments is independent of the others. Either one or more than one of them can be performed. If more than one is used, they will, of course, be done sequentially (user can adjust the sequence). The results could be different depending on the order in which they are performed. One of the methods may partially reconcile the currents, and then another could complete it. However, the results could be different depending on the order in which the methods are applied. It should be realized that the adjustments are used to compensate for incomplete knowledge of the ESPs operating conditions.

An alternative and more desirable approach, rather than allowing ESPVI 4.0W make the "adjustments", is to develop a deeper understanding of ESP operation and thereby make the adjustments to the various data inputs oneself. By developing this ability and understanding, adjustments that are more rational can usually be made to reconcile the two currents.

The remaining item "Compute Maldistribution" on the "Performance Calc" pull-down menu will be discussed in Chapter 4 of this manual.

3.6 The Effects of Varying the High Voltage

As previously discussed, changing the operating parameters on an ESP will change its performance. Changing those parameters in ESPVI 4.0W will cause the same change to the predicted performance. Among the more critical of the parameters is the high voltage supplied to the ESP.

For SAMPLE, the high voltages for all sections will first be increased by 1 kV and then reduced by 1 kV to observe the effect on current and penetration.

An ESP in good operating condition with a well operating controller for its energization source will be kept working at its optimum settings. It would be assumed, then, the electrical conditions for SAMPLE are set for the optimum conditions. Therefore, raising the voltages by 1 kV would generally not be a realistic thing to do. However, it is being done here to demonstrate the sensitivity of an ESP to changes in the very important parameter—voltage.

To work this example it is necessary to "Open" SAMPLE under "Files". Then go to "Operating Voltages" and change the voltages for each of the sections in the **Voltage** text boxes. The first entries will be to increase the voltage by 1kV. Then click **Accept** to close the window. Then use "Standard Method" followed by "All Results" to obtain the following voltages, currents and penetrations. After the completion of the calculations, go to "Files" and "Open" SAMPLE to restore the original parameters. Do not use "Save".

Repeat the procedure for the next set of calculations. This time decrease the voltage in each section by 1kV. The results of these two exercises are shown below in Table 3-1.

These are rather small changes in the voltages supplied to each of the sections, yet the change in emissions is significant. The change in power input to SAMPLE is also significant, which further indicates that a relationship exists. If SAMPLE were being subjected to regulations, it is possible that a small change in voltage could put it out of compliance with the regulations.

In practice, mechanical or electrical problems within the ESP could cause relatively low voltage on a section. The next example will explore this possibility.

Table 3-1. The Effects of Varying High Voltage on ESP Performance

Section	Parameter	Original Conditions	+1 kV	-1 kV
1	Voltage, kV	41.0	42.0	40.0
	Current, mA	0.180	0.199	0.161
2	Voltage, kV	40.0	41.0	39.0
	Current, mA	0.217	0.238	0.197
3	Voltage, kV	39.0	40.0	38.0
	Current, mA	0.216	0.237	0.197
Total	**Penetration, %**	2.37	2.17	2.61
	Emission Change, %	-	+8.4	-10.1

3.7 The Effect of Low Voltage on One Section

This example is similar to the one in Section 3.6 above, except that the voltage, first for Section 1, then 2, and finally 3, will be entered for 25 kV in separate computation runs. Occurrences such as these could be the result of TR-set problems or severe misalignment.

The reduction of voltages applied sequentially to the three sections produces the results shown in Table 3-2.

Table 3-2. The Effect of Low Voltage on One Section on ESP Performance

Section	Parameter	Original Conditions	Section 1 Low	Section 2 Low	Section 3 Low
1	Voltage, kV	41.0	25.0	41.0	41.0
	Current, mA	0.180	0.000	0.180	0.180
2	Voltage, kV	40.0	40.0	25.0	40.0
	Current, mA	0.217	0.176	0.001	0.217
3	Voltage, kV	39.0	39.0	39.0	25.0
	Current, mA	0.216	0.200	0.212	0.007
Total	**Penetration, %**	2.37	4.79	3.46	3.26
	Emission Change, %	-	-102	-46.0	-37.6

There is a reason for this difference in penetrations. With the first section almost completely without charging, all of the collection had to be done by the second and third sections. For the case in which the second section is subjected to the low voltage, the first section charged and collected normally. The second section, although it was not charging the particles, still had some electric field to collect the charged particles from the first field. For the last case, the third field received particles with an even higher level of charge. The particles that are being discussed here are generally the smaller ones that are subject to diffusion charging and that do not receive a saturation charge but whose level of charge acquired is time dependent.

An additional interesting and very important point is that, with the first section at lower voltage and therefore not charging and collecting particles, the electrical conditions in the second and third sections are significantly changed. In the second example, in which the voltage to the second section is lowered, only the third field experienced a change of electrical conditions; the inlet section was operating normally. For the last example, in which the voltage to the third section was lowered, the first two sections had normal operating conditions. This further illustrates the important concept that a change in the operating conditions of one of an ESPs sections or fields affects the sections downstream, but not the ones upstream. In practice, ESPs are often operating with such relatively low voltages due to uncorrected electrical and mechanical problems.

3.8 The Effect of Changing the Peak-to-Average Voltage Ratio

The peak-to-average voltage ratio is an often-overlooked factor in determining the performance of an ESP. ESPVI 4.0W asks for the peak-to-average voltage ratio as one of its inputs in “Operating Voltages”. If the measured peak-to-average voltage ratio is not available, it is suggested that a reasonable value of about 1.2 be used for full wave energization. This example is to illustrate the sensitivity of an ESP to a change in this value.

SAMPLE is currently set up with a peak-to-average ratio of 1.2 for all of its sections. This means that the peak voltage from the TR set is 1.2 times the average or high-voltage panel meter reading. It will be changed to another reasonable value of 1.1 for all the sections.

The procedure is the same as in the previous exercises. Make certain SAMPLE is “Open”. In the “Operating Voltages” window, enter the new **Peak-to-Average Voltage Ratio** of 1.1 into Section 1. Use **Copy Right** to copy into the other sections and then use **Accept** to close the window, Use “Standard Method” and then obtain the performance from “All Results”. This effect is shown in Table 3-3.

Table 3-3. Effect of Changing Peak-to-Average Voltage Ratio on ESP Performance

Section	Parameter	Peak-to-average	
		1.2	1.1
1	Voltage, kV	41.0	41.0
	Current, mA	0.180	0.119
2	Voltage, kV	40.0	40.0
	Current, mA	0.217	0.213
3	Voltage, kV	39.0	39.0
	Current, mA	0.216	0.214
Total	**Penetration, %**	2.37	2.63
	Emission Change, %	-	-11.0

The difference in emissions, which is about 11 percent, significantly affects the performance of the ESP, which reflects in ESPVI 4.0W. The peak-to-average ratio is not a parameter that is easily changed for an ESP. It is dependent on the TR-set properties; the electrical

capacitance, which is a function of the size of the energized bus section; and the corona current, which draws down the charge of the capacitance. It is presented here as an additional example of how important it is to try to obtain the best data possible to accurately characterize the operation of an ESP and predict its performance.

3.9 The Effect of Increasing Fly Ash Resistivity

In the examples and illustrations up to this point, the SAMPLE ESP has been operating with a fly ash having a resistivity of 1×10^8 ohm-m, shown as 1.0E+08 in ESPVI 4.0W, which is a moderate resistivity fly ash that collects well in an ESP. In Chapter 6 of this manual, PM on this resistivity is referred to as "normally favorable dust". If the resistivity of the fly ash were to be raised, the electrical conditions would have to be reduced to prevent the formation of reverse ionization or back corona. The reduction in the electrical conditions, as expected, would reduce the performance of the ESP.

In solving the problem of determining the proper electrical conditions, ESPVI 4.0W's calculation features are going to be used. The "Automatic V-I" curve does have the feature that allows it to suggest when reverse ionization is starting. The "Fixed V-I" curve does not have the automatic stop for reverse ionization. However, it does have other features. For this example, both will be used.

Reverse ionization or back corona starts when the electric field in the dust layer becomes sufficiently high so that the gas in its interstitial spaces breaks down and ionizes. The strength of the electric field is a function of both the dust resistivity and the current flowing through it. A typical dust-layer breakdown electric field is about 10,000 volts per cm. To avoid exceeding this breakdown field in the dust layer, as the resistivity increases, the corona current has to be reduced, which is accomplished by lowering the voltage. The electric field in the dust layer is the product of the resistivity and the current density.

This is essentially what ESPVI 4.0W does on "Automatic V-I". It shuts down when it senses that the criteria for reverse ionization has been reached on the ESP section for which it is developing V-I data. Some elements or electrodes have higher currents than others, which may stop the V-I calculations at what may appear to be a low average current density. For "Fixed V-I", sensing reverse ionization conditions causes ESPVI 4.0W to place an asterisk next to the average current density as an indicator.

The unevenness of the current density has prompted a suggestion that the average current density be reduced by factors of 5 to 10 for resistive dusts to prevent the onset of back corona (Hall, 1971). It is the opinion of the authors of this manual that a factor of 10 reduction is reasonable for very high space charge conditions that are common in the NIS. This would cause the average current to be no more than 1 nA/cm^2 for a resistivity of 1×10^{10} ohm-m and no more than 0.1 nA/cm^2 for a resistivity of 1×10^{11} ohm-m.

The "Automatic V-I" example will be done first. "Open" SAMPLE, go to "Operating Voltages", and change **Resistivity** from 1.0E+08 to 1.0E+10 ohm-m and then **Accept**, which closes the window. Then go to "Automatic V-I" and proceed, using the small window that

appears to develop the V-I curve data for all three sections. Figure 3-6 shows the display containing the V-I data on the left for the ESP's third section and the V-I curves for all three sections on the right side. The curves show, for a well operating ESP, the characteristic differences in sectional V-I curves that change with decreasing space charge. For the graph on Figure 3-6, **Graph full-scale current density** in "Calculation Options" was changed from its normal 20 nA/cm^2 to 10 nA/cm^2.

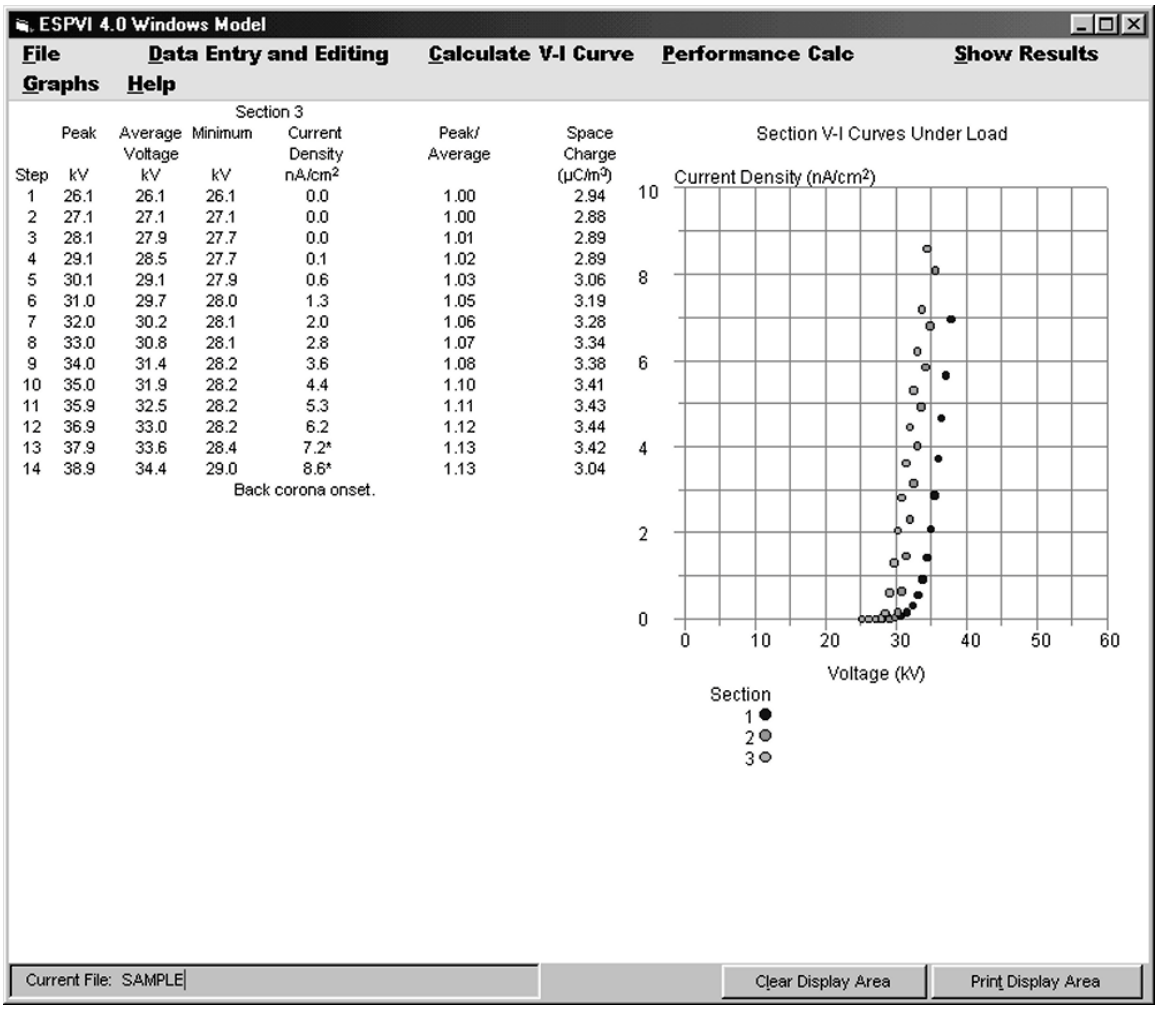

Figure 3-6. "Automatic V-I" calculations for SAMPLE operating with resistive dust.

The above procedure is repeated for "Fixed V-I". Changes to "Calculation Options" are that **Maximum local current density** is lowered to 1 nA/cm^2 as shown in Figure 3-7. Then go to "Show Results" to view the performance.

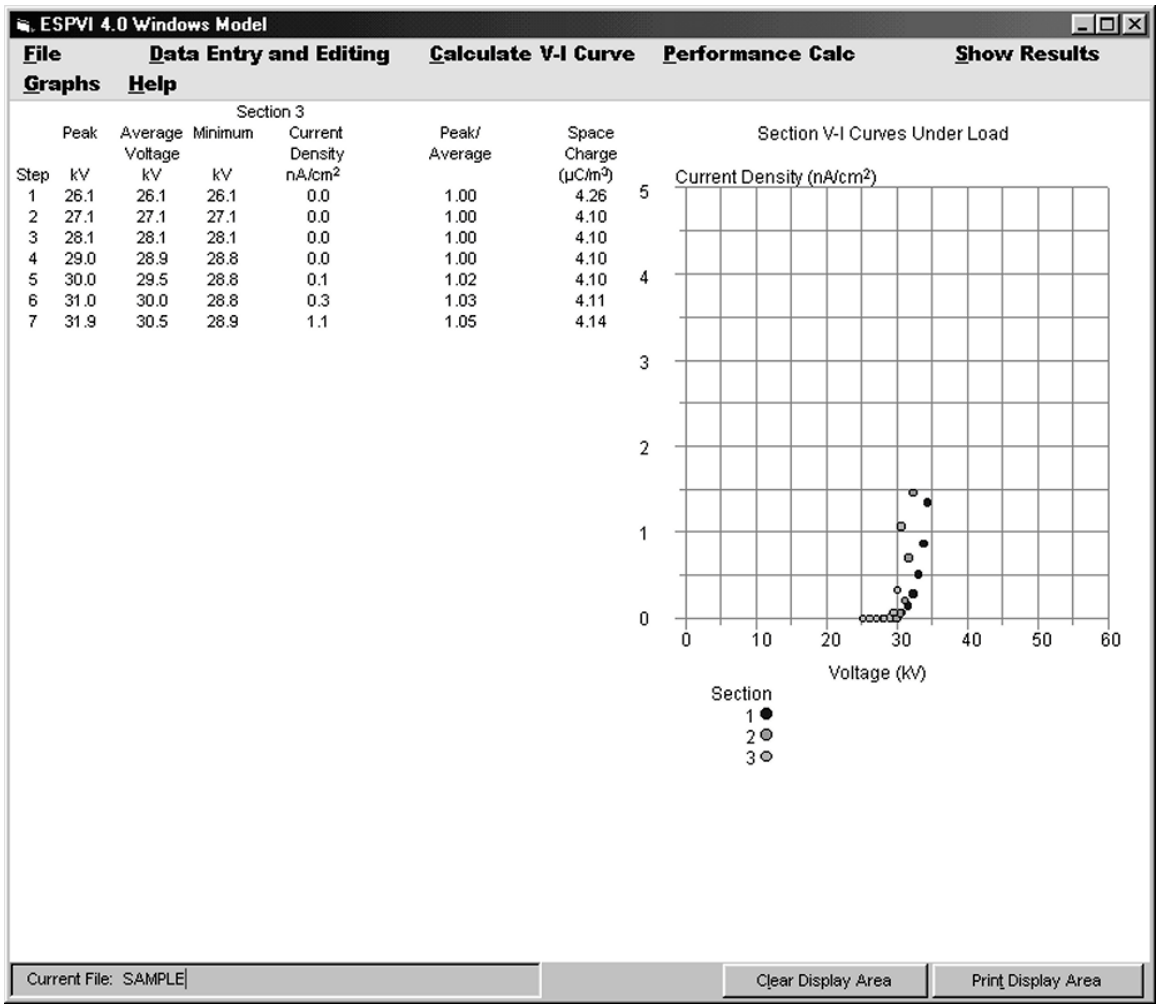

Figure 3-7. “Fixed V-I” calculations for SAMPLE operating with resistive dust.

The performance from “Show Results” for both examples is shown in Table 3-4.

Table 3-4. The Effect of Fly Ash Resistivity on ESP Performance

Section	Parameter	Original conditions	“Automatic V-I”	“Fixed V-I”
1	Voltage, kV	41.0	37.8	34.3
	Current, mA	0.180	0.077	0.016
2	Voltage, kV	40.0	36.2	32.2
	Current, mA	0.217	0.122	0.018
3	Voltage, kV	39.0	34.4	30.5
	Current, mA	0.216	0.100	0.013
Total	**Penetration, %**	2.37	5.19	8.61
	Emission Change, %	-	-119	-263

It is obvious that the performance of an ESP with a resistive dust will be worse than it is with a favorable dust. If an ESP in otherwise good condition is operating with a resistive dust, lowering its resistivity by a means such as gas conditioning will improve performance.

One additional and important point is that the conditions for the onset of reverse ionization are not adequately known. As seen by the above example it is best to approach it conservatively.

Reverse ionization or back corona will be explored more fully in subsequent parts of this manual.

Chapter 4
Impact of Mechanical Features on Electrical Operation

A number of mechanical aspects of an ESP's design are intimately related to its operation and performance. Some of these aspects are mainly mechanical while others, though mechanical in nature, have effects on the ESP's electrical operating conditions. These mechanical features will be considered in detail and, where applicable, will be related to ESPVI 4.0W.

4.1 Corona Discharge Electrodes

In an ESP, its size, shape, and distance from the grounded collector electrodes primarily govern the electrical characteristics of the corona discharge electrode. Generally, the smaller the physical cross-sectional size of the electrode, the lower the voltage at which it goes into corona. In commercial applications, the shape of these electrodes range from a very simple circular cross section up through complex fabricated assemblies. For certain applications, some of these are of the "controlled emission electrode" type used for high current applications, especially in a high space charge environment. Various means have been used to support the discharge electrodes within the ESP. Small sized electrodes have been hung from a supporting assembly with weights at the bottom to keep them taut. Other types of support means for the discharge electrodes make use of a mast and spar assembly or else positions them within a frame.

Figure 4-1 illustrates the variation in corona onset voltage and its effect on the V-I curves for three different discharge element diameters in a wire/tube ESP. It also shows that the corona onset voltage is influenced by the distance between the discharge and the collector electrodes. The same effect occurs in the more conventional wire/duct ESP.

The circular cross section discharge electrode lends itself most readily to analytic solutions to determine its corona onset voltage and its voltage current characteristics. For this reason, ESP models generally use the circular cross section or round electrode in their computations. The ESPVI 4.0W is no exception. However, features that are unique to ESPVI 4.0W allow it to simulate, by using round electrodes, virtually any complex electrode currently used in commercial practice. The ESPVI 4.0W accurately determines the corona onset voltages and voltage current relationships as a function of electrode size and spacing. Later in this chapter, information will be provided on how to enter data into the ESPVI 4.0W for round wire electrodes. Information is also provided for using one or more round wire electrodes to simulate some of the more complex electrode types. Figure 4-2 shows various typical corona "unbreakable" discharge electrode formats.

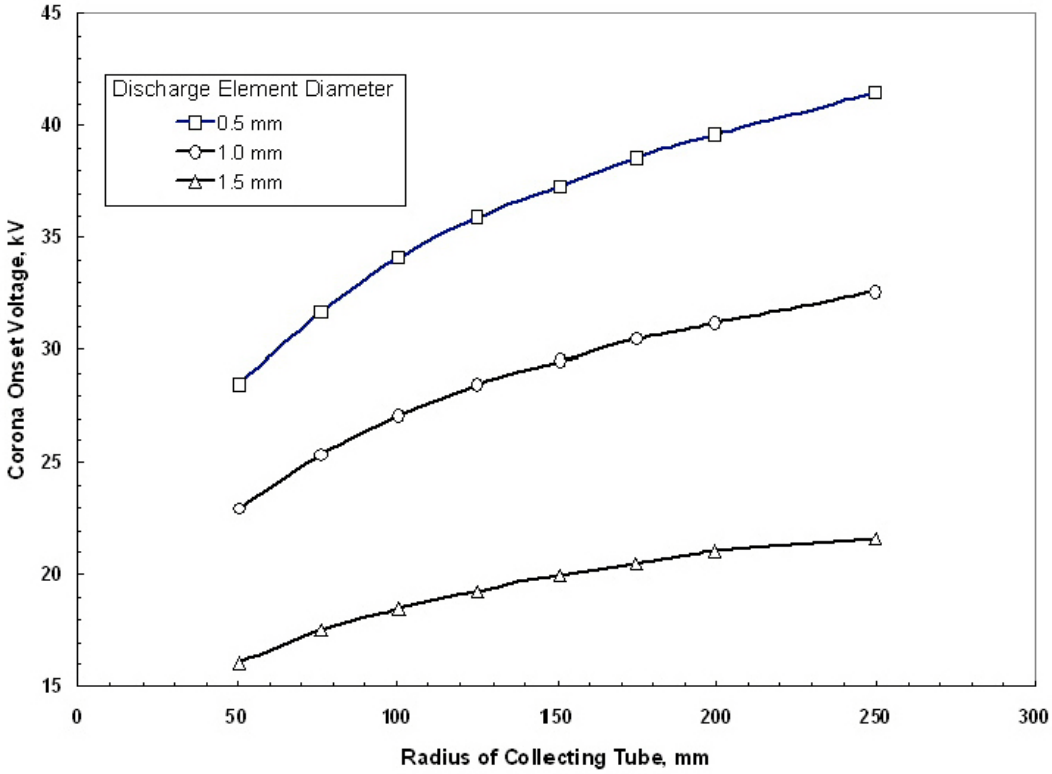

Figure 4-1. V-I characteristics indicating the corona threshold voltage for different electrode diameters.

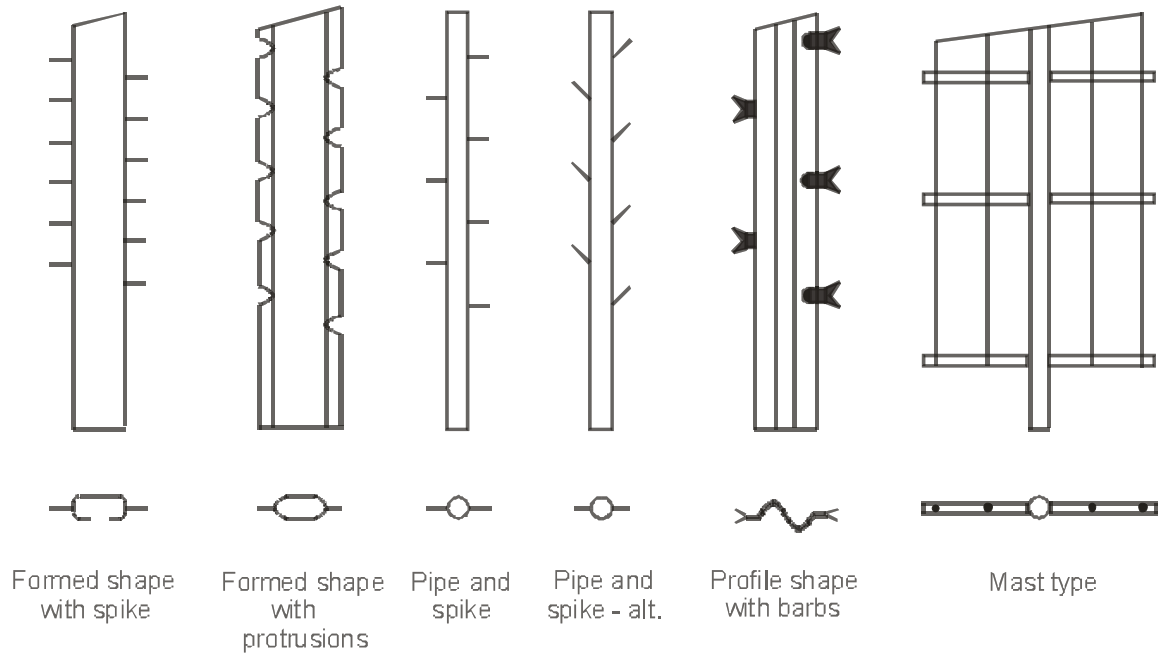

Figure 4-2. Typical discharge electrode types.

4.2 Discharge Electrode Formats

The type of discharge electrode used over the past century has taken many different forms and designs. These have ranged from the earliest of barbed wire to a pubescent electrode comprising a semi-conducting fibrous material, which produced a continuous corona at a relatively low voltage of 15 kV. Some of the present complex designs are termed by the suppliers as corona controlled or "unbreakable" types.

Most of the early installations were of the wire-tube design, many using a simple 2 to 3 mm diameter-weighted wire as the discharging element, the weight being necessary to hold and tension the wire in its proper location. Square and hexagonal shaped wires superseded the simple round wire of these early installations. These have greater mass to withstand flashover and rapping vibration while having similar discharge emission characteristics.

The practical significance of the space charge effect and corona suppression became recognized while handling large quantities of fine fume, especially as the target efficiency demands increased. This led to the development of the high emission, or controlled emission, electrode. This electrode is distinguished by having sharp protrusions where, as a result of the high field intensity at the sharp point location, optimum corona develops. Figure 4-3 indicates a range of discharge electrode formats of the controlled emission type, together with their experimentally determined "standard air" V-I characteristics. Standard air, or "air

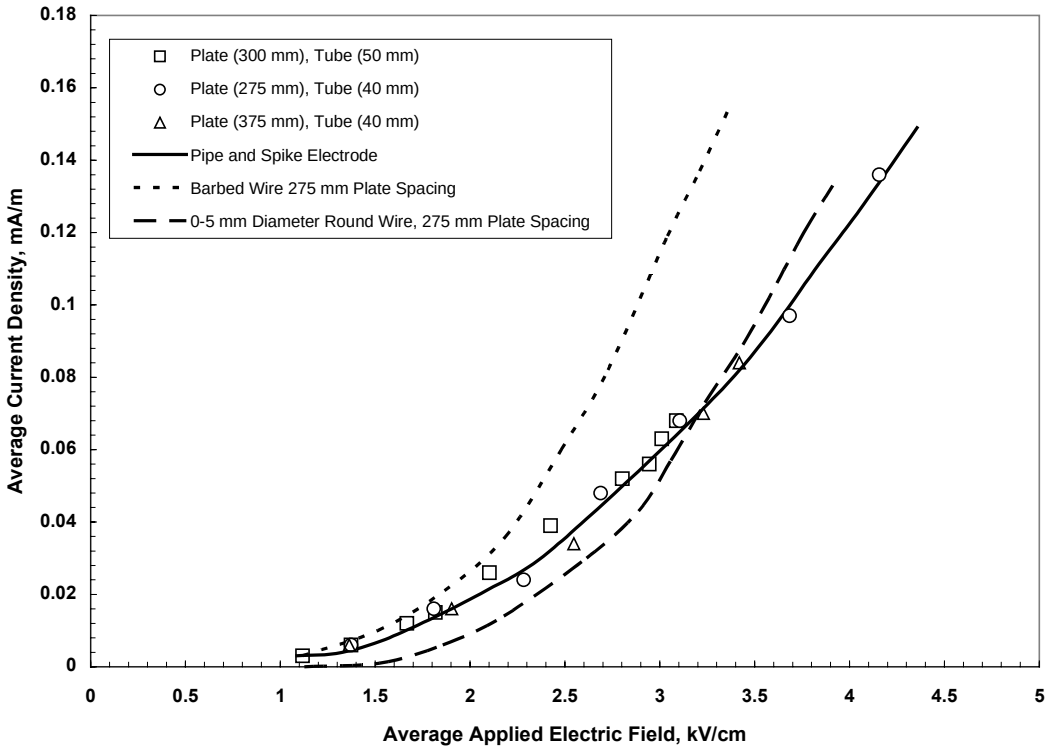

Figure 4-3. Typical air load V-I characteristics for various electrode formats

load," electrode characteristics are very useful for modeling complex electrodes with ESPVI 4.0W. In normal ESP service, the presence of particles and their accompanying space charge makes it difficult to identify the electrodes characteristics. Once modeled with air load data, the electrode's electrical characteristics can be applied to dust laden gas conditions. Examples of the procedure for doing this will be shown later in this chapter.

Because of the quantity of material used in the fabrication of the above electrodes, most are classified by the suppliers as "unbreakable" electrodes. This is partially true in comparison with the weighted wire electrode, which is subject to failure because of flashover, electric field induced oscillation, rapping vibration, and spark-induced erosion at the fixings. It should be pointed out that only a single electrode has to fail to produce a resultant drop in overall ESP performance, since it impacts on the electrical operating conditions within that particular ESP section.

Modern ESPs have become much larger to meet efficiency and improved reliability demands. At the same time, they also become taller to minimize cost and "foot print", or space occupied. With modern fabrication techniques and procedures, the present trend is to use collector plates up to 5 m wide by 15 m high, which precludes the use of weighted wire forms of discharge element, and some type of "unbreakable" discharge electrode is the usual practice. This form of electrode can be readily mounted within a frame, which secures better alignment than other designs and assists in distributing the transmitted rapping blow throughout the system.

The selection of a discharge electrode form for a specific duty demands careful consideration, since each electrode has its own specific emission characteristic. The controlled emission electrode has excellent high corona current capabilities, making it ideal to overcome corona suppression effects. In the absence of suppression conditions, the total corona current supplied can be significantly higher, which not only means that the TR equipment must be much larger, but the power consumption will also be significantly higher.

The effect of space charge or corona suppression can be readily observed in any ESP installation handling a gas containing particulates. For example, Figure 2-3 shows the electrical operating characteristics of the four sections of a 400-mm spaced-plate-type ESP application handling modest concentrations of fly ash. As shown before, the presence of space charge on an upstream section of any operational unit impacts the one immediately downstream. Therefore, if the upstream section is de-energized, the immediate downstream section takes on the properties of the original upstream section (the downstream section replicates the original space charge condition).

4.3 Spacing of Discharge Electrodes

With any ESP design, the separation/location of the discharge electrodes within the duct can significantly influence the electric field and the amount of ionization produced. For tube type ESPs, the number and location of the discharge electrodes for optimum performance is fixed, whereas with the plate type, there is an optimum location for the discharge electrodes within the duct walls.

In practice and from calculations, it can be shown that the optimum discharge electrode spacing is approximately equal to half the duct width. At about this spacing, all of the electric field lines terminate on the collector electrode. Too close an electrode spacing will result in corona suppression between adjacent elements, truncating some of the electric field lines and leading to reduced corona current flow. It will approach becoming a non-emitting system if the elements are too closely spaced. By spacing out the electrodes more widely in the ducting, the corona suppression situation will be minimized. This will lead to a point such that some areas will receive very little electric field. The electrically active area can decrease to such an extent that performance of the ESP is compromised.

Figure 4-4, presents an experimental plot of a simple electrode spacing in a 400 mm wide duct or passage against specific current and illustrates the effect of both too wide and too close a spacing (location) between the discharge electrodes. From this and other investigations using simple electrode forms, the optimum spacing for specific maximum corona current appears to be equal to half the duct separation regardless of actual duct width. Therefore, in respect to discharge electrode spacing, a good general rule is to space them at about half of the spacing of the grounded collector electrodes.

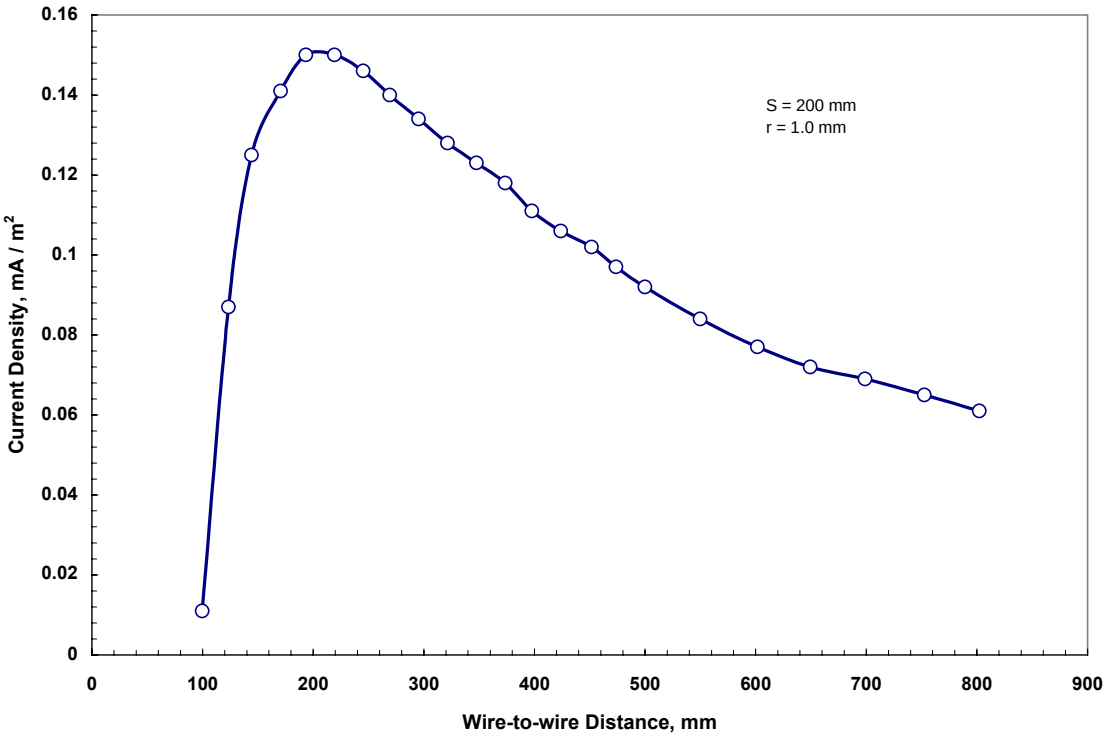

Figure 4-4. Effect of electrode spacing on specific current.

For more complex types of controlled emission electrodes, particularly those having protrusions lying parallel to the duct walls, the half duct spacing may not be correct since emission from adjacent points may suppress each other. In the past, it was necessary to determine the optimum element spacing from experimental procedures. Today the simplest

and most accurate method is to use modeling, considering electrode spacing in computations. Later, in this chapter, instructions will be provided to show how to set the electrode-to-electrode spacing. Once this is done, it will determine the correct electrical conditions for that configuration.

4.4 Collector Electrodes

For any form of ESP, the collector electrode should be non-emitting as regards corona emission. This is achieved by having a large radius of curvature in comparison with the discharge elements, which for a duct type ESP means a flat collector electrode profile.

With horizontal flow units having plate dimensions up to 5 m × 15 m, the collectors usually comprise a number of roll-formed channels, typically fabricated from 1.6 mm thick material, mounted between heavy upper and lower members to attain the required degree of straightness and stiffness. For optimum performance with the largest collectors, the degree of straightness which one is seeking is a tolerance of around ± 5 mm. Typical collector sheet profiles as used in the NIS are shown in Figure 4-5.

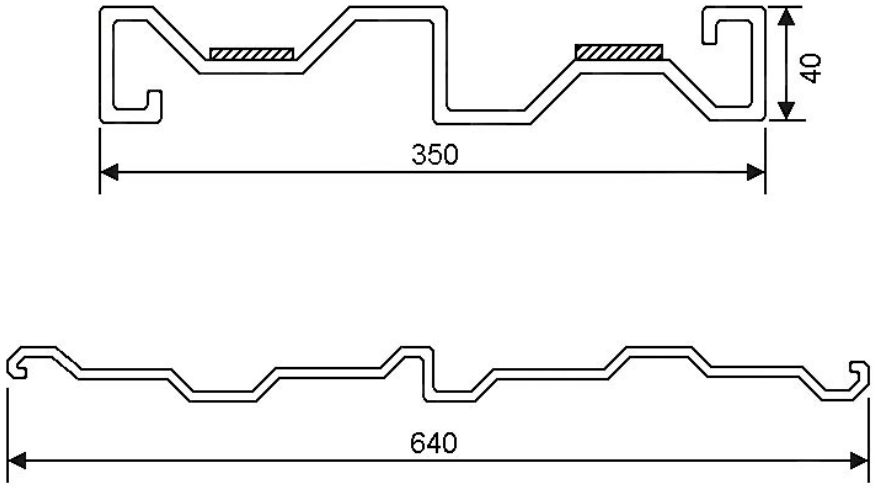

Figure 4-5. Typical NIS collector sheet profiles.

4.5 Specific Power Usage

An indicator of improved particle collection efficiency in an ESP is an apparent increase in the power that is used. Since the particle migration velocity is proportional to the voltage squared for field charged particles, it follows for a given electrode configuration, which determines the voltage/current relationship, that the efficiency is related to the specific power input (W/m^3). It can be shown that the performance, or collection efficiency, for a normally energized ESP can be related to the total power consumed. This relationship can be expressed simply as kV × mA for the gas flow in question, or more precisely, the specific power usage in W/m^3.

Although secondary voltage and current were originally used in the evaluation, with modern instrumentation it is possible to use either secondary or primary power metering, assuming the transformer losses are known or can be measured as discussed previously in Chapter 3. Figure 4-6, illustrates such a relationship for a power plant ESP installation. The significant increase in specific power required to achieve efficiencies in excess of 99.5 percent is related to the reduction in space charge. This leads to a much higher corona flow, and hence power consumption, as the gas becomes cleaner and particle concentration reduced towards the outlet end of the ESP.

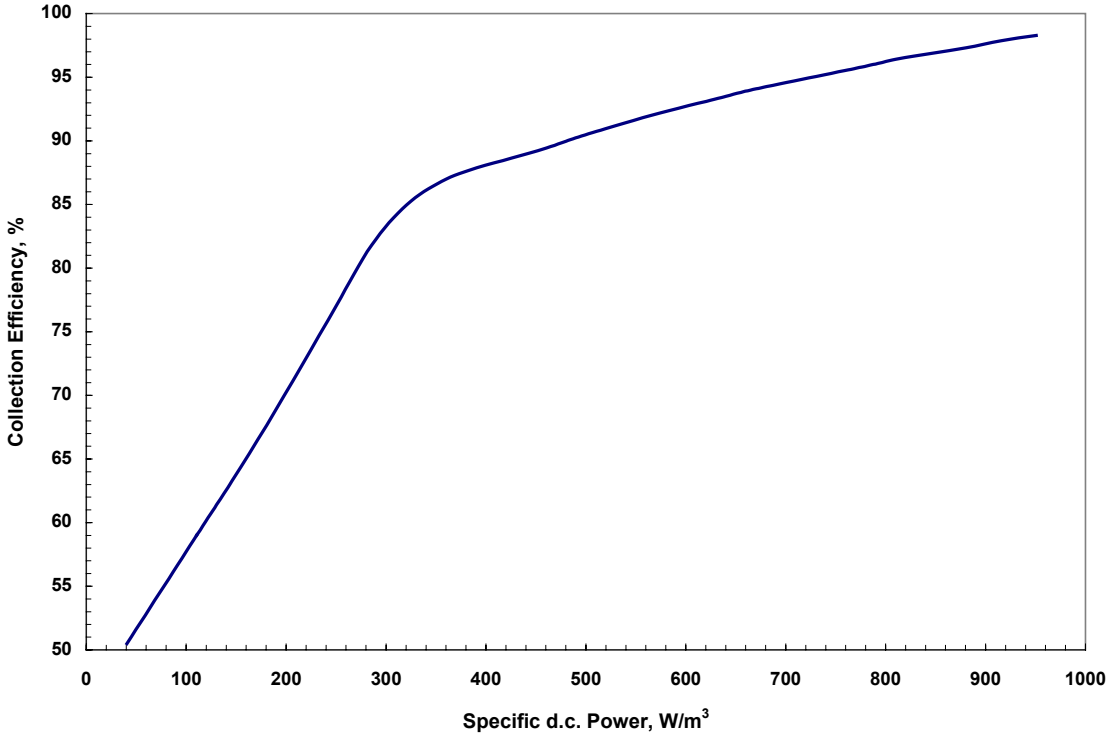

Figure 4-6. Effect of specific power absorption on ESP efficiency.

On most industrial applications, there is always a small amount of fine particulate material present in the waste gases. This fine PM arises from the condensation of initially volatilized feed stock contaminants in the cooler reaches of the plant. These fine particles are the ones that are in the size range of about 0.2 to 0.8 µm, for which neither diffusion nor field charging dominates, and are consequently more difficult to charge and collect. As the required collection efficiency approaches 100 percent, the effect of the reduction in the fractional efficiency with reducing particle sizing becomes significant. Therefore, a much larger plate area, and hence power usage, is required to achieve the necessary efficiency. This is the reason for the change of slope in the curve in Figure 4-6.

The form of the specific power/efficiency curve remains similar for all applications although the actual value of specific power will depend on the discharge electrode emission characteristics, particulate size analysis, gas composition, temperature, and, to a certain

extent, the ESP construction details. Generally, however, it can be considered that the higher the power that an ESP will usefully absorb without running into arcing conditions, back ionization, electrode misalignment, or effects of flow mal-distribution the higher is the efficiency attainable.

Depending on specific power absorption by itself as a means for improving ESP efficiency may lead to erroneous results. Specific power absorption is not an independent variable that will lead to improved ESP collection efficiency if increased. Instead, it is a dependent variable that often increases if correct measures are taken with the ESP. It is necessary to make certain that the ESP is in good operating condition both electrically and mechanically. Once this is done, changes can be made to the ESP that will improve the collection efficiency. It will likely be found that the specific power absorption will have increased at the same time.

ESPVI 4.0W can be used to optimize the performance of the ESP with the least increase in specific power usage. It will quantify the dust collection improvement and will also allow the calculation of the expected increase in specific power absorption. Furthermore, ESPVI 4.0W can be used to determine still further improvements in performance that can be achieved by making additional changes to the ESP.

4.6 ESP Sectionalization

To optimize the overall performance when treating a large flow rate, as on modern power plants, it is common practice to split the ESP into separate bus sections, both in the width and length, and to energize each section with its own TR equipment.

Splitting the unit across the width also allows any significant temperature or gas flow stratification to be more readily accommodated using individual TR sets rather than just one, which would only operate under the least onerous operating condition. By dividing the unit in length, as the gases move towards the outlet and become increasingly dust free, the decreasing space charge effect, and hence higher corona currents, are more able to be controlled/optimized by their individual TR equipment.

Although current designs of rectifier equipment can have current ratings up to some 2000 mA and can safely energize some 10,000 m^2 of total collector plate, it has been found that increases in the total plate area energized by a single rectifier has a detrimental effect on performance. Sparking in an ESP section is very much a probabilistic effect. The larger the section, the higher is the likelihood that there will be sparking because there are more sparking sites available. Therefore, the larger the section, the lower is the resultant voltage at which it can operate to keep flashover in check, which results in decreased corona current and, consequently, the accompanying specific power absorption. This effect is indicated in Figure 4-7, covering a range of U.S. power plant installations.

Not only does a flashover on one electrode have a larger impact on the overall efficiency, but the increase in capacitance of the larger section being energized—and the time required re-energizing it—results in a drop in the specific corona discharge such that the performance

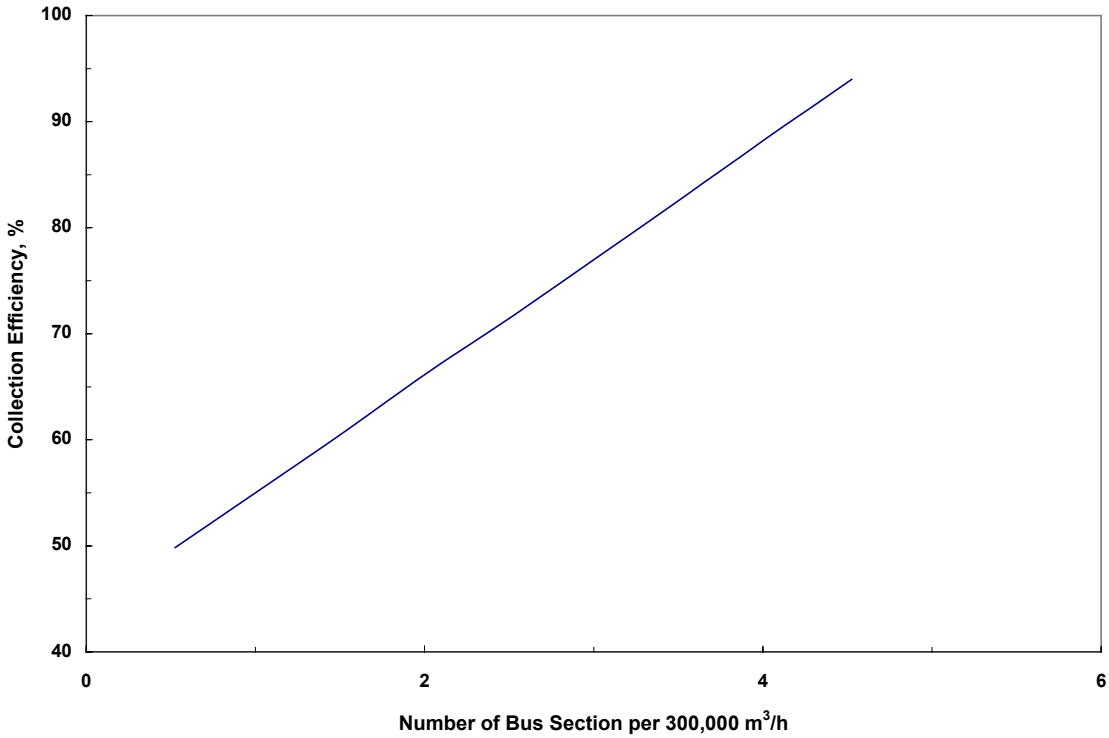

Figure 4-7. Effect of ESP sectionalization on performance.

decreases. Figure 4-8, indicates how the specific corona current (produced from a 4 mm square wire discharge electrode for a duct spacing of 300 mm) reduces as the size of the field energized by a single rectifier set increases. The curves depict ESPs treating normal fly ash at temperatures up to 150 °C and at temperatures around 300 °C, assuming that the discharge electrodes are optimally spaced and the plants are operating just at the point of flashover. In practice, the rate of reduction is not too significant for current power plant installations having individual field sizes of at least 5,000 m^2, and the impact on overall performance is therefore limited.

Accordingly, if an existing installation is not meeting the required performance level, it may be possible to improve the efficiency by splitting the field into smaller bus sections, each energized with its own rectifier equipment. ESPVI 4.0W can be used for determining this improvement.

From Figures 4.7 and 4.8, it will be noted that the performance of very small bus sections, such as those on pilot plants, is higher in terms of migration velocity than would be obtained from a large installation. This generally results from the inability of a large bus section to operate at the same higher voltage as a smaller bus section, with everything else being equal. Accordingly, caution should be used in scaling up from pilot- to full-scale operation, as some suppliers use a scale factor when considering pilot data while others reduce the specific corona input to equate to the full-scale consumption. Either approach can give satisfactory design information providing the pilot data is backed by full-scale performance results, with

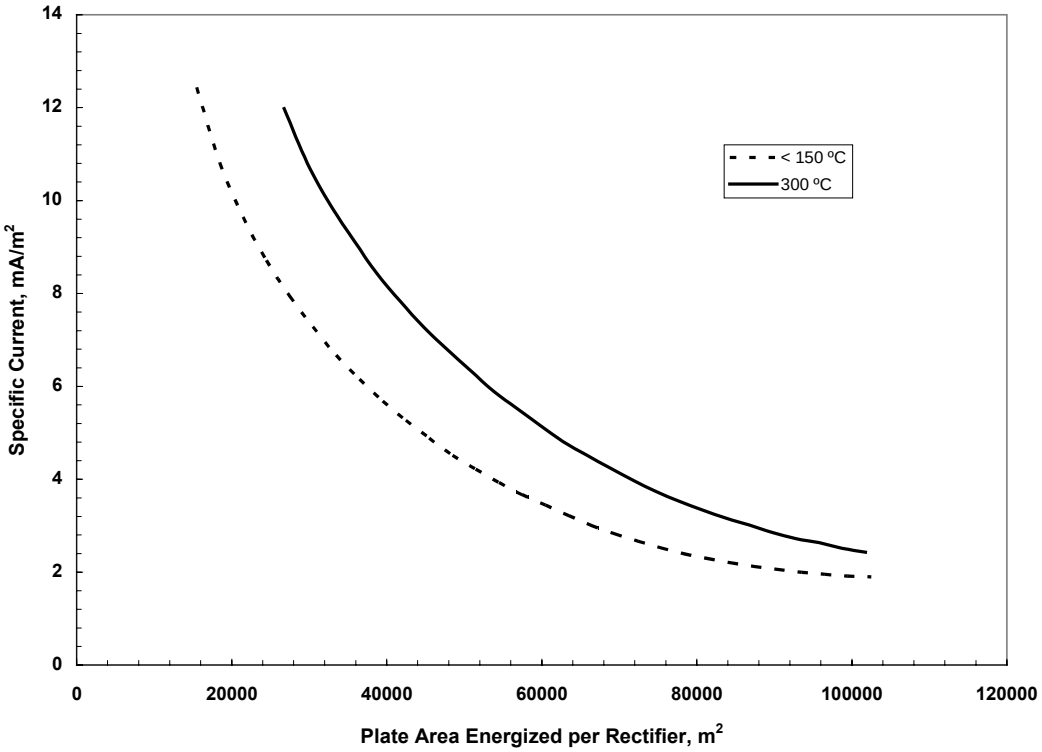

Figure 4-8. Effect of sectionalization on specific current production.

the caveat that the pilot testing must be carried out under the same inlet conditions as the full-scale plant.

A more modern, quicker, and more economical approach is to use modeling. Provided with information about the achievable electrical conditions between the pilot- and full-scale ESPs, ESPVI 4.0W will easily be able to relate the results of one to the other.

4.7 High Tension Insulators

Modern ceramic materials, such as high alumina porcelains, alumina, silicon nitride, silica, and such, are currently used for high tension insulators. Two approaches are employed to support the discharge frame. The first is directly vertically loaded, such as the “flower pot” design, and the second is outboard post insulators, in which the dead load of the discharge frame is carried from a cross structure. In either case, it is important that the insulator is maintained in a purged hot, dry condition such that deposition by any flue gas component and resultant electrical tracking or surface leakage is avoided. Generally, the requirements for any support insulator are that the material must have sufficient strength to support the weight of the discharge electrode system. It also must be electrically strong to withstand operational voltages of up to 110 kV in the case of 400 mm spaced collectors. Failure to do so would subject the rectifier equipment to electrical loading because of surface leakage.

ESPVI 4.0W, with its input parameters well calibrated to the operating conditions of the full-scale ESP, is a good means for indicating the presence of surface leakage of the ESP. The model will indicate what the corona onset voltage should be. If the ESP's panel meters indicate an ohmic type current at voltages less than the predicted corona start voltage, current leakage is probably present.

Figure 4-9, shows the effect of electrical tracking across the surface of a high-tension insulator as compared to a normal ESP section. This leakage, which is ohmic in nature, will indicate a current that starts at a low voltage and increases linearly until corona onset, at which point the corona current causes the curve to become non-linear. The tracking current is additional current that the energization equipment must supply to the section. As far as the ESP is concerned, tracking current appears as additional specific power adsorption that does not perform any useful function.

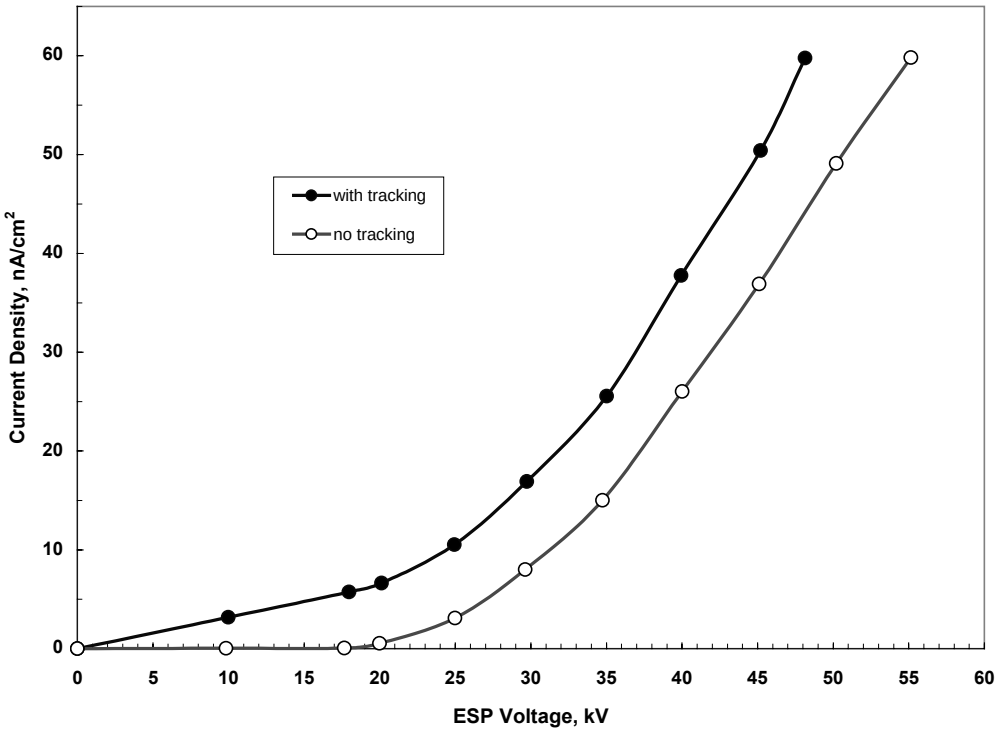

Figure 4-9. Effect of tracking across high tension insulator.

4.8 Electrical Clearances

The electrical clearances that must be carefully considered fall into two main categories. The first are those associated with the discharge electrodes and collectors. The second, which are sometimes overlooked, are the peripheral clearances in the high-voltage distribution system from the high-voltage energization sources to the ESP sections. Any electrical clearance that is too small will limit the operating voltage of the unit and affect the efficiency of precipitation.

In most cases, the electrodes are suspended so that they hang exactly mid-way between adjacent collectors at a separation of around half the collector/collector spacing. In practice, although the alignment is critical, a misalignment of up to ± 10mm on field heights of 10 m and above must be accepted because of erection and fabrication tolerances. It should be noted that some ESPs are designed with the corona sites located some distance off the center plane between the collector electrodes.

For collectors, the clearance between the stiffening channel edges and any emitting point should be greater than the collector half-spacing by 25 percent to provide satisfactory emission and voltage conditions. This distance applies in both the horizontal and vertical planes, since the electrodes or collectors may not hang exactly plumb.

Another area of concern with the discharge electrodes is the position where any support or carrier members pass through the collectors. In this case, not only should the member be low emitting, and have a large radius of curvature, they must also pass centrally between adjacent collectors.

For clearances outside the actual field area, the positioning of any live discharge electrode support members must be well clear of any grounded structural components. For safety, the following ‘rule of thumb’ minimum clearance distances should be adopted for any design. As positively energized components have lower breakdown strength than negatively energized elements, any sharp edges on the grounded collector, casing, or support members can result in premature breakdown.

For example, a separation of three times the discharge electrode/collector distance should be used for components having sharp edges opposing one another. Even with reasonably curved surfaces, such as those on rolled angles or joists, the minimum separation should be 1.5 times the discharge electrode/collector distance, with intermediate separations being adopted for differing profiles and edge conditions.

A special area of concern is where the discharge electrode support tubes pass through the casing and insulator. To minimize the quantity of heated purge air used with the cone or flowerpot insulator, the open area at the base is reduced by a restrictor in the form of a pro-filed electrical stress cone or bus ring. This, with a large diameter suspension tube (e.g., 50 mm), effectively minimizes the risk of breakdown in this area in spite of the actual clearance approaching, or being sometimes less than, the discharge electrode/collector separation. The location of the suspension tube must be truly central within the bus ring to be fully effective.

Where bus ducts rather than high tension (HT) cable are used to feed power to the electrodes, their diameter and profile must be such as to eliminate the risk of breakdown within the duct itself. If insulators are employed to centralize or carry the bus connection, these should have adequate tracking length to prevent breakdown resulting from atmospheric dust deposition, and such.

On large ESPs having discharge electrode frames spanning two or more hoppers, the actual distance between the frame and any cross-hopper apex member should take into account any potential dust deposition on the member to minimize the risk of breakdown.

Similar comments would apply to internal tumbling-hammer discharge electrode rapping systems, where the live shaft and hammers could give rise to suspect areas that would be difficult and expensive to overcome.

In general, the recommended clearances are given in Table 4-1 for any design of ESP.

Table 4-1. Recommended Clearances for ESPs

Condition	Minimum Clearance
Rounded Corner on DE System to Flat Earth	1.5 × ½ Duct Width
Sharp Edge on DE System to Flat Earth	2.0 × ½ Duct Width
Sharp Corner on DE System to Grounded Sharp Corner	2.5 × ½ Duct Width

Other components that may be built into the system should adopt the rule of thumb minimum clearance distances given in Table 4-1 in order that the maximum applied voltage is across the discharge electrode/collector system.

Although the above comments on clearances apply predominantly to new ESP designs, it should also be applied to older ones. Situations that do not meet the clearance criteria should be noted during inspections and maintenance. If they are corrected, higher voltages and currents can be applied to the ESP, which would result in improved collection efficiency.

4.9 Deposit Removal from the Collector and Discharge Systems

Dependent on the supplier, the rapping is achieved by a rotating tumble hammer, a lift and drop hammer, or by dropping a heavy rod onto an anvil connected to the component being rapped. The tumble hammer and lift and drop systems are normally operated through a motor-driven shaft and the drop rod by either a motor-driven camshaft or a magnetic lifting mechanism. Older systems, employing vibrators or mechanical lifting and dropping of the collectors, have been superseded by the foregoing, but can sometimes be found.

In order that the particles reach the hopper, the size of the agglomerate for power plant fly ash, when dislodged, must be some 1000 μm in effective diameter to overcome the horizontal component of gas flow. This means that a compromise has to be established on any operating plant, such that (a) the rapping provides sufficient energy to dislodge the deposited layer from the surface without causing the agglomerated layer to shatter and become re-entrained and (b) also limits mechanical damage to the components being rapped. Because the rate of deposition varies along the ESP, the rate or frequency of rapping is reduced from the inlet to the outlet fields. This is necessary to enable the deposited layer to achieve sufficient thickness to produce agglomerates of sufficient size to reach the hoppers when sheared from the surface by the rapping.

4.10 Hopper Dust Removal

Examination of the data logs from many operational plants, indicates that at least 70 percent of the reported dry ESP problems are associated with hopper dedusting difficulties of some sort. Accordingly, one cannot overemphasize the importance of developing a satisfactory hopper and dedusting system for any ESP installation.

There are numerous devices on the market for hopper level indication/detection, employing one or more of the following principles: ultrasonic or radioactive sensors; or a change in capacitance, in tuning fork frequency, in pressure/suction, or in the rotational speed of a driven disc. As any device will only determine a local dust situation, overfull hoppers can still arise in spite of an apparent 'empty' hopper indication. Should the hopper overfill with dust, not only will the dust short out the electrical supply but could also result in severe mechanical damage if the level should reach high enough into the field area.

To minimize the above, or at least give further early warning, in addition to the normal hopper level devices, flexible metal chains are sometimes hung from the four corners of the discharge frame. The dust on reaching the chains usually causes the electrics to trip on reduced kV output, thereby preventing further dust being precipitated.

One should remember, however, although dust will not be electrically precipitated within the inlet field, it could still deposit under gravity and hence create a problem. Therefore, action to remedy an over-full hopper situation must have a high priority if potential damage to the internals, with the attendant significant fall in performance, is to be avoided.

4.11 Reentrainment from Hoppers

As many ESPs operate under negative pressure, it is imperative that air in-leakage into the hopper region is prevented to eliminate possible reentrainment of already collected particles. Even an unmeasurable in-leakage flow can reentrain sufficient dust in passing through the hopper area to significantly affect the overall emission from the plant. This is particularly important with the outlet hoppers since there is no possibility of further precipitation occurring. For example, if there is hopper in-leakage equating to only 0.25 percent of the total flow but carrying 10 g/Nm^3 of re-entrained dust, an ESP designed to normally operate with an emission of 50mg/Nm^3 will produce a final emission approaching 75 mg/Nm^3, a 50 percent increase in emissions.

For volumetric systems such as conveyors of various types, rotary valves are often used and placed below the hopper take-off point to meter the dust flow. As the rotary valve acts as a pump on the return empty half-cycle, its position in the down leg and operation must be such as to provide a positive head of dust to eliminate in-leakage. For either dense or lean phase pneumatic conveying systems, the above pumping problem does not arise as both rely on slide-type gate valves for isolation and sealing; however, it is most important that these gate or slide valves effectively seal, particularly when positive pressure systems are used.

4.12 Electrode Design with ESPVI 4.0W

An ESP may have both simple and very complex electrodes. It may have the same or it may have different electrode configurations. In ESPVI 4.0W, each section (or field) has its own electrode file whether each electrode configuration is the same or whether it is different. The files that comprise the SAMPLE ESP are shown in Appendix B. The electrode files for the three sections, which are all configured the same, are SAMPLE01.elc, SAMPLE02.elc, and SAMPLE03.elc.

Examining the two files SAMPLE.mst and SAMPLE.esp, it should be noted that both designate as "Electrode File" the three electrode files. When creating a new ESP, ESPVI 4.0W will automatically prepare these files when it is saved. However, if the electrode configurations for the sections differ, a different procedure has to be used, which will be explained later in this chapter.

To use ESPVI 4.0W for electrode design, go through the pull-down menu "Data Entry and Editing" from the main window (Figure 1-2) to bring up the "Electrode Design" window, Figure 1-5.

In the upper portion of the "Electrode Design" window is a text box for the **Section Number**. The **Section Number** can be inserted manually to change from one section to another. Alternatively, the two arrows to the left of the text box can be used to change from one section to another number.

ESPVI 4.0W only considers round cross-sectional corona discharge electrodes. As has been discussed in a previous chapter, only electrodes having a round cross-section readily lend themselves to analytical solutions. If the ESP being modeled has round discharge electrodes, ESPVI 4.0W will use them directly. For complex shaped electrodes, one or more round electrodes that simulate the complex electrode's specific electrical characteristics must be used.

Directly underneath the **Section Number** box is a **Number of Elements** box. If the electrodes in the ESP section are all individual round cross sections, then the number of elements entered is equal to the number of electrodes. If complex electrodes are being simulated by an array of round electrodes, they must all be counted and entered as the total number. ESPVI 4.0W applies the same high-voltage value to all of the elements in one section.

Move down to the text boxes on the lower part of the "Electrode Design" window where the first three elements are shown. The horizontal scroll bars are used to view the remaining elements in the section. (The element numbers change as the elements are scrolled.)

The first row of the text box is labeled **Type 0, 1, 2**. The numbers 0, 1, and 2 signify the type of electrode. **Type 0** is a round cross-sectioned electrode. **Type 1** is for what is called a cold-pipe electrode. **Type 2** signifies a flat plate, high voltage electrode located midway between the grounded collector electrodes. Because of the way data is entered into the remaining text

boxes in the lower portion of “Electrode Design”, for each **Type**, they will be considered in more detail below.

Type 0 elements are the ordinary round cross-sectioned wire elements, which are used in many ESPs. Its diameter is the **Element Diameter**. The **Location (from inlet)** is its location relative to the entrance of the section: specifically, the distance from the leading edge of the section to the center of the electrode. Each electrode in a duct type ESP section has a different distance from the leading edge. The **Associated Parameter** is the distance between any barbs on the wire. Barbs tend to locate the corona at those spots thereby allowing no corona between them, which ESPVI 4.0W will take into account in its modeling. If there are no barbs, set the value to zero. The **Corona Onset Factor** is a number between 0.6 and 1, which provides tuft corona at the 0.6 setting and which gradually changes to full-glow corona as it is raised to a maximum value of 1. The corona onset factor was originally derived from experiments with round wire corona discharge electrodes. It was found that a smooth polished wire would go into corona onset at the correct voltage for the diameter, but which would decrease if corrosion or rust roughened it. The corona onset factor affects the corona onset voltage directly and the corona current density at any voltage indirectly. A typical value for this variable is 0.8; absolute limits are 0.6 to 1.0. This parameter is not considered highly important because changing the diameter of the round electrode essentially accomplishes the same thing. The important consideration is that the corona onset that ESPVI 4.0W predicts is the same as in the full-scale ESP being modeled. The corona onset factor does provide an additional means for helping to adjust the corona starting voltage for both a round and a non-round electrode to a measured value.

Type 1 elements are cold-pipe electrodes. The cold-pipe is an electrostatic section whose purpose is to put a very high level of charge on particles, especially those of high resistivity. Yamamoto, et al., 1990, described the reason for the high level of charge placed on the particles. The cold-pipe ESP consists of an array of pipes interspersed with corona discharge electrodes. It is shown as Figure 4-10, which was developed by ESPVI 4.0W, and came from “Electrode Arrangements” in the “Graphs” pull down menu. The length of the array is the diameter of the pipe. High resistivity particles are managed by putting sufficient cooling water through the pipes to cool the dust that collects on them, so that reverse ionization or back corona does not form. This device is placed upstream of a collector section with a corona discharge electrode configured to provide high electric fields and low currents. The cold-pipe charger is a section by itself, with its own power supply, since it is usually able to operate at a higher voltage than ordinary conventional electrodes in an ESP. It is possible to specify a cold-pipe element among other wires or flat plates, but it is not normally good practice. **Element Diameter** is the equivalent diameter of the round corona discharge electrode. The **Location (from inlet)** is the pipe radius. The **Associated Parameter** is the pipe diameter. The model is accurate up to a pipe radius approximately 1/3 the discharge electrode to pipe center separation. The **Corona Onset Factor** for **Type 1** is usually set to about 0.9.

Type 2 elements are flat plates connected to the high voltage. No current is ever allowed to flow from a flat plate in the model. If some current is needed, **Type 0** elements can be placed upstream and downstream of the flat plate. The Element Diameter for a flat plate is its

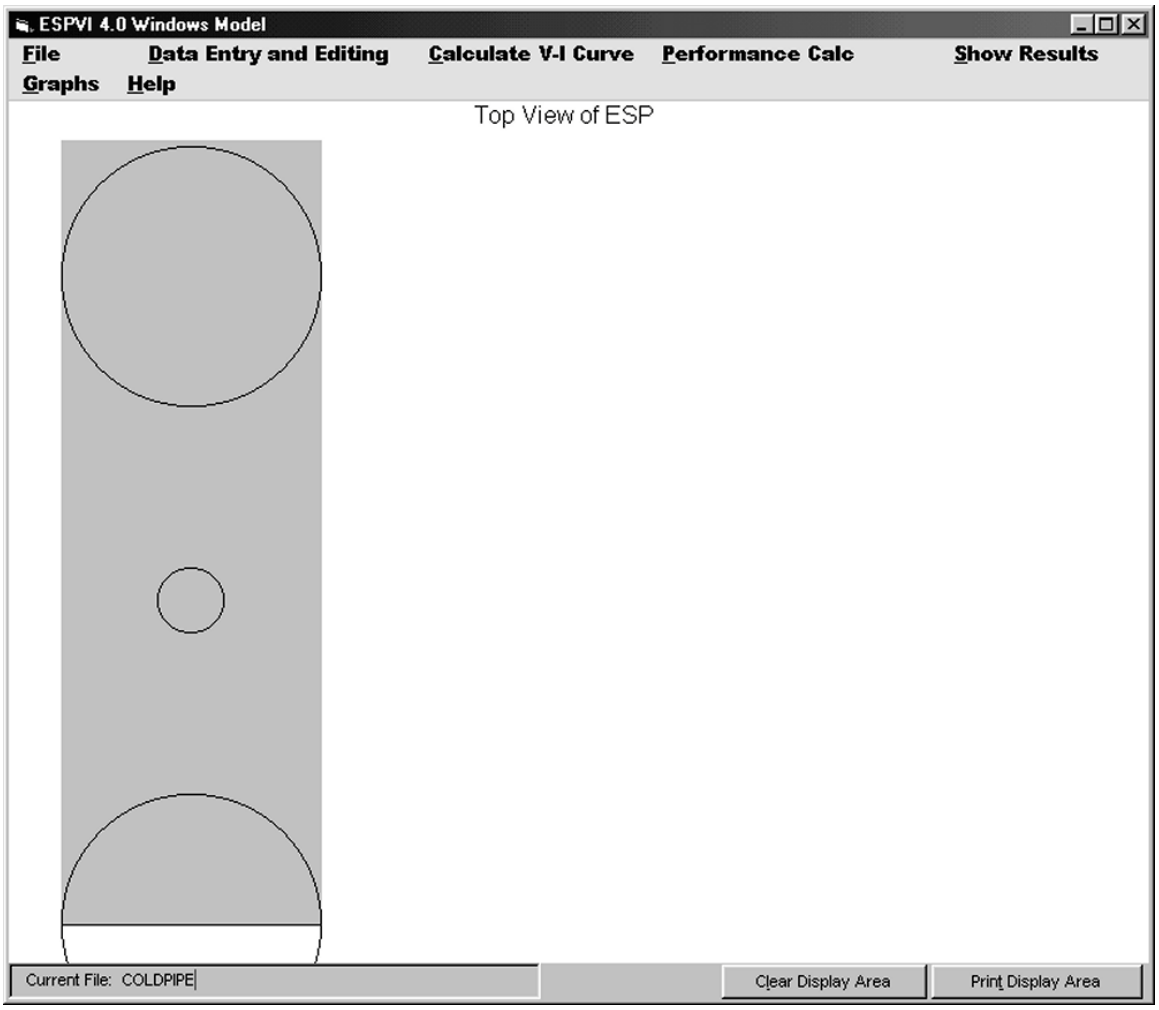

Figure 4-10. Cold-pipe electrode arrangement.

thickness; the value is used in calculating the electric field. The **Location (from inlet)** of the element is the distance from the leading edge of the section to the leading edge of the flat plate. The **Associated Parameter** of the flat plate is length in the direction of flow. Note that the location of the trailing edge of the flat plate is at the element's location plus its associated extent.

One has the option for loading the corona discharge electrodes manually with each element set by means of **Location (from inlet)**. These must be entered manually if the electrodes are not evenly spaced, which is usually true when entering an array of elements to simulate complex electrodes. However, for evenly spaced electrodes ESPVI 4.0W can help by loading the elements automatically.

Entering the element data manually is done in **Element Diameter** and **Location (from inlet)**. **Element Diameter** is the diameter of the round element. **Location (from inlet)** is the distance from the inlet to the center of the round element. Once the elements are entered, use

Update (located under the graphic representation) to update the new input. Especially, look at the graphic representation to see if the electrodes appear to be located correctly. Count the electrodes to see if the number in the graphic representation corresponds with the number that has been entered. If it is less, it is possible that two electrodes have been assigned the same distance from the inlet. Also, look at the text boxes to the left to see if any of the numbers are negative, which provides additional information about whether the location values are correct. It should be noted that, in the graphic representation, the size of the discharge electrodes increases with the entered diameter of the element. If the diameters of individual elements are sufficiently different, the differences will be readily visible in the graphical representation.

Copy Left and **Copy Right** are used with the input data portion of the window to allow data entered for one element to be copied to the other elements. These are applicable to all of the element-input rows.

If the elements are to be evenly spaced, ESPVI 4.0W provides a feature that allows the **Location (from inlet)** data to be entered automatically, thereby making it unnecessary for the distances to be computed manually. Returning to the "Electrode Design" window there are three additional text boxes in the upper left-hand corner. These are labeled **Average Spacing**, **Offset from Inlet**, and **Offset from Outlet**. They are used to facilitate setting the element locations with a constant spacing. Set **Offset from Inlet** to the distance from the section inlet to the first element. Then the **Offset from Outlet** is set to the distance from the last element to the outlet of the section. Clicking the **Perform Spacing** command button at the bottom left of the window will enter the appropriate **Location (from outlet)** distances for each of the uniformly spaced electrodes. The **Offset from Inlet** and **Offset from Outlet** distances must be set to values greater than zero for this automatic feature. This means that the first and last electrodes must be within the collection electrode plates. If the discharge electrodes, for some reason, are to be placed at the inlet and outlet of the section, it will have to be done manually.

The "Electrode Properties" window differs somewhat from the other windows accessible from the "Data Entry and Editing" pull-down menu. The differences are how data entries in "Electrode Properties" are saved and how differing electrode configurations among the ESP's sections are prepared.

The ESPs being modeled in ESPVI 4.0W up to this point had the same electrode configurations for each of the sections or fields. Quite often, a full-scale ESP can have different electrode configurations in each section. Having different electrode configurations for the ESP's sections in ESPVI 4.0W requires a somewhat different procedure than has been used up to now.

The data entry windows in the "Data Entry and Editing" pull-down menu all have **Accept** and **Cancel** command buttons. The **Accept** button allows the newly entered data to be used for computation; however, it does not save the data. To save the new data, which means writing it to the file, requires the use of the **Save** command. The **Accept** button for the

"Electrode Design" window writes the data to the file without the necessity for going through **Save**. **Cancel** will close the window and restore the original electrode configuration data.

Writing electrode files for ESPs having different electrode configurations in the various sections must be done on an individual sectional basis. Use **Open** to load the ESP. Go to "Electrode Design" and use the two horizontal scroll arrows to choose the section to which electrode changes will be made. In the text boxes, enter the data for the electrode configuration. If satisfied with the changes, use **Accept** to close the window and save the data.

At the lower left of the window is a **Copy** command button with its accompanying label **Copy current values to the next section**. If a section's electrode configurations are modified and the same change is desired for the following sections, use the **Copy** command. This function, which makes it unnecessary to enter the same data separately by section, should be done before using the **Accept** button.

In Appendix B, which shows the files for the SAMPLE ESP, all of the electrode files are the same. For an ESP with more than one electrode configuration, the electrode files will have differing values written into them.

4.13 Sneakage/Rapping/Turbulence with ESPVI 4.0W

Factors such as sneakage and rapping reentrainment, which cannot be determined analytically and must be introduced empirically, are called non-ideal factors. The sneakage, rapping, and turbulence data are important corrections to ESP performance calculations, but as the theoretical basis for such values is not strong, many of these should be viewed as "fitting" parameters.

"Sneakage/Rapping/Turbulence" on the "Data Entry and Editing" pull-down menu brings up the window shown as Figure 1-6, which allows entering of the non-ideal factors that affect ESP operation. The text box entries in the upper half of the window apply to the total ESP. The text boxes in the lower portion are for individual sectional entry.

In the lower or sectional portion of the "Sneakage/Rapping/Turbulence" window, the first set of text boxes is **Sneakage Fraction**. Sneakage is the fraction of gas that bypasses the collection zone of an ESP section, which is typically 0.03 to 0.06. Naturally, that fraction experiences no collection. At the end of each section, the model assumes that the sneakage fraction is totally mixed with that emerging from the section and then a new fraction of that gas bypasses the following collection section. It is believed that less attention was paid to sneakage in older ESP designs, and so a value nearer 0.10 can be used, although 0.05 seems adequate for most ESPs, especially newer ones. Sneakage is assumed to affect all particle sizes equally in the model. Sneakage has a more important effect on ESPs with fewer numbers of sections than on ones with a greater number. Cold-pipe sections have higher sneakage than conventional ESP sections because they require more clearance for the high voltages in their design. The sneakage can be estimated as the ratio of the corona length to the total height.

Rap reentrainment Fraction is the fraction of collected material reentrained into the gas flow with each rap, typically 0.05 to 0.15. There is some evidence that the rapping fraction should be closer to the 0.05 value for lower gas velocities. If the gas velocity exceeds 1.5 - 2 m/s, or if the dust is loosely held to the collector electrodes (as would be the case with very low resistivities), the fraction should be 0.15 or greater. This parameter is best adjusted if separate measurements of emissions with and without rapping have been made. The rapping fraction in ESPVI 4.0W can then be varied to make up the difference.

The calculated value for **Rap reentrainment Fraction**, in the parenthesis ( ) column, is a best estimate based on plate height, gas velocity, and distance between corona zones. It follows a square dependence with a change in gas velocity. It often agrees well with fitted input values and is useful in the absence of specific data. It is the opinion of the authors, that in the absence of supporting data, that a value less than 0.08 should not be used for the **Rap reentrainment Fraction**.

The **Turbulent Core Number** in the "Sneakage/Rapping/Turbulence" window represents a way to deviate from the highly turbulent Deutsch-type collection, which has been the basis for ESP modeling for many years. The **Turbulent Core Number** is not an ESP parameter that is used to help describe its performance. It cannot be derived either analytically or from first principles; instead, it is a designated value that can be entered into ESPVI 4.0W that may better allow it to match the performance of an ESP from which accurate and precise data for ESPVI 4.0W is available. This correction has been derived to account for the fact that many ESPs outperform the best models that use Deutsch collection. Instead of having full turbulence, varying the Turbulent Core Number allows the introduction of a series of laminar collection zones separated by regions of complete mixing. The core number describes the number of laminar zones per element and generally should have the value 1. That is, as particles pass under a discharge electrode, they experience an electrical force much stronger than the turbulent forces that cause mixing and are collected as if the mixing did not exist; once past the element, the mixing dominates again. To allow the mixing to continue under each element, set the core number to 5 or 10. Then, there would be five or ten mixing zones as the particles pass the elements. To allow for very low turbulence, the core number should be set to 0.2 to 0.5; then the particles would pass two to five elements before mixing would occur.

Some ESPs use baffles or pockets to shield the collected dust from the gas flow. These ESPs could use a lower turbulent core fraction to account for the quiescent zone, although the baffles themselves might increase the level of turbulence in the gas. On the other hand, a well-designed ESP with flat collector electrodes would be expected to have a lower turbulence, and one may use a turbulent core factor less than 1. An ESP operating at low gas velocity would also tend to have a lower degree of turbulence.

The lowest row of text boxes in this group contains the calculated **Reynolds Number** value that takes into the consideration the gas's velocity, density, and viscosity, as well as the duct dimension. The higher the **Reynolds Number,** the greater is the level of turbulence. This could provide some additional guidance on how to set the **Turbulent Core Number**.

The turbulent core fraction should be considered as a means for better matching the ESPVI 4.0W to the full-scale ESP if excellent data is available for the ESP. If the supporting data is unavailable, it is probably best that the turbulent core fraction should be set at the nominal value of 1.

Electrode Misalignment Fraction in "Sneakage/Rapping/Turbulence" is the maximum deviation of the corona discharge from the plane that bisects the gas passage lane. In most ESPs, the corona discharge electrodes are located in a plane that is midway between the two collection electrodes that form the gas passage lane. In some ESPs operating with high space charges, the corona discharge electrodes have sharpened points or spikes. The spikes are intended to address corona sites that are located off the center plane. Many ESPs may also have mechanical problems that cause the corona discharge to move from the center plane. These various situations, for the purpose of ESPVI 4.0W, make use of data entry into the **Electrode Misalignment Fraction** text box.

Electrode misalignment is considered to have two effects. The first is that the closer spacing between electrode and plates reduces the corona onset and sparking. The second effect is that the misalignment reduces the electric field in the wider spaced part of the electrode lane. Since that part carries more of the gas flow than the closer spaced part, the net effect is a reduction of collection efficiency.

The value for the **Electrode Misalignment Fraction,** which is entered into the text box, is the ratio of the displacement of the corona discharge electrodes from the centerline to the collector electrode. For example, if the collector electrode separation were 300 mm, the center plane to collector distance would be 150 mm. If any or all of the corona discharge sites were displaced 15 mm from the center plane the fraction would be 0.10.

The **Section Misalignment Fraction** sets the amount of the section for which the **Electrode Misalignment Fraction** should be applied. The maximum is 1, if the whole section is misaligned. The minimum is zero, if no fraction of the section is out of alignment. If half of the section were misaligned, than the value would be set to 0.5. If the whole corona discharge plane were purposely located away from the center plane such as the tape and needle corona discharge electrode normal to the gas flow, than the fraction value would obviously set to a value of 1. For the misalignment situations caused by mechanical problems, the **Section Misalignment Fraction** would be determined by an estimate based on observation and calculation of the amount of misalignment.

The first text box in the upper portion of the "Sneakage/Rapping/Turbulence" window, which is data entered for the total ESP, is **Velocity Std Deviation**. Generally, an ESP works best if the gas velocity entering it is uniform. However for practical reasons a completely uniform gas is unobtainable and some deviation from the ideal has to be accepted. Good operating practice accepts a deviation from the mean velocity of no more than 15 percent. For such a well operating ESP, the value inserted into the **Velocity Std Deviation** text box would be 0.15. ESPs with poor gas distributions would have higher values. If the available data indicates that the value entered is greater, insert the appropriate number. The effect of a higher velocity mal-distribution is to make the fraction of the ESP with higher velocities

collect particles less effectively and contribute more to the total emissions. Correcting any flow mal-distribution should improve ESP performance, but sometimes the potential improvement is not large enough to warrant the expense of correction.

When the “Adjust” methods in the “Performance Calc” pull-down menus were being presented in Chapter 3.5 there was an item “Compute Mal-distribution” that was by-passed at that time. In the “Standard Method”, ESPVI 4.0W computes the performance at seven different gas velocities distributed around the mean value according to the velocity standard deviation. This is done when “Standard Method” is run if: 1) it has never been run before for that ESP configuration, or 2) if parameters such as SCA, collector area, gas flow and the various reentrainment factors have been changed. If one of the alternate computational (Adjust) methods under “Performance Calc” has been run and if some significant changes have been made to the ESP, it may be best to use “Compute Mal-distribution”. Alternatively, “Standard Method” can be performed after one of the alternate computational methods has been carried out to do the necessary calculations.

Particle MMD (rap), is the mass median diameter of the particles re-entrained during rapping. The value is typically 5 - 9 micrometers for fly ash. One study has recommended the use of a fixed value of 6 micrometers. The exact reasons for the development of this size distribution are not known, but it may be due to breakup and recollection of large chunks of agglomerated fly ash dust cakes. Other studies have shown that, as ESP efficiencies are improved by increasing their size, a larger fraction of the residual emission is from rapping reentrainment. Therefore, it is beneficial to decrease the rapping reentrainment emissions in the ESP.

Geom Std Dev (rap), on the “Sneakage/Rapping/Turbulence” window, Figure 1-6, is the geometric standard deviation of the reentrained particles which accompanied the example indicating the mass mean diameter as 6 micrometers.

The **Back Corona Loss Fraction** is a value that computes the fraction of the particles that are near the collecting electrode that loose their negative charges due to neutralization by positive ions which result from the reverse ionization or back corona. It is not a measured value from an ESP to be provided as input to ESPVI 4.0W. Instead, it is speculation based on theoretical considerations about what happens to particles when back corona is present. It should be considered as a means for gaining insight and understanding and as an explanation of some of the observations from ESPs operating in the back corona regime. It only operates when the resistivity of the dust is sufficiently high that ESPVI 4.0W senses the ESP will be operating in the back corona regime. The input fractions range from 0.00 to 1.00, with the amount of charge neutralization increasing as the size of the fraction.

Back Corona Loss Fraction is a new concept that is being introduced into electrostatic precipitation modeling for the first time. As such, its usage is currently being explored. One obvious use is for evaluating a poorly behaving ESP that is subject to back corona and for which particle emission data is available. The **Back Corona Loss Fraction** can be used to determine what fraction value will explain the high particle emission level. The fraction value can then be reduced to see the effect on the emissions. Because back corona modifies

the electrical conditions in the ESP, it may be necessary to make similar changes in the data input to ESPVI 4.0W. With the current level of understanding, it is not believed that using a fraction greater than about 0.25 is justified.

It should be noted that if the **Back Corona Loss Fraction** is changed in "Sneakage/Rapping/Turbulence" and then **Accept** is used, the change is automatically saved in the data file. If the original default value of 0.100 is to be restored it is necessary to do it manually.

Steady Reentrainment Fraction is the fraction of collected particles that are immediately reentrained when they reach the collecting surface. This is a phenomenon that may be expected to occur with very low resistivity dusts or those with low cohesivity. Steady reentrainment may be a problem with fly ash treated with a spray dryer sorbent for sulfur dioxide control or for high carbon in ash carryover situations. Normally, the value should be set at zero.

One-section-out Fraction is the fraction of the ESP operating with one section out of order. This value must be in the range of 0 to 1. For example, for a two-chamber ESP having three-sections for each chamber, with one section out of operation, set this fraction to 0.5. It might be useful for evaluating a multi-chambered ESP that has to meet a guarantee.

The **Two-section-out Fraction** text box on the "Sneakage/Rapping/Turbulence" window is the fraction of the ESP operating with two sections in a row out of order. Use it for guarantee tests or to estimate operating margins. The value must be in the range of 0 to 1. As an example, for a four-chamber, four-section ESP, to evaluate the performance with two sections in one chamber out of operation, set this fraction to 0.25.

The one- and two-section outage fractions can be used together. The total fraction cannot exceed 1, and the one-section outage is assumed to be located in another chamber from the two-section outage situation. Using them simultaneously cannot simulate a three-section outage. In addition, the calculation is not performed unless there is at least one working section in each chamber.

Although the treatment of the non-ideal parameters is sketchy, due to the lack of understanding of the physics behind them, these parameters can adversely affect the performance of the ESP to a very large degree. In has been noted that measured performance of some high efficiency ESPs indicated that more than fifty percent of total emissions are due to rapping reentrainment. It is important, therefore, to consider the effects that any of these parameters may have, particularly when experimental measurements are not available.

Copy Left and **Copy Right** are used with the sectional input data portion of the window. These command buttons allow data that is entered for one section to be copied to the other sections.

The other command buttons along the bottom of the "Sneakage/Rapping/Turbulence" window form are labeled **Cancel**, and **Accept**. The **Accept** command button closes the

window with its current data contents so that the modeling can proceed. Clicking on **Accept** only allows the calculations to proceed with the window's current contents. It does not save the contents, which, if desired, must be done by means of **Save,** which is under "File" in the main window. Clicking on the **Cancel** command button closes the window and restores the original saved data entries.

4.14 Modeling a Complex Electrode

The objective in accurate modeling is to make the input data for ESPVI 4.0W represent the full-scale ESP's properties as closely as is possible. Usually the most difficult data to obtain is the particle size information and the corona discharge electrode's electrical characteristics. The usual order is first to determine the discharge electrodes electrical characteristics, which are then used to help determine the particle characteristics.

ESPVI 4.0W in its internal computations considers all corona discharge electrodes to be circular shaped, which lend themselves to analytical solutions. Many electrodes are merely round wires or rods, which are rather easily modeled. However, modeling is not always easy. As an example, the tape and needle electrode shown in Figure 4-11 and commonly used in the NIS certainly does not have a circular cross section and, therefore, is more difficult to model.

To determine the discharge electrode's electrical characteristics, it is necessary to separate the effect of the electrode from the space charge induced effects of the particles in the gas stream. The usual method for doing this is to use the voltage current curves from air load tests that are done at ambient temperature with air.

There are two approaches to modeling a corona discharge electrode. The simple approach is to find the diameter of a round electrode whose electrical characteristics are similar to that of the electrode of interest. The second approach is to set up an array of round electrodes in such a way, that it resembles the electrode in question. The simple approach will be adequate for much of the modeling that is done. Constructing the array requires considerably more effort and is usually justified if the quality of the data supports it and the need for higher accuracy exists. If the complex electrode has a significant dimension in the direction of flow, an array that simulates it adequately can place an equivalent electric field "footprint" on the collector electrode. Both approaches require that the air load gas properties be entered into the "Gas Properties" window to be covered in Chapter 5 and which was shown earlier as Figure 1-7. What will be entered there is the gas temperature and composition of ambient air.

The solutions that will be provided here are unique to both the spacing between the grounded collector electrodes and the spacing between electrodes. For ESPs with different collector and corona electrode spacings, it would be best to find solutions whose properties match those configurations.

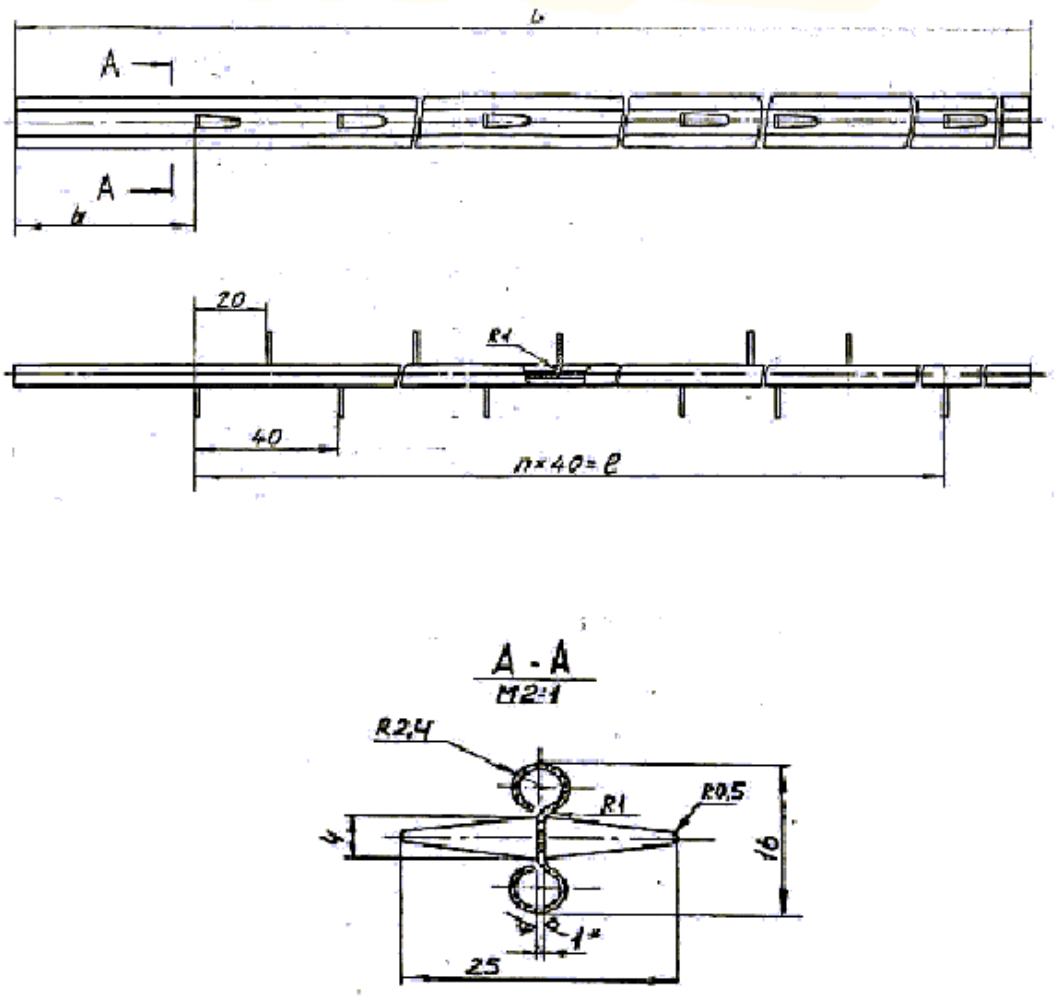

Figure 4-11. Tape and needle corona discharge electrode.

4.14.1 Modeling the Complex Tape and Needle Electrode with Needles Parallel to the Gas Flow Using a Single Electrode Element

The “tape and needle” electrode type, such as shown in Figure 4-11, may be used with the needles parallel to the gas flow or with the needles normal or perpendicular to the flow. In this example, the needles will be parallel to the flow.

Air load data from an ESP at a NIS power station using the tape and needle electrode configuration was obtained in graphical chart form. The air load data for the four sections of the ESP are shown in Table 4-2.

The original data for each ESP section was in amperes which, using the area of the collecting electrodes, was converted to a current density, nA/cm^2, to be consistent with the ESPVI 4.0W

Table 4-2. Comparison of Modeled Electrode Complex Tape and Needle Electrode with Needles Parallel to Gas Flow under Air Load Conditions

Voltage, kV	Current Density, nA/cm^2					
	Section 1	Section 2	Section 3	Section 4	Electrode 1	Electrode 2
20	-	-	-	2.5	-	0.9
21	-	-	-	-	-	1.6
22	2.5	2.5	2.5	-	-	-
23	-	-	-	-	-	3.2
24	-	5	5	5	-	-
25	5	-	-	-	2.7	5.5
26	-	-	-	-	-	6.7
27	-	10	-	10	6.4	-
28	-	-	10	-	-	9.7
29	10	-	-	-	10.7	-
30	-	15	-	15	13.6	-
31	-	20	-	-	-	-
32	15	25	15	20	18.6	17
33	-	-	20	25	21.7	-
34	20	-	-	-	-	21.5
35	-	30	25	30	-	-
36	25.25	35	-	-	-	26.4
37	-	-	30	34.75	35.5	-
38	30	40	35	-	-	31.6
39	-	45	40	40	-	-
40	40	-	-	-	-	-
41	45	50	45	45	51.9	-
42	-	-	-	-	-	-
43	50	-	50	-	-	-
44	-	-	-	50	-	-
45	-	-	-	-	-	-

output. The current density air load data for the four sections is plotted against voltage in Figure 4-12.

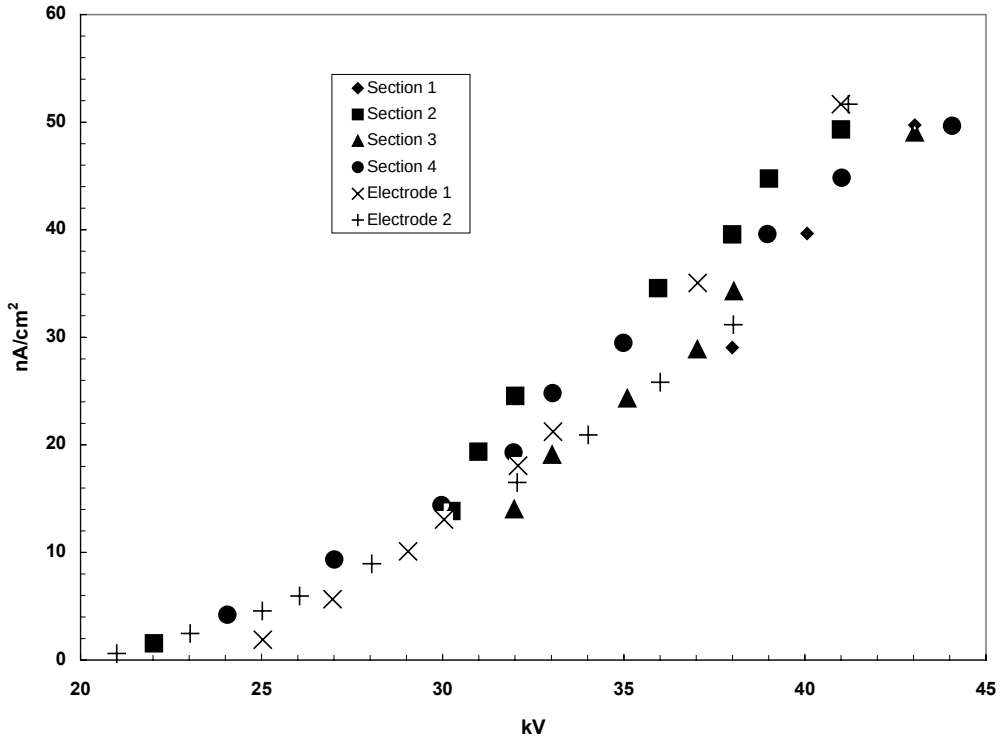

Figure 4-12. Complex tape and needle with needles parallel to gas flow using single element (Electrode 1) and array (Electrode 2) under air load conditions.

In examining the plotted air load data, it is noted that there are differences in the voltage current curves of the four sections. This is likely due to irregularities in the fabrication, installation, and the alignment of the sections. Although there are differences in the voltage current characteristics of the sections, the differences are relatively small and reasonable. The ESP that the air load data came from was similar to SAMPLE3, with its 275 mm spacing between collector plates.

The ambient conditions at the time that the air load tests were not available; therefore, it was assumed that the temperature of the air was 20 °C, which was entered into "Gas Properties". The other addition to "Gas Properties" was to set the SO_2 concentration to zero ppm. Do not leave the text box blank when the value is zero; it is necessary to insert a zero. Setting the SO_2 concentration to zero causes ESPVI 4.0W to use the ion mobility of air.

The particle concentration in "Particle Properties" has to be set to some very low value so that there is no space charge. The value arbitrarily chosen was $1x10^{-3}$ mg/m^3. The particle concentration must be a small finite value.

The other ESP input values were those of the actual ESP under air load operation. Because no particles were being collected and there was no interest in performance, the other values were not critical. The ESP with the entered air load data was saved as SAMPLE4.

As stated earlier, there is no unique solution in defining the electrode properties that will allow a match to the air load conditions. The objective is to find a solution that does allow a reasonable match between the air load electrical conditions and the electrical conditions predicted by ESPVI 4.0W. As much as possible is kept the same. The number of elements, which in this case was 14, and their location were kept the same.

Referring back to Figure 4-11, the needles are spaced at intervals of 20 mm, with each one facing the opposite direction from the adjacent one. Thus, the tips of adjacent needles, where the corona sites are located, are approximately 30 mm apart. Therefore, it seemed reasonable to set the **Associated Parameter** to a value of 0.03.

The next step was to try to determine what round cross section electrode element will have electrical conditions that would simulate the tape and needle electrodes. There are two variables. The first is **Element Diameter** and the second is **Corona Onset Factor**. The **Element Diameter** can be set to any diameter. The smaller the diameter, the lower is the corona onset voltage and the higher is the current density for a given voltage. This means that the voltage current curve also shifts with a change of element diameter. The **Corona Onset Factor** essentially reduces the corona onset voltage from its normal value to as low as a factor of 0.6 of that value. When it shifts the corona onset voltage, it shifts the whole voltage current curve. From the above descriptions of **Element Diameter** and **Corona Onset Factor**, it is apparent that their actions are quite similar.

A number of combinations of the **Element Diameter** and **Corona Onset Factor** were tried. A value of 2 mm, which is 0.0020 m, in “Electrode Designs”, was finally chosen as the element diameter. This was done by graphically comparing the original air load data to data from “Fixed V-I”. This was accompanied by a corona factor of 0.70. Using the air load conditions, “Fixed V-I” was used to generate the values shown in Table 4-2 in the column labeled Electrode 1. This data was also plotted into Figure 4-12, for comparison to the original air load electrical data.

Comparing the ESPVI 4.0W developed data to the original air load values shows a reasonably good match over the operating range of the ESP. It does deviate at the low voltage end of the chart around corona onset. It also starts to deviate at the higher voltages. There is a reason for this deviation. It is due to the ideal electrode conditions that are entered into ESPVI 4.0W, which is compared to the non-ideal electrode conditions that exist in the ESP. ESPVI 4.0W assumes that all electrode elements in the ESP have precisely the same characteristics. However, because of the fabrication process, the discharge electrodes in the ESP do not all have the same characteristics. Some sites on the electrodes will go into corona at lower voltages, while other sites require higher voltages.

The round 2 mm corona discharge electrode is not too realistic in modern ESP practice. Round discharge electrodes of 4 to 5 mm have been used with weights to keep them taut.

4.14.2 Modeling the Complex Tape and Needle Electrode with the Needles Parallel to the Gas Flow Using an Array of Electrode Elements

The array is made up of single elements in such a manner that it "resembles" the complex electrode being modeled. As with the single electrode approach, there is no unique solution when using the array approach.

If it were possible to view the tape and needle electrode from the collector electrode, each one would appear as two rows of corona points separated by a central supporting member, which is the tape. Therefore, it was reasonable to use a single circular element on each side of the supporting member for the corona sites. The supporting member, or tape, which does not have corona, is represented by a larger diameter element, which would have a corona onset voltage more than the operating voltage. The resulting array of three elements is seen in Figure 4-13. The large diameter element (2) in the center represents the tape. It is made sufficiently large so that it does not go into corona at the operating voltages. The smaller diameter elements (1) on either side represent the corona sites at the end of the needle. The elements in Figure 4-13 are not drawn to scale. In adapting this electrode configuration to SAMPLE, the large diameter element is located in the same position as was the 14 original elements. The small diameter elements are located 12 mm in front of, and in back of, the larger diameter elements, respectively. Thus, instead of 14 elements in each passage there are 42. Unlike the evenly spaced electrodes of SAMPLE and SAMPLE4, which ESPVI 4.0W will input automatically by its Space Elements Equally feature, these 42 elements must be installed manually. The location of each element must be calculated and entered individually. This was done and the modeled ESP was named SAMPLE5.

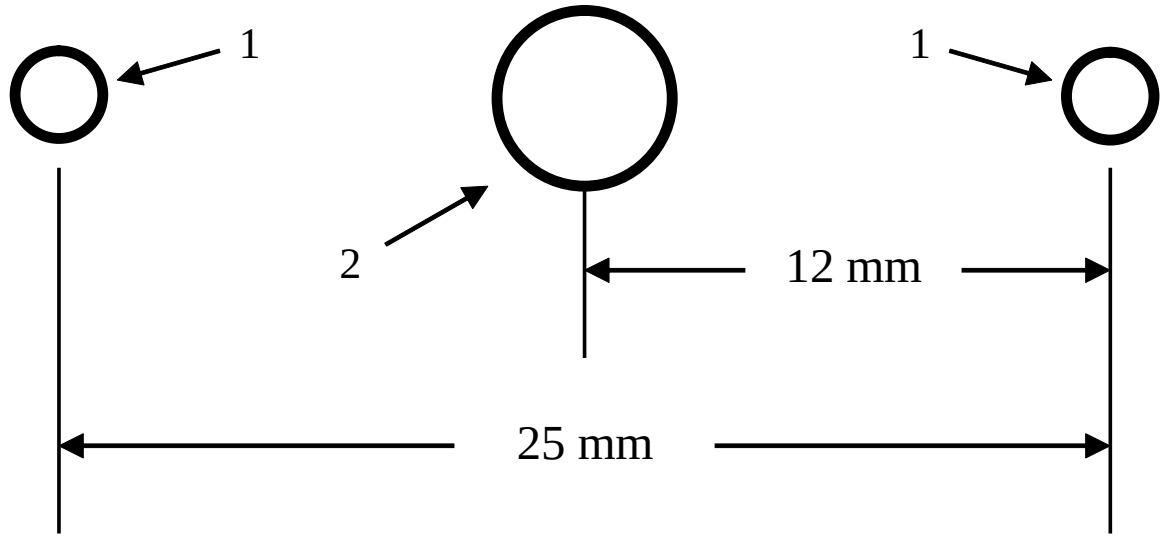

Figure 4-13. An array simulating the tape and needle electrode parallel to flow.

As in Chapter 4.14.1, the two sets of voltage current curves were evaluated by comparing them graphically. The results are presented as Electrode 2 on Table 4-2 and graphically on

Figure 4-12. The numbers that were entered were 0.0004 m for the small elements (1) and 0.0090 m for the larger elements (2). The corona factors were 0.68 for the small elements and 1.0 for the larger element.

Whether to use the simple element or the array is related to the circumstances. The array would be expected to provide some greater accuracy to the modeling than would the single element approach. However, it is more difficult and time consuming to input and adjust. The difficulty increases with the number of elements used in the array and the number of electrodes in each passage.

4.14.3 Modeling the Complex Tape and Needle Electrode with Needles Normal to the Flow

As described in previous sections, the tape and needle electrode with the needles parallel to the flow of gas was modeled. It was done with two different approaches. These were by using a single element and by an array of elements.

In a number of ESPs in the NIS, the tape and needle electrode is used normal to the gas flow. The corona sites at the ends of the needles in this configuration are located off of the center plane between the grounded collector electrodes.

Again visualizing the viewing of the corona electrodes from the surface of the grounded collector electrode, what would be visible would be a row of corona points. This suggests that a single element electrode would be suitable.

A major difference between this situation and the previous case is the location of the corona sites off the center plane. The deviation from the center plane is very similar to misalignment, which in this case is deliberate. To handle this, the **Electrode Misalignment Fraction** and the **Section Misalignment Fraction** of "Sneakage/Rapping/Turbulence" of Figure 1-6 will be put to use.

The procedure is very similar to the one used in Section 4.14.1. A set of air load data was obtained for an ESP very similar to the illustrative example that is provided as SAMPLE5, having a grounded electrode spacing of 275 mm. The needles in the two inlet sections are 12 mm in length and are 6 mm long for the two outlet sections. The tape and needle electrodes with the 12 mm needles were chosen for modeling for this illustrative example. SAMPLE5 was loaded and saved as SAMPLE6.

The air load data for the two inlet sections is shown in Table 4-3. The data originally provided as amperes per section was recalculated as nA/cm^2 to be consistent with ESPVI 4.0W and is listed in the columns labeled Sections 1 and 2.

In "Sneakage/Rapping/Turbulence" the Electrode Misalignment Fraction was set in SAMPLE6 to the ratio of the 12-mm offset to the distance from the center plane to the collector electrode, which is 137.5 mm. The fraction is 12/137.5 = 0.087 was entered into the the Electrode Misalignment Fraction text box, and then copied right. Because the

Table 4-3. Comparison of Modeled Electrode Complex Tape and Needle Electrode with Needles Normal to Gas Flow under Air Load Conditions

Voltage, kV	Current Density, nA/cm^2		
	Section 1	Section 2	Electrode
18.3	-	0.00	-
20.0	0.00	-	-
22.1	-	0.45	-
23.8	0.34	-	-
25.0	0.90	0.90	-
25.8	-	-	0.0
26.9	-	-	0.9
27.3	1.35	1.92	-
27.4	-	-	1.4
27.9	-	-	2.0
28.5	-	-	2.5
29.2	-	3.16	-
29.5	-	-	3.8
30.0	2.82	4.51	-
30.6	-	-	5.2
31.1	-	-	5.9
31.2	4.17	-	-
31.6	-	-	6.6
31.7	-	6.54	-
32.2	5.75	-	7.4
32.5	-	8.34	-
32.7	6.76	-	8.3
33.2	7.89	9.70	9.1
33.7	9.02	-	-
33.8	-	11.27	10.0

"misalignment" is throughout the section, the Section Misalignment Fraction was set to the value of 1. The window is then closed with Accept. The needle spacing of 40 mm was used for setting the Associated Parameter to 0.04 m.

Different combinations of **Element Diameter** and **Corona Onset Fraction** were tried in SAMPLE6, with the final settings being 0.0019 m and 0.80, respectively. The results are given in the column labeled Electrode in Table 4-3. The comparative results are presented graphically in Figure 4-14. It should be noted again that these data entries are just one possible solution.

Comparing the modeled electrode with the actual air load data indicates a reasonable match over much of the electrode's operating range. The deviation down at the low voltage end of the curve is probably due to surface conditions such as sharp edges and burrs left on the electrodes during fabrication.

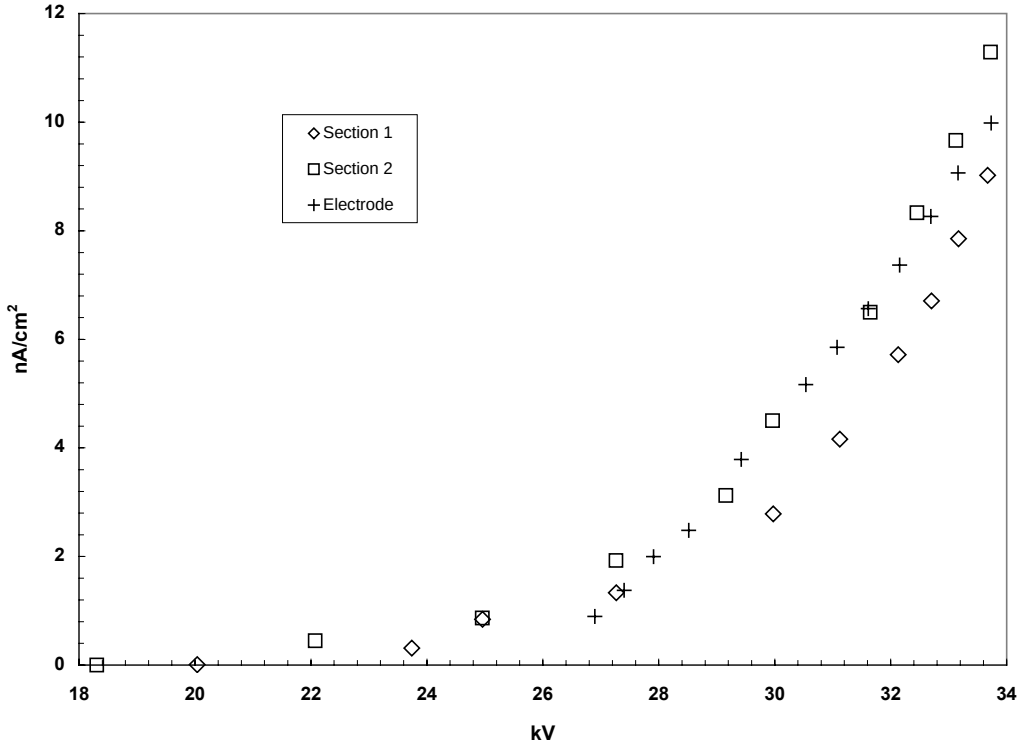

Figure 4-14. Complex tape and needle with needles normal to gas flow using single element under air load conditions.

Chapter 5
Gas Characteristics that Impact ESP Design and Operation

This chapter discusses the effect of gas properties such as composition, flow, and temperature on the performance of an ESP. It also explains the introduction of these parameters into the model.

5.1 Composition

The main requirement of the gas carrying the particles is that it must be capable of maintaining as high an electric field as possible and permit the flow of corona current. The composition of some gases, however, can impact the electric operating conditions of the ESP, since the corona characteristics are modified by the presence of electropositive or electronegative gases, or gases that readily absorb or reject negative ions.

Corona inception, as indicated, occurs when the electric field adjacent to the discharge element reaches a certain gradient irrespective of whether positive or negative energization is used. The actual corona current flow, however, depends on the energizing voltage and on whether the gases have electropositive or electronegative characteristics. Gases such as oxygen, sulfur dioxide, and the like are termed electronegative gases because, being deficient in electrons in their outer shell, they have a great affinity for electron attachment, producing negative ions. Other gases such as nitrogen, hydrogen, and the like are termed electropositive gases because they have little affinity for electron attachment and, consequently, do not produce negative ions in any great quantity.

While the foregoing is true for pure electropositive gases, the presence of trace quantities of electronegative gases typically met in practice significantly modifies the corona characteristics, as indicated in Figure 5-1.

In the case of pure sulfur dioxide, the number of ions produced is small and consequently results in little corona current flow even up to the breakdown voltage of the system. The presence of water vapor and sulfur dioxide in the gases, however, has a significant impact on the electrical operation and hence performance. This is because small quantities of electronegative gases modify the corona characteristics so as to enable the system to adequately charge and, hence, precipitate any entrained particles.

The significance of Figure 5-1 is that for flue gases, which consist mainly of nitrogen, the relatively small quantities of other constituents will have a significant effect on the electrical characteristics of an ESP. For this reason, ESPVI 4.0W considers the gas composition as will be seen in a later part of this chapter. For accurate performance prediction, it is important to have a good analysis of the constituents of the flue gas that the model requires as input.

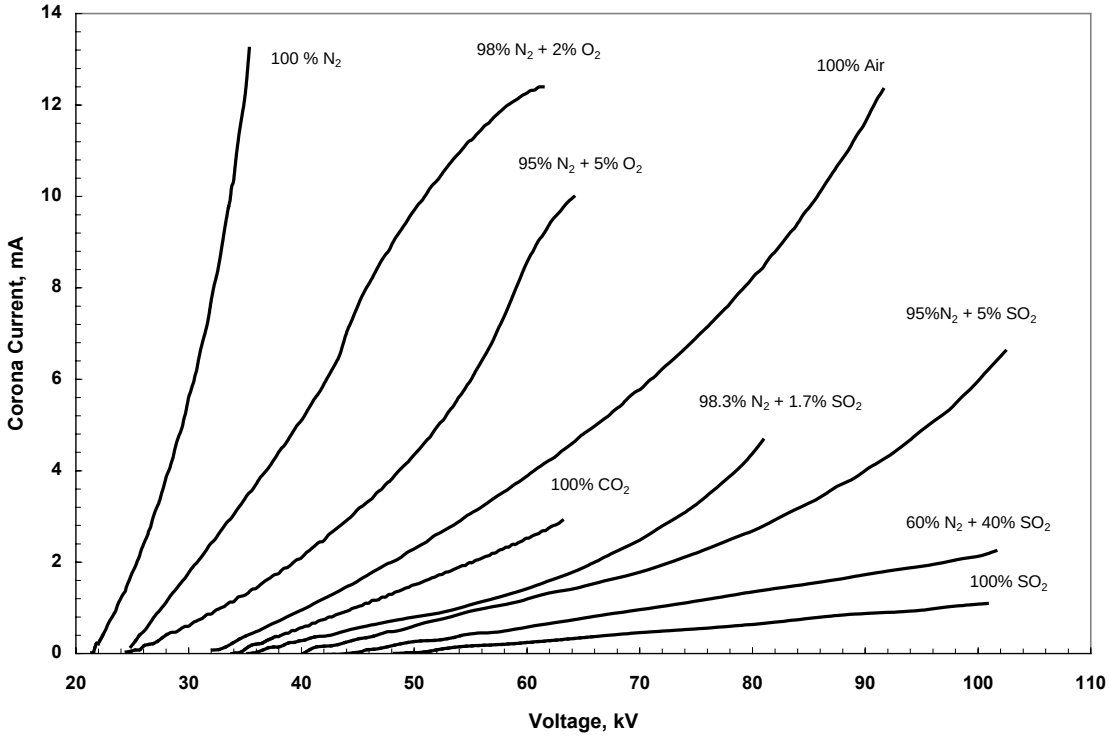

Figure 5-1. Typical corona characteristics of gas mixtures.

5.2 Temperature

An advantage of the dry type of ESP is that the gas can be delivered directly to the ESP without the need for additional cooling or treatment. This means that the collected material is captured in a dry state for subsequent disposal/reuse and that the cleaned gases are emitted from the chimney very buoyant and usually at a temperature high enough to result in a steam free discharge.

The gas volume being treated by the ESP is temperature dependent, according to Charles' Law, and since the performance of an ESP is related to the contact time, any increase above the design temperature will increase the gas volume and, therefore, reduce the overall collection efficiency.

Another impact of temperature, which affects the electrical operation and hence performance, is that, as the temperature increases, the kinetic energy of the gas molecules rises, which increases the corona current flow but at the expense of a reducing breakdown voltage. ESPVI 4.0W requires the temperature of the gas as input data. The model relates changes in current flow to changes in temperature in the same manner as in a full-scale ESP.

Temperature has an important impact on construction materials because mild (low carbon) steel is cost effective in most utility applications and is used for temperatures up to some 400 °C. Whatever material is used for fabrication, thermal expansion must be carefully considered to avoid alignment problems during operation.

In view of the influence of the temperature on particle electrical resistivity (Chapter 6), which has an impact on ESP sizing and performance, it is important that the operational temperature range for any installation is fully and carefully considered. The impact of temperature on performance is demonstrated in Figure 5-2; these curves were obtained using a large pilot ESP treating fly ash from two low sulfur fuels that formed high resistivity ash. The use of the pilot in this investigation enabled inlet conditions other than temperature to be maintained constant. Therefore, the results indicate the true effect of temperature in isolation. As can be seen later in Figure 6-1, particle resistivity peaks at about 150 to 170 °C. This requires operation at reduced voltages and corona current. This is not the situation with lower resistivity dusts of up to about 2×10^8 ohm-m, which does not suffer from reverse ionization under normal conditions. However, even low resistivity fly ash has a resistivity peak in the 150 to 170 °C range.

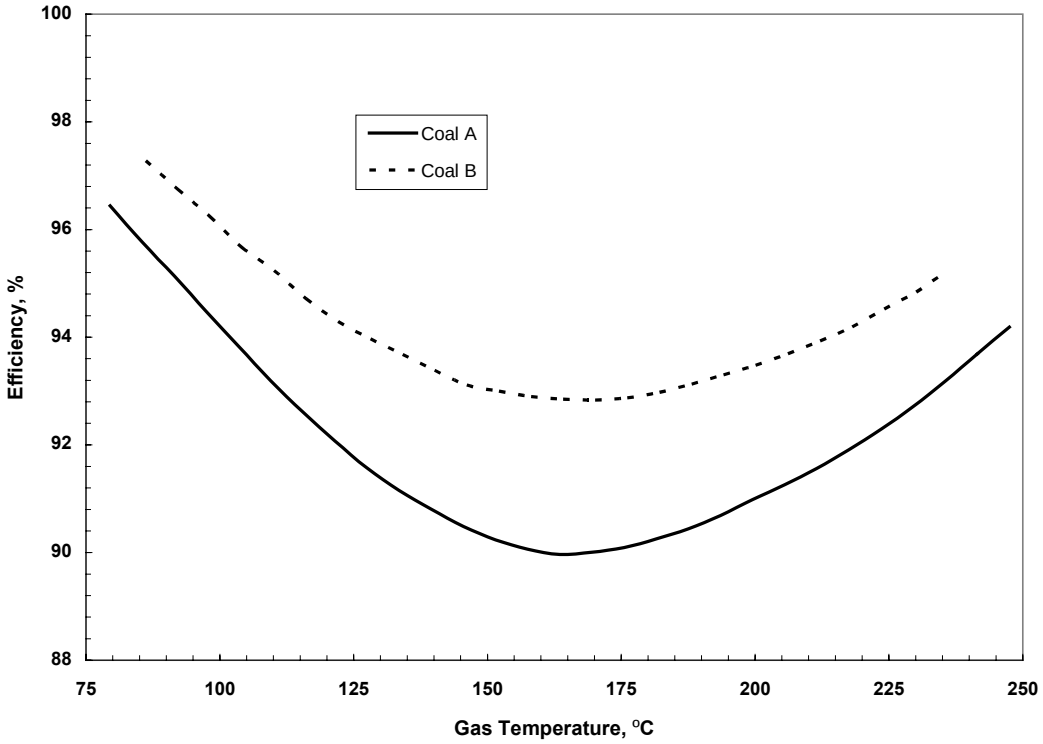

Figure 5-2. Effect of gas temperature on ESP efficiency.

5.3 Pressure

For ESPs that operate close to ambient pressure (sea level) conditions, gas pressure is not a major issue except to ensure the casing is “gas tight” and will withstand the operating conditions, that is, to prevent either the egress of process gas or the in-leakage of ambient air.

There are ESPs, located above sea level that operate at significantly reduced pressure, which affects the performance of the unit. To determine the performance of the ESP, it is important to determine the effect of the pressure change. The ESPVI 4.0W does this automatically if the correct pressure is provided as input, as will be seen in Section 5.5.

5.4 Gas Flow Rate and Velocity

It is clear from the Deutsch Formula that the size and, consequently, the performance of an ESP is dependent on the gas flow rate and, hence, contact time. For a given plate area and migration velocity, the efficiency is related to the gas volume. Any change in gas flow rate affects the efficiency in order to maintain the equation balance.

Figure 5-3 indicates how the efficiency for particle sizes of 3.5, 11, and 51 micrometers diameter changes with gas velocity through a precipitator designed with a nominal operating velocity of 1.4 m/s. A gas velocity that is too low will detract from the collection efficiency, since the deposition along the collector plate (most particles being collected adjacent to the inlet) adversely distorts the electric field. For increasing velocities, the collection efficiency tends to rise to a maximum; however, dependent on the cohesive properties of the dust, reentrainment at higher gas velocities results in significant degrading and a fall in collection efficiency. In general, gas velocities approaching 2 m/s should be avoided for a dry precipitator design because of the scouring and reentrainment risks.

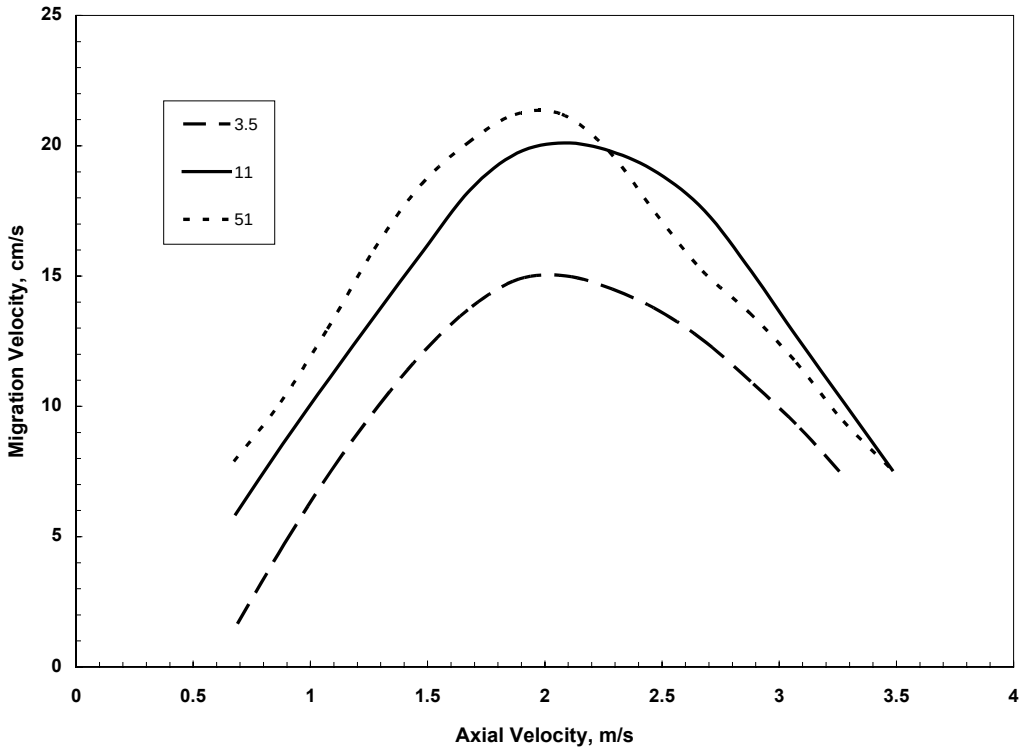

Figure 5-3. Effect of gas velocity on ESP efficiency.

Under-performance as a result of operating with too high a gas velocity coupled with poor cohesiveness is probably best illustrated for an ESP used in the power generation industry. Developments to limit NO_X emissions within the furnace area have lead to the introduction of low-NO_X burners, which, although minimizing NO_X formation, can produce a high carryover of large unburnt carbon particles. These particles have a large surface area, low mass, and low electrical resistivity, are susceptible to reentrainment and/or scouring under

high velocity gas conditions, and can pass through the precipitation fields without being collected. In the worst case, a unit with 12 percent unburnt carbon at the ESP inlet resulted in an emission comprising 90 percent combustible material, some 9 times greater than the actual fly ash.

It is important that the gas distribution across the frontal area of the ESP be as uniform as possible in order to optimize the collection efficiency. Good ESP practice dictates that the specific collection area, which is the collector electrode area divided by the gas flow volume, remains constant over the whole ESP. To produce a typical operational gas velocity of around 1.5 m/s that has been decelerated from some 15 m/s in the inlet approach ductwork is not an easy task. An acceptable velocity distribution has a standard deviation of 15 percent. This can be achieved through field corrective testing, large-scale model tests, or, more recently, by Computational Fluid Dynamic approaches. Figure 5-4 indicates how the efficiency varies with changing percent standard deviation fraction of velocity at a constant effective migration velocity and how the 15 percent value has become accepted as a cost effective measure.

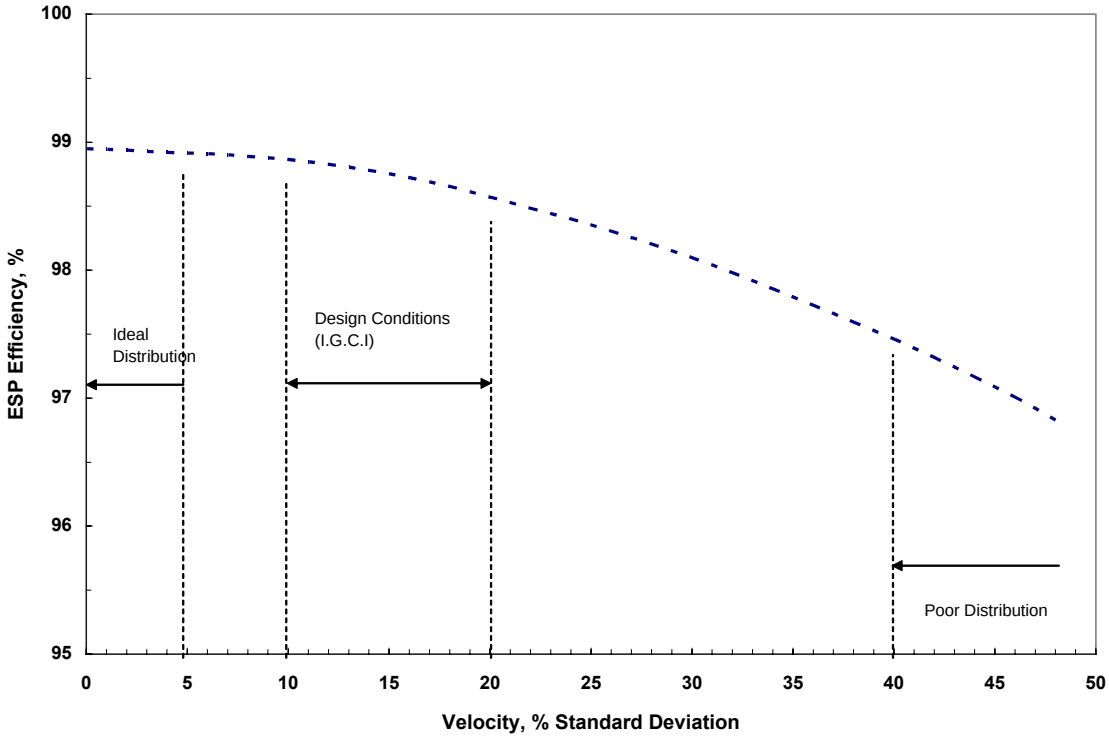

Figure 5-4. Variation of efficiency with gas velocity standard deviation.

In most process plants, the carrier gas velocity at full load is typically between 13 and 20 m/s in order to minimize cost, pressure loss, erosion, particle deposition, and thermal losses through interconnecting ducts. In order to reduce this duct velocity to around 1.5 m/s in the precipitation field, a diffuser with an expansion ratio of 10 or more is required. The expansion ratio depends on the design gas velocity and type of particle to be collected. The

design of this transition section, usually as pressure drop, is critical to achieve a uniform flow profile through the precipitation field if optimum performance is to be obtained.

With many installations, cost and space restrictions mean that sharp angled diffusers are used to decelerate the gas velocity and distribute the flow through the ESP. There are two main diffuser types used in practice; one is to use a fully-splintered transition section, based on an "egg-box" principle, to control the spread of the gas followed by a smoothing screen further downstream across the face of the field. The other type of approach is to use a series of perforated screens. If the transition is short and has steep angles, the flow will separate from the duct walls, creating a central high velocity jet that hits the perforated plate and spreads sideways, which results in a recirculating gas flow adjacent to the walls. To minimize this effect, it is normal to have a series of perforated plates having different porosity along the length of the transition to obtain the degree of smoothing required.

Although, it has been generally accepted throughout the precipitation industry that a 15 percent standard deviation will produce a satisfactory velocity distribution profile, there has been a recent trend to consider a skewed distribution, particularly in the vertical plane, for units having high levels of unburnt carbon or very high particulate loading. In these instances, some ESPs have the gas distribution modified so as to increase the gas velocity in the lower part of the inlet field to 30 percent higher than at the top of the field, while the converse flow profile is adopted in the outlet field, as indicated in Figure 5-5. The theory

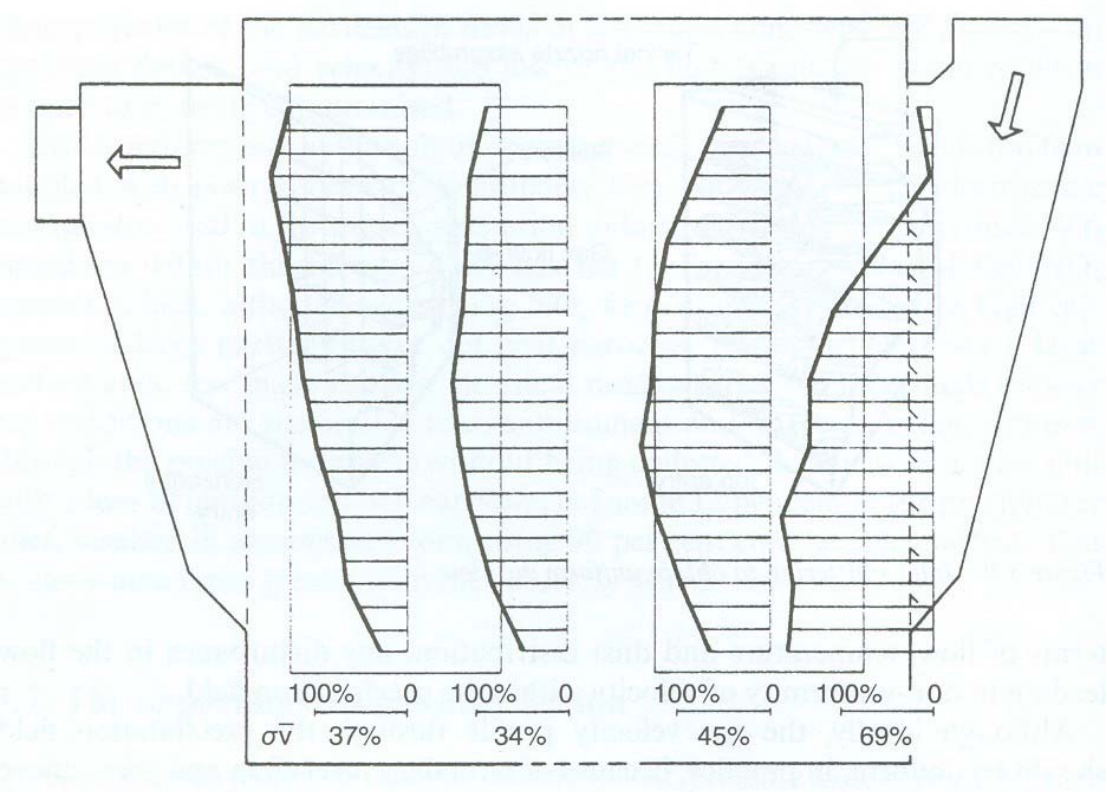

Figure 5-5. Skewed velocity distribution profile.

behind this form of distribution is that the bulk of the collected material at the inlet, with higher mass loading or readily entrainable dusts, has the least distance to fall after release from the collectors, which should reduce reentrainment into the downstream sections of the ESP. At the outlet, by having the high flow towards the roof of the ESP, any dust released from the collectors will pass through a lower axial velocity area, which again should reduce any incipient reentrainment.

Regardless of whether a standard or skewed velocity distribution approach is considered, it is important that the gas distribution in the horizontal plane is as uniform as possible, otherwise the performance will be adversely affected. A further practical consideration is the avoidance or minimization of gas bypassing over or under the actual precipitation field. This bypass results from boundary layer drag forces producing a slightly higher-pressure drop across the field because of the internals. To minimize the risk of this bypassing gas impacting overall performance, small "kicker" baffles are typically installed at the top and bottom of the field to break the gas from the walls and divert the flow into the field area. Although this is a palliative solution, since gas will still tend to loop, plant performance measurements have produced emissions of less than $1mg/Nm^3$ on some high efficiency installations. An alternative approach used by some suppliers is to install full height hopper baffles to minimize looping.

5.5 Viscosity and Density

These parameters are determined by the composition and temperature of the gases and affect the precipitation process as follows:

- As the charged particles migrate through the inter-electrode space, they are retarded by the effects of gas viscosity.
- As the temperature rises, although the gas density decreases assisting ion movement, the viscosity rises and hinders the particle transportation mechanism.

With ESPVI 4.0W, the effects of viscosity and density are automatically considered. The model with inputs of composition, temperature, and pressure, as will be seen later in this chapter, will automatically and accurately compute the viscosity and density of the gas, which it will then use in the determining the ESP's performance.

5.6 Flue Gas Properties with ESPVI 4.0W

"Gas Properties" on the "Data Entry and Editing" pull-down menu brings up the window shown as Figure 1-7, which allows input of the gas properties that are among the major parameter inputs needed to define ESP operation. The text box entries on this window apply to the whole ESP. The gas volume, composition, and temperature are important for determining the load on the ESP and the viscosity and mobility of the gas.

Between some of the labels and text boxes are values enclosed either in brackets [ ] or in parentheses ( ). Those values enclosed in the brackets are typical values that are provided for guidance. It does not necessarily mean that those values should be used. The values enclosed

in parentheses are calculated based on other data that has been provided as input elsewhere in ESPVI 4.0W.

Temperature on the "Gas Properties" window is the temperature at the inlet to the ESP, in degrees Celsius. This value is important for determining the gas properties that are temperature dependent. Operating temperature typically falls in the range of 140–180 °C. ESPs collecting high resistivity dusts have been operated at temperatures up to 450 °C to allow operation on the hot side of the resistivity temperature curve of Figure 6-1.

Temperature is provided as input to allow ESPVI 4.0W to calculate the gas viscosity and ion mobility within the V-I calculations and the electrical breakdown conditions. Resistivity is generally responsive to temperature changes. If the ESP experiences a range of temperatures, either across its face or along its length, the effects of temperature on the particulate resistivity should be examined and used for the modeling. Aside from affecting resistivity, temperature changes cause relatively small differences in performance, provided the volumetric flow rate is held constant.

Pressure on the "Gas Properties" window is set to the value of atmospheric pressure at the ESPs. This is primarily to indicate altitude effects because pressure affects ion mobility slightly and electrical breakdown to a larger extent. Values of 101.3–87.3 kPa (1–0.86 atm.) have been encountered for ESP installations. The internal pressure within some ESPs differs slightly from atmospheric as a result of the forced draft. It is not considered worthwhile to attempt to enter this slight difference in pressure.

The Volumetric Flow is the actual volume flow of the gas stream at the inlet temperature of the ESP. If the flow volume is available as flow volume at normal conditions, it must be corrected by multiplication with the factor $T_a/273$ in which T_a is the actual gas temperature.

The next group of text boxes in the "Gas Properties" window is used to enter the composition of the flue gas in percentages of N_2, O_2, CO_2, H_2O, SO_2, and SO_3, after including any excess air. These percentages should sum to 100 percent. If not, the program will display a message asking that the data either be reentered or allow it to normalize the data to 100 percent. ESPVI 4.0W will not allow the process to continue unless the composition data is correctly entered. Note that the sulfur oxides are displayed in ppm although they are stored in the files as percentages.

The Viscosity is the gas viscosity, which is dependent on the gas temperature and composition, and is used as part of ESPVI 4.0W's internal computations. A value calculated from those parameters is shown between the parentheses, which allows the option of either the calculated viscosity or some other value. If the calculated value is to be used, it should be entered in the text box.

The Mobility is the equivalent ion mobility of the gas, which is dependent on its composition, temperature, and pressure. Most of the current in an ESP is transported by the ions. The greater the value of the ion mobility, the greater is the current for a given secondary voltage. ESPVI 4.0W calculates the ion mobility as part of its internal computations. SO_2 has

a dominant role in the ionic conduction properties of the gas, and it is the only component in the composition that is allowed by ESPVI 4.0W to affect the ion mobility. If the SO_2 concentration is set to zero, ESPVI 4.0W uses the ion mobility of air. If the SO_2 concentration is changed and then **Accept** is used to close the window, the "Gas Properties" window should be reopened to calculate ion mobility. If the calculated ion mobility in the parentheses differs from the value in the text box, replace it with the calculated value and then close the window with **Accept**.

If the calculated values for Viscosity and Mobility differ by one percent or less from the values in the text box, ESPVI 4.0W will ignore the updating of the text box value. The "Gas Properties" window and Viscosity and Mobility, in particular, are the only places where this occurs.

There are command buttons along the bottom of the "Electrode Design" window labeled **Cancel**, and **Accept**. The **Accept** command button closes the window with its current data contents so that the modeling can proceed. Clicking on **Accept** only allows the calculations to proceed with the window's current contents. It does not save the contents, which must be done by means of **Save** under "File" in the main window. Clicking on the **Cancel** command button closes the window and restores the saved data entries.

5.7 Changing Gas Temperature

The inlet gas temperature can change for various reasons. Two cases will be examined. The first will be a change of temperature without a change in the volume flow rate of the gas. The second will be a change of temperature that causes a resultant change of volume flow rate. In both cases, the temperature change will be 20 °C.

To change the temperature without changing the volume flow rate, enter "Gas Properties" and change Temperature from 141 to 121 °C. Set the Viscosity and the Mobility in the text box to the calculated values in parentheses. Go to "Standard Method" and then to "All Results" to view the change. The results are seen below in Table 5-1.

Table 5-1. The Effect of Gas Temperature on ESP Efficiency

Section	Parameter	Original Temperature	Lower Temperature	Lower Temperature & Volume
1	Voltage, kV	41.0	41.0	41.0
	Current, mA	0.180	0.161	0.163
2	Voltage, kV	40.0	40.0	40.0
	Current, mA	0.217	0.196	0.197
3	Voltage, kV	39.0	39.0	39.0
	Current, mA	0.216	0.195	0.196
Total	**Penetration, %**	2.37	2.32	2.12
	Emission Change, %	-	-2.1	-10.5

Lowering the temperature with an accompanying change in gas volume requires that the gas volume of 119 m^3/s be multiplied by the ratio of the new to the original absolute temperature. That is, 119 × (273 + 121)/(273 + 141) = 113.25 m^3/s.

Enter the new temperature and volume into the appropriate text boxes, Temperature and Volumetric Flow. Because we have changed the volume flow rate, we know that the Gas Velocity and SCA should change. Therefore, go to "ESP Design" and try to close the window with **Accept**. It is noticed that the small "Consistency" window opens. Go through the same routine as previously choosing only those items that have to change. If this particular run is performed immediately after the previous run, with just the reduction of temperature, the correct Viscosity and Mobility settings would already be in place. Also, notice that, because Volumetric Flow was lowered, the gas velocity changed from 1.8 to 1.72 m/s.

In both cases, the voltages remained the same because "Standard Method" was used. However, the currents changed because of the change of ion mobility. On the second screen of "All Results", on the lower right side, is an item called "Reduced Mobility", which is immediately to the right of "Mobility". The value in "Mobility" is the ion mobility entered in the "Gas Properties" window. "Reduced Mobility" is the ion mobility corrected for changes of temperature, pressure, and composition. The change to the ion mobility from the temperature reduction caused the reduction in current. In the second case, the change in volume increased the particle concentration and the SCA. The change in current, therefore, resulted from both the decrease in temperature and the increase in space charge. In this case, both working together gave a greater improvement in performance.

5.8 Changing SO_2 Concentration

This example is intended to show the effect of a change of gas composition on an ESP's performance. The normal SO_2 concentration for SAMPLE is 805 ppm. It will be lowered to 100 ppm. The change will affect the ion mobility, thereby modifying the currents. Because "Standard Method" will be used for the ESPVI 4.0W computations, the voltages will remain the same. Small changes in some gas components, and most especially SO_2, will have a significant effect on the ion mobility of the gas in the ESP.

In actual practice, this type of reduction would usually not be expected to occur without an accompanying increase in particle resistivity, but the resistivity will remain unchanged for this example. The purpose of this exercise is to show the importance of good gas composition data in addition to other good ESP data needed for modeling.

To lower the SO_2 concentration from 805 to 100 ppm, open the "Gas Properties" window and enter the 100 into the "SO_2 Fraction" text box. Use **Accept** to close the window. Reopen "Gas Properties" and notice that the calculated "Mobility" in parentheses no longer agrees with the text box. Replace the text box mobility with the calculated value and close the window. Go to "Standard Method" and then to "All Results".

The results, shown in Table 5-2, show the increase of the ion mobility caused by low SO_2 concentration resulted in a significant increase in the corona currents and, consequently, to the input power to the ESP, resulting in decreased particle emissions. In actual practice, as will be seen in the next chapter of this manual, a decreased amount of SO_2 in the gas would likely have been accompanied by an accompanying increase in the particle resistivity. With increased dust resistivity, voltages and currents for the ESP would have to have been reduced. At the same time it is worth examining "All Results" as a means for determining what other effects are occurring within an ESP for this exercise as well as the other ones in the manual.

Table 5-2. The Effect of SO_2 Concentration on ESP Efficiency

Section	Parameter	SO_2 Concentration, ppm	
		805	100
1	Voltage, kV	41.0	41.0
	Current, mA	0.180	0.369
2	Voltage, kV	40.0	40.0
	Current, mA	0.217	0.458
3	Voltage, kV	39.0	39.0
	Current, mA	0.216	0.456
Total	Penetration, %	2.37	2.22
	Emission Change, %	-	-6.3

Chapter 6
Characteristics of the Particles and their Impact on ESP Performance

The properties of suspended particles that impact ESP performance are size distribution, concentration, resistivity, shape, and composition. In this chapter, these properties will be discussed as well as how they impact ESP performance.

6.1 Space Charge

As particles enter an ESP with the gas stream, they acquire an electric charge from the ions formed by the corona process and then are collected by means of the electric field between the corona discharge electrodes and the grounded collector plates. In addition to those events, another very important event is occurring. This is the generation of the space charge.

Each charged entity, both particles and ions, in the gas stream has its own electric field. Each volume of the gas has an electric field that is the sum of the electric fields of the entities. Space charge is the quantity of charge per unit of volume (C/m^3).

As particles enter the ESP and acquire a charge from the first discharge electrode, the space charge will start to increase. The effect of the space charge is to decrease the electric field near the first corona discharge electrode. This, according to Equation 2.3, raises the corona onset voltage, which decreases the corona current, an effect known as corona suppression.

As the space charge moves to the next corona discharge electrode, the process repeats itself by suppressing its corona. However, suppression is not as severe. A portion of the particles has been collected, which lowers the space charge thus causing less corona suppression. At the same time, the particles are likely to acquire additional charge. This repeats itself from discharge electrode to electrode. For each electrode, the corona current becomes increasingly greater. For the section, the total current is the sum of the currents for all of the corona discharge electrodes from inlet to outlet.

The process repeats itself for the subsequent sections of the ESP. However, because quantities of the particles have been collected, the corona suppression will not be as severe and the section current will be higher. Figure 2-2 shows typical V-I curves for a well operating four-section ESP with a collector electrode spacing of 400 mm operating with moderate space charge. The increasing current that results from the reduction in space charge is clearly shown in going from the inlet to outlet sections. V-I curves for other collector electrode spacing are similar. For ESPs operating with greater amounts of PM, the space charge will be stronger; the differences in the section curves will be even more apparent.

Table 6-1 presents the electrical operating conditions for a three section ESP having 400 mm spaced collectors, which, like Figure 2-2, shows the effect of corona suppression. The decreasing space charge from inlet to outlet results in the decreasing voltages and increasing

currents. Should the inlet field become inoperative for any reason, then the second section would assume the operating characteristics of the first, and so forth.

Table 6-1. Electrical Operating Conditions for a 3-Section ESP

Section	Voltage, kV	Current, mA
Inlet	70	392
Center	68	601
Outlet	64	1020

The overall effect of space charge in suppressing corona is not all that bad. Up to some point at which the corona current is so severely suppressed that the charging essentially stops, the effect of increasing space charge is to actually increase the collection efficiency of the section. This is because the decrease in the electric field in the central zone around the discharge electrode is made up by an increase in the electric field in the zone close to the collecting electrode, which, in turn increases the migration velocities.

A user of the ESPVI 4.0W does not have to worry about the complexity of computing the space charge, determining the amount of corona suppression, the resultant reduction of particle charge, and computing the increased electric field and migration velocities. The model computes these values for each discharge electrode in an electrode-by-electrode fashion in each section.

Because space charge is a function of the number of particles and their charge in the volume of gas under consideration, it is obvious that their concentration is an important factor. For the same total mass weight of particles, there could be either a greater or lesser number of the fine particles, which dominate the formation of space charge. Less obvious is the effect of particle size distribution on the space charge. For spherical shaped particles, which are the dominant shape in fly ash, the difference is in the ratio of the cube of their diameters. Larger particles will acquire a greater charge than will smaller ones. However, by number, fly ash will usually contain many more and finer particles than larger ones. In fact, the major contributor to the space charge is those particles that are less than 1 μm in size. Therefore, the two contributors to space charge are concentration and size distribution.

6.2 Concentration

In initial design of an ESP, its later upgrading, or analysis by modeling, the inlet fly ash concentration needs to be known. It is expressed in mg/m^3, which is the value that ESPVI 4.0W's internal calculations use.

An ESP, except for changes in load, is often operating under relatively steady state conditions. The main effect of changes to the inlet fly ash concentration is minimal and normally only impacts the outlet emission level. Generally, increases in the inlet loading over that specified tend to arise from an "upset condition" on the process plant and are normally associated with the carryover of larger sized particles, which are more readily precipitated

than the finer ones. Nevertheless, it is possible that the “upset condition” can modify other characteristics of the gas and result in an unacceptable emission increase. Although these upset conditions are generally transitory, they need to be addressed if the plant has to comply with strict legislative emissions.

6.3 Particle Sizing

Determination of the performance of an ESP is very much dependent on accurately knowing the size distribution of the particles that enter the unit. Fly ash particles generally follow a log normal distribution, which is totally described by the geometric mass mean diameter and the geometric standard deviation. ESPVI 4.0W uses these two numbers, which it can accept directly as input, in its internal calculations. Alternatively, it can accept the particle size information as histogram data, which is usually in the form of the cumulative amount contained for each size. ESPVI 4.0W internally converts the histogram data into its equivalent log normal distribution.

If accurate particle size data is available, it should be used directly in ESPVI 4.0W. Otherwise, other procedures discussed later in this chapter, called reverse modeling, are used to calculate the particle size distribution that has caused the electrical conditions and the observed amount of corona suppression for the full-scale ESP being analyzed.

6.4 Particle Shape and Composition

For most applications, the particle shape can be either granular (resulting from the comminution of the feed material by grinding, milling, or other means) or small spherical fumes. Where fumes are involved, these usually result from material being initially volatilized in the high temperature zone of the process to subsequently condense into a fume upon cooling. For coal combustion, about 1 percent of the ash components can be volatilized within the furnace and condense out in the cooler reaches of the boiler to form submicrometer sized fume; however, this quantity is significant for the formation of space charge and resists collection.

It has been noted that the NIS ESPs generally operate with high particle concentrations, which results in a large amount of space charge. As stated previously, the greatest contributor to the space charge are particles of the one-micrometer size or smaller. These submicrometer particles are usually of the spherical type.

The analytic solutions, including the ESPVI 4.0W, of particle charging and collection in an ESP usually assume that the particles are spherical. Fortunately, the larger particles, which are easily charged and collected, are consequently of little concern. The concern is the submicrometer particles, which not only establish the electrical conditions in the ESP, but are also the most difficult to collect. Because submicrometer particles are generally spherical, the modeling of the ESP by ESPVI 4.0W is accurate.

The shapes that can seriously impact performance are usually those having a thread like form, where the precipitated fibers can link together and short circuit the electrical supply. A similar particle-linking phenomenon can sometimes arise with platelet-type materials, which

have a fairly large surface area but virtually no thickness; these are very light in terms of mass and tend to attach themselves end-on to the collectors and each other.

In general, the chemical composition of the particles does not have a significant effect on the mechanical design of an ESP. However, if a particle is chemically reactive, corrosion resistant materials must be used for ESP fabrication.

If carbon becomes trapped in the spherical particles, “cenospheres” (hollow spheres) can be produced, which have a large surface area but little mass and are subject to scouring and reentrainment from the collectors. These cenospheres do not impact on electrical operation or plant design but generally, because of their low mass and poor cohesiveness, can be readily reentrained, thereby detracting from overall performance.

6.5 Particle Resistivity

The electrical resistivity of any PM is controlled by one of two mechanisms. One is the bulk volume conductivity, which is a function of the particle matrix constituents, and the other is surface conduction, which is controlled by the particle surface reactivity and gas components.

Figure 6-1, illustrates the effects of moisture and temperature on a typical high-resistivity fly ash. On the left side of the curve, surface conduction dominates, but bulk volume conductivity dominates on the right side. What is obvious is that the resistivity is at its peak level for the usual operating temperature of about 150 °C and typical moisture levels.

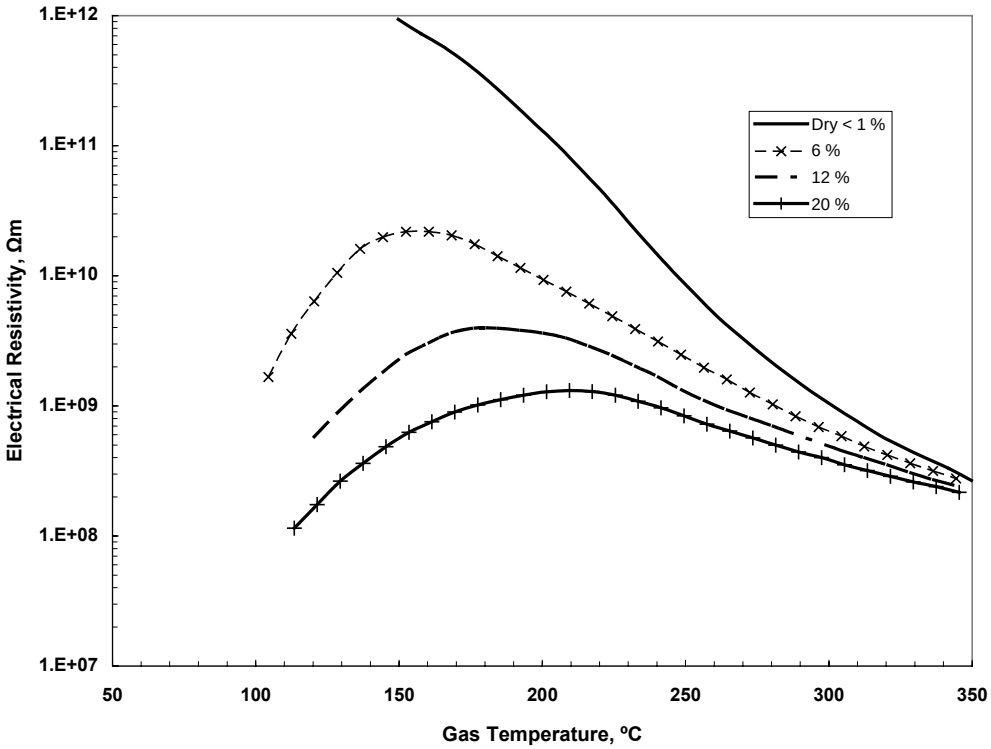

Figure 6-1. Effects of temperature and moisture on fly ash resistivity.

Some ESPs that operate with high resistivity fly ash are designed to operate at temperatures more than 350 °C, to take advantage of the lower bulk volume conductivity. ESPs operating at these high temperatures, or on the right side of the curve, are commonly referred to as “hot side” ESPs.

More commonly encountered are ESPs that operate on the left, or “cold side”, of the curve where surface conduction dominates. As far as “cold side” ESP performance is concerned, the surface condition of the particle is generally more important than the chemical composition of the matrix. For applications firing sulfur-containing carbonaceous fuels, the flue gas on cooling can pass through an acid dew point temperature. Any resultant sulfuric acid mist produced subsequently uses the particles as condensation nuclei to deposit a thin layer of highly conductive material on their surface.

For steam-raising units, the coal ash carried forward to the ESP normally is composed of a high percentage of silica and alumina, both excellent insulators having extremely high resistivities. Units with sulfur in the coal and sodium oxide in the ash tend to reduce the resistivity in “cold side” applications. For “hot side” units, situated upstream of the air heater and operated at a temperature of 300 °C or more, there is no possibility of reaching any dew point temperature. Hence, this mechanism relies more on improved electrical conductance within the particle matrix.

6.5.1 Factors that Affect Particle Resistivity

During combustion, most of the coal’s pyritic sulfur burns to produce sulfur dioxide, although a small percentage converts to sulfur trioxide. Sulfur trioxide may reduce the fly ash electrical resistivity in “cold side” ESP applications. There is generally at least 6 percent moisture present in boiler flue gas, either from the moisture or converted hydrogen in the coal or from atmospheric moisture in the combustion air. At the equivalent dew point temperature, any free gaseous SO_3 reacts with this gas phase moisture to produce sulfuric acid mist, which then uses the particles as condensation nuclei. The subsequent thin layer of highly conductive sulfuric acid deposited on the fly ash enables charge transference to occur. The actual effect of surface conditioning in this case depends on the amount of sulfur trioxide and moisture present and on the gas temperature, which dictates the saturation vapor pressure.

For coals containing in excess of 1 percent sulfur, there is generally sufficient natural surface conditioning at normal operating temperatures of around 130 $^{\circ}$C to give acceptable values of resistivity for effective precipitation. Although this is generally true, there are incidents where the fuel can promote a severe reverse ionization type of operation. This may particularly be the case if the hydrocarbon content is not totally combusted but is initially volatilized and later condenses on the fly ash particles as an insulating type of coating. This phenomena/occurrence is probably more prevalent during plant start-up, when the furnace is cold and the oil start-up burners are not ideally set up; however, the situation can arise at other times, so one must be aware of this potential problem.

Calcium and magnesium present in the ash tend to produce sulfates with exposure to and reaction with sulfur trioxide in the gas stream. These sulfates are chemically produced and, having low conductivity, tend to interfere with the potential resistivity reduction from sulfur trioxide condensing as sulfuric acid mist onto the fly ash. Calcium and magnesium components present in the fly ash, therefore, must be considered as leading to lower ESP performance through increased resistivity effects and requiring appropriate adjustments in the design/sizing of any installation. The ash from certain lignite and sub-bituminous coals can have calcium oxide contents of around 20 percent, which have a significant impact on the initial ESP sizing.

The presence of sodium in the ash behaves in a very different manner. The sodium ions within the particle matrix act as charge carriers instead of surface conditioners, which assists in negating the effect of high resistivity fly ash to a certain extent. Measurements of fly ash resistivity directly within an ESP show acceptable agreement with those calculated from the Bickelhaupt relation. Figure 6-2 shows how the resistivity varies with sulfur in the coal and sodium oxide content of the ash. It is interesting to note that at around a resistivity 2×10^8 ohm-m, the curve steeply increases with reduced values of sulfur plus sodium, whereas for higher values of sulfur plus sodium oxide the resistivity decreases only slowly.

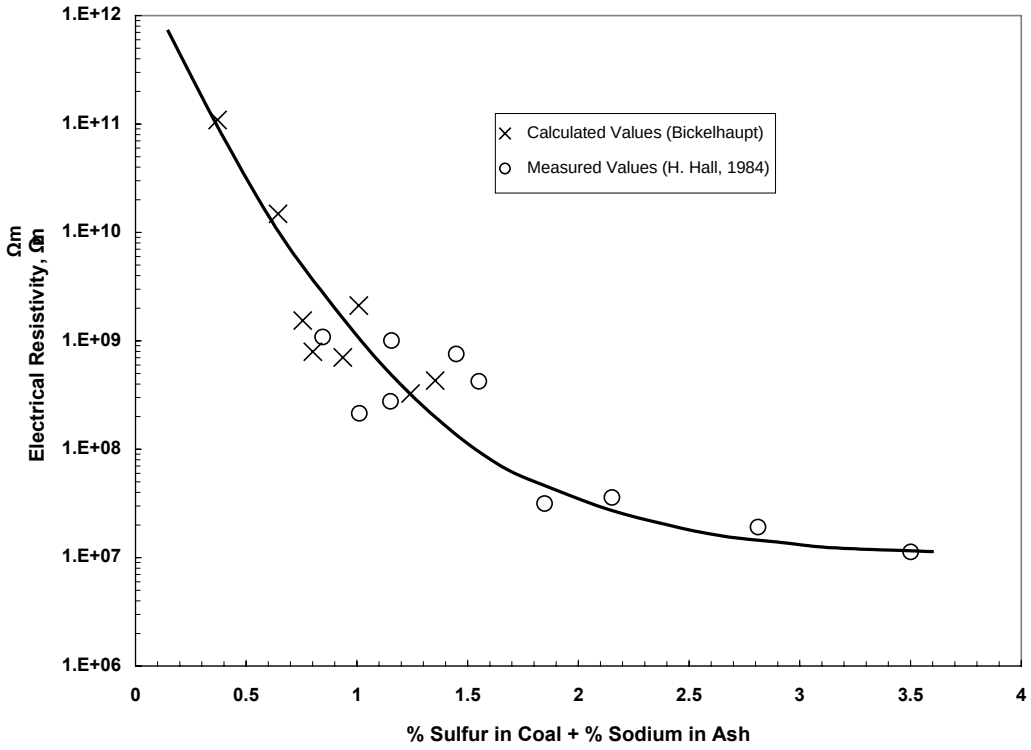

Figure 6-2. The effect of sulfur in coal and sodium in ash on fly ash resistivity.

6.5.2 The Effect of High Resistivity on the ESP

Resistivity effects on an ESP mainly relate to its action on the particles in the layer that forms on the grounded collector plate. In practice this layer usually consists of a permanent bonded

layer (resulting from repeated boiler start-ups and shut-downs when the temperature passes through the dew point) covered by a layer of relatively recently deposited dust. Only this recently deposited layer will shear off when rapped; dust is only dislodged from dust and not the metal surface. This is shown schematically in Figure 6-3.

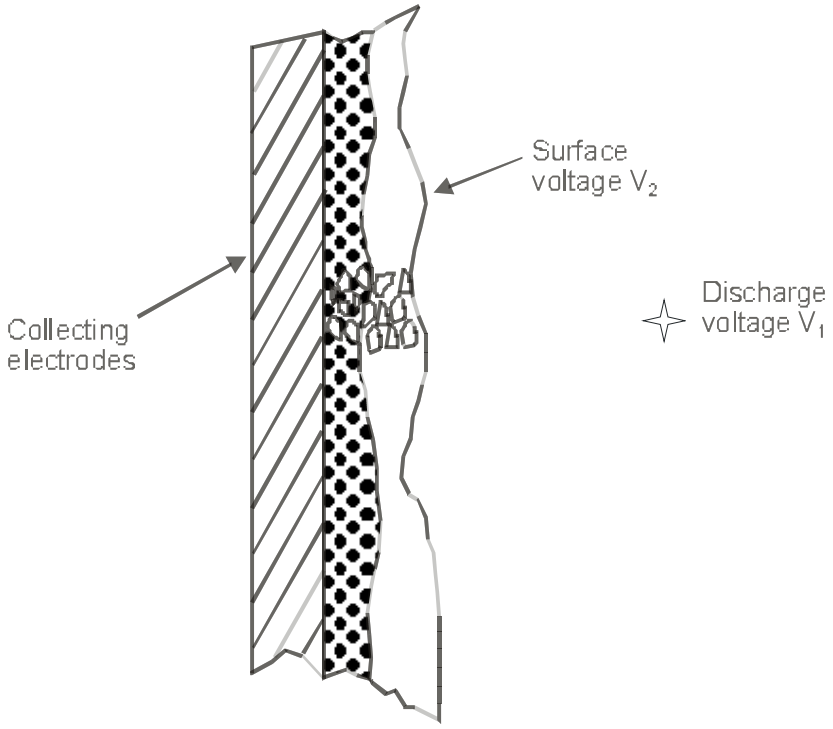

Figure 6-3. Representation of the conditions arising across a collector dust deposit.

The presence of this dust layer can seriously affect the electrical operating conditions. A voltage drop across the dust, which depends on the dust's thickness and resistivity and on the corona current flow, produces a voltage on the surface of the dust layer that influences the electrical operation of the section as will be shown for three fly ash resistivities:

- Normal Favorable Dust — Resistivities less than 2×10^{8} ohm-m with typical full-scale corona current flow up to around 10^{-4} A/m^2
- Resistive Dust — Resistivities around 1×10^{9} ohm-m and an average corona current of about 5×10^{-5} A/m^2. High corona currents cause local electrical breakdown in the dust layer, which causes sparking, propagated to the discharge electrode. To limit corona current voltage, average voltage is reduced, which results in reduced collection. The area of the dust layer directly under the corona discharge electrode, where the current is highest, suggests the formation of reverse ionization.
- High Resistivity Dust — The electric field in dust layer ionizes gas in interstitial spaces causing an effect known as reverse ionization, or back corona. Positive corona current flows from collecting electrodes to discharge electrodes in addition to the

negative flow. The two currents are additive and normal metering will not discriminate between them. Reverse ionization is a complex phenomenon, and analysis of it does not really lend itself to the approach used for the other two conditions, where there is only negative corona discharge. The primary procedure for resisting the formation of reverse ionization is to severely limit the corona current, which decreases the average voltage to a level that approaches the corona onset voltage. The reduced collection requires a larger ESP to meet the efficiency requirements.

Figure 6-3 shows enlarged representations of the interstitial gas spaces in the dust layer directly under the negative discharge electrode, where the corona current is highest. For a dust of sufficient resistivity, the electric field in these interstitial spaces causes the contained gas to break down and form positive ions. This break down of the gas in the interstitial spaces can cause various effects that will dominate the operation of the electric precipitator.

The effects of various resistivity dusts are shown in Figure 6-4. Curve A is what may be observed with a “normal favorable dust”. The resistivity is sufficiently low so that the electric field in the dust layer never does reach the point at which its contained gases break down. Instead, the voltage increases to a point at which the electric field in the inter-electrode space is sufficiently high to allow a spark to propagate across the gap. The inception site for the spark is generally a small region of high electric field somewhere on the surface of the dust layer on the positively charged collecting electrode.

A “high resistive dust” has a sufficiently high resistivity to cause the formation of a significant electric field in the layer under conditions of low corona current and applied voltage. In this situation, V-I Curve B in Figure 6-4, the electric field in the dust layer becomes sufficiently strong to cause breakdown of the gas in the interstitial spaces. However, the voltage applied to the electrodes is too low to allow a spark to propagate. Instead, the ionized gas in the dust layer’s interstitial space causes the formation of positive ions that flow to the negatively charged corona discharge electrode. This has a two-fold effect, the first of which is to neutralize some of the negatively charged particles waiting to be collected, thereby decreasing the precipitator’s efficiency. At the same time, the flow of ions in two directions causes the high currents along with decreasing high voltage as shown by curve B.

Curve C shows a typical intermediate resistivity or “resistive dust”. For this situation, there is a combination of both a reasonably high-applied voltage with a corresponding high current. The reasonably high current in the dust layer causes formation of an electric field that is sufficiently high to breakdown, or ionize, the gas in its interstitial space. The breakdown of the electric field in the dust layer causes the transfer of its electric field to the gas in the inter-electrode space, allowing it to become sufficiently high so that a spark can propagate across it.

The explanation of the effects of particle resistivity is somewhat simplistic. However, it is sufficient to provide an understanding of what is happening in the precipitator and how it relates to ESPVI 4.0W.

Further examining curves A, B, and C in Figure 6-4 provides additional insight. The operating points curves for a precipitator operating with A and C will be at point where sparking commences. The electrical conditions for A are obviously superior to those for C. Therefore, one would expect that the same precipitator operating with A will have a significantly higher collection efficiency than it will if operating with C. Optimum performance with B would be at some point towards the bottom of the V-I curve, before it starts to turn steeply upwards. Therefore, its electrical conditions would be inferior to those of C, which is inferior to those of A. Therefore, the same precipitator operating with a dust having the resistivity of B, would have the poorest performance.

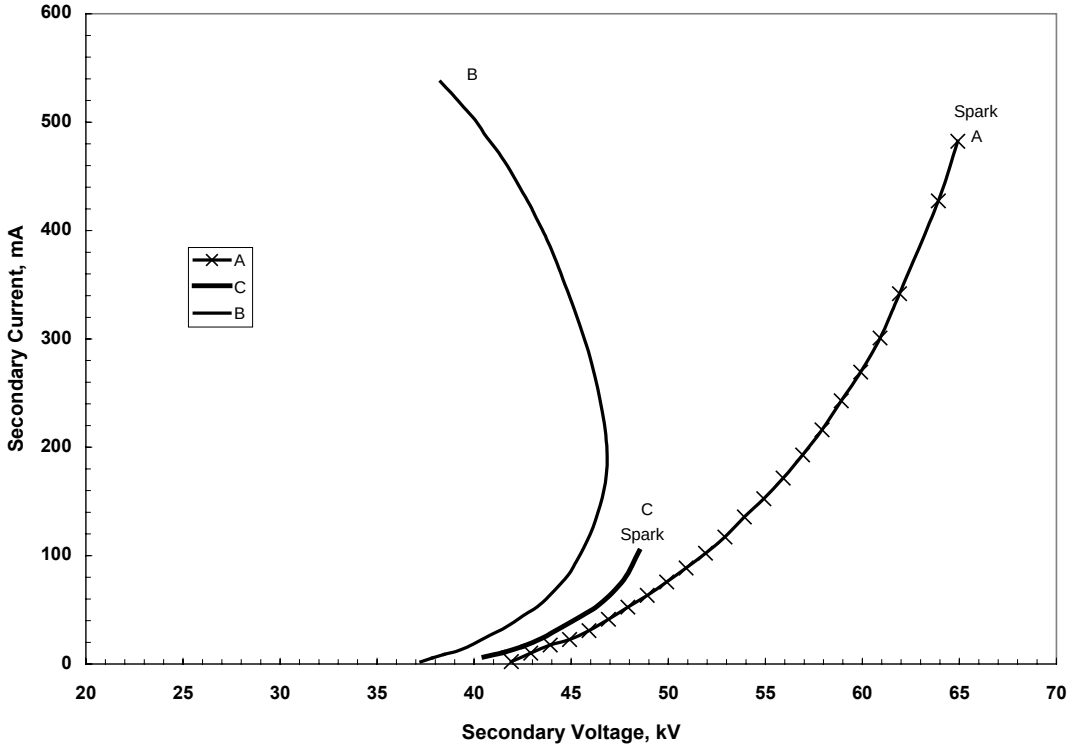

Figure 6-4. Typical V-I curves for different dust resistivities.

Although the greatest rate of dust deposition occurs on the collectors, even small accumulations on the discharge electrodes can have a deleterious effect on the electrode emission characteristics. It is therefore important to ensure that the discharge electrodes are effectively rapped. Dust deposits that are retained on the discharge electrodes will significantly change their electrical characteristics. Unless the corona discharge electrodes are kept continuously clean by effective rapping, the ESP may not operate at its design capability, and dust collection may degrade.

6.5.3 Correlation between ESP Performance and Particulate Resistivity

Measurements on a Japanese ESP firing Australian low sulfur (0.5 percent) coal, and therefore expected to give ‘difficult’ precipitation, showed that the ESP emission was very dependent on the sodium oxide content of the fly ash, as illustrated in Figure 6-5. The

decrease in emissions, as the sodium oxide in the ash increases, was due to back ionization, or back corona, as the resistivity of the fly ash increased. It should be noted that that this is the result of a test for a specific ESP and is provided here for illustrative purposes.

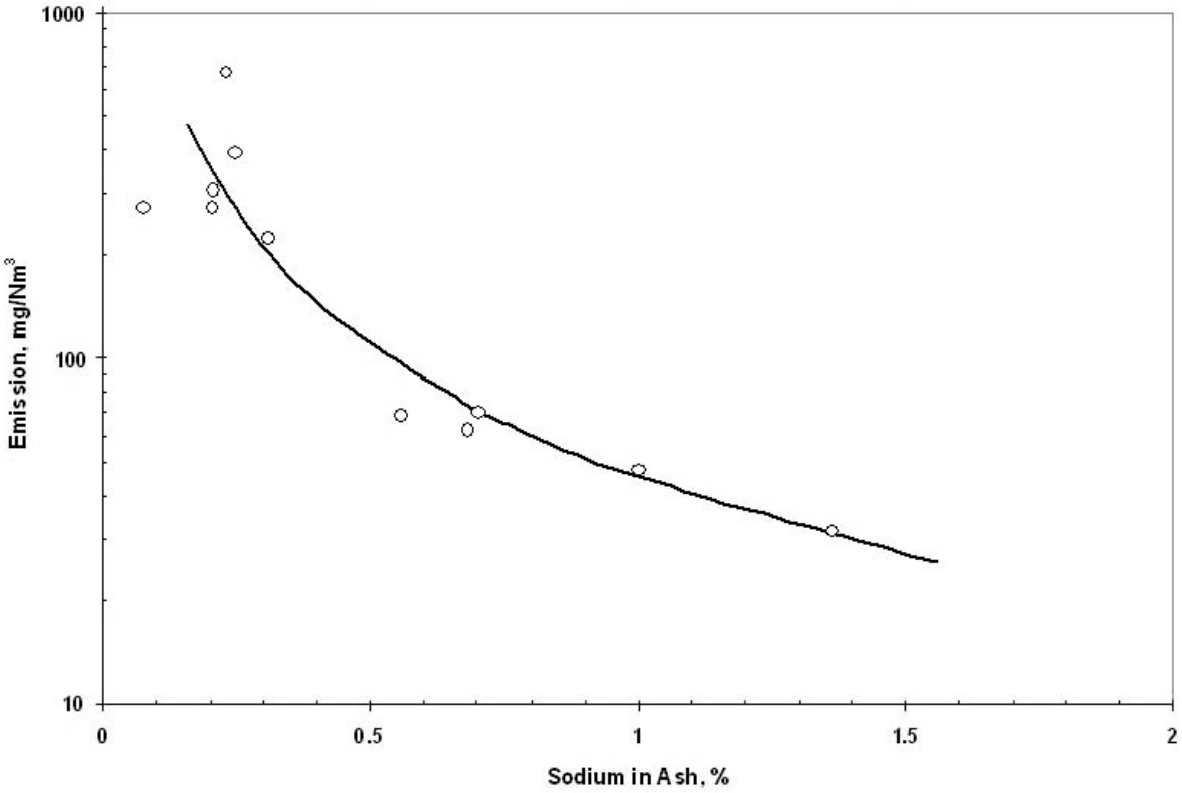

Figure 6-5. The effect of sodium oxide in the ash on an ESP's efficiency.

In the past, performance measurements on a large number of ESPs have been correlated with the coal and fly ash analyses, enabling first-order ESP sizing curves to be developed. Figure 6-6 indicates the effective migration velocity achieved for one ESP under normalized conditions of temperature, dust loading, and such against the coal sulfur and ash sodium oxide contents. Other curves, incorporating silica, alumina, calcium, and magnesium in addition to coal sulfur and sodium oxide in the ash have been developed, but these do not appear to significantly affect ESP-sizing requirements seen in Figure 6-6. Effective migration velocities can be useful as an approximate means for evaluating the performance of an ESP, especially for users who have a knowledge base of the performance of similar ESPs. It should be remembered that, in solving the modified Deutsch equation for effective migration velocity, there is one other variable to work with, which is the ratio of the collector area to the volumetric flow rate. It does not take into account differences in particle resistivity, level of space charge, sectionalization of the ESP, and such, which can skew the results when trying to apply effective migration velocity.

Gas components, ash chemistry, and reactivity at the ESP inlet are important in that they determine the particle resistivity, and hence performance, of the installed ESP. However, the only source of information available at the design stage is the raw coal and ash analyses,

together with operating temperatures at the inlet to the ESP. These analyses are able to provide the ESP design engineer with invaluable information on the probable fly ash resistivity and hence the potential ESP size for a specific efficiency. For new applications, the fly ash electrical resistivity is computed from the coal and ash chemistry by using a relationship developed by Bickelhaupt. This has proved extremely useful, since one can assess what changes can be applied to the inlet gas conditions or fly ash chemistry in order to modify the resistivity and thus enhance the performance.

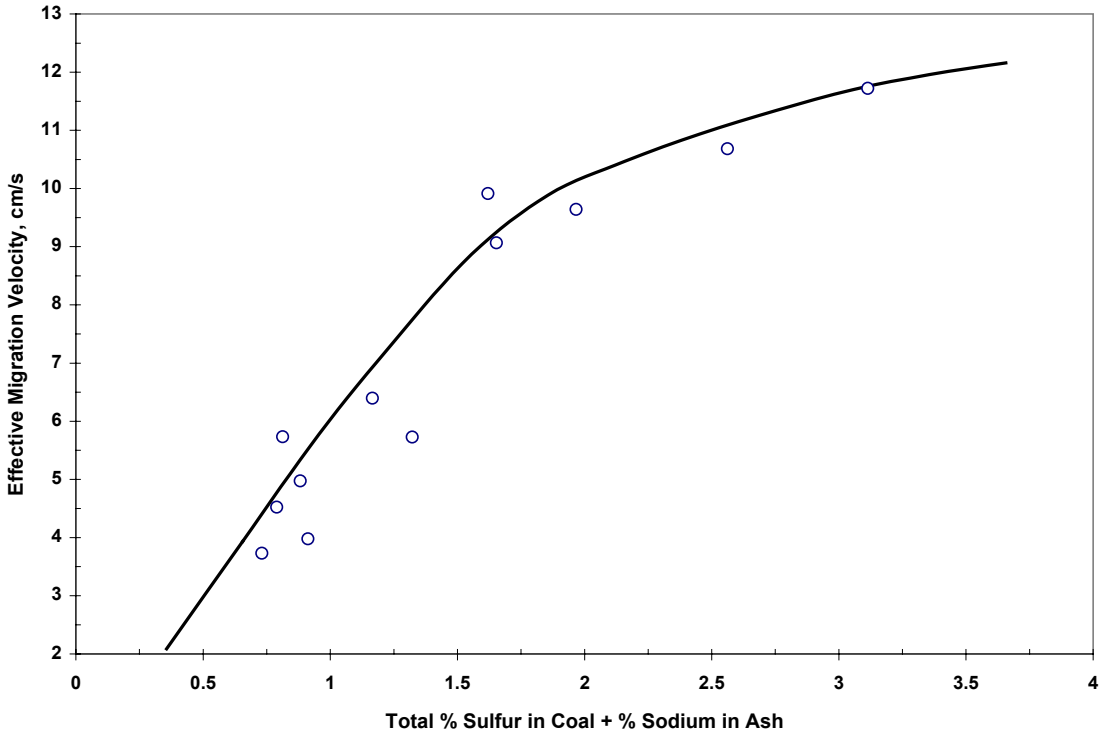

Figure 6-6. The effect of sulfur in coal and sodium in ash on ESP performance.

6.5.4 Electrical Conditions for ESPs Collecting Resistive and High Resistivity Dust

As should be realized by now, the higher the resistivity of the particle matter, the lower the allowable corona current to prevent the occurrence of reverse ionization, or back corona. For operation with dusts of higher resistivity, the current is reduced which causes the voltage to be reduced. The question becomes, what should the current and, thereby the voltage, be?

An example previously discussed touched on the approach by setting up some guidelines involving the resistivity of the dust and the electric field that would cause the breakdown of the field. It also suggested that the current be further reduced because of the space charge effect, which can cause increasing currents from the inlet to the outlet of the section. It was suggested that the maximum local current be reduced by a factor of 5 to 10. It was further

recommended by the authors that for very high space charge, as is common in the combustion of NIS coals, the factor of 10 be considered.
To make the matter simpler and more easily applied, Figure 6-7 is presented as adapted from McDonald and Dean (1980). Curve 1 is the adaptation of Hall's 1971 experimental data for the maximum average current as a function of the resistivity. Curves 2 and 3, added by the authors of this manual, represent the reduction in average current by factors of 5 and 10, respectively.

Once the maximum average current is chosen, the "Fixed V-I" on the "Calculate V-I Curve" pull-down menu is used. To set the point at which "Fixed V-I" stops its calculations, use **Maximum local current density** in "Calculation Options".

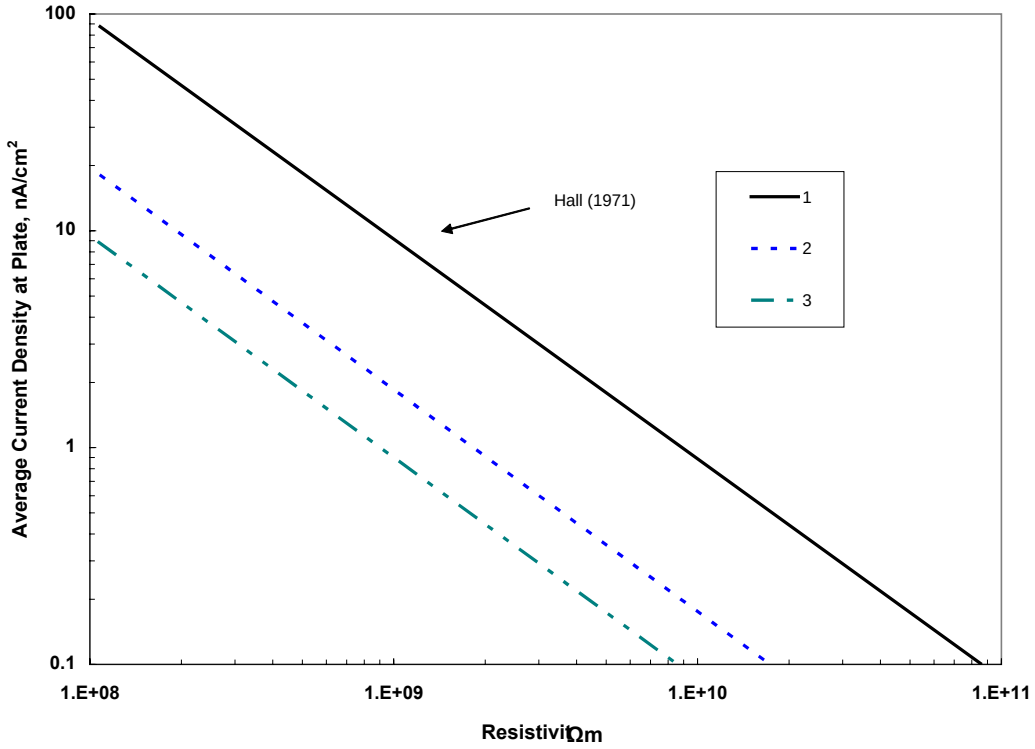

Figure 6-7. Effect of resistivity on allowable current density in an ESP.

6.5.5 Low Resistivity Ash and Its Effect on Performance

It is customary in the power industry to consider unburnt carbon as approximately equal to the loss on ignition at 800 °C. This carbon is usually present in the form of partially burnt coal, comprising large particles of low mass and typically having a bulk resistivity of about 1×10^6 ohm-m. As such, although the carbon particles can be satisfactorily charged by the corona, they loose their charge so rapidly as they approach the collectors that they can be repelled back into the gas stream where they can be reentrained. This charging and repulsion situation can occur several times as the particles progress through the ESP, and some can eventually escape without being collected. Even if the particles are retained on the collectors, the fly ash plus carbon deposit has very low cohesiveness and tends to shatter and explode

upon rapping rather than being sheared off the collector, so it can be readily reentrained by the horizontal gas flow. In either situation the efficiency of collection will be reduced. Although the larger carbon particles are deleterious to ESP performance, carbon in the form of fine particles, such as carbon black, have a low saturation charge that is insufficient to repel them back into the gas stream, and they are collected with the other materials. The mixture of fine carbon plus the other materials can result in a significant reduction in the bulk resistivity of the deposit, which aids performance.

6.6 Particle Properties in ESPVI 4.0W

From the main window, Figure 1-2, go through the pull-down menu "Data Entry and Editing" to bring up the "Particle Properties" window, Figure 1-8, which allows entering properties specific to the particulate material needed for ESP performance calculations.

The first text box on the top of the "Particle Properties" window is **Mass Load,** or concentration of particles by mass in the gas stream. The value is expressed in mg/m^3 and can range from 200 to 60,000 mg/m^3. The **Mass Load** is important for determining emission compliance, because the outlet emissions are directly related to the inlet concentration through the ESP collection efficiency. The operation of the ESP is also affected heavily by the **Mass Load**, which influences the space charge and electrical conditions. Some of the V-I characteristics of the ESP are also affected by the concentration. This is because the accumulation of charges on the particles creates a space charge component to the electric field that opposes the further flow of ions from the corona. This is particularly true for particle size distributions with mass median diameters less than about 2 micrometers and for higher values of mass loading. In extreme cases of high space charge, the apparent current density at the collecting plate can approach zero, but some charge is deposited on the particles and some collection will take place. It should be noted that the mass loading is for the gas at the actual ESP operating temperature and pressure. Accordingly, if the data is provided as g/Nm^3, it must be converted to mg/m^3.

The next two text boxes are **Mass Mean Diameter** and **Geometric Standard Deviation**. The log-normal particle size distribution is defined by the two variables geometric mass mean diameter and the geometric standard deviation, which are the **Mass Mean Diameter** and **Geometric Standard Deviation**, respectively, on the "Particle Properties" window. If these values have been accurately measured, they may be entered directly. ESPVI 4.0W uses the particle data in log-normal form for its internal calculations. Upon loading the particle size data as the geometric mass mean value and the geometric standard deviation, ESPVI 4.0W will automatically divide the particle size distribution defined by these values into the 27 size fractions and load them into the proper bin.

Frequently particle size data is available only in a histogram form rather than as log-normal values. To enter histogram data, the text boxes on the lower portion of the "Particle Properties" window are used. There are 27 text boxes for entering the histogram data, which is nominally one for each of ESPVI 4.0W's particle size bins. However, it is not necessary to have 27 individual histogram data points. If there are fewer than 27 histogram data points, ESPVI 4.0W will use them first to compute the equivalent log-normal distribution. Once the

log-normal distribution is computed ESPVI 4.0W will populate all 27 histogram text boxes with their values.

The histogram text boxes on the lower left side accept cumulative histogram data. That means that the value of each bin is the sum of its contents and all the bins containing smaller particles. The first bin holds the fraction of the particles in its size range. The second bin holds the fraction of the particles in its size range plus those of the first bin. This continues with each bin containing the cumulative fraction of the particles up to the size that it contains. The cumulative fraction is the value of the upper limit of that size bin.

Up to 27 sets of cumulative data may be entered in **Diameter** and **Cumulative Fraction**. It is not necessary to extrapolate to sizes above and below the actual range of the data if less than 27 sets are to be entered. The fitting procedure within ESPVI 4.0W will do that automatically. Thus, if the data, such as from an impactor, has its lowest value at 0.3 μm, that will be the value placed in the first size bin in the data entry form. The size distribution will then be extrapolated down to 0.08 μm when the **Accept** command button is used to close the window. For the cumulative histogram, the **Diameter** value is the upper limit for each of the bins.

The text boxes on the right side of the "Particle Properties" window under the heading **Particle Properties at Average Diameter** serve additional purposes. "Particle Properties" window also consists of 27 bins. The first column, labeled **Diameter,** is the average particle size based on the bin's upper and lower limit. The second column, called **Relative Fraction,** is the relative fraction of the particles contained in that size bin with respect to the total value, which is taken as the value 1. It is called a differential distribution, which is also can be called a "frequency" distribution. The **Cumulative Fraction** values are used to initially derive **Relative Fraction** values that can be edited. If **Relative Fraction** is used for editing, the resulting **Cumulative Fraction** values may change slightly because the sum of the **Relative Fraction** values is normalized to 1, which means that their sum equals 1. The **Cumulative Fraction** input does not require that their sum be equal to 1. **Relative Fraction** inputs may be useful in emphasizing or reducing particular particle size contributions, such as in submicrometer sizes, or in transferring differential size distributions from published graphs.

Inputs in differential form are usually used in one of two ways. The first is to enter particle size data that is available from a graph in which the data is plotted in differential form. A second, and more important use, is to edit the cumulative distribution by modifying individual size bins.

Next to the column of **Relative Fraction** text boxes is a column for the particle **Density**, which value is the actual particle density rather than the bulk density for some amount of collected particulates. Particle density is used within ESPVI 4.0W for calculations such as computing the electrical migration velocity. A particle density value of about 2400 kg/m^3 is typical of many fly ashes. The ability to enter the particle density might be useful if there is data that indicates that the particle density of a fly ash varies by size.

Still further to the right of the **Relative Fraction** and **Density** text boxes are two columns entitled **Real Index of Refraction** and **Imaginary Index of Refraction**. Referring back to

"ESP Design", in Figure 1-3, there was an entry called **Stack Diameter** for the location in the stack in which an opacity meter or transmissometer would be located. The opacity is described by a complex number containing both the real index of refraction and the imaginary index of refraction. The real index of refraction is that component which subjects the light passing across the stack to some amount of scattering. The imaginary index of refraction is that component of the light that is absorbed by the particles. If there is an interest in determining stack opacity it would be desirable to obtain precise values for both the **Real Index of Refraction** and **Imaginary Index of Refraction** for the fly ash in question, and then enter them into the appropriate text boxes on the "Particle Properties" window. If there is no interest in having ESPVI 4.0W compute opacity, **Real Index of Refraction** and **Imaginary Index of Refraction** have no other function and can be ignored.

On the lower left hand side of the "Particle Properties" window are the two command buttons labeled **Insert Row** and **Delete Row**, which are used to add and delete values to the **Cumulative Mass Fraction** text boxes for entering cumulative histogram data values. To **Insert Row** or **Delete Row** it is necessary to highlight the number in the **Bin** column.

Copy Up and **Copy Down** are used to enter **Relative Fraction** data. Individual size values can be increased, decreased, or set to zero. Then use **Calculate** to recompute the **Cumulative Mass Fraction** and the log-normal distribution. Each of the **Cumulative Mass Fraction** boxes must have a value in them; none can be left blank.

The **Calculate** command button performs various calculations if particle parameters are changed. If log-normal parameters are entered, it will repopulate the **Cumulative Mass Fraction** and **Relative Fraction** boxes with appropriate values. If new **Cumulative Mass Fraction** or **Relative Fraction** data is provided, it will compute the log-normal distribution and all of the **Cumulative Mass Fraction** and **Relative Fraction** boxes.

The **Accept** command button closes the "ESP Design" window with its current data contents so that the modeling can proceed; ESPVI 4.0W will not allow the modeling calculation to proceed if there are data inconsistencies. Clicking on **Accept** merely allows the calculations to proceed with the window's current contents. It does not save the contents, which must be done by means of **Save**, under "File" in the main window. The **Cancel** command button also closes the window but does not restore the original saved data entries.

6.7 Reverse Modeling Particle Size Distribution Using the Space Charge Effect on the Electrical Conditions

Often, particle size data is not sufficiently detailed for accurate modeling of ESP installations. Therefore, it is necessary to use the very essential ability to "reverse model" the particle characteristics by making use of the abilities of ESPVI 4.0W.

There are two steps required to reverse model the particle size distribution. The first is to model the corona discharge electrodes as was done in Section 4.13. Once the electrical characteristics of the electrodes have been produced, the next step is to determine the characteristics of the fine particles that would result in the observed space charge suppression

and the resulting electrical conditions. It should be noted that the formation of space charge is dominated by the fine particles, predominantly in the range of 1 μm and less. There is little interest in the larger particles, which are captured easily in any event.

Three unknown properties, or variables, define the inlet particle characteristics of an ESP. These are the concentration, the log-normal mass mean diameter, and the geometric standard deviation. Unless these variables have been accurately measured, three unknowns, or variables, have to be determined. If the particle distribution differs from log-normal, then the size distribution will make use of histogram input.

Defining the values of concentration, mass mean diameter, and standard deviation that makes ESPVI 4.0W's V-I curves match those of the ESP in question, can range from a relatively easy to a complex and difficult procedure. The degree of complexity is directly related to the accuracy of the other data that has been entered to ESPVI 4.0W, especially those that impact the electrical conditions. This is the reason so much emphasis has been placed on determining the electrical characteristics of the corona discharge electrodes.

The quality of the electrical data is especially important. V-I curve data from corona onset up to the usual operating point is much more useful than just having the electrical operating points by themselves. Therefore, it is desirable to obtain V-I data for each of the ESP sections from inlet to outlet and from corona onset up to full operating voltage. Changing the electrical conditions of an ESP section will affect the operating characteristics of the ESP sections downstream. Therefore, once an upstream section's electrical conditions have been characterized and its electrical conditions are reset, those electrical conditions should be recorded and made part of the test report.

In situations in which the ESP is collecting a highly resistive dust, an upstream section must be kept out of reverse ionization, or back corona, while determining the V-I curves for a downstream section. This is because a section operating in back corona will have lost its V-I curve that was recorded for operation without back corona. The V-I data must be gathered from the area of the curve in which there is no reverse ionization. This means that meaningful data must be obtained in the narrow region between corona onset and the point at which reverse ionization starts. Gathering downstream section data requires that the upstream section's electrical conditions be within the zone in which there is no reverse ionization.

To determine the particle characteristics, which have at least three unknowns, there has to be at least the same number of independent data sets to find a solution. Because most ESPs have at least three sections, there can be as many sets of data as there are unknowns.

A log-normal mass mean diameter of 16 μm and geometric standard deviation of 3.4 μm has been recommended by Dahlin and Altman (1983) for bituminous coals fired in conventional (not including cyclone) pulverized coal fired boilers. They presented a complex procedure for sizing ash from sub-bituminous coals but did not present any recommendations for lignite and anthracite. If there is no better data available, the log-normal distribution of 16 μm and 3.4 μm is probably a reasonable size distribution from which to start.

An example of reverse modeling is included in ESPVI 4.0W based on a set of V-I curve data obtained from air load electrode modeling done in Section 4.14.1 as SAMPLE4 and in Section 4.14.2 as SAMPLE5. Some V-I data had also been provided for the same ESP treating hot flue gases. It was apparent from the V-I data that the ESP had severe back corona, which meant that the inlet electrical condition was the only data that was usable. There were more unknown than known conditions. Additional operating conditions were also provided; however, no information was available to indicate that the data was assembled under the same set of operating conditions. In fact, an analysis of the data suggested that the data likely came from more than one set of operating conditions.

The data that were available were used to set up SAMPLE7. The SAMPLE7 data set was saved from SAMPLE 5, which means that the electrodes are configured with the 42-element array as discussed in Section 4.14.2. The data set for the original ESP included dust concentration of 13,600 mg/m^3, and the ash contained a considerable amount of unburnt carbon, particles of which are usually quite large. The supplied data also indicated a particle resistivity of 3×10^9 ohm-m. A Bickelhaupt resistivity analysis suggested a resistivity more than 1×10^{10} ohm-m.

The V-I electrical data plotted in Figure 6-8 is labeled as “Original”. An extended plot of this data set would show the curve moving up and to the left with increasing current. This is an obvious indication of severe back corona, which provides further evidence of high resistivity and back corona.

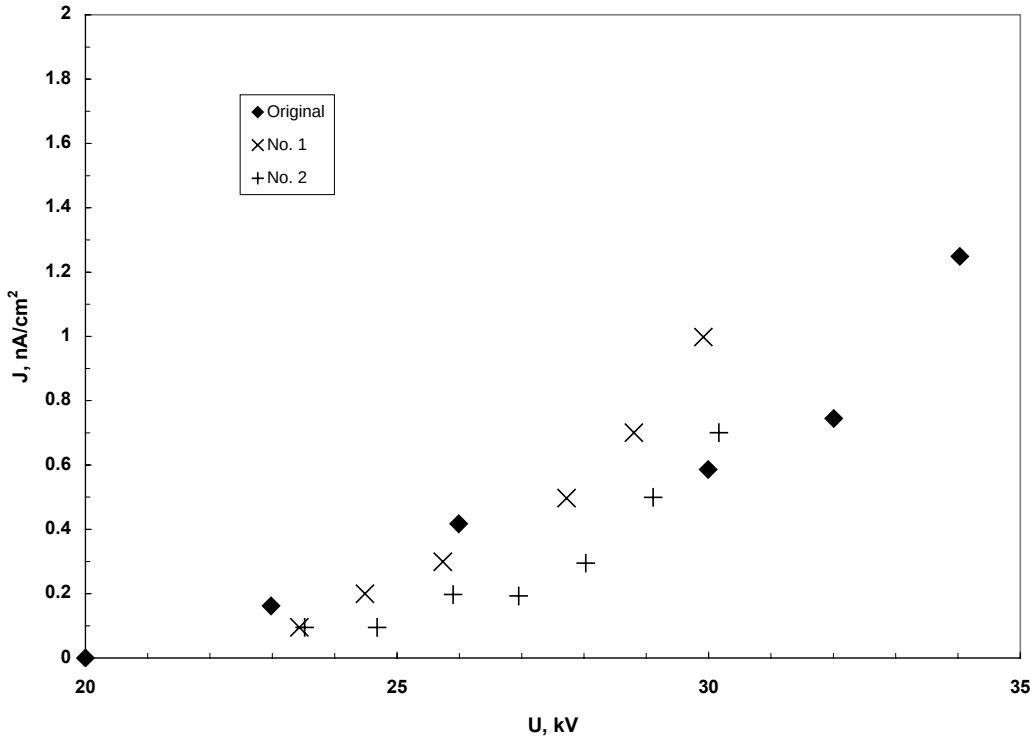

Figure 6-8. V-I curves from unknown particle and two different known particle characteristics in SAMPLE7.

A number of different V-I curves were evaluated in which the three variables log-normal mean mass diameter, standard deviation, and concentration were changed. Two of these evaluations are included in Figure 6-8. The first, which is titled in the legend as No 1, is for the mass mean diameter and standard deviation set to 16 μm and 3.4 μm, respectively, (as recommended by Dahlin and Altman) and the concentration to 10,000 mg/m^3. Curve No. 2 has the standard deviation increased from 3.4 to 3.5 with the mass mean diameter and concentration remaining the same as for curve No 1.

Both of the particle characteristics for No.1 and No.2 provide electrical conditions that are similar to that of the original over the portion of the V-I curve before back corona starts to become strong. It should be noticed that the relatively small increase in the standard deviation from 3.4 to 3.5 raised the space charge enough to cause a significant change in the corona current. If the ESP were operated at those electrical conditions, these particle size representations would provide an approximate idea of the efficiency of the ESP. For information that is more precise it would have been necessary to observe the effects of the various particle characteristics on the remaining sections of the ESP.

To gain more insight into how changes to the inlet particle characteristics affect subsequent sections, it is recommended that SAMPLE7 be used to investigate the effects on its various sections of varying the particle characteristics. It would be readily seen that the effect on the inlet section is profound. The effect on the second section would also be significant, but less strong than the effect on the inlet section. Progressing through the ESP, the space charge decreases, and the effects become increasingly weaker. The space charge effects on the outlet sections could be quite subtle for a well operating ESP.

To gain good insight on the emission level of particles exiting the ESP, it is necessary to accurately know the concentration of particles entering as well as the penetration. The concentration is one of the unknown particle characteristics.

An important lesson that comes out of all of this is the necessity of good quality data. The electrical data must be both detailed and precise. When gathering V-I data for a downstream section of the ESP, the electrical operating points of the upstream sections must also be known. The upstream sections should not be in back corona while evaluating the downstream sections. Finally, the other input data for ESPVI 4.0W that affects the electrical characteristics of the ESP must be known. With this done, it is possible to “reverse model” the ESP and thereby determine the particle characteristics that cause it to perform in the manner that it does.

Chapter 7
Enhancing the Performance of Existing ESPs—Mechanical

ESPVI 4.0W is a very useful tool to enhance the performance of an existing ESP. Modeling the ESP's mechanical and electrical design and intended operation will indicate its performance capability. Then by comparing the various aspects of ESP operation that will be addressed in this chapter, ESPVI 4.0W will predict how they affect that performance. Once this is done, decisions can be made on how to proceed with the enhancement in the most cost-effective manner.

To determine if the current operation of the ESP deviates from the original operation and design, some tests and determinations may have to be made. There are a number of approaches that can be used to enhance the performance of an under-performing ESP. Assuming the mechanical and electrical design of the ESP is satisfactory, the characteristics of the gas and dust entering the ESP can have a major impact on its performance.

One of the initial approaches is to check if the ESP's gas volume is higher than design, because of either operation with excess air or air leaking in upstream of the ESP. The next is to consider whether the gas temperature is higher than predicted, because of either air heater ash build up or combustion difficulties, since this may increase the electrical resistivity of the fly ash, as indicated in Figure 6-1, in addition to increasing the gas volume.

As mentioned before, poor gas distribution has an adverse effect on the performance of an ESP. Therefore, conducting a field check of gas distribution within the field area will confirm if corrections need to be made. Mitigation of field bypassing or ducting build up should be addressed during the field measurements. These field measurements will also allow an assessment of the effectiveness of rapping in terms of keeping the system relatively dust free in addition to checking the alignment of the discharge electrodes and collectors.

In Chapter 9, Troubleshooting, Fault Finding, and Identification, the electrical operating conditions should identify possible deficiencies in operation, as a result of obtaining V-I curves for each precipitation field. The main advantage of determining the V-I curves is that they can be taken while the unit is on line. Although correction of these deficiencies may be carried out only with the unit off line, the maintenance team will have some idea of the problems.

7.1 Increasing the Size of the ESP

From time-to-time, ESPs are increased in size. This is usually done when a major increase in performance is required that is beyond the capability of simpler approaches. This would be a major, costly undertaking for which there may not be an alternative.

Increasing the size of the ESP can be done in either of several ways. The first is to increase the height, which requires that the superstructure be raised and new internal electrodes be

installed. The second is to add one or more additional sections, which of course requires the room to do it. A third possibility would be to increase the width of the unit.

7.2 Flue Gas Conditioning

From the coal and ash analyses and electrical operation, one can identify if the ESP is electrically operating under reverse ionization, or back corona, conditions. One approach to enhance performance on "cold side" applications is to modify the ash resistivity by the injection of chemical conditioning agents. Possibly the most widely adopted method is the injection of sulfur trioxide. Where reverse ionization conditions arise on "hot side" applications as a result of sodium migration in the collected dust layer, then injection of sodium salts is used to mitigate the effect of sodium migration in the particle matrix.

An assessment of the opacity traces and a chemical analysis of the inlet and outlet dusts should indicate if the plant is subject to reentrainment problems, either because of excessive rapping or because the fly ash lacks cohesiveness. As indicated, unburnt carbon or the presence of cenospheres is particularly subject to producing low cohesivity deposits. One approach to improving cohesiveness and reducing reentrainment is to inject small quantities of ammonia upstream of the ESP. The ammonia reacts with the sulfur dioxide and sulfur trioxide to produce ammonium salts, some of which will be fused at the operating temperature, helping to bind the collected particles together.

Table 7-1 lists a number of situations in which flue gas conditioning has been successfully used to enhance the performance of the ESPs. A minimum emission reduction of 50 percent and a maximum reduction of some 90 percent were attained.

Table 7-1. Performance Enhancement from Flue Gas Conditioning Approaches

Fuel Type	Conditioning Agent, SO_3 ppm	Conditioning Agent, NH_3 ppm	Emission Reduction, %
U.S. low sulfur Eastern	12	6	74
U.S. low sulfur Western	8	0	>75
Spanish Lignite + South African Bituminous	0	15	87
Australian low sulfur	20	0	81
Polish low sulfur	10	0	57
Indian high ash, low sulfur	20	0	50
Indian high ash, low sulfur	0	15	80
Australian low sulfur high Al_2O_3+SiO_2 plus I.E.	0	15	80

To minimize site installation costs, all equipment is largely skid mounted, pre-wired and checked prior to delivery. The site work is thus limited to the final injection manifold and distribution pipe-work, electrical hook-up, and interfacing with the plant control system. The basic approach to produce the conditioning agents for SO_3 injection is for the system to convert the SO_2 to the trioxide by means of a catalyst before being diluted with heated air and dispersion into the ductwork. For the ammonia system, liquefied ammonia is evaporated and mixed with air prior to injection into the flue system.

Sulfur Trioxide Conditioning

For sulfur trioxide conditioning, the feedstock can be either liquefied sulfur dioxide or sulfur. The liquid sulfur dioxide is stored and evaporated adjacent to the plant and mixed with heated air before entering the vanadium pentoxide catalyst chamber. For sulfur feed stock, the sulfur is fired in a sulfur burner with a balanced amount of air to produce around a 5 percent concentration of SO_2. The SO_2 is then passed through the catalyst chamber where the sulfur dioxide is converted to sulfur trioxide with an efficiency of some 95 percent. The sulfur trioxide exiting the catalyst bed is then diluted with hot air and passed through a distribution manifold into the ducting upstream of the ESP.

To maximize the conditioning effect, in a contact time of less than 1 second, it is important that the reagent gases are introduced into the flue gas having as wide a contacting area as possible. A typical injection manifold would comprise a number of probes spaced across the duct, each having injection nozzles positioned at the “centers of equal areas”. To maintain the gas as active sulfur trioxide and to avoid corrosion and plugging within the gas distribution network, the manifold system is constantly maintained at a temperature above any potential acid dew point.

Investigations into the conversion of naturally occurring sulfur dioxide in the flue gases on power plants are being actively conducted as an alternative to imported feed stock conditioning. With these, a parallel side stream catalyst bed is installed upstream of the economizer, where the temperature is around 400 °C, and the raw flue gas passed through the catalyst to convert some of the sulfur dioxide to sulfur trioxide. These approaches, although avoiding the need to import feedstock material, not only impact the overall boiler efficiency, but also can prove very expensive in that the cost of new or replacement catalyst beds can be significant unless gas pre-cleaning is adopted. There is also a catalyst-aging factor to be considered, which will reduce the nominal design conversion efficiencies and hence produce potential ESP performance shortfalls.

Ammonia Conditioning

The equipment for ammonia injection is simpler in that anhydrous liquefied ammonia is stored and evaporated adjacent to the plant and mixed with air before passing through a distribution pipe manifold system. Although 25 percent ammoniacal liquor, a by-product from a coke oven, can be used, this requires additional thermal evaporation prior to dilution. The lack of availability of ammoniacal liquor to the site may mean this approach is not viable in spite of a much lower cost and easier handling.

With some particulates, such as Australian high-silica-plus-alumina fly ashes, dual conditioning is required. This is achieved by having both a sulfur trioxide and ammonia injection system operating in parallel, as indicated in Figure 7-1, but injecting the ammonia upstream of the sulfur trioxide. This enables the ammonia to initially react with the gaseous sulfur dioxide to produce ammonium bisulfate/bisulfite to enhance the particulate cohesiveness; the sulfur trioxide is then able to reduce the fly ash resistivity to improve ESP performance electrically.

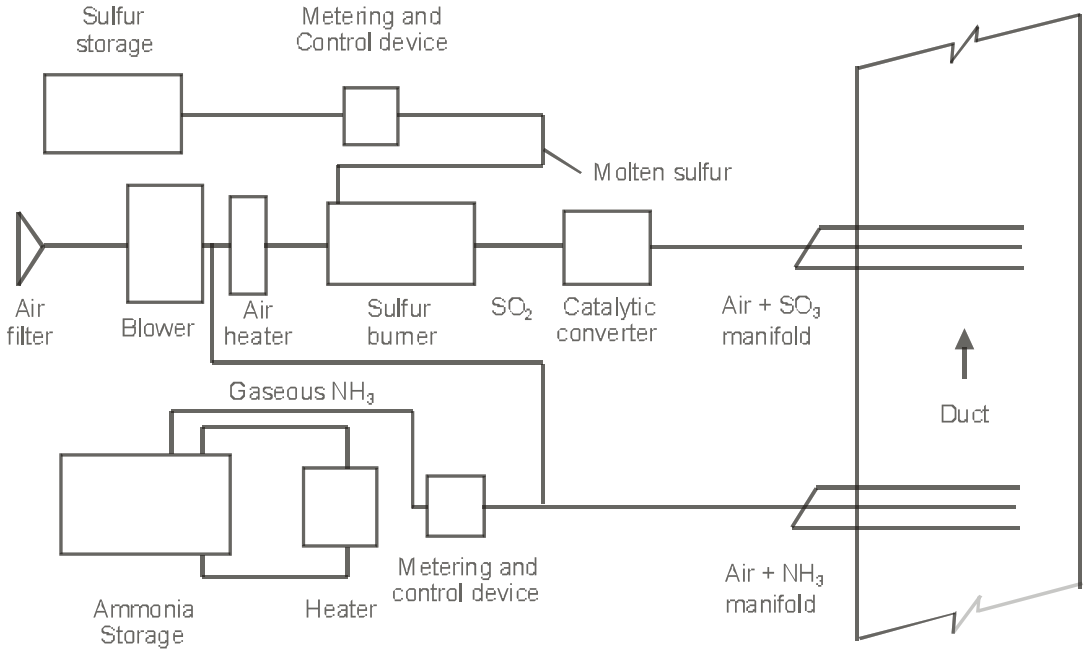

Figure 7-1. Generic arrangement of a dual, sulfur trioxide plus ammonia, conditioning system.

The actual injection rate into the flue gas, usually controlled by microprocessor devices, can be up to 15 ppm by volume for each reagent. These tend to be site dependent and are controlled by feedback data from the boiler loading, the continuous emissions monitoring system, and the ESP electrical operation. The results carried out on ESPs employing flue gas conditioning indicate that, dependent on the application, flue gas conditioning can bring about a minimum emission reduction of 50 per cent and can approach nearly 90 per cent in certain circumstances.

7.3 Humidity Conditioning

The moisture content of flue gases has an important role in determining the electrical resistivity of the particulates and, hence, ESP electrical characteristics and performance. As an alternative to chemical conditioning moisture has been injected on some power plants into the ductwork immediately in front of the ESPs and achieved significant improvements in performance. The difficulty with this approach is that, with an exposure time of less than 1 second and a gas temperature of around 130 °C, the size of injected water droplet is critical.

To minimize the injected droplet size, two fluid atomizers are essential to ensure complete evaporation in order to eliminate fall out and build up problems downstream of the injection point.

7.4 Reducing Inlet Gas Temperature

Rather than injecting moisture to lower the gas temperature and, thus, reduce the electrical resistivity, work in Japan employing gas/gas heat exchangers in front of the ESP to lower the temperature and, thus, reduce the electrical resistivity of the particles has been shown to be effective. Cooling the gas decreases its volume flow rate, which increases the efficiency of the ESP. This is now a fairly standard practice employed by a number of Japanese coal-fired installations using difficult low sulfur fuels. The effect of reducing the gas temperature on particle resistivity for a range of low sulfur coals is shown in Figure 7-2, from Fujishima, et al. (2001), in which it is referred to as the "Advanced System ESP". With the difficult coals, the ash resistivity is decreased as much as an order of magnitude, which is a significant amount.

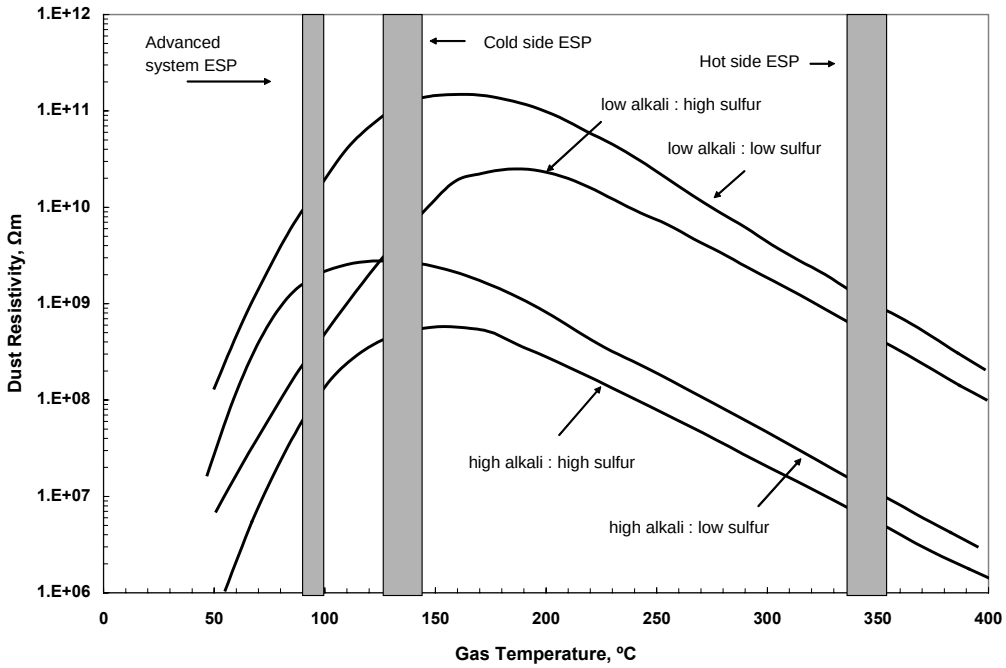

Figure 7-2. Impact of temperature variations for a range of fuels.

7.5 Mechanical Enhancement Evaluations with ESPVI 4.0W

In practice, without employing electrical means to enhance the performance of an ESP installation, one can only really consider changing its physical size, changing the inlet conditions, or modifying the fly ash resistivity presented to it.

If any of these approaches are chosen, ESPVI 4.0W will provide a simple and economical means for determining the expected performance of the modification. These approaches were

explored with some of the various modifications that were made to SAMPLE. Using the same approach on the ESP of interest with ESPVI 4.0W can quickly provide information on the improved performance the various options will provide.

Several different mechanical enhancements have been suggested earlier in this chapter these are:

- Increasing the size of the ESP
- Flue gas conditioning
- Humidity conditioning
- Reducing inlet gas temperature

"Increasing the Size of the ESP" has been discussed in Chapter 2 of this manual. The options are to increase the height, increase the width, or add additional sections or fields. ESPVI 4.0W allows rapid and economical evaluations of the various options. For a desired performance improvement, ESPVI 4.0W can easily determine how much additional electrostatic precipitation is required. Once this is done, the cost analysis for each approach can then be performed and an intelligent choice made.

"Flue Gas Conditioning" allows a reduction of the resistivity of the fly ash which then allows a higher operating voltage and current. Generally, the unknown is what the resistivity of the dust will be once the conditioning agent is used on it. This information usually has to be obtained from other sources. An analysis by the Bickelhaupt method could provide useful results. In some situations, it may be desirable to obtain results from other installations which have boilers fired with similar coals. Tests conducted on the fly ash can also provide information. Once the expected resistivity is determined, ESPVI 4.0W will help determine the new electrical conditions and the expected improvement of the ESP's performance. This will allow an intelligent decision to be made.

With the addition of flue gas conditioning the most significant change will be the electrical conditions. If the ESP has high current electrodes such as the tape and needle, consideration might be given to a new electrode configuration, especially in the downstream sections where the space charge has been reduced significantly by the higher voltages and currents upstream. With high current corona discharge electrodes operating in low space charge sections, the currents will be higher than needed, the average voltage will be reduced, and increased turbulence may result due to the elevated corona wind.

"Humidity Conditioning" provides increased humidity, which lowers the resistivity of the dust, and evaporative cooling, which decreases the temperature and the gas volume. The temperature and volume of the gas are calculated first for various levels of increased humidity. In calculating the new gas volume, the contribution of the water has to be added. Data will be needed on the change in resistivity due to the reduced moisture level and increase of the humidity. ESPVI 4.0W will accept the new gas flow rate and temperature. The viscosity and ion mobility under "Gas Properties" along with the change in SO_2 concentration will have to be entered. The reduction of the gas volume flow rate will cause an increase of the SCA, which is consistent with the expected performance improvement.

Once this is done, ESPVI 4.0W will help determine the new electrical conditions and the expected improvement of the ESP's performance.

"Reducing the Inlet Gas Temperature" is somewhat similar to the "Humidity Conditioning". The major difference is that there is no increase in humidity to help lower the resistivity of the dust. The reduction of the resistivity will be totally due to the lowering of the temperature. The resistivity may be lowered sufficiently to allow operating with significantly higher voltages and currents. The improved electrical conditions and reduction of the volume flow rate, which increases the SCA, will allow ESPVI 4.0W to predict the improvement of the performance.

Chapter 8
Enhancing the Performance of Existing ESPs—Electrical

This chapter will be concerned with ESP performance enhancement by improving the electrical characteristics. Mechanical and electrical ESP enhancement sections are separated for convenience and not because they are truly different. In fact, they are very closely related. It is difficult if not impossible to modify one without affecting the other. An important segment of Chapter 6 was concerned with the effects of resistivity, particularly high resistivity, on the ESP. This chapter is also very much concerned with high resistivity conditions. Other interests are with maintaining optimum operating conditions within the ESP.

8.1 Electrical Methods of Mitigating Reverse Ionization

The methods of overcoming the difficulties of a highly resistive fly ash in Chapter 7 are based on changing the properties of the gas or particulate at the inlet to the ESP. There are methods for mitigating some of the effects of reverse ionization on performance that use an electrical approach.

8.1.1 Intermittent Energization (IE)

One of the newer methods for reducing the impact of reverse ionization has been to use intermittent energization (IE) techniques in which, instead of a continuous DC energization, the thyristors are held off to produce an intermittent current. As the ESP has a certain capacitance, the voltage between thyristor firing tends to hold, while the intermittent arrival of current allows the charge on the collected particle to dissipate before the arrival of the next charge and, hence, prevents the build up of voltage typical of reverse ionization operation. It serves the dual purpose of saving energy and improving the collection efficiency of ESPs when handling high resistivity dusts.

IE is obtained with the same electrical equipment as employed in traditional full wave power supplies. The difference is in the automatic voltage control equipment, which has the capability to suppress a certain number of half-cycles of the primary current delivered to the transformer by the AC supply. The suppression is obtained by not firing the phase control thyristors in the respective half-cycles or, alternatively, by using a firing angle of 180°.

The principle of operation is illustrated for a 50 Hz rectified supply by the wave forms shown in Figure 8-1. This example shows six half-cycles (three full cycles) of the line frequency voltages and currents. For every three half cycles, two half cycles are suppressed. These waveforms were obtained with a firing angle corresponding to 3 ms after the zero crossing of the line voltage.

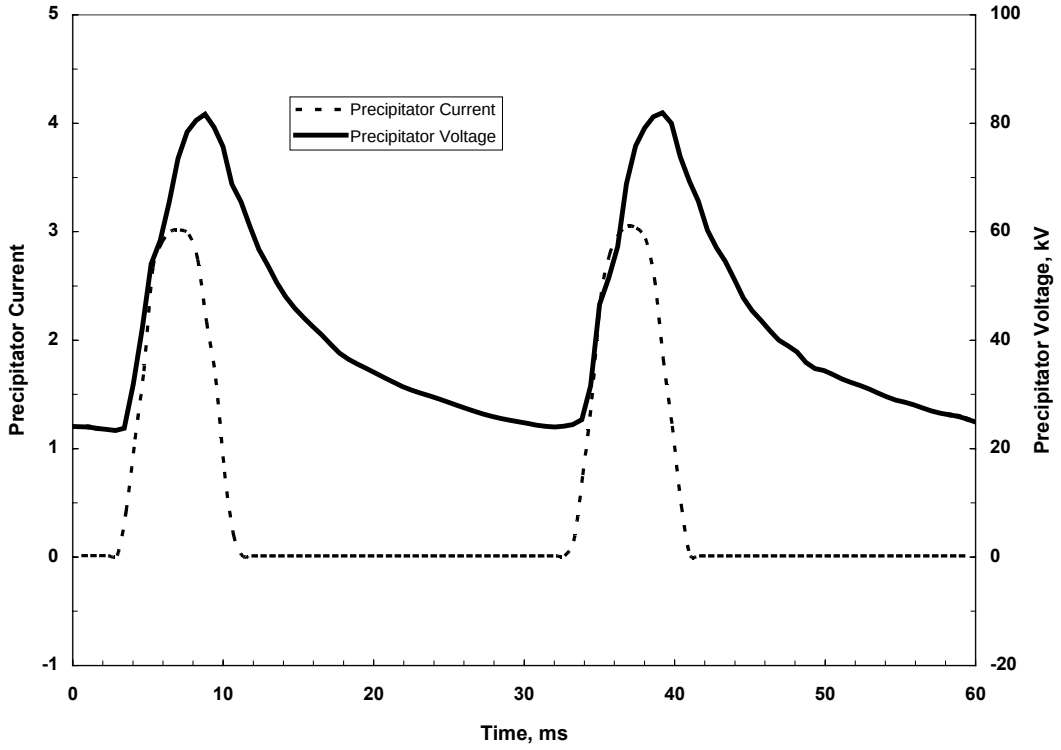

Figure 8-1. Typical wave forms with IE.

The wave forms in Figure 8-1 show the following differences compared with DC energization for the same firing angle as in Figure 3-2:

- The peak value of the ESP voltage is higher.
- The minimum (trough) value of the ESP voltage is lower.
- Due to the suppression of two current pulses, the mean and the RMS values of the ESP current are significantly reduced.

With IE, since the current to the ESP is discontinuous, the operation is normally specified in terms of the Degree of Intermittence, or D, which is derived by dividing the number of half-cycles included in one energization duty cycle by the number of current pulses in this time interval. In the example shown in Figure 8-1, the energization cycle is three, so the degree of intermittence, D, is 3. In another example of IE, where the thyristors are fired once and then kept blocked for the next ten half-cycles, then the degree of intermittence D would be 11.

The degree of intermittence is also expressed by other names such as the “charge ratio”, *D*, which is defined as the number of current pulses in one duty cycle divided by the number of half-cycles included in the energization cycle. For instance, the charge ratio, *D*, in Figure 8-1 is 1/3, that is, the wave form comprises one current pulse out of every three. This means that the charge ratio (*D*) is basically the reciprocal of the degree of intermittence (D). Remember that the degree of intermittence is the SemiPulse ratio of ESPVI 4.0W.

Table 8-1 presents a direct comparison of the electrical operation between IE, with a 3 ms firing angle, in comparison with conventional DC energization.

Table 8-1. Current and Voltages with IE Compared to Values obtained with DC Energization

Energization Form	IE	DC
Firing Time, ms	3	
Primary Current I_p, A	172	223
Peak Precipitator Current I_p, mA	3100	2350
Precipitator Current I_o RMS, mA	476	1030
Peak Precipitator Voltage V_o peak, kV	82	78
Mean Precipitator Voltage V_o mean, kV	41	61
Min Precipitator Voltage V_o min, kV	24	46

8.1.2 Comparison of IE with Traditional DC Energization

As a consequence, the impact of IE on ESP operating conditions compared to DC energization can be summarized as follows:

- The peak voltage is higher because the area under the current pulse is greater. Because this area corresponds to the electric charge Q_p delivered to the ESP section, the larger the value of Q_p, the higher the peak voltage since the ESP load has an inherent capacitive component.
- Because of the longer time interval between successive current pulses, or periods, without receiving electrical charge, the ESP discharges towards the corona onset voltage, resulting in a lower Minimum Voltage value.
- The Mean Voltage is proportional to the area under the ESP voltage in one energization duty cycle (in this example: three half-cycles of the line frequency). Because of the lower minimum voltage, the mean voltage value is also reduced.

The mean value of the ESP current is reduced due to the suppression of a number of current pulses, where the suppression is typically expressed as the "degree of intermittence", D. If it is assumed the area under the current pulse is the same for both IE and DC energization, and the mean current obtained with DC energization is $\mathbf{I_{DC}}$, then the mean current obtained with IE $\mathbf{I_{IE}}$ can be expressed as shown in Equation 8.1 below

$$\mathbf{I_{IE} = I_{DC}/D} \qquad 8.1$$

The area under the current pulses with IE may sometimes be higher than that from conventional energization by a factor k. Then, the mean current is given by Equation 8.2:

$$\mathbf{I_{IE} = kI_{DC}/D} \qquad 8.2$$

where **k** may vary between 1 and 1.5 and in the example shown in Table 8.1, **k** is 1.39. In this situation, the mean current is reduced by a factor **k/D**. (Assuming that the primary current pulse has a similar wave form in both cases, then the RMS value is reduced by a factor equal to **k** divided by $\sqrt{\mathbf{D}}$). Summarizing, there are two aspects where IE can be considered inferior to DC energization: the higher form factor of the primary current and the potential saturation of the transformer magnetic core.

The relationship between the RMS and mean ESP current values in Table 8.1, clearly indicates that the form factor is higher with IE than that obtained with DC energization. This results in a corresponding higher form factor for the primary current, which is equivalent to a higher harmonic content. Also, because of the pause interval in primary current flow with IE, the change in the magnetic induction is reduced, resulting in a reduced and inferior transformer core saturation. This situation can be minimized in the design using different approaches such as:

- Using a larger transformer core.
- Using a core with higher remanence (residual flux) and low eddy losses.
- Firing a smaller auxiliary current pulse before the main one.
- Installing a larger linear series reactor to modify the wave form.

8.1.3 Pulse Energization

Pulse energization has been used as an alternative to IE as an electrical means of overcoming reverse ionization difficulties. Although the approach has been used to mitigate the problems of reverse ionization, the equipment usually requires one additional high voltage supply and control, which not only complicates the operation but is expensive. Although pulse energization has been superseded by other approaches, it is included to complete the various approaches that have been adopted to overcome reverse ionization difficulties. In addition, there is currently no means for modeling pulse energization; ESPVI 4.0W does not include it in its capabilities.

The principle of pulse energization is to inject short duration high voltage pulses onto a reduced base DC voltage, which is maintained close to the corona onset voltage. The high voltage pulses are repeated at a certain frequency, in the range of 1 to 400 pulses per second (pps), in order to allow time for the collected particles to discharge themselves. In operation, the pulse amplitude, base voltage, and pulse repetition frequency have to be varied according to a certain programmable strategy, requiring a special control unit to perform this function.

A typical wave form of the applied voltage for a frequency of 100 pps is depicted in Figure 8-2, which also includes the voltage wave form for traditional DC energization for comparison purposes. The differences are quite clear in that the narrow pulse voltages have much higher amplitude with pulse energization. With the narrow pulse width, the peak voltage applied to the ESP can be much higher than with DC energization without running into breakdown problems and, therefore, can provide much higher field strengths for both ion production and precipitation.

In principle, there are two main design architectures for single pulse operation; one based on switching at low potential and one based on switching at high potential. The first type normally uses two high voltage tanks (one for the pulse generator and one for the base voltage) and separate cabinets for the automatic voltage and power control devices. The second type normally uses one control cabinet and one high voltage tank resembling a traditional power supply. Both use a series LC (inductance capacitance) resonant circuit, where the ESP, represented by its capacitance, is one of the circuit components. The pulsing

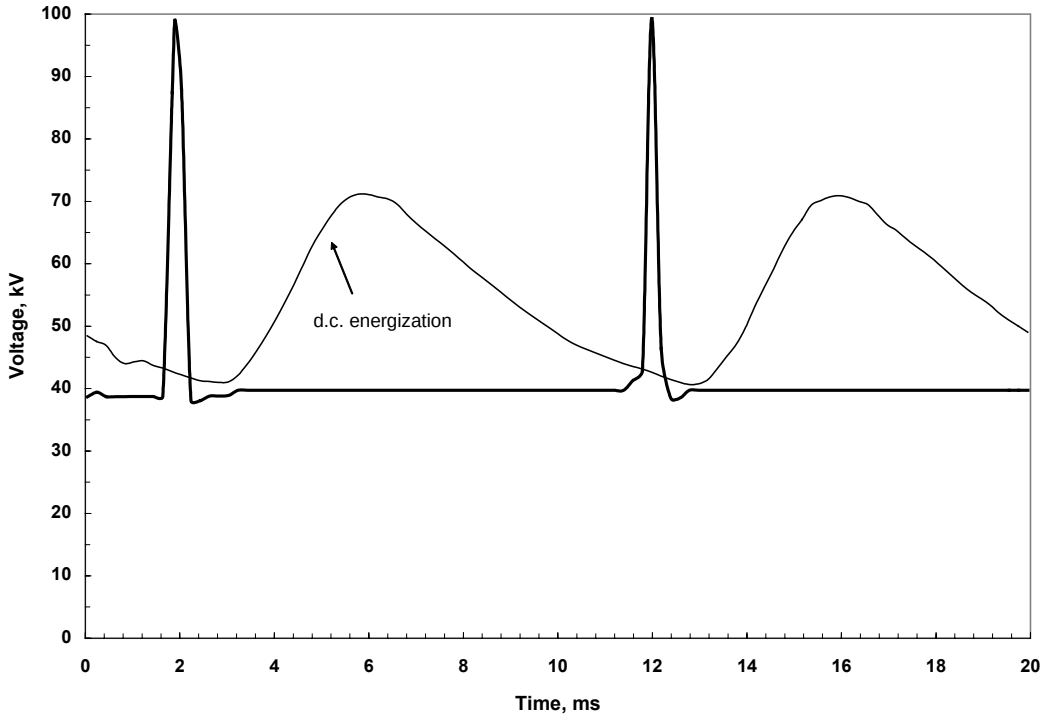

Figure 8-2. Typical voltage wave form comparison obtained with pulse and DC energization.

high voltage initiation switch, typically a large power thyristor having an anti-parallel breakover diode, is essential for energy recovery.

Another approach is multipulse energization. In this approach, instead of supplying a single pulse, the system uses a burst of short duration pulses derived from an inductor/capacitor discharge in the secondary circuit. Except for the generation of multipulses, the operation and performance is very similar to the single pulser system.

8.1.4 Summary of Resistivity Effects on ESP Performance

The effect of resistivity on ESP operation and performance is shown in Figure 8-3 and can be summarized as follows:

- For particles having resistivity in the range 1×10^{7} to 1×10^{9} ohm-m, the particle charging and discharging regime when the particle arrives at the collector proceeds normally and so has minimum impact on performance (Curve A).
- As the resistivity increases, although the charging occurs normally, the particle only slowly loses its charge on arriving at the collector, and a voltage begins to develop across the dust layer according to Ohm's Law. Depending on the resistivity, layer thickness, and local currents, the voltage for resistivities in the 10^{10} ohm-m range can reach a point at which positive ions begin to be emitted from the surface of the dust. These positive ions cross the inter-electrode space and collide with and neutralize negative ions and charged particles, which significantly reduces ESP performance. This condition is termed reverse ionization, or back-corona, and the operating electrical characteristics exhibit a much-reduced average voltage but an extremely

high current (Curve B).

Recent investigations of the applied voltage and current wave forms have shown that, under reverse ionization conditions, the peak applied voltage tends to be maintained; but, with the high current flow, the ripple voltage significantly increases, with its main feature being that the minimum ripple voltage level dramatically falls. To control or minimize the deleterious effects, modern AVC units monitor this minimum voltage condition and take appropriate corrective action to prevent the positive current "runaway".

- For slightly lower resistivities or for dusts having poor packing density, although a voltage develops across the dust layer, interstitial breakdown occurs through the layer and gives rise to a "streamer", which results in field breakdown. The symptoms of this condition are a slightly reduced average operating voltage but a very low discharge current, with any attempt to raise the current immediately resulting in increased flashover. Examination of the voltage wave form shows a minimum ripple voltage, and any attempt to increase the current raises the threshold voltage, resulting in breakdown. While this condition does not have as much impact on performance as the classical reverse ionization, or back-corona, scenario, it nevertheless causes an efficiency limitation. (Curve C).

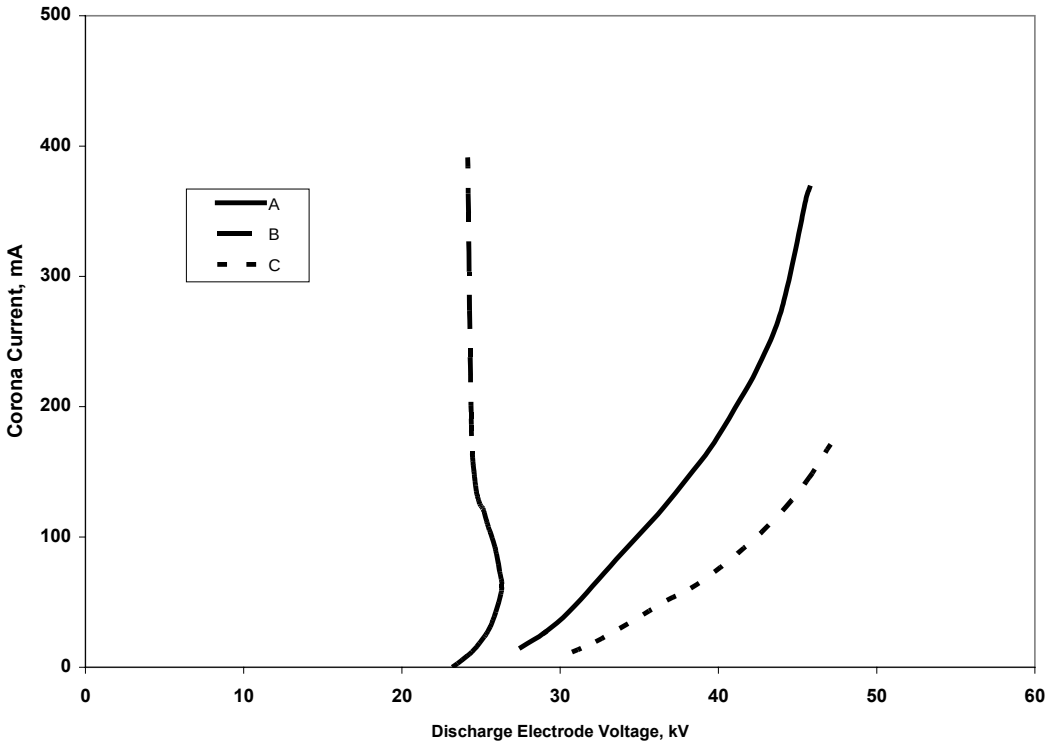

Figure 8-3. Voltage/current characteristics for different fly ash resistivities.

At the lower end of the resistivity range, the charge on very conductive particles is lost so quickly when arriving at the collector that the particle either sits on the surface as a neutral

particle that can be readily reentrained by the gas stream, or the rapid charge transfer repels the particle back into the gas stream.

The extent of the reentrainment depends on a number of factors such as particle cohesion, gas stream velocity and turbulence, and the electrostatic forces acting on the particle. Examination of outlet dust samples from plants dealing with low resistivity particulates, specifically unburnt carbon, shows an increasing quantity of these conductive particles. For pulverized coal fired units having low NO_X burners and producing around 10 percent unburnt carbon, the increase in carbon in the outlet gases can be at least 30 percent, whereas, for unburnt carbon in the 15–20 percent range, the carbon content on the outlet dusts can be as high as 90 percent. Although these low resistivity particles generally have no significant effect on electrical operating conditions, the emission from the ESP is high as a direct result of particle reentrainment from the collectors.

8.2 Reverse Ionization Detection and Corona Power Control

Normally, the occurrence of reverse ionization in one or more ESP sections has been determined by examining the corresponding V-I curve. The criterion used for determination of reverse ionization is the slope of the V-I curve; if it is negative (falling kV), it indicates reverse ionization. In the early 1980s it was considered that this method was not sensitive enough, and a better indication was obtained by using a V-I curve in which the minimum value of the ESP voltage is plotted against the mean current, as illustrated in Figure 8-4.

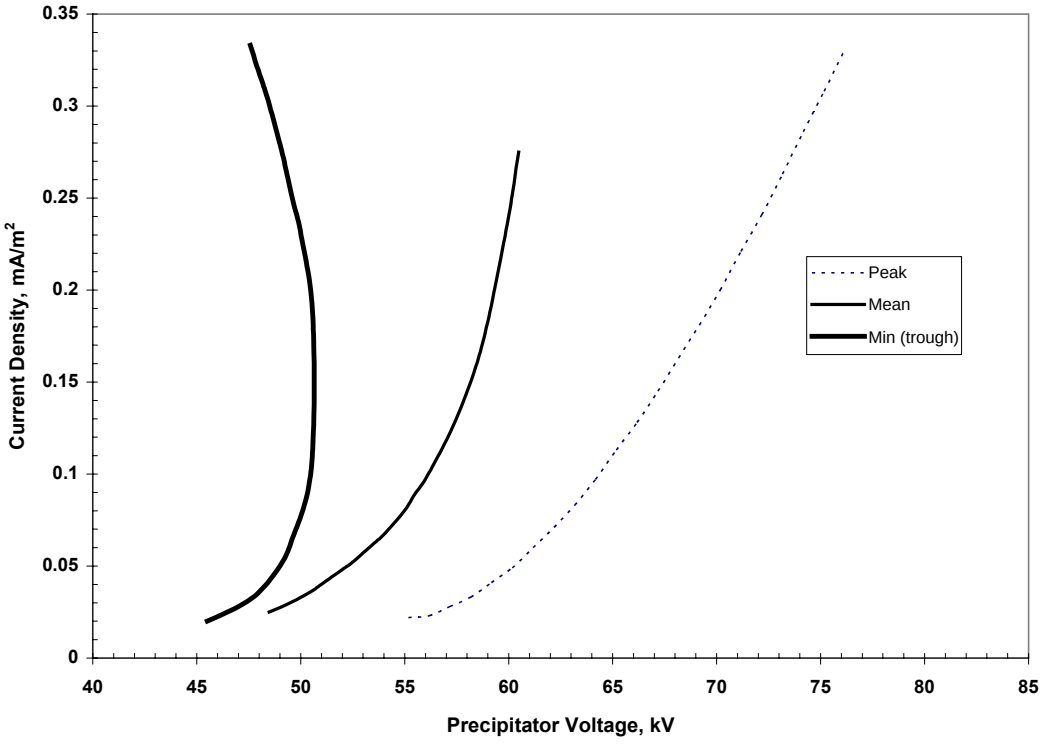

Figure 8-4. V-I curves indicating peak, mean, and trough voltage levels.

Figure 8-4 shows that the curve changes slope at a relatively low current level, where the curve based on the mean voltage still has a positive slope. The curve based on peak voltage shows a positive slope, irrespective of the presence of reverse ionization. Not all voltage control units include means of reverse ionization detection, but those which have, invariably use the following control principles:

- The slope of the V-I curve. This corresponds to the method described above in which the minimum voltage of the ESP is used. However, his approach has the disadvantage that the power levels have to be systematically reduced in order to find the actual inflection point.
- Voltage wave form at sparking level. This method is also based in the minimum value of the ESP voltage, and the occurrence of reverse ionization can be determined by comparing its value before and after spark. Reverse ionization exists if the minimum value after the spark is higher than the value before the spark.

The second approach has the advantage that it does not need to reduce power levels because sparking is used as the monitoring control. In the case of a “no sparking” condition, a blocking period during which the thyristors are not fired is used instead.

8.3 Automatic Voltage Control and Instrumentation

To obtain the maximum collection efficiency it is of the utmost importance to optimize the electrical energization. To accomplish this, the size of the TR set and the energized bus section must be reasonably matched and there must be an efficient automatic voltage control (AVC) unit to optimize electrical operation under all operating conditions. As indicated, the key parameter governing the total corona power delivered by the TR set to a particular bus section is the firing angle of the thyristors. This angle is determined by the control unit for every half-cycle of the supply frequency and must have the correct value according to the existing operating conditions within the ESP.

The performance of any automatic control system is closely related to the type of instrumentation used to establish the ESP conditions at any given time. In general, the primary voltage and current are measured across the transformer using voltage and current transformers, but the secondary voltage is determined by either a resistance or capacitance divider and the secondary current by a resistant shunt in the earth leg. It is imperative that the secondary voltage and current measuring devices are adequately grounded to ensure personnel safety.

The use of RMS measuring devices along with high-resolution analog to digital converters enables modern microprocessors to accurately sample the average operational voltage and current values of the precipitation fields. The actual parameters, which are used for control purposes to optimize performance in these microprocessor-based AVC units, are stored in a non-volatile memory using a key pad approach and are not subject to change as could occur with earlier forms of controller.

By using satisfactory monitoring signals coupled with a satisfactory control algorithm, it is possible to improve the controller response such that arcs within the ESP are extinguished on

a timely basis, thereby promoting improved ESP performance. It is therefore important that the detector can recognize the type of spark and take appropriate corrective action without a new spark arising; “multiple sparking” should be avoided. When handling difficult high resistivity dusts, improved control techniques such as IE, as described in the following section, can be used to mitigate any fall in performance with the latest forms of algorithm.

8.4 Specific Power Control

In order to mitigate reverse ionization and maximize performance, the corona current has to be reduced. In practice, there are two means to accomplish this reduction; either reduce the electric charge (Q_p) delivered to the ESP (described as the area under a current pulse) by delaying the firing angle of the thyristors, or change to IE sequence and find the optimal degree of intermittence.

8.4.1 Control by the Use of IE

Plant personnel have traditionally performed power control manually, but the tendency over the last decade has been to do it automatically. One approach has been to include this function in the AVC units where the optimization of the degree of intermittence (D) can be performed in combination with the automatic detection of reverse ionization. If reverse ionization is found during the detection, then D is increased, but D is reduced if reverse ionization is not detected. The optimization of the electric charge delivered by each current pulse, Q_p, is difficult. One method employed is to maximize the minimum value of the ESP voltage while remaining at the optimal degree of intermittence.

To improve this task, some units incorporate an opacity signal into the algorithm to optimize the corona power. This simple approach, however, can never be 100 percent effective because a particular control unit does not know if there has been a change in the settings of another control unit or a variation in the operating conditions of the ESP. Therefore, the present tendency is to place this task in a “supervisory computer”, which receives all the relevant process and stack emission signal information. With this data, the computer can then optimize the settings of the individual control units accordingly.

8.4.2 Supervisory Computer Control Using a Gateway Approach

A typical solution for a supervisory computer control using a gateway approach is depicted in Figure 8-5. The common communication bus for the control units is an accepted industrial standard; however, if this is not available, either the feature has to be included in the automatic voltage control units (AVCs) or a suitable converter has to be used. When this requirement is met, the gateway unit makes communication possible between the standard bus and various types of common programmable logic control (PLC) systems. This communication problem is similar for types of equipment used in other industrial plants, which has led to the development of the required low cost communication drivers; these gateway units can now be obtained as stock components, enabling their wide spread use in the precipitation industry.

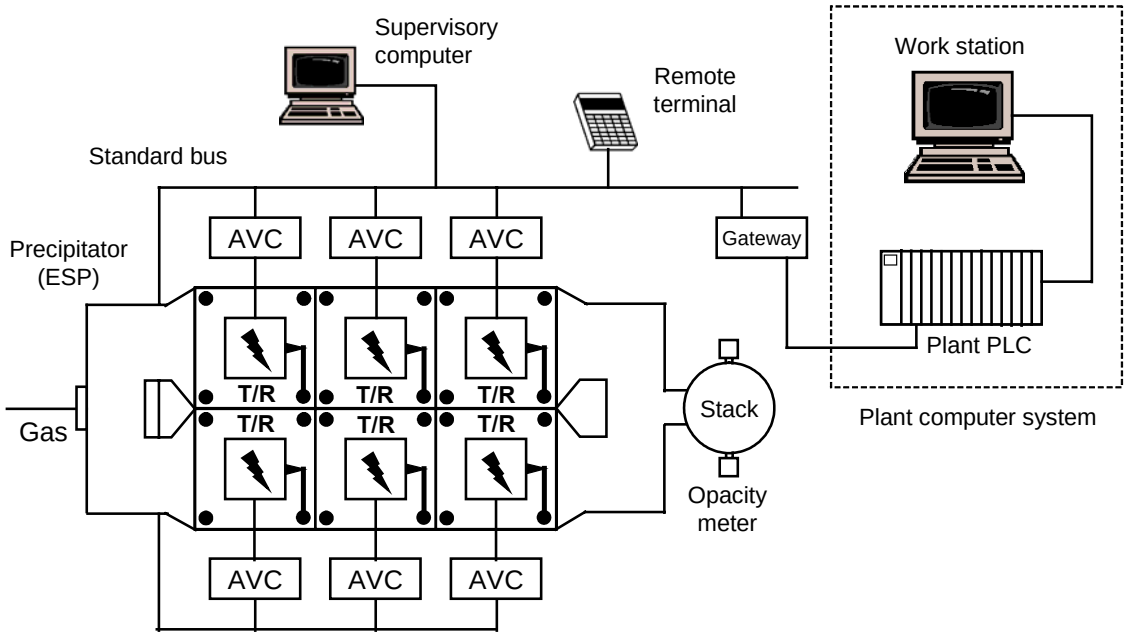

Figure 8-5. Supervisory computer control system.

Once a connection of the AVCs via a standard bus and a gateway to the computer has been established, the supplier normally has other modules that can be connected to the standard bus to exchange data with each other. The standard bus runs through the whole plant, and different modules can be physically connected at the point where they are required.

8.5 Advanced Computer Control Functions

Among the features offered by an ESP supervisory computer, one of the most important is an advanced control strategy by including functions like optimization of:

- The corona power
- The degree of intermittence (D)
- The charge delivered per current pulse (Q~)
- The spark rate and current setback
- The rapping sequences, including optimization of the off-time between rapping of the collecting plates
- Synchronization between rapping of adjacent sections, programmable power-off rapping sequences
- Energy management and control.

A supervisory computer is able to fulfill these requirements in a satisfactory way because it is constantly receiving information about:

- Process condition (for example, gas temperature, flow, feed rate, O_2, SO_2)
- Stack opacity (dust emission)
- Currents and voltages from the individual bus sections
- Status of TR sets, rappers, timers, parameters, and similar equipment.

Based on this data, the supervisory computer can therefore optimize the relevant settings in each AVC, such as:

- Degree of intermittence – (D)
- Upper current limit – (Q_0)
- Spark rate – maximizing kV
- Rapping off time – reentrainment.

These settings are changed at regular intervals or when required, and their positive effect is assessed by analyzing the opacity signal while simultaneously checking, by means of a trend analysis of their respective signals, that the process conditions have not changed. These relevant settings cannot be optimized by the AVCs operating as stand-alone units—only relying on the electrical mA and kV feedback signals— to the same degree as under the direction of a supervisory computer.

With these advantages, it is considered that the architecture depicted in Figure 8-5 will become more and more accepted. The control room personnel will operate the ESP from their monitor stations in the normal way but via a gateway communication with the ESP supervisory computer running in the background. This computer will take over and perform more and more advanced control and monitoring functions, like ESP event and alarm indication and handling, fault diagnosis, and the like. These features, complemented with ESP automatic start-up and shut-down routines, will result in an intelligent and powerful supervisory computer control, thereby relieving plant personnel from tedious work routines, and will provide cost advantages because of power savings, easier and better maintenance, higher plant availability, and a lower average dust emission.

8.6 Switched Mode Power Supplies (SMPS)

There have been few departures in the past from the use of traditional main frequency rectified supplies for ESP energization, due in part to the lack of available suitable high frequency high voltage transformers and high speed switching power thyristors. Consequently, the conventional 50/60 Hz design has dominated the precipitation market. The circuit architecture of the conventional design, while being robust and simple, has a number of technical drawbacks that can be summarized as follows:

- The regulator output current may be discontinuous or non-sinusoidal, depending on the thyristor firing angle and the current demanded by the ESP. Consequently, the input power factor is very poor if there is a high harmonic distortion in the main supply.
- Because the power supply operates at main frequency, any required step change in ESP operation can only be met through a sluggish transition of 8.3 or 10 ms to the new working level. Under certain operating conditions, flashover can occur up to 100 times per minute. Therefore, the supply must be capable of being interrupted rapidly to ensure that the flashover does not lead to an arc. This is achieved with the single phase AC regulator by interrupting the current for at least a full cycle of the main supply, which can mean that the ESP is dead for 20 ms up to 100 times per minute or more. In addition, there will be a significant time delay when the ESP is being recharged (around 100 ms or more) on resuming the input voltage supply. Since the

transformer is operating at main frequency, its physical dimensions and weight will be high, depending on the power rating. A typical 100 kVA unit will have dimensions around 600 × 800 × 1200 mm and weigh 1500 kg or more. Additionally, the high reactance of the transformer core will result in the main supply having a low overall efficiency.

Although various attempts were made to address factors such as phase balancing and poor power by using three phase rectification approaches, these initially experienced severe arcing that could only be overcome by completely switching off the supply. This compromised the electrical operating conditions and, hence, ESP performance such that the three phase approach was not actively exploited at the time because of the lack of suitable switching devices for control purposes.

The problem of arcing from a three-phase system was addressed, and an early form of SMPS was developed. In this design, the three-phase bridge comprised a series of diodes and thyristors that were used as the power control element. The resultant controlled DC output was then chopped at a frequency of some 5 kHz to supply a fairly standard transformer. Although this was a reasonably successful design, lighter and cheaper designs of later SMPS systems rapidly supplanted commercial usage of this early low frequency system for ESP energization.

8.6.1 The Development of SMPS

The improvements resulting from using a high frequency SMPS are:

- High frequency switching operation, compared to the present 8.3 or 10 ms periodicity, allow a much more precise control over the ESP operating parameters, such as operating voltage, corona discharge, and flashover rates. Hence there will be an increase in both the ESP collection performance and power supply efficiency.
- High frequency switching will allow a significant reduction in the size and weight of the high voltage transformer since flux excursions within the core will be minimized. This reduction in size and weight will lead to a more compact design, which will minimize the installation and maintenance costs.
- The adoption of high frequency switching will allow more precise control of the electrical operation, and it will be possible to operate the ESP much closer to its optimum working point—nearer to breakdown—with a very low incidence of flashover, leading to higher performance levels.

8.6.2 System Requirements

A block diagram of such a system is shown in Figure 8-6. In this system, the incoming three-phase supply is initially rectified, and the resultant DC feeds a power inverter operating at a frequency of 20 to 50 kHz. This DC link can then be modulated by using semi-conductor power switches to any desired amplitude before feeding the ferrite-cored HT transformer. The transformer output, which after rectification supplies the ESP, is controlled by varying the on/off times of the power switches. This is accomplished by using a feedback system,

which continuously monitors the output voltage and current levels to achieve optimum conditions on the ESP.

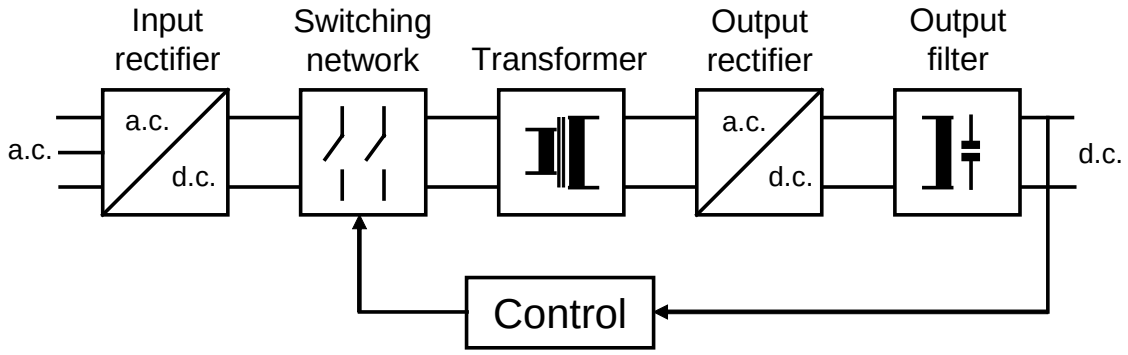

Figure 8-6. Block diagram of a typical SMPS system.

The operational problems of interrupting the power supply in order to quench an arc/flashover are considerably reduced by operation at high frequency because the minimum switching time is 0.02 ms at 50 kHz, compared with 10 ms at 50 Hz, and the recovery time to recharge the ESP can be more controlled using smaller time step increments to speedily re-establish optimum ESP performance.

8.6.3 SMPS Design Considerations

The development of a SMPS presents ESP designers with various challenges from the main input topology through to the final rectification stage. The first objective, however, is to establish the exact requirements of the supply and to ensure that the chosen topology will satisfy the following key areas:

- The operating frequency, voltage, and current levels required by the system are obtainable using readily available, tried, and proven power semiconductor devices.
- Ability to respond to any required control variations in order to adjust for changes in the ESP inlet parameters, specifically the voltage (or current) must be capable of being varied, either automatically or manually. Programmable ramps and timings must be able to vary from fractions of a millisecond to several seconds depending on the prevailing conditions within the ESP.
- When a flashover occurs within the ESP, the power supply must be capable of detecting it and interrupting the power flow rapidly to minimize the amount of energy lost. The system must then be capable of recharging the ESP to a specified level with programmable times and methods.
- High operating efficiency, high power factor operation, and good quality sinusoidal input currents are a prerequisite of any modern power electronic installation. Poorly designed topology could easily exceed the limits on current harmonics set by European standards.
- Finally, the topology should be simple, and the chosen approach must be cost effective.

8.6.4 SMPS Circuit Configurations

Although the actual circuit design/configuration and components will depend on the supplier's preference to a certain extent, the basic equipment arrangement comprises the basic steps as indicated in Figure 8-6 above:

- Rectification of the incoming three-phase supply
- Generation of a controllable square wave output in an inverter
- Providing necessary primary supply to the HV transformer
- Rectification of the high voltage transformer output and supplying ESP
- A control and monitoring system
- Possible "pulse energization" capability. In effect, this is the application of a short duration wave (typical pulse width 50 to 100 microseconds) supplied by the inverter feeding the HV transformer.

8.6.5 Practical Application of SMPS Systems

The following illustrates an example of SMPS energization compared to the same ESP when energized from a conventional main frequency rectifier set. The trials were carried out on a wood chip fired boiler unit producing a dust having a moderately low resistivity of 1×10^{8} ohm-m. The ESP under test comprised two fields, and the SMPS equipment, rated at 80 kV and 250 mA running at ~ 50 kHz, was installed in parallel with one of the existing TRs through a changeover switch.

The results from these initial field trials showed that the ripple voltage was significantly reduced with the faster charging rate of the SMPS system, 0.02 ms compared to 10 ms with conventional energization. This resulted, not only in the corona current increasing from 110 mA to 220 mA, but also in the mean operating voltage rising by 10 kV. These changes in active power input produce a significant enhancement in ESP performance.

Figure 8-7 shows wave forms comparing the voltages obtained with SMPS operation and conventional energization. Although the sparking/flashover voltages are similar, the large ripple voltage clearly illustrated with conventional energization results in a significant reduction in the mean operating voltage, whereas that from SMPS energization is almost a pure DC.

The wave forms in Figure 8-8 illustrate that, with the improved control available with the SMPS system, the time "lost" in recovering optimum electrical conditions following a flash over is reduced, as is the "quench" time, leading to an overall enhanced performance being achievable with SMPS energization.

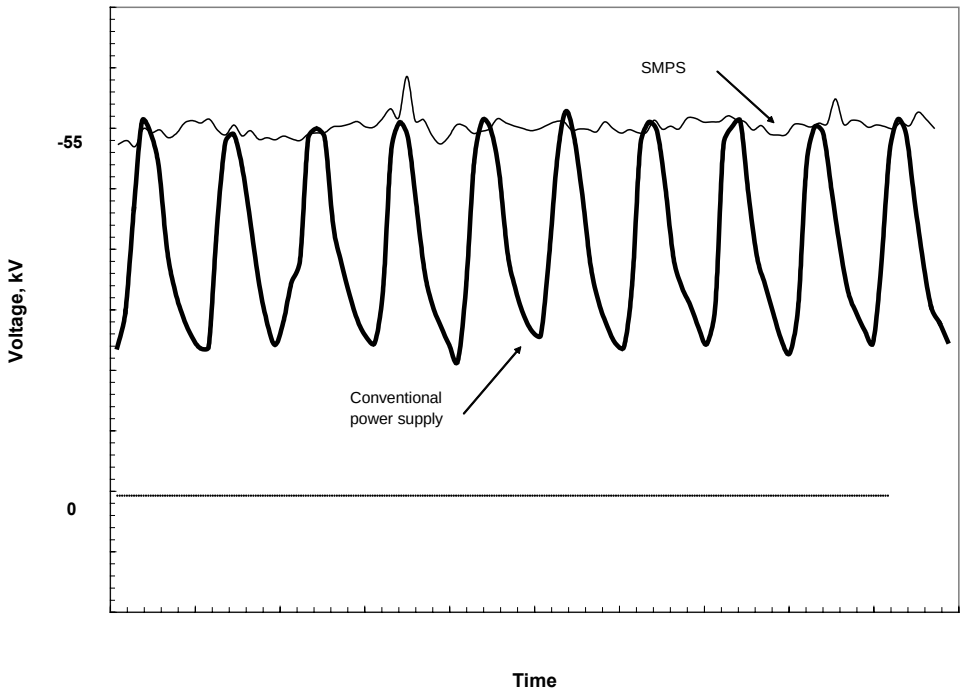

Figure 8-7. Comparison of voltage wave forms from conventional and SMPS energization systems.

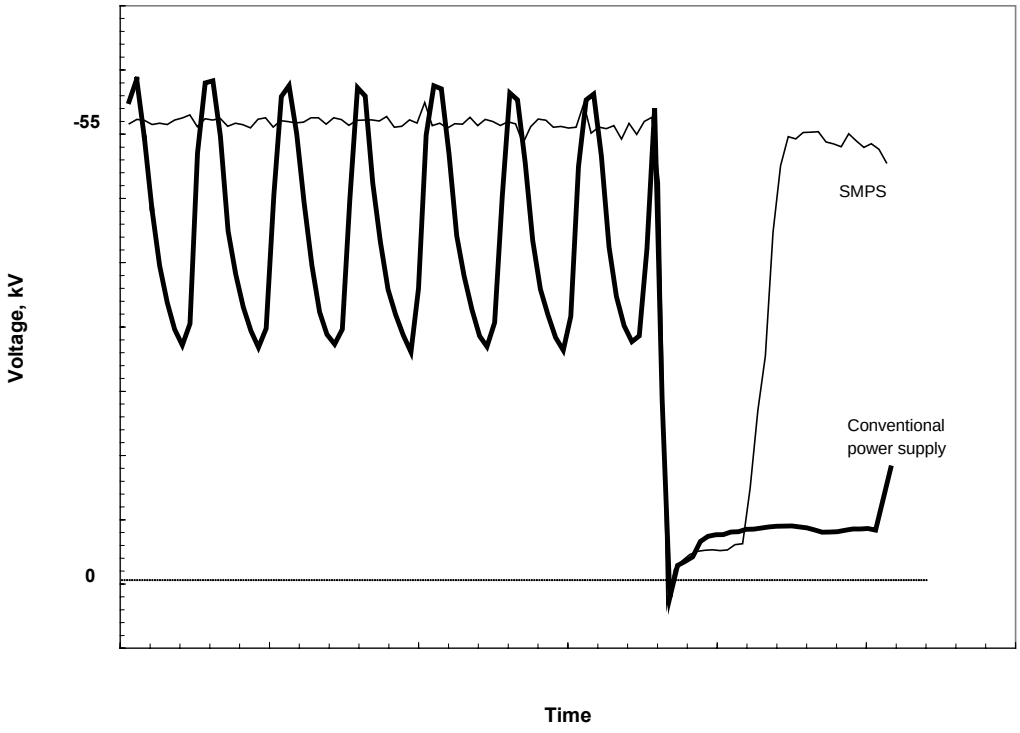

Figure 8-8. Reduction in electrical recovery times following a flashover with SMPS operation.

8.6.6 Summary of SMPS Equipment Operation

A number of suppliers have proven SMPS equipment operating in the field, and the results of these installations can be summarized as:

- SMPS energization generally results in significant particulate emission reductions.
- SMPS energization significantly increases the useful power input into a precipitation field.
- SMPS is a more efficient power converter than a conventional TR (approximately 95 percent efficiency for SMPS versus the maximum of approximately 85 percent efficiency for a conventional TR). This improvement in efficiency results in considerable energy savings.
- SMPS readily achieves compliance with “main cleanliness codes”. A conventional single phase main operated TR disturbs the main supply significantly and in an unbalanced way. A (3-phase) SMPS system complies with such codes automatically because of the way in which it is designed.
- Retrofitting of an ESP with complete an SMPS system, instead of making an upgrade with only new microprocessor controls for a conventional TR, is more cost effective, and additionally, the performance advantages of the SMPS approach are obtained.
- A SMPS system only contains a minimal coolant volume; no oil tray with expensive drainage pipes and collector tanks are needed, thereby reducing site costs.
- The simplicity of the SMPS installation reduces installation costs, and it is readily connected to the same process and monitoring PCs because it can operate through the same communication network as conventional TR controllers.
- The replacement of old conventional TRs containing PCB oil with new SMPS systems is a very cost effective and viable alternative, particularly as the performance advantages from the ESP effectively do not bear additional cost.

Having the above advantages, the SMPS approach will have a significant impact on future ESP technology, and it is suggested that most new applications will have SMPS energization. Not only should this result in smaller and lower cost installations but also, with the ability to readily modify the output wave forms, the impact of reverse ionization problems should be minimized without the need of further equipment additions.

Chapter 9
Troubleshooting, Faultfinding, and Identification

Although many of the problems associated with potential performance difficulties have been discussed in the manual under their relevant chapters, the purpose of this chapter is to provide the operators with a separate working document that will assist in identifying both electrical and mechanical problems without having to bring the unit off line.

As has been stated a number of times in various ways in this manual, ESPVI 4.0W, when provided the proper parameters of the full-scale ESP, will precisely match the performance of that ESP. This allows ESPVI 4.0W to become a very important tool in the troubleshooting, faultfinding, and identification of problems and their cause.

A large number of charts have been presented portraying both good and bad operation of ESPs. These are general charts that, in most cases, do not portray any specific ESP. In that respect, those charts are useful, but ESPVI 4.0W provides an opportunity to improve on them.

Because ESPVI 4.0W has the capability of precisely matching the performance of the full-scale ESP, it should be used as a standard against which to judge the performance of it. This requires that ESPVI 4.0W be set up so that it portrays the full-scale ESP operating correctly. Because so many of the problems of an ailing ESP are related to its electrical conditions, there would then be some standard against which to compare those electrical conditions.

Setting up ESPVI 4.0W properly for an ESP that is not operating well is more difficult than it is for one that is performing well. With the methods learned in this manual, it can be done. However, it may be necessary to search for data from times in the past when the ESP had been operating well. It may also be necessary to borrow data from other ESPs of the same type or that use the same fuel. This data can then be translated with ESPVI 4.0W to the unit that is being modeled.

Instead of waiting for an ESP to start operating badly, use ESPVI 4.0W to model it for both current and optimal conditions. That way, a model will be available when it is needed.

It would not be too strong a statement to say that every operating ESP should be modeled with ESPVI 4.0W. Once this is done, ESPVI 4.0W should be run on a computer alongside the ESP. Doing this would provide several important benefits including:

- The real time ability to judge the performance of the ESP against the standard, which is the well performing unit in the computer.
- Real time ability to judge the level of particulate emissions from the ESP against what it would be emitting if it were operating well.
- The provision of considerable insight consistent with this manual and particularly with this chapter in identifying problems and their probable cause.

- The availability of an economical and easy-to-use method for determining future upgrade options for improving the performance of the ESP.

9.1 Electrical Operating Conditions

The areas in an ESP installation where typical difficulties arise are shown in Figure 9-1. In identifying these areas, it is assumed that the ESP installation has been satisfactorily erected and commissioned and that a performance problem, as evidenced by the opacity meter, or high stack emission, develops during normal plant operation.

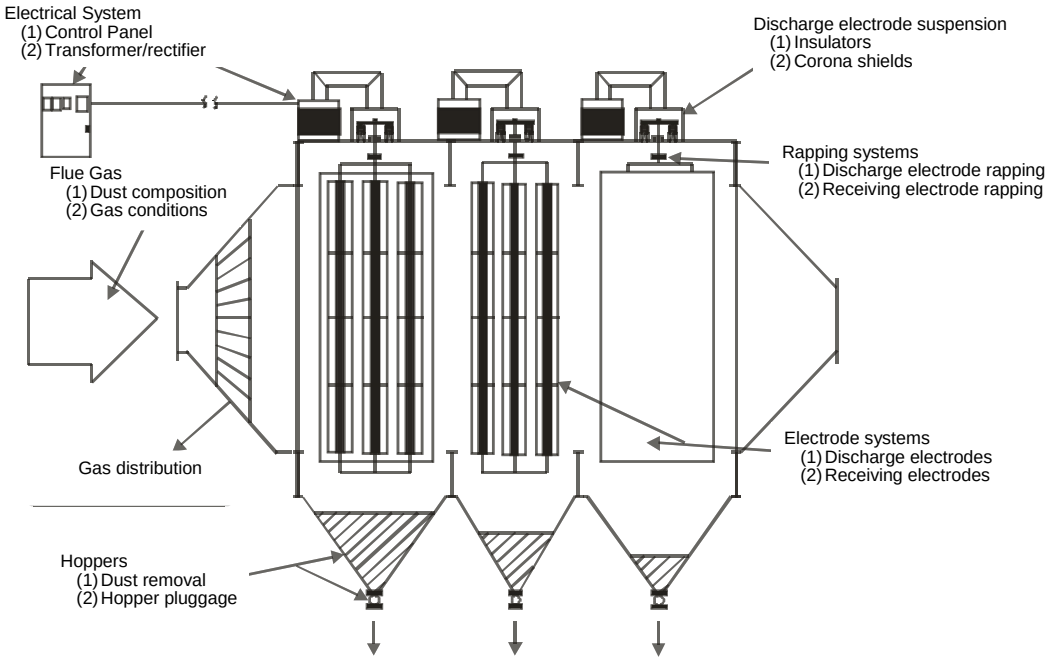

Figure 9-1. Identification of potential ESP fault areas.

As with any item of equipment, if problems arise, it is important that a systematic approach be adopted to identify and rectify the situation.

The areas that need to be examined are in Table 9-1 and given below:

- Rectifier equipment
- Deposit removal from the ESP internals
- Electrical characteristic curves
- Discharge electrode and collector alignment
- High voltage insulator systems
- Hoppers and de-dusting
- Gas distribution and air in-leakage
- Changes in Gas Inlet Conditions

Table 9-1. Most Common Electrical Problems—Control Cubicle Information

Symptom	Likely Fault
Green lamp fails to light on closing isolator	▪ No supply voltage ▪ Bulb filament burnt out ▪ Auxiliary contacts on isolator not closing ▪ Auxiliary isolator fuse O/S
HT "On" contactor fails to close on operating switch	▪ Contactor failing to close correctly ▪ Contactor fuse O/S ▪ TR Set tripped, for example, because of High Oil Temperature ▪ Local/remote selector switch in remote condition
Red lamp fails to light when HT contactor is closed	▪ Bulb filament burnt out ▪ Auxiliary contacts not closing ▪ Auxiliary fuse O/S
Contactor trips on closing	▪ No fluid in dash pots ▪ Overload setting too low ▪ Dead short on electrode system
Contactor trips High mA but low kV	▪ Partial or high resistance short of electrode system ▪ Hopper dust level ▪ HT insulators tracking ▪ Dust deposits on electrode system
Contactor fails to trip on continuous overload short	▪ Check if dash pot fluid is correct viscosity ▪ Check if dash pot piston release hole is clear

It is not suggested that these are the only areas where difficulties may arise that impact the overall performance of the unit, but the following checks can often identify the likely cause of the problem and, more important, most corrections can be made without having the unit off line. Consequently they should be considered as the first approach to any ESP faultfinding procedure, that is, on-line monitoring.

Although problems associated with the TR equipment are rare, the signal lamps and meters can give invaluable information as to a likely cause of the difficulty being experienced. While this analysis applies specifically to conventional single-phase main rectified electrical equipment, many of the symptoms equally apply to other forms of energization, but are not necessarily mirrored by some of the examples shown.

Although the foregoing identifies difficulties that may prevent the TR Set being energized, the following table assumes the field has been successfully energized and the panel meters are operating satisfactorily.

Examination of the TR panel meter readings shown in Table 9-2 can often indicate the likely fault, which makes locating and addressing the issue easier. The following specifically refers to ESPs that are energized by conventional main rectified equipment, although some of the symptoms can equally apply to other forms of energization.

Table 9-2. Examination of TR Panel Meter Readings

Meter Readings				Likely Fault
Primary Volts V	Primary Amps A	Secondary Volts kV	Secondary Amps mA	
Zero	Zero	Zero	Zero	▪ Main supply fault ▪ Thyristor fault ▪ AVC fault ▪ AC Inductor O/C if fitted ▪ Control Circuit fault
Zero or Low	High	Zero or Low	High	Possible short circuit on: ▪ Precipitator misalignment, dust short or build up, etc. ▪ High dust level in hoppers ▪ Earth switches closed ▪ HT Cable or Connection down ▪ Internal TR fault—shorting to earth
High	Low	High	Zero	Possible open circuit on: ▪ HT Feed lines ▪ HT Changeover switches if fitted ▪ Internal TR fault—open circuit
Zero or Low	High	Zero or Low	Low	▪ TR set fault of some type, e.g., primary short.
Normal	Normal	Zero	Normal	▪ Voltage divider fault ▪ Meter fault ▪ Wiring O/C
Zero	Normal	Normal	Normal	▪ Meter fault ▪ Fuses O/C on meter if fitted
Normal	Zero or Low	Normal	Normal	▪ Current transformer fault ▪ Meter fault ▪ Wiring fault
High or Normal	Low or Normal	High	Low	▪ Dust deposits on discharge electrode system, check rapping
Normal	Normal	Normal	Zero	▪ Faulty meter ▪ Shunt short circuit
Indication of excessive arcing on either manual or automatic control				▪ Precipitator fault, e.g. broken element ▪ Cracked or broken HT insulator ▪ Cracked/contaminated rapping drive insulator ▪ Transformer fault condition ▪ Change in inlet gas conditions
A higher kV and or performance can be obtained under manual rather than automatic control				▪ The AVC requires setting up to meet operating gas conditions or is faulty

In general, a quick check on the effectiveness of the metering system is to compare the ratio of primary volts times primary current ($V_p \times I_p$) against the secondary product (kV × mA). If the secondary value is between 60 and 70 percent of the primary, the metering is probably satisfactory; otherwise, one must investigate which metering is incorrect.

9.2 Deposit Removal from the Internals

In order that the precipitation process can proceed unhindered, it is important that the internal components are kept relatively free of deposits that can adversely impact on the electrical operation and hence reduce performance. General problems that can arise and impair performance are described below.

Deposits on the collector plates, which receive the majority of the material, reduces the electrical clearance and hence flashover voltage. Depending on the electrical resistivity of the particulates, deposits produce a significant voltage drop, which impairs the electric field distribution and particle charging. Deposits on the discharge elements can significantly reduce the corona current generation because they increase the radius of curvature of the element, which can effect particle charging and hence performance.

If there is a significant fall in electrical operating conditions from the “clean plant” V-I characteristics, then examination of the rapping control panel instrumentation can often indicate the likely fault, which makes subsequent location and rectification easier. Where the rapping is computer controlled, motor indicator lights can be used to check operation. Schematic of rapping system examination is given in Table 9-3.

Table 9-3. Schematic of Rapping System Examination

Location	Symptom	Likely Cause
Rapping motor starter panel	Motor fails to start	▪ Check selector switch position ▪ Check if “stop” buttons locked off ▪ Check electronic shear pin setting if fitted
Rapping motor starter panel	Motor trips immediately	▪ Check if rapping shafts are jammed ▪ Check if gearbox for jamming ▪ Check overload settings on electronic shear pin, if fitted
Rapping control panel	Motors do not operate In correct timing sequence	▪ Check PLC or computer settings
Rapping control panel	Discharge electrode rappers not operating	▪ Check for broken drive insulator ▪ Check gearbox

9.3 Discharge Electrode and Collector System Voltage-Current Relationships

As a diagnostic tool, the V-I curve can provide invaluable information as to possible faults within the precipitation field. There are three types of curve to be considered; the first is under static air conditions on a clean plant (air load); the second is with process gas passing through the plant; and the third is under dirty conditions without process gas but with hot gas conditions prevailing.

9.3.1 Clean Air Load Characteristic

The first relationship is normally termed an Air Load Test, and the initial test should be carried out during plant commissioning. The resultant information forms the basis on which later comparative assessments can be made.

To produce a V-I curve, the discharge currents are recorded for, say, 5 kV increments of secondary voltage. It is also useful for later reference to record at the same time the corresponding primary voltages and currents for each incremental step. The corresponding current for each incremental step is then plotted until the flashover voltage occurs or the secondary current or voltage limit is reached. For later modeling work, it is desirable to have even closer voltage increments of about 1 kV starting at corona onset.

With air, the low space charge that prevails usually means that the current is the limiting condition rather than secondary voltage. If possible, when carrying out this air test, the access doors should be left open to avoid the build up of ions within the ESP, which can have an impact on the final, measured values. The resultant curve, shown in Figure 9-2, provides the basic electrical "foot print" of the ESP field. If all fields have the same type of discharge element and collector spacing, then the curves for each field or precipitation zone should be similar in terms of corona inception and breakdown voltage. If the curves indicate serious deviations, it usually means that the alignment of electrodes is faulty or there is an internal or external electrical clearance between the energized sections and ground that adversely impacts the operating conditions.

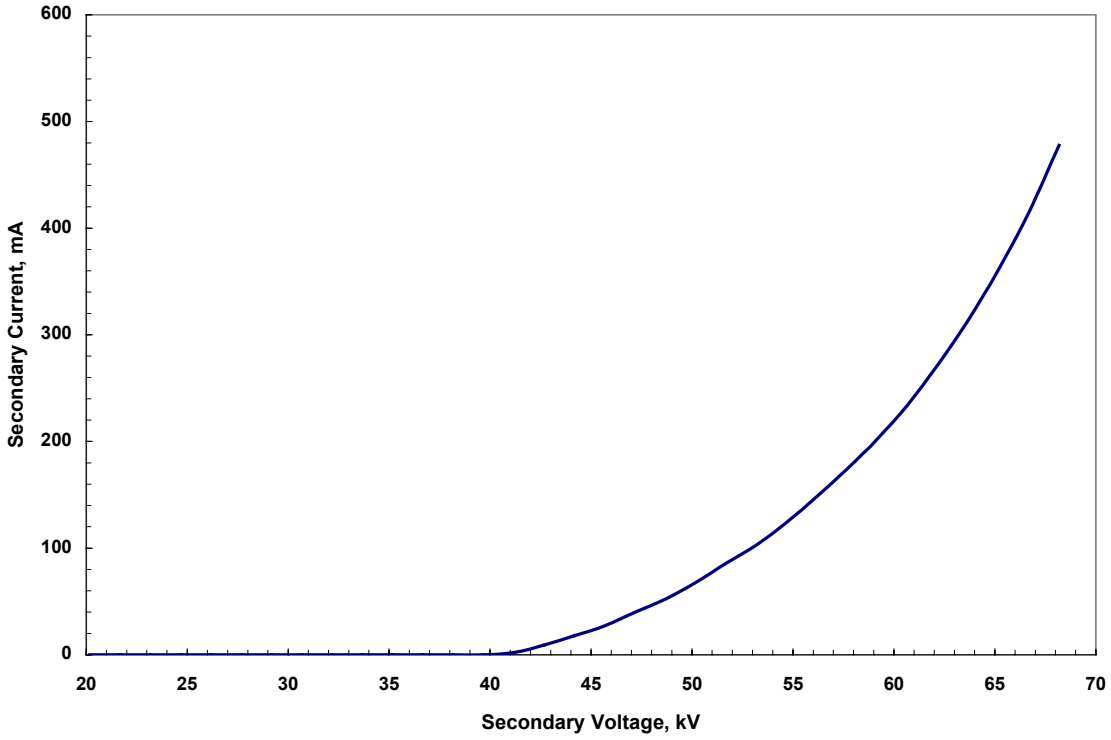

Figure 9-2. Static V-I characteristic of an ESP field.

9.3.2 Operational Curves with Gas passing through the System

These operational curves under process gas conditions are determined in a similar manner to the basic air load test by slowly raising the operating voltage and plotting the corresponding secondary current flow until flashover or the set limits are reached.

In the case of operational characteristics with dusty gas passing through the electrode system, the effect of space charge becomes evident; as the gas passes through the ESP, the particle concentration decreases, which reduces the space charge effects, and the corona current flow significantly increases. This effect is illustrated in Figure 9-3 for a conventional three field ESP handling a precipitable dust having a particulate electrical resistivity on the order of 10^8 to 10^{10} ohm-m. Because the electrical breakdown voltage will be similar for the same collector spacing and electrode system, the mean voltage as shown on the kV meter will be lower than upstream fields due to the increasing voltage ripple in supplying the increased current.

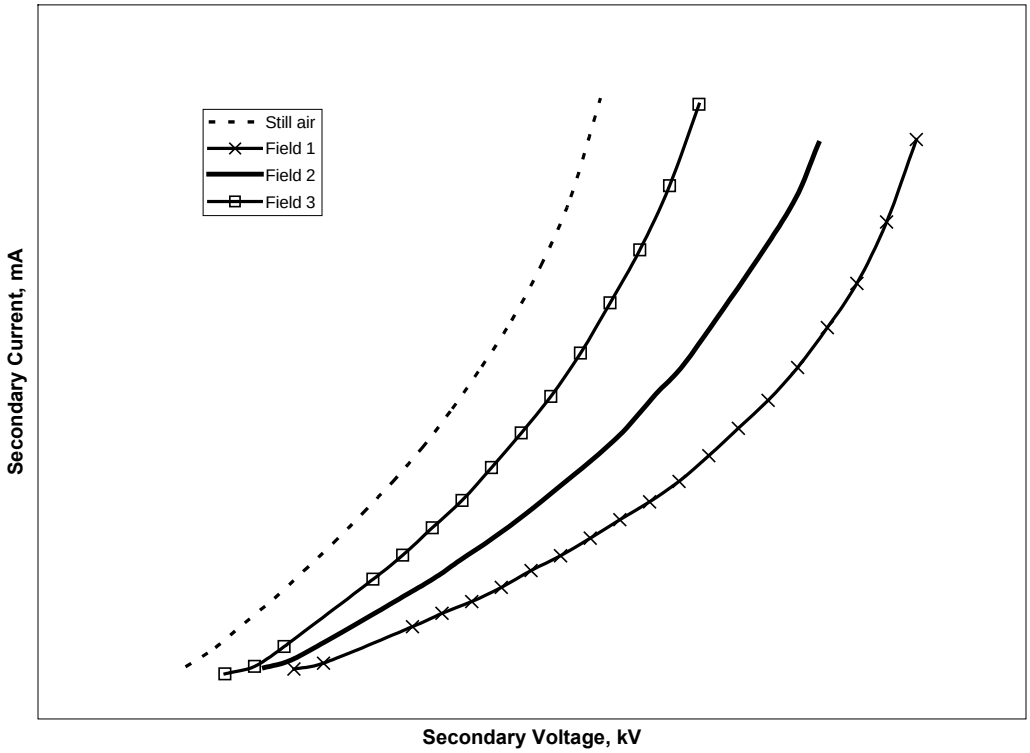

Figure 9-3. Typical V-I characteristics for good fly ash.

Figure 9-4, illustrates some shortcomings and operating restrictions arising because of mechanical limitations on the ESP. In all cases, the collection efficiency will be reduced because the electrical parameters are compromised.

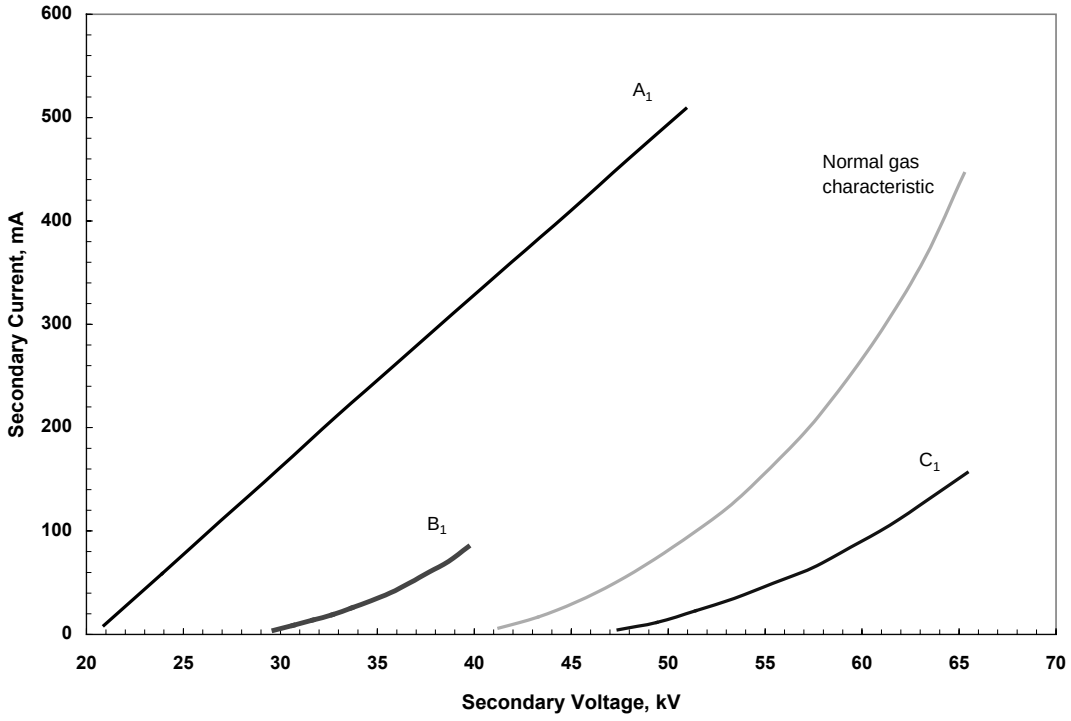

Figure 9-4. V-I characteristics indicating operational performance problems.

Curve A_1, shows a resistive path to ground as a straight line. This may be the result of a contaminated HT support, a failed rapping drive insulator, or a high hopper dust level. It should be noted that if the resistance path is very low, it may not be possible to energize the TR Set at all. A_1, as portrayed, shows the current going to zero at about 20 kV. In many cases it would be totally ohmic and would go to zero current at zero voltage.

Curve B_1 illustrates severe mal-alignment between the collectors and discharge electrodes, being characterized by a low corona onset voltage followed by breakdown at a low secondary voltage. This type of curve can also be the result of excessive collector dust build up.

Curve C_1 represents the type of characteristic attributable to heavily built up discharge electrodes, which is raising the corona onset voltage by increasing the effective diameter of the discharge elements. In this event, it is normal for the breakdown voltage to be significantly reduced, depending on the degree of build up experienced.

Abnormal characteristics that can arise are illustrated in Figure 9-5, these are usually because the ESP must handle a difficult dust, which is one having an electrical resistivity greater than 10^9 to 10^{10} ohm-m.

Curve A_2 is characteristic of severe reverse ionization. This occurs when the resistivity is so high that the particle negative charge is unable to leak to earth, resulting in a voltage build up on the surface of the deposit that gives rise to the production of positive ions. These leave the collector and migrate towards the discharge electrodes, adversely modifying the electric field

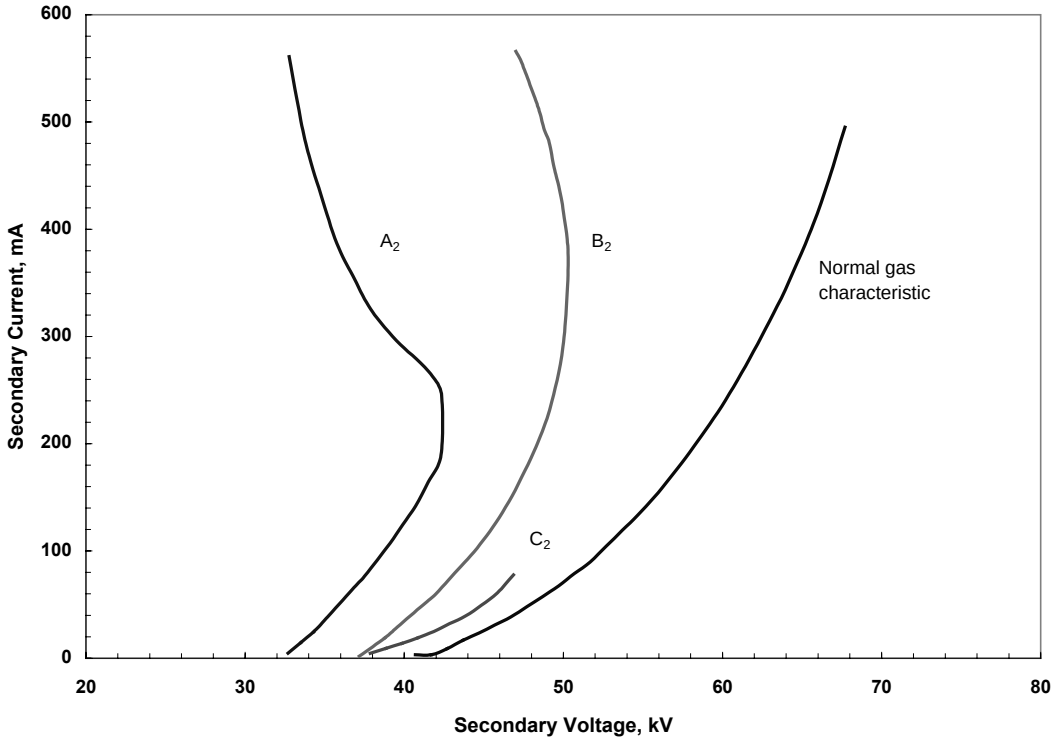

Figure 9-5. Abnormal operational V-I characteristics.

pattern and neutralizing the negative corona flow. Under this condition, emissions have been known to increase by at least a factor of 10.

Curve B_2 indicates high resistivity dust, but without full reverse ionization developing. As with severe reverse ionization, the TR Set current limit may be reached before electrical breakdown occurs.

Curve C_2 represents the electrical operating characteristics for a dust having a borderline electrical resistivity. Instead of positive ions developing and leaving the deposit, the voltage across the deposit increases only to a point where breakdown occurs, the value of voltage being dependent on the resistivity of the material.

When examining the operational curves, it is sometimes difficult to distinguish between the characteristic arising because of electrode mal-alignment as in Curve B_1, because of deposit build up as in Curve C_1, or because of a moderately high electrical resistivity fly ash as in Curve C_2. Comparing these curves with those taken immediately following commissioning, when alignment is good and there is no serious deposit build up, should indicate which symptom is the most likely, particularly when handling a low resistivity fly ash.

9.4 Dirty Air Load Test, without Gas Passing through System

Occasionally it may not be possible to internally inspect the unit, even without gas passing through it. In this case, an air load test taken under hot conditions can provide useful

information as to both the likely cause of changing electrical characteristics and the increase the corona current resulting from the increased temperature.

Figure 9-6 shows the impact on the electrical characteristics of dust deposition on a dirty plate compared to a clean plate under ambient conditions. Generally, the operational voltage with the clean collector, A_3, appears higher than for a dirty collector plate, B_3, for similar corona conditions because of the voltage drop across the deposited layer. When comparing the inlet, center, and outlet field characteristics, the corresponding curves under dirty conditions may not be identical, even if the alignment is acceptable, since the resistivity of the deposit, and hence the voltage drop, can vary with particle size, dust composition, and humidity of the air.

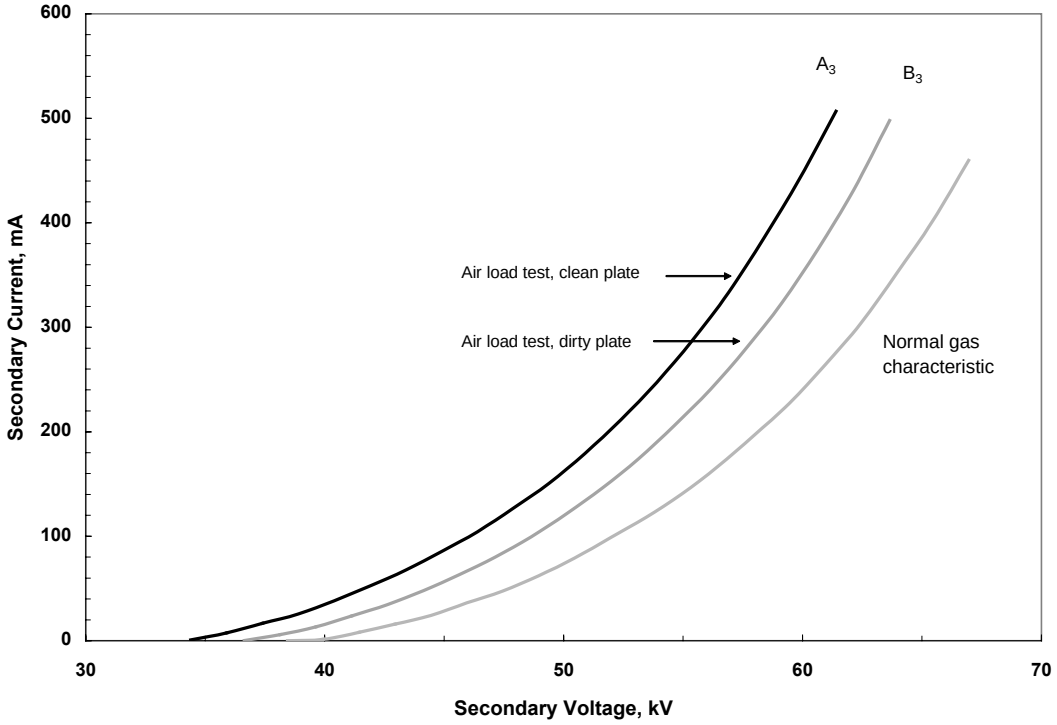

Figure 9-6. Comparison of V-I characteristics for clean and dirty collector plates.

Compared to the process gas characteristics represented in Figure 9-3, these dirty air tests tend to lie on the left side of the axes, with higher currents, mainly as a result of the reduced space charge effects and a higher voltage level because of the drop across the deposited dust layer.

9.5 Collector and Discharge Electrode Alignment

Curve B_1 in Figure 9-4 indicates that the electrical characteristics can be predetermined by the alignment of the internal components. Generally with the height of collectors and discharge electrodes in common usage for large ESP installations, the optimum alignment that can be achieved in practice is around 10 mm because of fabrication and erection tolerances.

For plants having collector spacings of 400 mm, the alignment can be out by around 5 percent, which reduces the optimum operational voltage by a similar amount; for closer collector spacing, the optimum voltages are reduced even further. It should be remembered that the flashover voltage is determined by the lowest electrical clearance, so even one misaligned discharge element has a significant effect on the operating voltage and, hence, performance.

Although discharge electrodes in current use are designed to have a long life, occasionally one may break or come adrift from the frame. If this occurs, then the free end is drawn towards the collector plate by the electric field. Flashover occurs as it nears the plate, and the electrode tends to fall back under gravity. Once the field is reestablished, the free end is again drawn towards the collector and flashover recurs. This collapsing and reestablishing of the field following breakdown results in a cyclical pattern of power on, power off, the periodicity of which is determined by the free length of the element that is swinging.

One of the reasons for carrying out an air load test following commissioning or internal work on the unit, is to ensure that not only is the electrode alignment and internal clearances satisfactory, but nothing has been left inside the unit which can later impact the electrical operation. Items which have been found are welding wires used to support lamps, lengths of rope, and such, which tend to lie in a vertical plane but stand out horizontally across the inter-electrode region when energized, significantly reducing the flashover voltage.

9.6 High Tension Insulators

Operational difficulties can arise with the HT support or lead through insulators used for isolating the discharge electrode system from the casing, which is at ground potential. These generally arise through contamination of the insulator surface with flue gas components, typically dust, moisture, or sulfuric acid deposition. If deposition occurs, depending on the degree of contamination and its resistivity, the secondary voltage can short out through the deposit, initially leading to a very low operating voltage and high current discharge.

To avoid this, it is normal practice to purge the insulator with hot air, such that the insulator, whether it is for discharge electrode support or rapping, remains out of the gas stream and the surface ideally remains above any potential acid dew point temperature. If the heating or purging system fails, then the insulators are subject to possible contamination and tracking as was shown in Figure 4-9.

9.7 Hopper Problems

In any operational unit, build up in the collecting hoppers can cause performance shortfalls, usually because of limitations resulting from the discharge or evacuation systems failing to remove the collected material. If this occurs, the dust level can build up and will eventually short out the discharge electrode system. Depending on the build up resistance, the form of the characteristic curve is as depicted as Curve A_1 in Figure 9-4.

If the inlet field evacuation system fails, then de-energizing the inlet will not necessarily prevent further hopper deposition, since the coarser and heavier particles reaching the ESP will have been decelerated sufficiently to fall out under gravity. Unless the hopper is cleared, the dust level can reach a height to short out or damage the internals.

The inlet field hoppers will have the largest quantity of deposited dust, which will also have the coarsest particle sizing and hence lowest cohesive interstitial forces, and therefore be the easiest to discharge. Dust collected further down stream will have progressively smaller and narrower particle sizes and will be more difficult to evacuate in spite of the smaller mass. This needs to be carefully considered in the design and during process commissioning to ensure evacuation of all hoppers is satisfactory.

Steps are taken in the gas distribution system to prevent untreated hopper gas bypass impacting on the performance of the ESP. As a result, the gas and material in the hopper is heated only by radiation from the horizontal gas stream. As the hoppers have relatively large surface areas, heaters are generally applied to match the heat loss through the thermal insulation and prevent the walls cooling to below a dew point temperature. Keeping the dust hot and dry is essential to minimize dust plugs, bridging, and other hopper de-dusting difficulties. On some plants, air distribution pads injecting warm air into the hoppers are used to fluidize the dust to assist its discharge. Although vibrators have been fitted to some installations, these can result in compaction of the dust and actually make the de-dusting situation worse.

9.8 Gas Distribution and Air In-leakage

Since there is an inverse exponential relationship between efficiency and gas volume, hence gas velocity, it is important, as was discussed in Chapter 5, for the gas distribution to be maintained at the correct standard. Although the gas distribution through the unit should have been checked and confirmed prior to full scale commissioning, it is possible for the inlet ducting, in particular, to become partially blocked by dust deposition during operation, which can upset subsequent gas distribution patterns. Only an internal inspection will reveal if duct deposition is having an adverse effect of gas distribution and, hence, performance.

If a hole develops in the casing or an access door leaks cold air in, typically as a jet several meters in length, a local gas distribution upset is invariably produced. This cold air leakage usually results in rapid electrical flashover at a voltage level much lower than would be anticipated from the characteristic curves as a result of the change in gas composition and local gas temperature.

Air leakage into the hopper region, either through ill sealing doors or leaking joints in the evacuation system, can reentrain previously collected and deposited dust and, in so doing, can convey it directly into the outlet duct at a high concentration, which can seriously impact emissions.

9.9 Changing Inlet Gas Conditions

9.9.1 Particle Resistivity

The most significant change in electrical operating conditions typically arises with changes in the electrical resistivity of the particulates presented to the ESP. With boiler plant applications handling fly ash from different coals, the electrical resistivity is largely determined by the sulfur content of the coal plus the sodium oxide content of the ash, as was discussed in Chapter 6. As the electrical resistivity increases, the electrical characteristics alter as indicated in Figure 9-5, Curves A_2, B_2, and C_2. By modifying the resistivity through injection of chemical conditioning agents, it is possible to change the electrical operating conditions back towards a more normal characteristic.

9.9.2 Particle Sizing and Opacity Monitoring

Examination of an opacity chart can also give invaluable information as to the likely cause of performance degradation. This is because, if the particle size changes with different fuels or conditions, the electrical operating conditions may not change significantly in spite of an increased emission. In this situation, examination of the opacity traces can indicate the source of degradation.

The emission increase may be a result of a general shift to a lower outlet particle size range, which may not alter the collection efficiency since many opacity meters are particle size sensitive. But care should be exercised in reaching this conclusion since, depending on the system of measurement, the variation may not be due to a reduced mean particle size. For example, a light transmission type of device is particle size sensitive since the absorption coefficient depends on the number of particles present in the light beam, whereas, the surface area of the particles is more important than their size for backscatter devices.

A cyclic “spiky” trace can be the result of particle reentrainment because the particulates have poorer cohesive properties than those precipitated before the performance degradation and consequently, on rapping, are released to pass into the outlet ductwork and have a serious impact on the overall collection efficiency. In this situation one must carry out a full rapping investigation by altering the rapping cycle systematically and observing the resultant opacity traces until a satisfactory trace is obtained.

9.10 Systematic Fault Finding Procedure

Although the foregoing sections generally relate to the identification of possible faults using the electrical operating conditions and other plant instrumentation, they must only be considered as the initial step in any investigative procedure. Although some likely faults will be readily identified using the above approaches, it will be eventually necessary to have the unit off line to carry out an internal inspection and to perform corrective work on some of the more serious faults in order that optimum ESP performance can be reestablished.

The main purpose of this chapter is to indicate how an examination of the installed monitoring equipment and instrumentation can be effective in not only identifying possible faults but also in optimizing the performance of the ESPs. With the introduction of more powerful supervisory computer control systems, as reviewed in Chapter 8, being installed as a norm, many of the electrical and other operational difficulties discussed above can now be identified from in-built fault finding menus.

Chapter 10
References

Cochet, R., Lois. *Charge des Fines Particules (submicroniques) Etudes Théoriques – Controles Récents Spectre de Particules.* Coll. Int. la Physique des Forces Electrostatiques et Leurs Application. Centre National de la Recherche Scientifique. Vol. 102. pp 331–338, Paris, 1961.

Bickelhaupt, R.E. *A Technique for Predicting Ash Resistivity.* EPA-600/7-79-204 [NTIS PB80-102379], August 1979.

Dahlin, R.S. and Altman, R.F. *Prediction of Mass Loading and Particle Size Distribution for use in an ESP Sizing Model*; Proceedings: Conference on ESP Technology for Coal-Fired Power Plants, EPRI April 1983.

Deutsch, W. *Bewegung und Ladung der Elektricitatstrager im Zylinder Kondensator*, Annalen der Physik 68, 335 (1922).

Fujishima, H. et.al. *Trend of ESP Design in Japan*; Procceedings of the 8th ICESP Conference. Birmingham, AL; May 2001. II Paper B 4-1.

Gaugain, J.M. *On the Disruptive Discharge*. Annales de Chimie et de Physique. 1862 Vol. 64. p 175.

Hall, H.J. *Trends in Electrical Energization of ESPs*; In Proceedings: ESP Symposium, Birmingham, AL; 1971.

Hall. H.J. *Fly Ash Chemistry Indices for Resistivity and Effects on ESP Design and Performance*; Proceedings Fourth Symposium on the Transfer and Utilisation of Particulate Control Technology. Vol. II. Houston, TX; EPA 600-9-84-025b [NTIS PB85-161909], pp 459–473, Nov. 1984.

Lawless, P. *Particle Charging Bounds, Symmetry Relations, and an Analytic Charging Rate Model for the Continuum Regime*; J. Aerosol Sci.; Vol 27, pp 191–215, 1996.

Matts, S. and Ohnfeldt, P. *Efficient Gas Cleaning with SF ESPs*; AB Svenska Flaktfabriken; Stockholm, Sweden; 1963-1964.

McDonald, J.R and Dean, A.H. *A Manual for the Use of ESPs to Collect Fly Ash Particles*; EPA-600/8-80-025 [NTIS PB81-112757], p 333, May 1980.

Plaks, N. *CAM and ESP Modeling*; Clear Stacks; Reinhold Environmental Ltd.; pp 3-6, January 1998.

Roentgen, V. *Gottinger Nach*; 1878. p 390.

Smith, W.B., and McDonald, J.R. De*velopment of Theory for the Charging of Particles by Unipolar Ions*; J. Aerosol Sci.; Vol. 7, pp 151–166, 1976.

Townsend, J.S. *Electricity in Gases*; Oxford University Press; 1915.

Trichel, G.W. *The Mechanism of the Negative Point–to-Plane Corona near Onset*. Physical Review; Vol. 54, p 1078, 1938.

Yamamoto, T., Lawless, P.A., and Plaks N. *Evaluation of the Cold Pipe Precharger, IEEE Transactions on Industry Applications*; Vol. 26, No. 4, July/August 1990.

Appendix A
Installing and Setting Up ESPVI 4.0W

The ESPVI 4.0W installation program is on a CD ROM. Insert the CD ROM into the CD drive. If the CD is set for automatic install, an instruction screen will appear and should be followed.

If the automatic install is not operating, then go to the Start button and then to Run. Type D:\setup.exe, in which D is the designation of the CD drive. If the CD drive has a designation other than D, use the correct letter in place of it. Then click OK, and follow the screen instructions.

It is always good practice when installing a Windows program, to shut down other programs that may be open.

Appendix B
Internal Composition and Text of the Data Files

The internal texts of the five sets of data files and one electrode file for each of the sections or fields that describe an ESP are shown below. The illustrative case here is for SAMPLE. Because SAMPLE has three sections, the total number of files is 8, since in this case the electrode configuration for each of the sections is the same. As such, only one of the three is shown here. They are viewed with a text editor such as Notepad. Occasionally it is necessary to enter them to look for and correct problem-causing errors. Another need may arise if one wants to bring in electrode files from another modeled ESP. The new electrode files must be in the same folder and the electrode file names must be entered in the *.mst and *.esp files in the appropriate order. If any work is performed on the files with the text editor, maintain the precise format.

SAMPLE.mst

```
Esp Design file = ;SAMPLE
Electrode file  = ;SAMPLE01;SAMPLE02;SAMPLE03
Non-ideal file  = ;SAMPLE
Flue gas file   = ;SAMPLE
Particle file   = ;SAMPLE
Note 1: ;SAMPLE is a relatively small three section ESP that is supplied with
Note 2: ;the program. It is featured in the manual and is used as the basis from which to
develop
Note 3: ;other ESP files for modeling.
Note 4: ;
```

SAMPLE.esp

```
Units (0=SI) =; 0
SCA    =;30.30
Total area   =;3600.0
Gas velocity =;1.800
Number Sects =; 3
Total Length =;7.50
Total Height =;7.50
Total Width  =;8.80
Stack diam   =;3.05
Sect SCA=;10.101;10.101;10.101
Sect Area     =;1200.00;1200.00;1200.00
Sect Length   =;2.500;2.500;2.500
Sect wire-plt =;0.1250;0.1250;0.1250
Sect Dust Thk =;0.000;0.000;0.000
Resistivity  =;1.00E+08
```

Peak-to-avg =;1.200;1.200;1.200
Operating V =;41000.0;40000.0;39000.0
Operating cd =;1.12E-04;1.42E-04;1.57E-04
Electrode file=;SAMPLE01;SAMPLE02;SAMPLE03
Calculation =; 0
Waveform =; 2 ;Full Wave1:1
Max Voltage =;60000;60000;60000
Max Peak Volt =;84000;84000;84000
Max current =;0.500;0.500;0.500
CO additions =;0.000;0.000;0.000
ect Wav Frms =;2;2;2
Mobility factors =;1.00E00;1.00E00;1.00E00
Resistivity =;1.00E+08;1.00E+08;1.00E+08

SAMPLE01.elc

Number Elements = ; 14
Electrode Type = ;0;0;0;0;0;0;0;0;0;0;0;0;0;0
Electrode diam = ;3.00E-03;3.00E-03;3.00E-03;3.00E-03;3.00E-03;3.00E-03;3.00E-03;3.00E-03;3.00E-03;3.00E-03;3.00E-03;3.00E-03;3.00E-03;3.00E-03
Electrode loc = ;8.90E-02;2.68E-01;4.46E-01;6.25E-01;8.03E-01;9.82E-01;1.16E+00;1.34E+00;1.52E+00;1.70E+00;1.88E+00;2.05E+00;2.23E+00;2.41E+00
Electrode extent=
;0.00E+00;0.00E+00;0.00E+00;0.00E+00;0.00E+00;0.00E+00;0.00E+00;0.00E+00;0.00E+00;0.00E+00;0.00E+00;0.00E+00;0.00E+00;0.00E+00
Corona factor =
;0.800;0.800;0.800;0.800;0.800;0.800;0.800;0.800;0.800;0.800;0.800;0.800;0.800;0.800

SAMPLE02.elc

Number Elements = ; 14
Electrode Type = ;0;0;0;0;0;0;0;0;0;0;0;0;0;0
Electrode diam = ;3.00E-03;3.00E-03;3.00E-03;3.00E-03;3.00E-03;3.00E-03;3.00E-03;3.00E-03;3.00E-03;3.00E-03;3.00E-03;3.00E-03;3.00E-03;3.00E-03
Electrode loc = ;8.90E-02;2.68E-01;4.46E-01;6.25E-01;8.03E-01;9.82E-01;1.16E+00;1.34E+00;1.52E+00;1.70E+00;1.88E+00;2.05E+00;2.23E+00;2.41E+00
Electrode extent=
;0.00E+00;0.00E+00;0.00E+00;0.00E+00;0.00E+00;0.00E+00;0.00E+00;0.00E+00;0.00E+00;0.00E+00;0.00E+00;0.00E+00;0.00E+00;0.00E+00
Corona factor =
;0.800;0.800;0.800;0.800;0.800;0.800;0.800;0.800;0.800;0.800;0.800;0.800;0.800;0.800

SAMPLE03.elc

Number Elements = ; 14
Electrode Type = ;0;0;0;0;0;0;0;0;0;0;0;0;0;0

Electrode diam = ;3.00E-03;3.00E-03;3.00E-03;3.00E-03;3.00E-03;3.00E-03;3.00E-03;3.00E-03;3.00E-03;3.00E-03;3.00E-03;3.00E-03;3.00E-03;3.00E-03;3.00E-03
Electrode loc = ;8.90E-02;2.68E-01;4.46E-01;6.25E-01;8.03E-01;9.82E-01;1.16E+00;1.34E+00;1.52E+00;1.70E+00;1.88E+00;2.05E+00;2.23E+00;2.41E+00
Electrode extent= ;0.00E+00;0.00E+00;0.00E+00;0.00E+00;0.00E+00;0.00E+00;0.00E+00;0.00E+00;0.00E+00;0.00E+00;0.00E+00;0.00E+00;0.00E+00;0.00E+00;0.00E+00
Corona factor = ;0.800;0.800;0.800;0.800;0.800;0.800;0.800;0.800;0.800;0.800;0.800;0.800;0.800;0.800;0.800

SAMPLE.srt

Sneakage fraction = ;0.050;0.050;0.050
Rapping re-entrainment = ;0.100;0.100;0.100
Core turbulent number = ;1.000;1.000;1.000
Section misalignment fraction = ;0.000;0.000;0.000
Fraction misaligned = ;0.000;0.000;0.000
Velocity sigma = ;0.150
Rap MMD = ;6.00
Rap sigma = ;1.600
1-section Out fraction = ;0.00
2-section Out fraction = ;0.00
Steady reentrain fr. = ;0.000
Total maldist. factor = ;1.002
RapTot maldist. factor = ;1.056
Sneakage maldist. factor = ;1.00418;1.00339;1.00289;1.00233;1.00194;1.00177;1.00163;1.00155;1.00146;1.00136;1.00142;1.00153;1.00152;1.00159;1.00175;1.00180;1.00194;1.00224;1.00308;1.00442;1.00538;1.00453;1.00256;1.00044;1.00003;1.00000;1.00000
Rapping maldist. factor = ;1.00418;1.00339;1.00289;1.00233;1.00194;1.00177;1.00163;1.00155;1.00146;1.00138;1.00152;1.00196;1.00295;1.00532;1.01042;1.01700;1.02843;1.04986;1.08609;1.12006;1.13918;1.15245;1.15289;1.13690;1.07404;1.01736;1.00167
Back Corona Loss fr. = ;0.100

SAMPLE.gas

Units (0=SI/1=US) = ; 0
N2 = ;7.350E01
O2 = ;3.300E00
CO2 = ;1.490E01
H2O = ;8.00E00
SO2 = ;8.050E-02
SO3 = ;3.200E-04
Gas Temp (K) = ;4.14E02
Gas Volume = ;1.19E02

Gas Pressure (kPa) = ;1.01E02
Gas Viscosity (kg/ms) = ;2.60E-05
Gas Mobility (mý/Vs) = ;8.81E-05

SAMPLE.prt

Units (0=SI/1=US) = ; 0
Particle density = ;2400.0
Mass loading = ;6.00E-03
Lognormal MMD = ;16.00
Lognormal sigma = ;3.402
Distribution type = ;0
Fraction @ 0.07 =; 5.34E-06
Fraction @ 0.09 =; 1.22E-05
Fraction @ 0.11 =; 2.50E-05
Fraction @ 0.14 =; 5.50E-05
Fraction @ 0.18 =; 1.33E-04
Fraction @ 0.23 =; 2.62E-04
Fraction @ 0.29 =; 5.02E-04
Fraction @ 0.36 =; 0.0009
Fraction @ 0.45 =; 0.0017
Fraction @ 0.55 =; 0.0029
Fraction @ 0.69 =; 0.0051
Fraction @ 0.89 =; 0.0091
Fraction @ 1.10 =; 0.0143
Fraction @ 1.30 =; 0.0201
Fraction @ 1.54 =; 0.0281
Fraction @ 1.80 =; 0.0370
Fraction @ 2.04 =; 0.0464
Fraction @ 2.44 =; 0.0620
Fraction @ 3.29 =; 0.0980
Fraction @ 4.90 =; 0.1666
Fraction @ 6.93 =; 0.2470
Fraction @ 9.38 =; 0.3315
Fraction @ 12.41 =; 0.4179
Fraction @ 16.73 =; 0.5146
Fraction @ 23.66 =; 0.6254
Fraction @ 31.30 =; 0.7082
Fraction @ 41.83 =; 0.7838
Fraction @ 59.76 =; 0.8592
Density,Index,Charge # 0.08 =; 2400; 1.500; 0.010; 0.00E00
Density,Index,Charge # 0.10 =; 2400; 1.500; 0.010; 0.00E00
Density,Index,Charge # 0.12 =; 2400; 1.500; 0.010; 0.00E00
Density,Index,Charge # 0.16 =; 2400; 1.500; 0.010; 0.00E00
Density,Index,Charge # 0.21 =; 2400; 1.500; 0.010; 0.00E00
Density,Index,Charge # 0.25 =; 2400; 1.500; 0.010; 0.00E00

Density,Index,Charge # 0.33 =; 2400; 1.500; 0.010; 0.00E00
Density,Index,Charge # 0.40 =; 2400; 1.500; 0.010; 0.00E00
Density,Index,Charge # 0.50 =; 2400; 1.500; 0.010; 0.00E00
Density,Index,Charge # 0.60 =; 2400; 1.500; 0.010; 0.00E00
Density,Index,Charge # 0.80 =; 2400; 1.500; 0.010; 0.00E00
Density,Index,Charge # 1.00 =; 2400; 1.500; 0.010; 0.00E00
Density,Index,Charge # 1.20 =; 2400; 1.500; 0.010; 0.00E00
Density,Index,Charge # 1.40 =; 2400; 1.500; 0.010; 0.00E00
Density,Index,Charge # 1.70 =; 2400; 1.500; 0.010; 0.00E00
Density,Index,Charge # 1.90 =; 2400; 1.500; 0.010; 0.00E00
Density,Index,Charge # 2.20 =; 2400; 1.500; 0.010; 0.00E00
Density,Index,Charge # 2.70 =; 2400; 1.500; 0.010; 0.00E00
Density,Index,Charge # 4.00 =; 2400; 1.500; 0.010; 0.00E00
Density,Index,Charge # 6.00 =; 2400; 1.500; 0.010; 0.00E00
Density,Index,Charge # 8.00 =; 2400; 1.500; 0.010; 0.00E00
Density,Index,Charge # 11.00 =; 2400; 1.500; 0.010; 0.00E00
Density,Index,Charge # 14.00 =; 2400; 1.500; 0.010; 0.00E00
Density,Index,Charge # 20.00 =; 2400; 1.500; 0.010; 0.00E00
Density,Index,Charge # 28.00 =; 2400; 1.500; 0.010; 0.00E00
Density,Index,Charge # 35.00 =; 2400; 1.500; 0.010; 0.00E00
Density,Index,Charge # 50.00 =; 2400; 1.500; 0.010; 0.00E00

TECHNICAL REPORT DATA
(Please read Instructions on the reverse before completing)

1. REPORT NO.	2.	3. RECIPIENT'S ACCESSION NO.
EPA-600/R-04/072		

4. TITLE AND SUBTITLE	5. REPORT DATE
Electrostatic Precipitator (ESP) Training Manual	July 2004
	6. PERFORMING ORGANIZATION CODE

7. AUTHORS	8. PERFORMING ORGANIZATION REPORT NO.
Kenneth Parker and Norman Plaks	

9. PERFORMING ORGANIZATION NAME AND ADDRESS	10. PROGRAM ELEMENT NO.
ARCADIS Geraghty & Miller 4915 Prospectus Drive, Suite F Durham, NC 27713	11. CONTRACT/GRANT NO. 68-C-99-201, W.A. 4-30

12. SPONSORING AGENCY NAME AND ADDRESS	13. TYPE OF REPORT AND PERIOD COVERED
U. S. EPA, Office of Research and Development Air Pollution Prevention and Control Division Research Triangle Park, North Carolina 27711	Final 14. SPONSORING AGENCY CODE EPA/600/13

15. SUPPLEMENTARY NOTES

The EPA Project Officer is Ravi K. Srivastava, Mail Drop E305-01, phone (919) 541-3444, e-mail srivastava.ravi@epa.gov

16. ABSTRACT

The manual assists engineers in using a computer program, the ESPVI 4.0W, that models all elements of an electrostatic precipitator (ESP). Once an ESP is accurately modeled, the model can be used as an analytical tool to diagnose problems and to suggest ways to improve efficiency. In terms of emissions or electrical use, it can predict the results from various fuels and predict the benefit of equipment additions such as gas conditioning. The manual teaches the engineer how to operate the program and discusses the underlying mathematics. A great deal of attention is given to the practical workings of an ESP. Electrical issues are considered, including the detection and control of reverse ionization, electrode design, and various strategies for controlling and optimizing electric energy use. Mechanical matters such as flue gas cooling and conditioning are discussed as are the characteristics of flue gas that result from various fuels, the particles the flue gases contain, and the electrical qualities of the particles.

17. KEY WORDS AND DOCUMENT ANALYSIS

a. DESCRIPTORS	b. IDENTIFIERS/OPEN ENDED TERMS	c. COSATI Field/Group
Air Pollution Electrostatic Precipitator Electric Corona Particles Sulfur Oxides Flue Gases	Pollution Control Stationary Sources	13B 13I 20C 14G 07B 21B

18. DISTRIBUTION STATEMENT	19. SECURITY CLASS *(This Report)*	21. NO. OF PAGES
Release to Public	Unclassified	184
	20. SECURITY CLASS *(This Page)*	22. PRICE
	Unclassified	

EPA Form 2220-1 (Rev. 4-77) PREVIOUS EDITION IS OBSOLETE